Characterizing the role of the Negative Elongation Factor complex in myogenic cell state changes

Daniel Curtis Louis Robinson

A thesis submitted to the University of Ottawa in partial fulfillment of
the requirements for the Doctorate of Philosophy in Cellular & Molecular Medicine

Department of Cellular & Molecular Medicine
Faculty of Medicine
University of Ottawa

Abstract

The robust regenerative capacity of muscle stem cells (MuSCs) and their progenitors depends on their ability to undergo rapid and vast changes to their transcriptome during cell state changes. While transcription factors and epigenetic remodelling proteins are critical to render genes permissive for transcription, often these genes are found to have paused promoter proximal RNA Polymerase II (Pol II) which remains in a rate-limiting poised state. Indeed, while prior studies have shown poised Pol II is often regulated by the Negative Elongation Factor (NELF) to induce rapid changes in gene expression, the specific need for NELF in somatic stem cell populations has not been previously examined. In this thesis, we identify a specific requirement for NELF-dependent promoter proximal Pol II pausing in proliferating myogenic progenitors. Here, NELF stabilizes nascent transcripts associated with the paused RNA Pol II at genes required to maintain muscle progenitors in cell cycle. This promotes expansion of the pool of myogenic progenitors required to adequately repair damaged skeletal muscle. Our molecular analysis suggests that in proliferating progenitors, NELF-bound Pol II ensures the stabilization of transcripts, and continued expression of genes that prevent p53-mediated cell cycle withdrawal and terminal differentiation. Unexpectedly, this work revealed a previously unappreciated contribution of proliferating myogenic progenitors to replenish the stem cell niche in support of MuSC self-renewal during skeletal muscle regeneration. Based on our results, new therapeutic avenues which could treat muscle wasting disease are also discussed.

Acknowledgements

First and foremost, I would like to thank my research supervisor, Dr. Jeff Dilworth, who has excelled as a mentor throughout my journey in graduate school. Through exceptional leadership, Jeff has nurtured my scientific curiosity, guided me through experimental obstacles, and provided numerous opportunities towards my professional development, all while providing a supportive environment to pursue my academic interests. The skills I have learned while working with Jeff have been instrumental to establish a foundation to develop my career.

I am grateful for the bountiful resources provided by the Ottawa Hospital Research Institute which assured success during my time in graduate school. Their modern facilities and strong research community has vastly contributed to my growth, and allowed me to overcome various hurdles towards achieving my research objectives. I am particularly thankful for the contributions and support provided by my Thesis Advisory Committee members, namely Dr. Nadine Wiper-Bergeron, Dr. Michael Rudnicki, and Dr. Jing Wang.

I would like to thank the many funding organizations which have provided financial opportunity during my training in graduate school. This includes studentships provided by the Canadian Institute of Health Research, Ontario Graduate Scholarship, Queen Elizabeth II Scholarship in Science and Technology, and funding towards international training by the CIHR Michael Smith Foreign Study Supplement and the Stem Cell Network. Scholarships provided by the University of

Ottawa have additionally eased financial burdens which have allowed me to focus on my research.

Finally, I would like to thank my colleagues, friends, and family for their endless support throughout my time in graduate school, and has made the process quite enjoyable. I am exceptionally grateful for my academic colleagues at the OHRI and the many laughs we shared along the way. Lastly, I am especially thankful for my mother, who fostered my interest in science from a young age, encouraged me to follow my passion, and has always been a pillar of support.

Table of Contents.

List of Abbreviations

4-OHT	–	4-hydroxytamoxifen
AI7	–	Alpha integrin 7
BGS	–	Bovine Growth Serum
Cdk	–	Cycling Dependant Kinase
Cdk9dn	–	Cyclin Dependant Kinase 9, dominant negative
CTD	–	C-Terminal Domain (RNA Pol II)
CUT&Tag	–	Cleavage Under Targets and Tagmentation
Dpi	–	Days post-injury
DSIF	–	DRB-sensitive Inducing Factor
ECM	–	Extracellular Matrix
EDL	–	Extensor Digitorum Longus
ERK	–	Extracellular signal-Regulated Kinase
FACS	–	Fluorescence Activated Cell Sorting
FAP	–	Fibroadipogenic Progenitor
FGF	–	Fibroblast Growth Factor
GAF	–	GAGA Associated Factor
GO	–	Gene Ontology
H3K4me3	–	Histone 3 Lysine 4, tri-methylated
HDAC4	–	Histone Deacetylase 4
HEK 293T	–	Human Embryonic Kidney 293T (cells)
Hpi	–	Hours post-injury

IL-(#)	–	Interleukin
IP	–	Intraperitoneal
MAPK	–	Mitogen Activated Protein Kinase
MEF2	–	Myocyte Enhancer Factor 2
MRF	–	Myogenic Regulatory Factor
MuSC	–	Muscle Stem Cell
NELF	–	Negative Elongation Factor
NSG	–	Nod Scid Gamma (mouse)
PBS	–	Phosphate-buffered Saline
PEDF	–	Pigment Epithelium Derived Factor
PFA	–	Paraformaldehyde
PGC1-α	–	Peroxisome proliferator-activated receptor gamma coactivator-alpha
PIC	–	Preinitiation complex
Pol II	–	RNA Polymerase II
PRO-seq	–	Precision Run-On Sequencing
pTEFb	–	Positive Transcription Elongation Factor
RRM	–	RNA Recognition Motif
SEM	–	Standard Error of the Mean
shRNA	–	short hairpin RNA
SIX	–	Sine Oculis Homeobox
TA	–	Tibialis Anterior
TBS	–	Tris-buffered Saline
TBST	–	Tris-buffered Saline with Tween

TdT	–	TdTomato
TF	–	Transcription Factor
TGF	–	Transforming Growth Factor
TSS	–	Transcription Start Site
UTR	–	Untranslated Region
VEGFa	–	Vascular Endothelial Growth Factor A

List of Figures

Chapter 1

Chapter 3

Chapter 4

CHAPTER 1

Introduction

1.1 – Adult stem cells and skeletal muscle regeneration: a cellular perspective

1.1.1 ***Brief overview of stem cells and their function***. Stem cells have garnered extensive excitement based on their vast potential therapeutic applications towards the repair and regeneration of damaged tissues, organs, and age-related deterioration (1). In fully developed adults, the population of somatic or adult stem cells reside in specialized niches within their respective tissues and support tissue repair and general maintenance for continued tissue function. To do so, adult stem cells must exhibit two fundamental criteria which includes self-renewal and differentiation into another cell type (2). This assures an abundant supply of stem cells remain for future repair, while permitting the repair of the damaged host tissue (3). Together, the diverse abilities of adult stem cells boast great therapeutic potential to regenerate and rejuvenate tissues.

While unlocking the secrets behind adult stem cell behavior to regulate their function would offer vast therapeutic potential, there are currently several limitations which prevents their use. This includes problems inherent to isolation protocols which limits the ability to propagate viable stem cell populations suitable for transplant, the inability of some adult stem cells to adequately repopulate a recipient tissue upon transplant, and general safety concerns relating to potential transplant rejection which require further investigations and clinical trials (3).

1.1.2 *Robust regenerative capacity of skeletal muscle*. Additional investigations focused on molecular functions which govern stem cell behaviors may provide the necessary insight to permit therapeutic use of stem cells. In doing so, an ideal adult stem cell model for these studies must be both abundant and easy to manipulate to provide the necessary populations to probe molecular mechanisms which regulate adult stem cell behavior. Amongst candidate tissues, skeletal muscle is an excellent model as it is largely abundant, boasts robust regeneration capacity, and harbours many adult muscle stem cells which permits its regenerative capacity (4). To illustrate, the population of adult muscle stem cells (MuSC) exhibit dynamic behavior in response to environmental requirements. This includes MuSCs support towards myofiber viability during homeostasis (5), preservation of MuSC populations despite myofiber hypotrophy when skeletal muscle becomes immobilized (6, 7), and expansions of MuSC populations to support myofiber hypertrophy during increased use of skeletal muscle (8-10). In addition, MuSCs may enter a dormant protective state to remain viable in hostile environments, as observed with viable MuSC populations harvested from a carcass at up to 17 days post-mortem (11).

The regenerative program of MuSCs is additionally quite resistant towards errors. Although skeletal muscle comprises 40% of human body mass and contains over half of all body proteins (12), it exhibits a strikingly low occurrence of cancers and tumours. Indeed, rhabdomyosarcoma is the only reported skeletal muscle cancer, and it accounts for only 3% of pediatric cancers (13, 14), and less than 1% of adult solid tumours (15, 16). Thus, the dynamic ability of MuSCs to regulate environmentally responsive changes to skeletal muscle, and the robust regeneration program makes it an ideal model system in the study of somatic stem cell populations.

1.1.3 *Skeletal muscle regeneration is a highly-coordinated process between many cell types.*

The robust regenerative capacity of skeletal muscle relies on several tissue-resident and infiltrating cell types, whose interactions dictate myogenic cell state changes during skeletal muscle regeneration. The primary cell population engaged in actual myofiber repair are the muscle stem cells (MuSCs), also termed satellite cells owing to their peripheral location on individual myofibers (17). While these permit myofiber repair, their ability to do so is strongly dependent on accessory cell types, and their effects on the extracellular environment. These extracellular cues in turn controls MuSC cell state changes to permit myofiber repair and MuSC self-renewal. A brief look at these cell types is described in the following sections.

1.1.3a *Myogenic cell state changes during myofiber repair*. In undamaged muscle, quiescent MuSCs reside within a protective niche situated between the sarcolemma and the basal lamina of the extracellular matrix (18). When intact, this niche offers physical contacts between MuSCs and a basal lamina enriched in cytokines, mitogens, and secondary cell types which support MuSCs to remain in a quiescent state (19). In addition, this niche forms a physical barrier which deters certain mitogens from interacting with and activating MuSCs (20). In response to injury, breaks in the myofiber sarcolemma disrupts the MuSC niche and exposes quiescent MuSCs to a cascade of signaling molecules and accessory cell types which initiate the myogenic program. Here, MuSCs undergo either a symmetric or asymmetric division, which is strongly influenced by the extent of skeletal muscle damage (21). Acute injury favours symmetric divisions to produce two activated

myogenic daughter cells committed to the cell cycle (22) (Figure 1.1A), while lesser injury favours asymmetric division to produce one daughter cell committed to the cell cycle and another which remains as a quiescent MuSC (23) (Figure 1.1B). While activated MuSCs rapidly enter the cell cycle to become proliferating myogenic progenitors, some retain the ability to return to a dormant state (Figure 1.1C) and form a population of satellite progenitors. These may enter the cell cycle in response to future injury, but are not considered true quiescent MuSCs as they cannot undergo self-renewal (23).

Upon entry in the cell cycle, myogenic cells undergo a massive proliferation to produce the necessary cell numbers required to repair damaged myofibers. Typically, proliferation is sustained until extracellular signaling or cell-cell contacts induce cell cycle withdrawal and irreversibly commit to terminal differentiation (23). Once committed, these myocytes may either fuse with damaged myofibers or with one

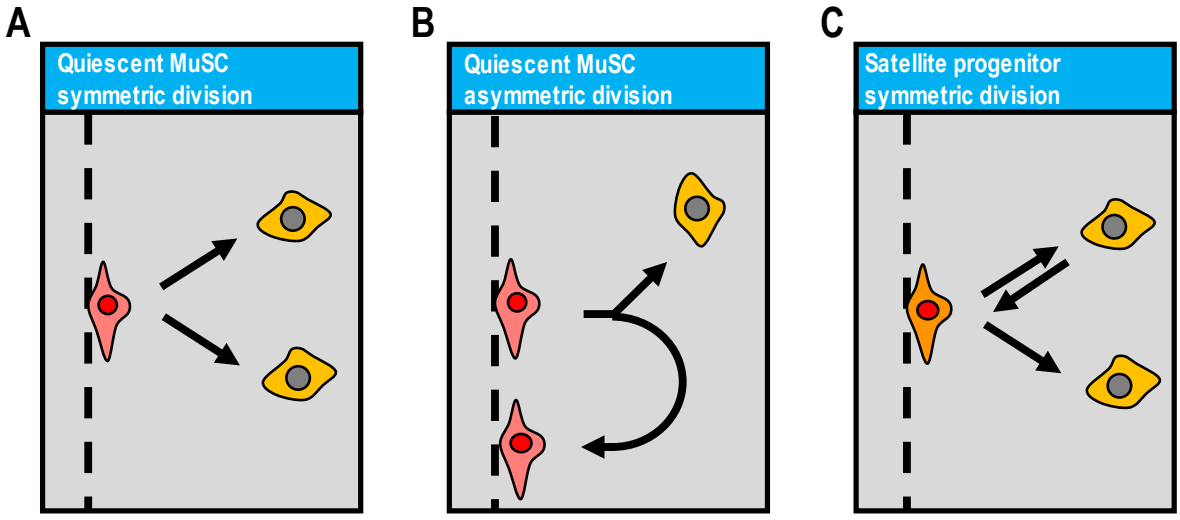

Figure 1.1 – Types of quiescent MuSC and satellite progenitor divisions. In response to acute injury, ***(A)*** quiescent MuSCs (red) undergo symmetric division to produce two activated MuSCs (light orange). ***(B)*** During homeostasis, only quiescent MuSCs (red) may undergo asymmetric divisions to produce one activated MuSC (light orange) primed towards the cell cycle and another quiescent MuSC (red) ***(C)*** dormant satellite progenitors (dark orange) may undergo a symmetric division to produce two activated MuSCs (light orange) which are primed towards the cell cycle. Activated MuSCs may resume a quiescent state and become a dormant satellite progenitor.

another to create *de novo* myofibers. In either case, the resulting multinucleated myofiber continues to mature to produce functional actinomyosin myofibrils to restore contractile function to the myofibers, as summarized in Figure 1.2. During late proliferation and early differentiation, quiescent MuSCs also undergo symmetric divisions, which marks their self-renewal to increase populations of quiescent MuSCs ready to respond to future rounds of injury (24, 25). Collectively, this designates five different myogenic cell states which are critical for skeletal muscle regeneration, namely quiescent MuSCs, satellite progenitors, activated MuSCs, myogenic progenitors, and myocytes.

1.1.3b *Accessory cell types coordinate skeletal muscle regeneration*. The regulated activity of MuSCs behavior in myogenesis is strongly influenced by

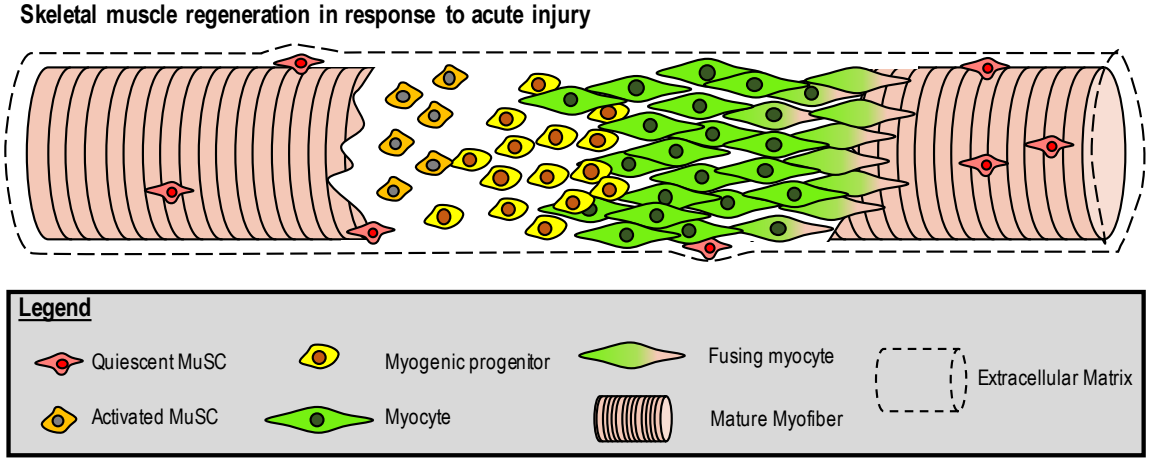

Figure 1.2 – General overview of myogenic cell state transitions during skeletal muscle regeneration. In response to acute skeletal muscle injury, damaged myofiber debris are cleared by immune cells (not shown), which primes MuSCs for skeletal muscle repair. This prompts a symmetric division amongst quiescent MuSCs to produce two activated MuSCs. These enter the cell cycle, and form a population of massively expanding proliferating myogenic progenitors. In response to cell-cell contacts or signaling pathways, myogenic progenitors withdraw from the cell cycle, and form a population of myocytes which are committed to terminal differentiation, where they fuse with one another or damaged myofibers. During late stages of proliferation, quiescent MuSCs undergo self-renewal to increase the populations of quiescent MuSCs available for skeletal muscle maintenance.

accessory cell types in the surrounding environment from both cell-cell contacts and cellular cross-talk networks, arising from tissue-resident and infiltrating cell types. In all instances, these accessory cell types reformulate the extracellular environment, secrete cytokines, mitogens, and other effectors to influence the downstream behavior of MuSCs. While many accessory cell types participate in this process, they may be broadly classified into three categories which represent inflammatory cells, extracellular matrix remodellers, and vasculature remodellers.

Inflammatory cells. Muscle-resident and infiltrating immune cells orchestrate the early processes in response to skeletal muscle damage (26). To do so, tissue-resident mast cells and neutrophils are the first to act in response to acute injury, where they immediately begin to clear damaged myofiber debris. While doing so, they recruit additional infiltrating mast cells and neutrophils to strengthen their response. This is followed by activation and recruitment of both tissue-resident and infiltrating M1 macrophages to support damaged myofiber clearing. The M1 macrophages also recruit anti-inflammatory M2 macrophages and T cells, both of which secrete cytokines to help control the myogenic program (27-29).

Extracellular matrix remodellers. The implications of the extracellular matrix (ECM) to regulate MuSC and myogenic progenitor behavior have been well established. To name a few, it provides a niche environment conducive to MuSC quiescence, provides structural integrity to permit myofiber contractions, and its specific composition directs MuSC symmetric and asymmetric divisions (30). To maintain its functional purpose, the ECM depends largely on maintenance

contributions by skeletal muscle resident fibroblasts. Here, fibroblasts secrete structural constituents of the ECM such as collagens, fibronectin, and proteoglycans, in addition to matrix metalloproteinases to restructure the ECM (31). The effect of fibroblasts on ECM composition directly affects regenerated myofiber diameter and MuSCs self-renewal (32), along with myofiber maturation and fiber type (33). Skeletal muscle resident mesenchymal progenitors known as fibro-adipogenic progenitors (FAPs) may also differentiate into fibroblasts or adipocytes to support skeletal muscle regeneration (34, 35).

Vasculature and neurosmuscular junctions. During later stages of skeletal muscle regeneration, neuromuscular junctions are repaired by resident glial cells (36), while vasculature is supported by pericytes, endothelial cells, and smooth muscle cells. These cells reside within special localized niches in skeletal muscle (37), and contribute to maintain MuSC quiescence (38).

1.1.3C *Cellular cross-talk supports skeletal muscle regeneration.* Structured paracrine signaling networks are critical to permit the necessary cellular cross-talk between different cell types to orchestrate skeletal muscle regeneration. This includes early responses to skeletal muscle damage, where damaged myofibers recruit macrophages to initiate debris clearing. Once recruited, paracrine signaling by macrophages activates the surrounding pericytes, smooth muscle cells, and endothelial cells to stimulate angiogenesis (39, 40). At later stages of regeneration, self-renewing MuSCs secrete VEGFa to localize endothelial cells within their proximity (38), and these recruited endothelial cells express the notch ligand Dll4 to support

maintenance of MuSCs in a quiescent state (38, 41, 42). During this early response to damage, FAPs similarly exhibits a large secretome to support myogenic cell behavior during skeletal muscle regeneration (43, 44): Wisp1 regulates MuSC asymmetric division (45), follistatin promotes terminal differentiation of myogenic progenitors (46), IL-33 activates and potentiates resident T cells (47), and IL-6 and IL-10 act as myokines which direct the activity of myogenic progenitors (44). Similarly, proliferating myogenic progenitors secrete exosomes that contain miR-206 (48) which are internalized by fibroblasts. Here, miR-206 represses the master regulator of collagen biosynthesis Rrbp1, and this prevents overproduction of collagen deposits in the ECM by fibroblasts (48). During their expansion, heterogeneous populations of proliferating myogenic progenitors additionally exhibit a highly dynamic landscape of syndecan receptors on their extracellular membrane, and this changes their ability to detect and respond to specific extracellular environment signals (49).

Overall, the ability of MuSCs to effectively participate in skeletal muscle regeneration is largely defined by their extracellular interaction with accessory cell types and paracrine signaling networks. In turn, this controls cell state transitions as quiescent MuSCs progress towards terminal differentiation. When perturbations disrupt MuSC cell state transitions, it often culminates in drastic outcomes which affect the integrity of skeletal muscle. As an example, the reduced ability of aged MuSCs to proliferate produces fewer downstream myocytes available to fuse with and repair damaged myofibers, which contributes to myofiber hypotrophy reported in sarcopenia (50).

1.2 Molecular regulation of MuSC and progenitors in regeneration

1.2.1 ***Myogenic transcription factors control changes in gene expression networks to permit myogenic cell state changes***. The ability of accessory cell types to regulate MuSC activity relies largely on signal transduction cascades to detect changes in the extracellular environment and elicit an internal response within MuSCs. In turn, this evokes changes to intracellular regulators, which exert control on cellular activity and gene expression. What remains relevant to this research is doing so allows to control the activity and interactions between epigenetic modifiers which reorganize the chromatin landscape, and myogenic transcription factors (MRFs) which localize these chromatin modifiers to specific genomic areas (51). This is additionally supported by accessory transcription factors such as the sine oculis homeobox (SIX) protein family (52, 53), and myocyte enhancer factor 2 (MEF2) proteins (54). In turn, these different combinations and activities of MRFs, accessory transcription factors, and epigenetic modifiers directly controls which gene networks are activated or suppressed to define different myogenic cell states. Therefore, myogenic cell states may be defined through their active expression of Pax7, and the MRFs Myf5, MyoD, Myog, and Mrf4 (23, 55), as summarized (Figure 1.3).

A. Dormant MuSC populations The population of dormant MuSCs are sub-categorized into two different G_0 populations, defined by their expression of Pax7 and Myf5. Populations that exhibit a molecular signature of $Pax7^+/Myf5^-$ define the true quiescent populations, while $Pax7^+/Myf5^+$ form a satellite progenitor population (56). While both populations remain dormant and ready to respond to skeletal muscle

damage, only quiescent MuSCs can undergo asymmetric divisions to produce another quiescent MuSC ($Pax7^+/Myf5^-$) and satellite progenitor ($Pax7^+/Myf5^+$). As previously described, satellite progenitors are restricted to symmetric divisions to produce activated MuSCs, and cannot undergo self-renewal (56). Quiescent MuSCs may additionally undergo symmetric divisions (56) to permit self-renewal and repopulate quiescent MuSCs populations following acute skeletal muscle injury. Unless further specified, the use of MuSCs will be used to denote both true quiescent MuSCs and dormant satellite progenitors.

B. Activation and proliferation During MuSC activation, a rapid increase in the protein levels of Myf5 and MyoD activates gene networks which support myogenic progenitor proliferation (57), and stimulates maintenance within the cell cycle (58, 59). Dynamic changes in protein levels of MyoD and Myf5 that correlate with the cell cycle stage is in part regulated by targeted degradation of these MRFs by cell cycle regulators (60, 61) and this assures progression between cell cycle stages (62). Together, the interplay between Myf5, MyoD, and cyclin dependent kinases (Cdks)

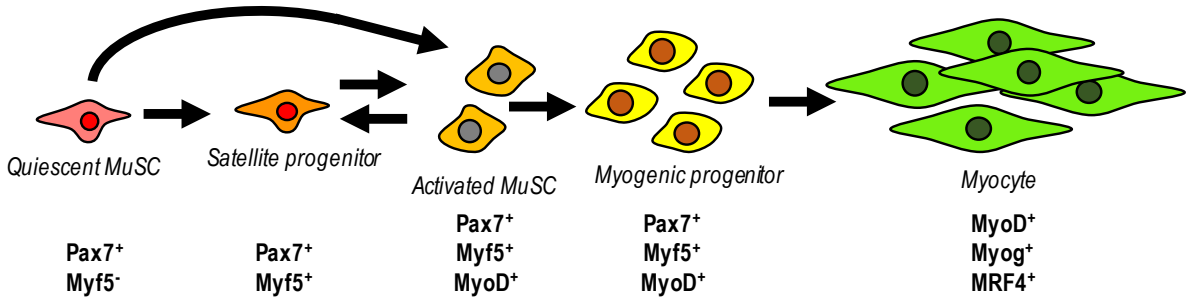

Figure 1.3 – Myogenic cell states defined by their expression of myogenic transcription factors. During myogenic cell state transitions, different expression patterns of Pax7 and the myogenic regulatory factors Myf5, MyoD, Myog, and Mrf4 are required to express gene programs specific to each cell state. Specific myogenic cell states are often characterized by their molecular signature of these transcription factors.

favours maintenance of myogenic progenitors within the cell cycle, which supports massive population expansions.

Myogenic progenitor proliferation is additionally marked with a gradual depletion of Pax7 (63). This favours maintenance within the cell cycle, as overexpressed Pax7 causes myoblasts to enter a non-differentiated G_0 cell stage (64), which arises from reciprocal interactions between Pax7 and the MRFs (65). During proliferation, Pax7 and accessory transcription factors additionally support chromatin remodelling towards a permissive state of genes required for terminal differentiation (66). To do so, Pax7 anchors super-enhancer regions to promoter sites, which remain even after Pax7 is fully depleted (66). Thus, chromatin remodelling primes gene networks for rapid induction during terminal differentiation.

C. Terminal Differentiation. At the onset of terminal differentiation, myogenic progenitors withdraw from the cell cycle and begin to fuse with one another and/or to damaged myofibers to support regeneration. This is facilitated by the actions of MyoD which binds the promoter of *Myog* to initiate its expression. Once expressed, Myog elicits rapid changes to the transcriptome to favour cell state transitions. This includes suppression of genes which define the transcriptome of proliferating myogenic progenitors such as *Myf5* (67), and genes which support cell cycle maintenance (68). In addition, Myog activates expression of *Cdkn1a* to produce the cell cycle arrest protein p21 (69). Supported by MyoD and Myog, an increase in *Mrf4* expression proceeds to activate many genes implicated in post-fusion myofiber maturation, so that the myofibers remain functional (70, 71). In later states of differentiation, Mrf4 interacts with HDAC4 (72), and together these antagonize the function of Mef2

proteins to control myofiber growth (73). Taken together, MyoD, Myog, and Mrf4 regulate changes in the transcriptome to accompany cell cycle withdrawal, myocyte fusion, and myofiber maturation.

1.2.2 ***Rapid changes in myogenic cell states are carefully regulated.*** During skeletal muscle regeneration, vast changes in the transcriptome which define myogenic cell states occur quite rapidly. Such an example stems from recent advances in MuSC isolation protocols, which demonstrate vast differences in the transcriptional profile of *in situ* fixed and unfixed MuSCs which arise during the isolation period (74, 75). This rapid change in transcriptome may in part be regulated through post-transcriptional regulation of Myf5 and MyoD mRNA abundance and translation in MuSCs: *Myf5* mRNA is sequestered in mRNP granules by miRNA-31 (76), whereas *MyoD* mRNA is degraded by tristetrapolin (77). During MuSC activation, disruption of granules releases *Myf5* mRNA and inactivation of tristetrapolin by the p38/MAPK α and β prevents degradation of *MyoD* mRNA. The rapid translation of these pre-produced transcripts bypasses lengthy processes implicated in transcription initiation, expression, and mRNA maturation, which fast-tracks their functional presence to elicit changes in the transcriptome.

1.2.3 ***Permissive chromatin is required to recruit Pol II for transcription initiation***. The ability of Pax7 and the MRFs to direct epigenetic changes is critical to produce permissive chromatin prior to gene expression. Once gene regions become accessible, this exposes the necessary binding sites for general and accessory transcription factors to recruit and assemble a functional RNA Polymerase

II (Pol II) transcription complex. Here, general transcription factors (TF) IID, IIB, IIF, IIE, and IIH assist Pol II recruitment and positioning within the promoter region to form a preinitiation complex (PIC) (78). Within the PIC, the C-terminal domain (CTD) of Pol II remains unphosphorylated, and this facilitates its interactions with the mediator complex to hold Pol II within the PIC and prevent its premature release. Subsequent post-translational modifications to the Pol II CTD heptad repeats causes Pol II to disengage from the PIC, and interact with downstream effectors of Pol II activity (79). This includes phosphorylation of Ser5 within the CTD heptad repeat by TFIIH-associated Cdk7, which disrupts the interaction of Pol II with the mediator complex to prompt Pol II escape from the PIC (80, 81) (Figure 1.4A)

1.2.4 ***Pax7, the MRFs, and epigenetic regulation of myogenic cells.*** The importance of Pax7 and the MRFs to regulate myogenic cell state changes have been the center of focus for quite some time, and many reviews elegantly describe their roles in myogenic cell state changes well beyond what was described above (23, 82). What remains pertinent to Pax7 and the MRFs is their ability to direct vast changes in the epigenome, which tunes gene networks, and permits myogenic cell state changes (51). Although these regulatory pathways are often described as intrinsic cell changes, their activity is strongly influenced by the dynamic extracellular environment (43, 83). Therefore, cell state changes require vast changes in the transcriptome, which is dictated by Pax7, the MRFs, and epigenetic modifiers, and this occurs in response to signaling events in the extracellular environment.

1.3 NELF, DSIF, and pTEFb act to regulate Pol II promoter proximal pausing

1.3.1 ***Active Pol II is strongly regulated beyond the transcription start site.*** While chromatin accessibility represents an important regulatory step in controlling gene expression to permit cell state transitions, genomic mapping of Pol II suggests an additional regulatory step in gene expression beyond transcription initiation. Specifically, an abundance of Pol II peaks slightly downstream of the transcription start site (TSS) (84, 85) suggests active Pol II is poised for downstream gene expression in various tissues, including skeletal muscle (86, 87). While it is now known that engaged Pol II paused in the promoter-proximal region can resume active elongation (88, 89), this presents a rate-limiting regulatory step in gene expression, where active Pol II is poised for rapid gene expression. Indeed, early investigations in this phenomenon have identified a role for Pol II promoter proximal pausing as an important regulatory step of gene expression in rapid-response genes, such as induction of *hsp70* as part of the heat shock response in *Drosophila* (90).

The prevalence of promoter proximal paused Pol II, and its regulatory activity in gene expression has enticed vast research efforts to understand its regulatory mechanisms and functional implications. These propose a potential mechanism which explains the cause and maintenance of Pol II pausing. This starts at the later stages of the preinitiation complex after Pol II is recruited and localized to its promoter regions by general transcription factors as previously discussed. Here, post-translational phosphorylation of Ser5 on the Pol II CTD disrupts interactions with the mediator complex (Figure 1.4A), which allows Pol II to escape from the preinitiation complex and begin active elongation. Once Pol II bypasses the transcription start site (TSS), TFIID initiates pausing of the active Pol II around 20 – 60 nucleotides downstream of

the TSS (Figure 1.4B) (86, 91, 92). In this paused state, a tilted conformation between the DNA:RNA hybrid within the Pol II active site causes nascent RNA to translocate out of the active site while DNA remains stably bound to DNA (93). While Pol II remains stably associated with DNA, its blocked active site precludes the entry of nucleotides for RNA synthesis, and this effectively halts transcription. Variability within the Pol II pause site suggests the DNA sequence may influence the distance from which Pol II becomes paused by TFIID, but this remains under investigation.

Generally, TFIIS supports paused Pol II to permit backtracking to correct misaligned DNA:RNA hybrids, and resume productive elongation (94). In the case of promoter-proximal pausing, Pol II is stabilized by accessory factors which include the DRB sensitive inducing factor (DSIF) and the negative elongation factor (NELF) to support an extended pausing state. Once recruited, NELF acts as a steric block towards TFIIS and prevents Pol II backtracking. This retains Pol II engaged in the paused state (93, 95-97), poised for rapid gene expression in response to stimulus. Earlier research suggests this requires the positive transcription elongation factor (pTEFb) complex to associate with paused Pol II, where it phosphorylates DSIF to evoke release of NELF from the paused complex, and permits a release of paused Pol II towards active elongation for gene expression (Figure 1.4C) (92). The pTEFb additionally phosphorylates Ser2 of the Pol II CTD heptad repeat which stabilizes Pol II during active elongation.

Previous decay assays (98) show promoter proximal paused Pol II is highly stable (80, 99-102), which suggests promoter proximal paused Pol II may be a regulatory step in gene expression (80). This pausing step likely functions as a hub to

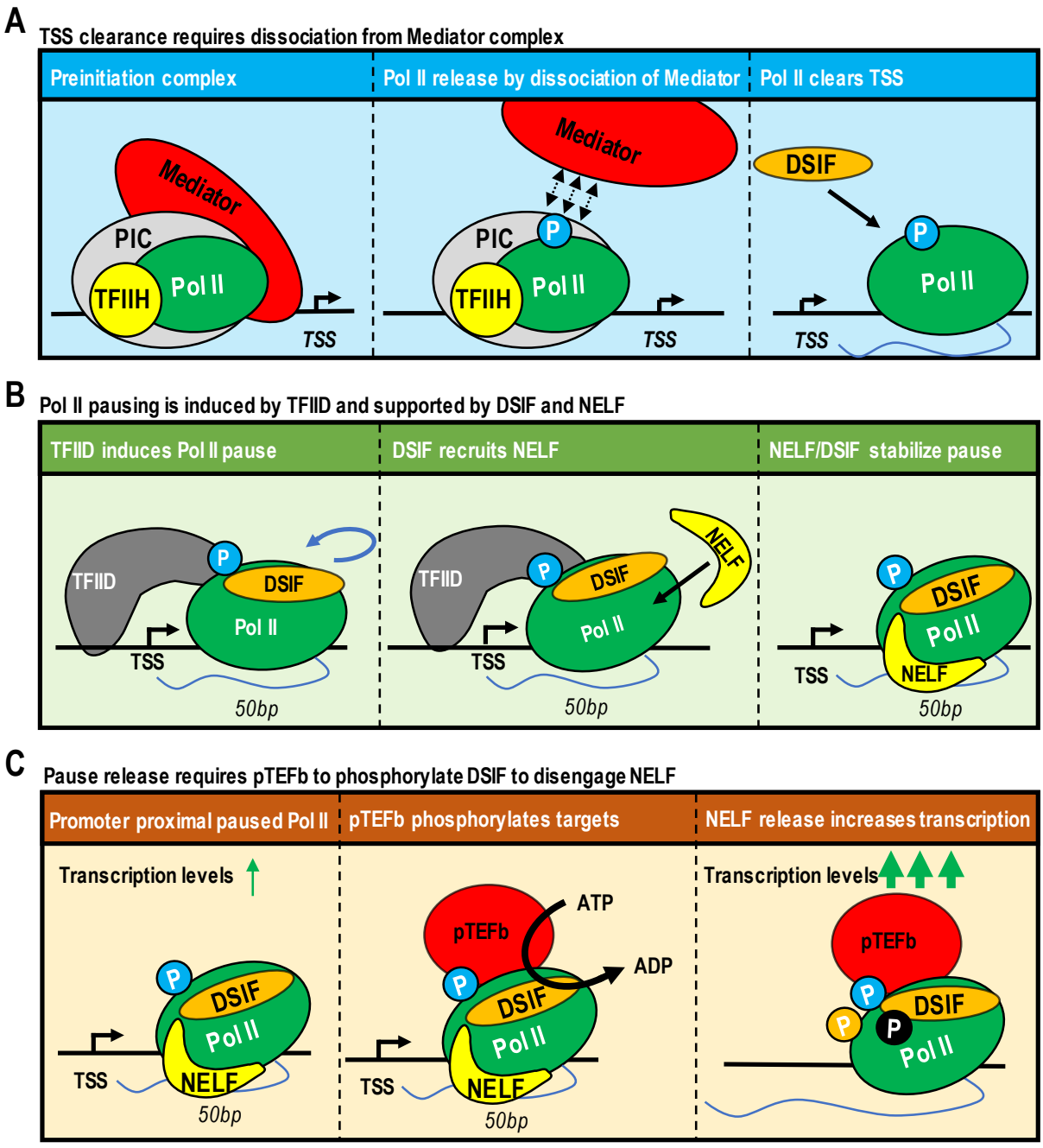

Figure 1.4 – Regulation of Pol II activity in the promoter proximal region. ***(A)*** During transcription initiation, Pol II is retained in the PIC through interactions with the Mediator complex. Phosphorylation of Ser5 in the heptad repeat of the Pol II CTD by TFIIH, disrupts interactions with Mediator and permits TSS clearance. While clearing the TSS, DSIF docks Pol II. ***(B)*** Upon TSS clearance, TFIID from the PIC initiates Pol II pausing in the promoter proximal region. DSIF acts as a docking site for NELF, and together DSIF and NELF stabilize the paused Pol II complex. ***(C)*** Paused Pol II is susceptible to some escape from the paused complex. When pTEFb binds the paused Pol II complex, it phosphorylates DSIF (orange) and prompts dissociation of NELF. This permits Pol II escape from the promoter proximal region and vastly increases gene expression. pTEFb remains associated with Pol II and phosphorylates Ser2 of the CTD heptad repeat to stabilize elongating Pol II.

integrate regulatory signals (99) while preventing nucleosome encroaching and subsequent gene silencing (103), and this maintains genes poised for rapid gene expression. When accessory factors NELF and DSIF associate with promoter proximal paused Pol II, it further stabilizes and extends paused Pol II duration (93, 99, 104). While DSIF and NELF stabilize promoter proximal Pol II pausing, these factors are not always present at the pause site (105), which suggests promoter proximal Pol II pausing may be influenced by additional regulatory proteins.

Studies which have rendered the NELF complex non-functional report a high turnover of Pol II (99, 106), but the specific effects on Pol II distribution remain enigmatic. In some instances, ablated NELF produces lower Pol II abundance in the promoter proximal region without affecting Pol II abundance in the gene body, consistent with Pol II termination near the transcription start site (89, 103, 107, 108). In other instances, a loss of functional NELF causes upregulated expression of specific target genes (92), which suggests processive elongation of Pol II upon a loss in function of NELF. Collectively, this supports dual roles for NELF-mediated Pol II pausing which acts as a type of rate-limiting step to integrate regulatory signals to influence Pol II activity and downstream gene expression.

1.3.2 *Fate of paused Pol II stabilized by NELF and DSIF*. Advancements in sequencing resolution by transcription run-on assays have brought some insight into the fate of Pol II and gene expression at NELF-bound genes. After Pol II becomes paused at the promoter proximal region, NELF and DSIF stabilize the paused Pol II which is subject to different fates. When the integrator complex subunit 11 (Ints11) interacts with the paused Pol II, its endonuclease activity cleaves the nascent RNA

which destabilizes paused Pol II and prompts its termination (109, 110). While a low amount of Pol II does escape the pause site and enter the gene body, this state is still viewed as an overall 'off' mode, where most of the paused Pol II is subject to transcription termination (Figure 1.5). When pTEFb associates with the paused NELF-DSIF-Pol II complex, it phosphorylates DSIF and Pol II which prompts release of NELF and permits gene expression. While the integrator complex still conducts transcription termination, disengagement of NELF by pTEFb produces a vast increase in Pol II escape from the pause site, producing an upregulation in gene expression. In this state, this classifies active gene expression, which is rapidly inducible upon association of pTEFb. Thus, the function of NELF and DSIF to stabilize promoter proximal paused Pol II may act as a rate-limiting step to permit signal integration and dictate the outcome of Pol II towards either productive or abortive transcription. While some Pol II escapes pausing towards active elongation for low-level expression, most Pol II succumbs to abortive transcription by the integrator complex. This may be avoided upon association of pTEFb, which permits release of the poised Pol II prior

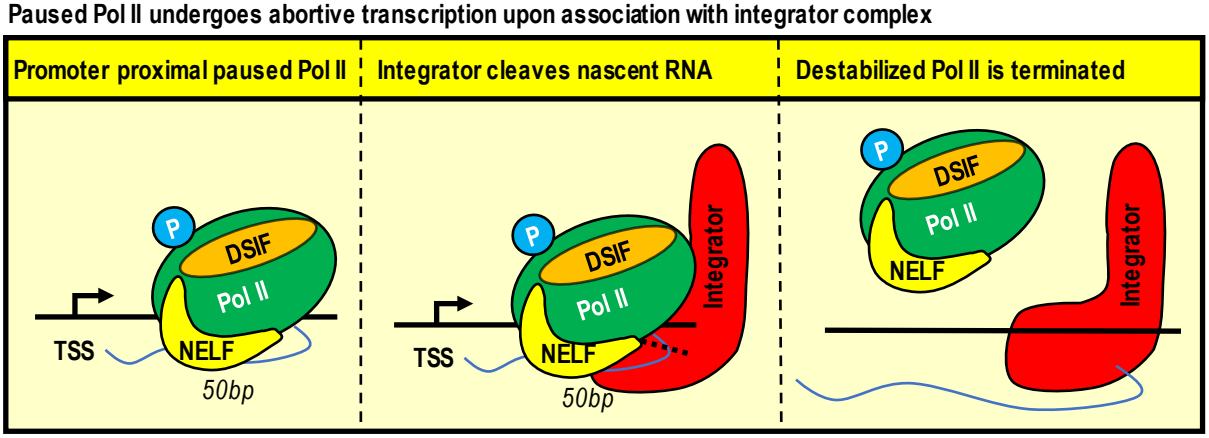

Figure 1.5 – Promoter-proximal paused Pol II is susceptible to abortive transcription by the integrator complex. When the integrator complex binds promoter proximal paused Pol II, its endonuclease activity cleaves the nascent RNA transcript. This destabilizes the paused Pol II complex, which undergoes abortive transcription.

to the integrator complex being recruited to produce an elevated level of gene expression. Thus, the fate of promoter proximal paused Pol II appears to be a competition between the integrator complex to promote abortive transcription, and pTEFb to promote active gene elongation.

1.3.3 ***The NELF complex plays an important role to regulate Pol II in rapid response genes.*** Past research efforts have identified a functional importance of NELF to control rapid changes in gene expression in response to extracellular stimulus. These responses may arise from signaling pathways which exert their effects on NELF, as is the case during estrogen signaling (111), FGF / ERK signaling (108), inflammatory response (112), and signaling by IL-6 (92). Indeed, the demonstrated ability of NELF to regulate rapid changes in gene expression are bountiful, as shown in its ability to regulate the heat shock response in *Drosophila* (113, 114), activate neuronal immediate early genes (115), and regulate cell state changes in embryonic development (116-118). Thus, this implies that the NELF complex exerts stability on Pol II poised in the promoter-proximal region to evoke changes in gene expression in response to stimulus.

Structural analysis of NELF has identified it is a heterotetrameric complex formed of four subunits known as NELFa, NELFb, NELFc/d, and NELFe and all four subunits must be present to form a functional complex (93, 119) (Figure 1.6A). Because all four subunits of the NELF complex are required to form an active NELF complex, eliminating any one of the subunits prevents assembly of a functional NELF complex. The assembled NELF complex forms a three-lobed structure which interact with different segments of Pol II: the NELF-AC lobe acts to dock the NELF complex

on paused Pol II, the C-B lobe does not make contact with Pol II but provides structural integrity to the NELF complex, while the B-E lobe facilitates interactions with the nascent RNA (93). In addition, two unstructured tentacle-like domains in NELF may facilitate its interactions: the NELFa tentacle supports interactions with DSIF, while the NELFe tentacle is partially supported by NELFb to form an RNA Recognition Motif (RRM), while a distal segment of this tentacle interacts with RNA (93). While the RRM of NELFe binds nascent RNA to stabilize paused Pol II, enhancer RNA produced in cis-regulatory regions may interfere with this binding and facilitate dissociation of NELF from paused Pol II to permit downstream gene expression (115).

The function of NELF to regulate gene expression has garnered interest to understand regulatory mechanisms which may contribute to its recruitment and function. This first requires the Spt5 subunit of DSIF to bind Pol II near the RNA exit channel (105, 120), which creates a docking site to recruit NELF (89, 99). Once recruited, NELF and DSIF bind opposing sides of Pol II and interact with each other

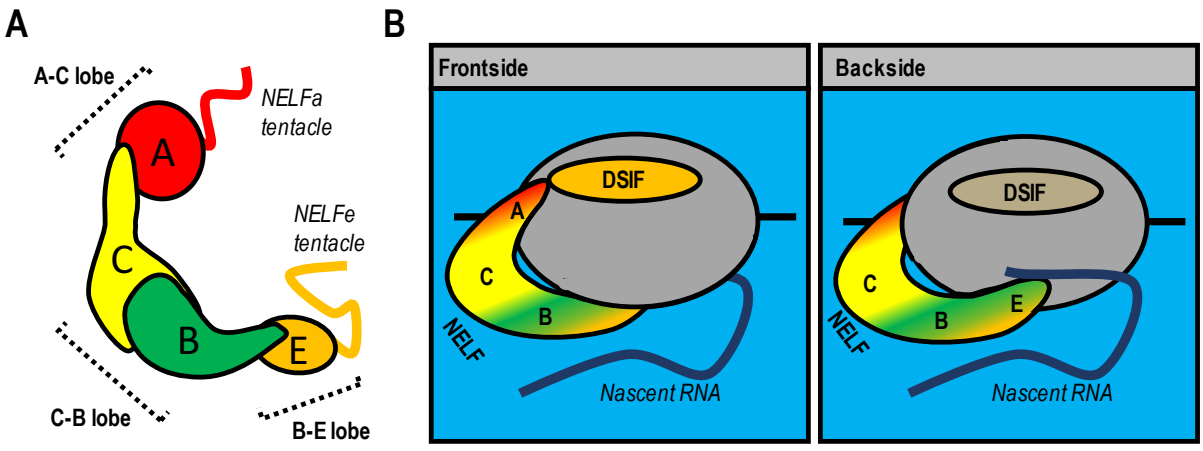

Figure 1.6 – Quaternary structure of NELF and the paused Pol II–DSIF–NELF. (*A*) The four NELF subunits, NELF(a, b, c/d, and e), organize in a linear fashion to form a three-lobed structure with two unstructured tentacle-like domains. ***(B)*** NELF binds Pol II with the AC-lobe, interacts with DSIF through the NELFa tentacle, and interacts with nascent RNA emerging from Pol II with its RRM and NELFe tentacle.

through unstructured tentacle-like domains which act as a clamp to help stabilize paused Pol II (93) (Figure 1.6B). While the nascent RNA transcript binds the NELFe RRM, secondary RNA structure does not contribute to the recruitment or stability of NELF at paused Pol II sites (80, 93, 121). In addition, the DNA sequence may participate in the precise location of Pol II pausing which remains variable but typically resides between 20 – 60 nucleotides downstream of the transcription start site. Here, a sequence-dictated G quadruplex may contribute to slowing of the Pol II during early transcription, which in turn facilitates pausing initiated by TFIID (91, 122, 123).

1.3.4 *Pol II activity is disrupted upon a non-functional NELF*. Studies focused on the functional role of NELF have often relied on preventing the expression of a NELF subunit (124), or rapidly degrading one of the NELF subunits (125). In either case, the absence of any of the four subunits prevents functional assembly of the NELF complex (119), which causes dysregulated gene expression of NELF-regulated genes. Many studies suggest that a loss of NELF decreases the abundance of paused promoter proximal Pol II without affecting its distribution within the gene body, which supports Pol II termination. While this causes an increased turnover of Pol II within the promoter regions of these genes (99, 106), it also destabilizes association of general transcription factors within these promoter regions (103). This leads to nucleosome encroachment within the promoter regions (126), reduces further transcription initiation at these genes (127, 128), and leads to silenced gene expression. In addition, a loss of NELF to stabilize paused Pol II may be more susceptible to abortive transcription by the integrator complex (110) previously discussed. While this mechanism of abortive transcription is typical at paused

promoter proximal Pol II, a loss of NELF may further destabilize Pol II and make it more susceptible to integrator-mediated abortive transcription (Figure 1.7).

In other instances, a loss in function of NELF produces an upregulation of the target gene. In these instances, this suggests that NELF typically acts to withhold Pol II and inhibit gene expression. Thus, this presents dual roles for NELF to either stabilize promoter-proximal paused Pol II in support of gene expression, or to inhibit gene expression. The function of NELF in these dual roles likely arises from differences within the chromatin environment which surround the promoter-proximal region.

1.3.5 ***Paused Pol II release requires pTEFb recruitment***. As previously discussed, NELF-DSIF stabilized paused Pol II is extremely stable and prone to retain Pol II in the poised state for an extended period. Indeed, this paused complex is only released once pTEFb associates with the paused complex and phosphorylates NELF, DSIF, and Pol II (89, 99, 129), which prompts dissociation of NELF, and permits Pol II to immediately proceed into processive elongation.

Regulatory activity of pTEFb to initiate release of paused Pol II is susceptible to many levels of regulation. This is dictated within the molecular composition of Cdk9 and the cyclin subunit with which it associates to form pTEFb. Here, residue T186 of Cdk9 must be phosphorylated to activate its kinase domain (130). This occurs primarily by Cdk7 or Brd4, but may also occur from auto-phosphorylation (131). Once activated, Cdk9 associates with a cyclin to form functional pTEFb. Here, Cdk9 associates with either Cyclin T1, T2a, T2b, or K, which depends largely on tissue-mediated cyclin availability (132). Once activated, pTEFb is rapidly sequestered by a

large inactivation complex formed of Hexim1/2, 7SK snRNA, LARP7, and MeCPE, which prevents its ability to phosphorylate any of its target proteins such as NELF (133). Thus, a release of pTEFb from the sequestered complex is required for it to associate with the super elongation complex or transcription factors to localize it to promoter proximal paused Pol II and initiate gene expression (134).

1.3.6 *Regulatory function of pTEFb.* The molecular activity of Cdk9 distinguishes it from other members of the cyclin dependent kinase family. Here, expression levels of Cdk9 tend to be reliant on tissue type (135) rather than cell cycle stage (136). In addition, mild increases in available pTEFb are speculated to induce large-scale dissociation of NELF to elicit rapid changes in gene regulatory networks. Indeed, prior investigations have identified that MyoD localizes pTEFb to specific gene loci to permit terminal differentiation of C2C12 myoblasts(132, 137) and a concomitant loss in function of pTEFb prevents formation of myotubes (137). While pTEFb may have over 100 protein targets besides DSIF and Pol II (138), it is highly regulated

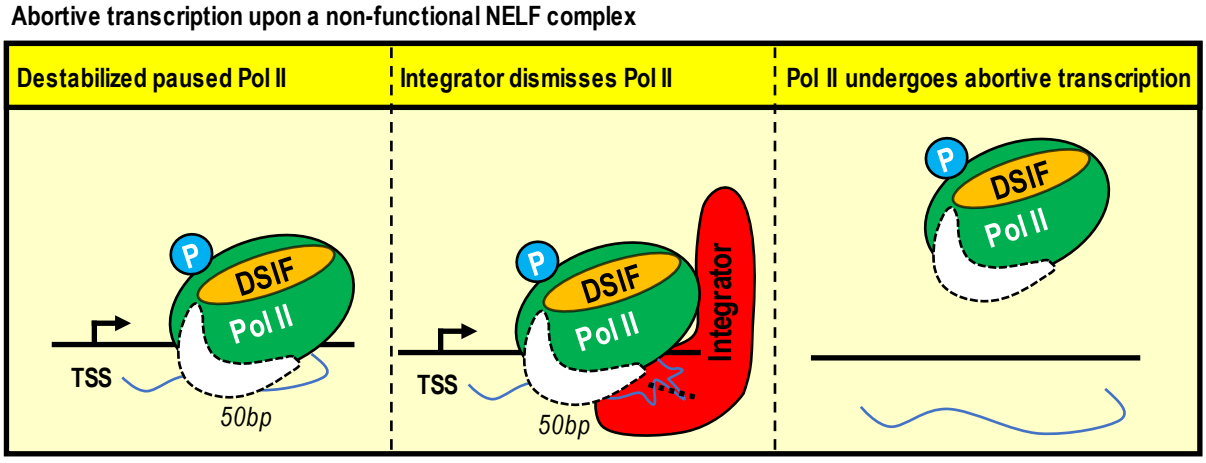

Figure 1.7 – Abortive transcription upon a non-functional NELF complex. In response to a non-functional NELF complex, paused Pol II is destabilized and prone to abortive transcription by the Integrator complex. This causes a reduced abundance of paused Pol II in the promoter proximal region, and reduced expression of the gene.

which may be of critical importance to control gene expression of NELF bound genes. Interestingly, when either NELF or DSIF are depleted, transcription occurs independently of pTEFb (104, 139, 140), which demonstrates a type of gene-regulatory axis which is capable to elicit rapid control of changes in gene activity. In addition,

1.4 Objectives and research questions

1.4.1 *Rationnale and Hypothesis.*

The prevalence of Pol II promoter proximal pausing amongst higher eukaryotes suggests this is a critical regulatory step in gene expression programs. When Pol II is paused in the promoter proximal region, its fate is strongly influenced by factors which support either abortive transcription or active elongation, and the ability of NELF to stabilize Pol II to permit signal integration is critical in the outcome of Pol II activity. Despite the prevalence of Pol II pausing in higher eukaryotes (87) and the role for NELF to regulate its activity, there remains little known about the specific role of NELF in controlling gene expression to mediate cellular activity during homeostasis and regenerative processes in adult somatic cells. One suitable model system to investigate this role is MuSC-mediated skeletal muscle regeneration owing to the system's regenerative capacity and the reported presence of NELF subunits within skeletal muscle (119). In addition, myogenic cell state changes during skeletal muscle regeneration are known to undergo rapid changes to their transcriptome which are highly responsive to the extracellular environment. Combined, this leads to speculate that the function of NELF to retain poised Pol II at

specific target genes permits the rapid changes in gene expression networks to permit myogenic cell state changes during myogenesis.

It is my hypothesis that the NELF complex stabilizes paused Pol II in the promoter-proximal region, so that Pol II remains in a 'poised and ready' state to permit rapid expression of specific target genes required to induce myogenic cell state changes during skeletal muscle regeneration.

1.4.2 *Research Objectives*. The first research objective explores the functional requirements of the NELF complex to regulate myogenic cell state changes during skeletal muscle regeneration. To do so, we first evaluate the effects of NELF to control C2C12 myoblast activity. These results are further translated *in vivo* using a MuSC specific NELF-b knockout mouse model alongside acute injury to skeletal muscle to study the implications of the NELF complex in myogenesis. Emphasis is placed on myogenic cell state changes to identify the influence of NELF on MuSCs as they progress from quiescent through to terminally differentiated myocytes during skeletal muscle regeneration. Collectively, this objective identifies the specific implications of NELF on Pol II activity to control myogenic cell state transitions in myogenesis.

As a second research objective, we investigate the specific molecular mechanisms regulated by NELF to control myogenic cell state transitions during skeletal muscle regeneration. This is supported by the first research objective, where investigations are focused on the disrupted myogenic cell states in response to a non-

functional NELF complex. To do so, molecular investigations using a series of deep-sequencing experiments are used to identify (I) the effect of a non-functional NELF complex on gene expression, (II) genes bound by the NELF complex, and (III) the fate of Pol II in response to a non-functional NELF complex.

As a last research objective, we investigate whether the NELF-pTEFb axis can be manipulated to control myogenic cell state changes. Emphasis is placed on the ability of a small molecular inhibitor to impede the function of the pTEFb complex, so that NELF binding is sustained at its target genes. Retained NELF binding may prevent the expression of genes required for myogenic cell state changes, and preserve myogenic cells within their current cell state. These results reveal that myogenic cell state transitions can be specifically manipulated along the NELF-pTEFb axis.

CHAPTER 2

Materials and Methods

2.1 – Animal models and subject details

Animal Models. All animal experiments were performed in accordance with the recommendations of the University of Ottawa Animal Care Facility, and the guidelines published by the Canadian Council on the Animal Care (CCAC). Experimental mice used in the study were in early adult stage (6 – 10 weeks of age), with equal repetitions performed between males and females. The exception to this falls within NSG recipient mice for animal studies, which were performed in mice 6 months of age (middle adulthood). Animal strains used for experiments are indicated in the table below. These strains were used to generate combined experimental strains, which include the $NELFb^{fl/fl}Pax7^{CreER}$, $NELFb^{fl/fl}Pax7^{CreER}TdT^{fl/fl}$, and $Pax7^{CreER}TdT^{fl/fl}$ strains described. Generating combined strains was performed through breeding of homozygous parental strains (F_0) to generate a heterozygote population (F_1), which was crossed amongst itself to generate the desired homozygous strain (F_2). Genotyping was performed throughout to assure the desired alleles were established and maintained (table 2, 3). Harem breeding in accordance with animal care protocols consisted of housing 2 females with 1 male. Mice of the same sex, from a same litter and of the same verified genotype were caged together to a maximum of 5 mice per cage, in accordance with our animal care protocols. Engraftment experiments were performed double-blinded until results were quantified and identities revealed.

Primary Cell Cultures. Primary cell cultures used for *ex vivo* experiments were derived from adult mice according to protocols described below. Experiments were performed with combined populations of male and female cells, isolated from adult mice (6- 10 weeks). Cells were cultured in a humid sterile environment at 37ºC and 5%CO_2. Cell authentication was performed by monitoring for TdT expression, and genotype verification of the adult mice prior to their use to derive cell cultures.

2.2 List of important reagents and dilutions used within experiments.

The following contains a list of important reagents which includes their supplier, original citations, and dilutions used, when applicable.

Table 1: Animal strains

Allele	**Jax strain identifier**	**Jax stock no.**	**Original Citation**
NELFb$^{fl/fl}$	C57BL/6N-*Nelfb*$^{tm1.1Ehs}$/J	033115	(124)
Pax7^{CreER}	B6.Cg-*Pax7*$^{tm1(cre/ERT2)Gaka}$/J	017763	(32)
TdTomato	B6.Cg-*Gt(ROSA)26Sor*$^{tm9(CAG-tdTomato)Hze}$/J	007909	(141)
NSG mouse	NOD.Cg-*Prkdc*^{scid} *Il2rg*^{tm1Wjl}/SzJ	005557	(142)

Table 2: Genotyping primers

Gene of interest	**Primers**	**product**
NELFb 3’	3’ Fwd : TGCCTGATGTAGGCACTAGGAGTT 3’ Rev : AAGCCAGTTCCAGGACACCCAGG	WT : 252 bp KO : 386 bp
NELFb 5’	5’ Fwd: ATGTAGGTGCTGGAACTGAACCCA 5’ Rev: TGCTGTCACACTTGGCAATGATGC	WT: 246 bp KO: 373 bp

TdTomato	WT Fwd: AAGGGAGCTGCAGTGGAGTA WT Rev: CCGAAAATCTGTGGGAAGTC Fl Fwd: GGCATTAAAGCAGCGTATCC Fl Rev: CTGTTCCTGTACGGCATGG	WT : 293 bp Fl : 196 bp
Pax7^{CreER}	WT Fwd : GCT GCT GTT GAT TAC CTG GC WT Rev : CTG CAC TGA GAC AGG ACC G Mut Fwd : GCT GCT GTT GAT TAC CTG GC Mut Rev : CAA AAG ACG GCA ATA TGG TG	WT: 235 bp KO: 419 bp

Table 3: Genotyping PCR parameters	
ID	**Conditions**
NELFb	**Denature** : 95°C 10:00 min **Cycling (35x) : 95°**C, 30 sec 58°C, 30 sec **72°C, 45 sec** **Hold 1**: 72°C, 10:00 min **Hold 2**: 4°C, hold
TdTomato	**Denature**: 95°C 10:00 min **Cycling 1** (10 x): **94°C 0:20 sec** **65°C 0:15 sec** **68°C, 10 sec** **Cycling 2 (28x): 94°C, 15s** **60°C, 15 s** **72°C 0:10 sec** **Hold 1**: 72°C, 10 min **Hold 2**: 4°C
Pax7^{CreER}	*Same conditions as described for the TdTomato allele, above*

Table 4: Reagents and Materials		
Reagent Name	**Catalog Number**	**Supplier**
Collagenase Type 1	C0130-1G	Sigma Aldrich
DMEM High Glucose with sodium pyruvate	SH3024301	Fisher Scientific
Ham's F10 medium	318-050-CL	Wisent Biocenter
Fibroblast Growth Factor	GF003AF-MG	Millipore Sigma
Penicilin / streptomycin antibiotic mix	450-201-EL	Wisent biocenter
Bovine Growth Serum	SH3054103	Fischer Scientific
DAKO fluorescent mounting media	S302380-2	Agilent

Mouse on mouse Ig blocking reagent	VECTMKB22131	Vector Laboratories
Dispase II	4942078001	Millipore Sigma
Matrigel	354234	Corning
Red blood cell lysis buffer	R7757	Millipore Sigma
DAPI	D9542	Millipore Sigma
Horse serum	H1138	Millipore Sigma
Insulin(bovine -10 mg/mL)	I0516	Millipore Sigma
Holo-transferrin (bovine)	T1283	Millipore Sigma
Nucleospin RNA plus XS, micro kit for RNA purification with DNA removal column	740990.50	Macherey-Nagel
2-mehtylbutane (isopentane)	320404	Millipore Sigma
Superfrost Plus microscope slides	12-550-15	FisherBrand (Fischer Scientific)
40 um cell strainer	CA21008-949	VWR
50 um cell strainer	CA21008-950	VWR
Cardiotoxin	L8102-CARDIOTOXIN	Latoxan
VWR Premium Frozen Section Compound	95057-838	VWR
PureLink RNA Mini Kit	12183020	Thermo Fischer Scientific
EdU	Ab146186	Abcam
Click-it™ EdU Cell Proliferation kit for imaging, Alexa Fluor™ 488 dye	C10337	Thermo Fischer Scientific
KAPA stranded mRNA sequencing kit	07962169001	Roche
Captisol™	RC-0C7-100	Ligand Technology
Recombinant Human PEDF Protein	Ab56289	Abcam
Pifithrin-alpha	P4359-5mg	Millipore Sigma
FAM-Flica Poly Caspase Kit	ICT091	Bio-Rad Antibodies
Digitonin	D151-500mg	Millipore Sigma
Concanavalin A-coated magnetic beads	BP531-10mL	Bangs Laboratories

Table 5: Antibodies and dilutions			
Antibody name	**Dilution**	**Catalog number**	**Supplier**
Pax7 hybridoma (culture supernatant)	1:4	Pax7	DSHB
Myogenin (F5D)	1:100	sc-12732	Santa Cruz Biotechnology
NELF-E (F9) (Monoclonal)	1:1000	Sc-377052	Santa Cruz Biotechnology
NELF-E (Polyclonal)	1:1000	10705-1-AP	ProteinTech
Alpha-integrin 7 (R2F2 clone)	1:1000	67-0010-05	UBC Antibody Lab (AbLab)
NELF-B (Cobra1)	1:1000	14894S	Cell Signal Technology
Rabbitα-Tubulin	1:1000	2125S	Cell Signal Technology
Calcitonin Receptor (CalcR)	1:1000	Ab11042	Abcam
Ki67	1:1000	Ab15580	Abcam
Histone H3K4me3		07-473	Millipore Sigma
Wheat Germ Agglutinin (WGA) Texax Red Conjugate	1:1000	W21405	Thermo Fisher Scientific
Wheat Germ Agglutinin (WGA) Alexa 488 Conjugate	1:1000	W11261	Thermo Fisher Scientific
Goat anti-Mouse IgG (H&L) cross-adsorbed secondary antibody, Alexa Fluor 647	1:1000	A21235	Thermo Fisher Scientific
Goat anti-Mouse IgG (H&L) cross-adsorbed secondary antibody, Alexa Fluor 546	1:1000	A11030	Thermo Fisher Scientific
Goat anti-Mouse IgG (H&L) cross-adsorbed secondary antibody, Alexa Fluor 488	1:1000	A11001	Thermo Fisher Scientific

Goat anti-Rabbit IgG (H&L) cross-adsorbed secondary antibody, Alexa Fluor 647	1:1000	A21244	Thermo Fisher Scientific
Goat anti-Rabbit IgG (H&L) cross-adsorbed secondary antibody, Alexa Fluor 546	1:1000	A11010	Thermo Fisher Scientific
Goat anti-Rabbit IgG (H&L) cross-adsorbed secondary antibody, Alexa Fluor 488	1:1000	A11034	Thermo Fisher Scientific

Table 6: Commercial plasmids used			
Plasmid ID	**Plasmid No.**	**Supplier**	**Original plasmid use citation**
pLKO.1 luciferase shRNA	30324	Addgene	(143)
pMD2.g	12259	Addgene	This plasmid was a gift from the Didier Trono lab (unpublished)
psPAX2	12260	Addgene	This plasmid was a gift from the Didier Trono lab (unpublished)

Table 7. shRNA constructs cloned in pLKO.1 plasmids		
Identifier	**Target Sequence (5' → 3')**	**mRNA target region**
shLuciferase	CGATATGGGCTGAATACAAAT	CDS
shNELFb-1	CCAAGGTGCATGGGACTTAAT	CDS
shNELFb-2	CCTGGACTTGTGGAAACGTTT	CDS
shNELFb-3	CCTGATATTCAATCTGCACAA	3UTR
shNELFb-4	GAGGCAGATTTGGCAAGACAA	CDS
shNELFb-5	CCTGAGAGTTTCACCAAGTTT	CDS

2.3 Detailed experimental methods.

2.3.1 *Phenotypic methods*

In vivo Muscle Regeneration**.** Animals were subject to four intraperitoneal (IP) tamoxifen injection (100 µL at 10 mg/mL in corn oil) at 24h intervals followed by a 72h recovery period. Mice were anesthetized with isoflurane (2% in oxygen), and skeletal muscle damaged through intra-muscular injection of cardiotoxin (10 µM in saline, 50 µL per muscle group) in the designated muscle group (TA, EDL, gastrocnemius, bicep posterior). Buprenorphine was concurrently administered (0.1 mg/kg) for pain management. Muscle regeneration periods were provided to experiment-specific endpoint. Re-injury experiments were performed through repeating the above steps at the specified time point. Upon experimental endpoint, mice were euthanized with CO_2 asphyxiation and cervical dislocation.

In vivo EdU pulse. *In vivo* EdU pulse experiments were adapted from (144). First, EdU was dissolved in sterile saline (10 mg/mL) and administered to mice by IP-injection (100 µL) at an experiment-specified timepoint. For EdU labeling of actively dividing cells using FACS analysis, *in vivo* EdU was administered at either 28 hours post-injury (hpi) followed with a 12h incubation to label activating satellite cells, or at 66 hpi followed with a 6h incubation to label actively dividing myogenic precursors. For Edu pulse-label on regenerating skeletal muscle, EdU was administered with a single IP-injection at 48 hpi or 72 hpi, and allowed to regenerate for 7days post-injury (dpi).

Muscle perfusion. To maintain the TdTomato fluorescence signal, mice were perfused prior to muscle processing. For this, mice were euthanized with sodium pentobarbital (200 mg/Kg bodyweight) without cervical dislocation. Once no reflex could be detected, mice were exsanguinated by cardiac perfusion with 25 mL chilled PBS, then 50 mL chilled PFA (4% w/V, 4°C), both delivered at a flow rate of 5 mL/min. Harvested TA muscle was post-fixed in 4% PFA (w/V) overnight (4°C) followed by overnight incubation at 4°C over a two-layer sucrose gradient (15% w/V layered on 30% w/V sucrose in PBS). Muscle was embedded in Frozen Section Compound, and frozen in isopentane cooled in liquid-nitrogen.

Isolation of Tibialis Anterior muscle. Isolation of TA muscle was modified from (145). Upon experimental endpoint, mice were euthanized as described above, and TA muscles harvested from the hindlimbs, submerged in a tinfoil cup containing Frozen Section Compound, then frozen in isopentane cooled in liquid nitrogen. For long-term storage, muscle was stored at -80°C. Skeletal muscle was processed by sectioning on a cryostat cooled to -20°C until the widest segment of the muscle was reached. From there, muscle was sectioned at 10 μm thickness and sections collected on positively-charged microscope slides. Slides were either immediately processed or placed at -80°C for long-term storage.

In vivo Rescue of Regeneration with pifithrin-α and PEDF. Mice were induced with tamoxifen to induce Cre-mediated recombination prior to cardiotoxin injury of the TA muscle as described above. For pifithirin-α treatment, at 40h, 64h, and 88 hpi, mice were administered an intraperitoneal injection of either the p53

inhibitor pifithrin-α (0.04mg dissolved in 50 µL of 20% captisol/saline solution (v/v)) or an untreated control (50 µL of 20% captisol/saline solution (v/v)). For PEDF treated populations, PEDF peptide was reconstituted in DMSO (5mM) then dilute in a 2% sodium alginate gel to a final concentration of 50 µM. This was provided as an intramuscular injection at 24hpi and 48hpi, while control populations received a vehicle control of 2% alginate solution. In all experiments, mice were sacrificed at 7-days post cardiotoxin-injury to assess regeneration of the TA as described above.

Single Myofiber Isolation. Single myofiber isolation from Extensor Digitorum Longus (EDL) muscle was performed using established protocols (146). EDL muscles were carefully harvested from a euthanized mouse and immediately placed in sterile PBS pre-warmed to 37°C. Paired EDL muscles from each mouse were processed together. EDLs were washed twice in pre-warmed PBS, then placed in digestion medium (2 mg/mL Collagenase Type 1 in DMEM high-glucose with sodium pyruvate). EDLs were gently swirled at 15 min intervals for 1.5h, then the digestion quenched through addition of primary growth medium (Ham's F10 medium, 20% Bovine Growth Serum, 1% pen/strep, Fibroblast Growth Factor 2.5 ng/µL). Fibers were allowed to settle at the bottom of the plate (5 min), and the medium replaced with fresh primary growth medium. Primary growth medium was changed at 24h intervals up to the endpoint of the fiber culture. For EdU-pulsed experiments, one volume of 2X EdU solution (20 µM in primary growth medium) was added to one volume of fibers in growth medium, and incubated (37°C, 5% CO_2) for 6h. Upon culturing endpoint, fibers were fixed (4%PFA, 20 min, RT) and stored in PBS for further immunofluorescent staining.

Primary myoblast isolation. Primary myoblast isolation was carried out as described in (147). First, skeletal muscle was dissected from hindlimbs of euthanized mice (TA, EDL, quadriceps, gastrocnemius, bicep posterior) and adipose tissue and tendons trimmed away. Skeletal muscle was minced with dissection scissors to small pieces (approx. 1 mm^3), then washed twice in PBS. Muscle was enzymatically digested in digestion medium (1 mg/mL Type 1 collagenase, 1 U/mL Dispase II in Ham's F10 medium, no serum) for 1h with gentle swirling at 15 min intervals (37°C, 5%CO_2). On ice, digested muscle tissue was suspended in two volumes of chilled PBS, passed through a 40 µm strainer, and the mononuclear cells were recovered as a pellet by centrifugation (150 x g, 10 min, 4°C). For cell culturing, cells were pre-plated on an uncoated tissue culture dish for 3h, then the supernatant collected and plated on a Matrigel coated dish (20 µL Matrigel resuspended in 1 mL DMEM High-glucose medium, swirled on a 10 cm dish, and allowed to solidify for 1h at 37°C°, 5% CO_2). For FACS sorting of MuSCs, cell pellets were resuspended in 350 µL Red Blood Cell lysis solution, then immediately resuspended in 10 mL FACS buffer (10% Bovine Growth serum in PBS, 3mM EDTA), and pelleted (350 x g, 4°C, 10 min). Cell pellets were resuspended in 1 mL FACS buffer, incubated with 647nm-fluorophore tagged alpha-integrin 7 (20 min, 4°C), washed, and exposed to Sytox 488 cell viability dye, then passed through a 50 µm cell strainer. Cells were stored on ice in a polystyrene tube while awaiting FACS sorting.

C2C12 cell culture. Immortalized C2C12 mouse myoblasts (CRL-1772, ATCC) were cultured as previously described (148)(149). Propagation was performed

at low confluence in growth medium (10% bovine growth serum, 1% pen/strep in DMEM high-glucose with sodium pyruvate) to retain cellular proliferation. To induce terminal differentiation, cells were replated at high-confluence on either uncoated or Matrigel-coated cell culture plates in differentiation medium (2% horse serum, 0.1% insulin, 0.1% transferrin, 1% pen/strep in DMEM high-glucose with sodium pyruvate) and were undisturbed for 48h – 72h.

Lentivirus production. Lentivirus was prepared according to previously established protocols (143). To do so, HEK 293T cells were cultured to 70% confluence and provided fresh growth medium. For each lentiviral preparation, pMD2.G (5.93 µg), psPAX2 (14.88 µg), and the pLKO.1-puro plasmid containing the shRNA construct (19.90 µg) were mixed in a conical tube, and the volume brought to 447.2 µL with sterilized distilled water. Dropwise, 48.8 µL of $CaCl_2$ (2.5M) solution was added to the plasmid mixtures, and provided a 5 min incubation. Afterwards, 496 uL of 2X HBS solution solution was added dropwise to the preceding plasmid mixture with continued vortexing throughout, and provided a 25 min incubation period. This solution was administered dropwise over HEK 293T cells (70% confluence in 10cm culture dish with primary growth medium), provided a 15h incubation period (37°C, 5%CO_2, with humidity) to permit transfection, then the growth medium refreshed. The growth medium was collected at 24 h, replaced with fresh growth medium, then collected again 48h later. The growth medium aliquots collected from both 24h and 48h incubations for a same transfection were pooled, centrifuged to remove cell debris (4,000xg, 10 min, RT), and stored in 5mL aliquots (-80°C). This unconcentrated medium contained the lentivirus for subsequent transductions.

C2C12 transductions. To initiate transductions, cultured C2C12 myoblasts (40% confluence, 10cm culture dish) received fresh growth medium (5mL), and exposed to an equal volume of unconcentrated lentivirus prepared above (dropwise). Subsequent to a 30h incubation, C2C12 myoblasts underwent positive puromycin selection (2 μg/mL) over 72h to eliminate non-transduced cells. The remaining viable cell populations were assessed for successful transduction by western blot analysis, focusing on the mRNA protein product which was targeted by the shRNA constructs.

Differentiation of cultured myoblasts. Primary myoblasts were expanded while maintaining low cell confluence to avoid cell-cell contact on Matrigel-coated dish. Upon sufficient population expansion, myoblasts were trypsinized, resuspended in primary growth medium, and the cell concentration quantified using a Countess^{TM} II Automated Cell Counter. Cells were plated on a Matrigel-coated dish at a density of 650 cells / mm^2 (650,000 cells per well in a 6-well dish), allowed to adhere for 1h, then changed to a low-serum differentiation medium (2% horse serum, 0.1% insulin, 0.1% transferrin, 1% pen/strep in DMEM high-glucose with sodium pyruvate). Differentiation was allowed to proceed for 48h (37°C, 5% CO_2) without any changes to the medium.

NSG mouse engraftment preparation. Allograft transplantation experiments were performed according to previously established protocols (150) with minor modifications. NSG mice were first anesthetized with isoflurane (2% in oxygen),

then the endogenous MuSC populations in the hindlimbs were incapacitated with 8 Gy irradiation, delivered at 0.89 Gy/min (X-rad 320, Precision X-ray), while the rest of the body was protected with a lead shield. If damaged TA muscle was experimentally required, cardiotoxin (50 µL, 10 µM) was immediately administered to both TAs of the NSG recipient mice, with buprenorphine (0.1 mg/Kg bodyweight) for pain management. Mice were provided a 48h recovery period, then each TA was injected with 12,000 MuSCs derived from either WT or NELFb^{scKO} donor mice. A 21-day regeneration period was provided, then mice euthanized and perfused as previously described.

Primary myoblast drug treatments. Primary myoblasts isolated from NELFb^{scKO} or wildtype mice were plated at low confluence in Matrigel-coated 12-well plates. Primary growth medium was refreshed with primary growth medium containing either pifithrin-α (27 µM), or untreated primary growth medium, and provided a 4h incubation period. Subsequently, 1 volume of untreated primary growth medium, or primary growth medium containing the same concentrations of PEDF and pifithrin-α as previously described was spiked with EdU (20 µM) and added to the corresponding wells for a 4h incubation period. Myoblasts were fixed with PFA (4% (w/v) in PBS) and treated for subsequent immunofluorescent characterization (see '*immunofluorescent staining of cell cultures'*, below).

Apoptosis screening assay. Primary myoblasts were isolated and expanded in culture as previously described. Apoptosis screening was performed using an activated capsase screening kit, following the manufacturer's protocol (FAM-

FLICA poly caspase kit, Bio-Rad Antibodies, ICT091). A positive control was prepared alongside experimental samples by adding staurosporine (5 µM in DMSO) for 3h to the culture medium of WT myoblasts.

2.3.2 *Immunofluorescent Characterization.*

Myofiber Immunofluorescent staining. Isolation of myofibers was performed according to protocols described in (146). Fixed fibers were permeabilized (5% Triton X-100 vol/vol in 100 mM glycine in TBS), reacted with EdU Click-It chemistry according to manufacturer protocol, pre-blocked in Goat anti-mouse IgG (100 µg/mL in TBS), then blocked for 1h (5% goat serum, 2% BSA in TBST). Fibers were subsequently incubated with primary antibody (overnight, 4°C) according to the specified dilution (Table 5), then with secondary antibody dilute in TBST, counterstained with DAPI (0.2 mg/mL in PBS), and mounted with fluorescent mounting media. Immunofluorescence images were captured using a Zeiss Z1 inverted epifluorescent microscope.

Immunofluorescent staining of muscle cross-sections. Slides containing muscle cross-sections were thawed to room temperature, washed (PBS), then fixed with PFA (4% w/v, 10 min). Antigen retrieval was performed (heat-induced epitope retrieval, 98°C°, 10 min), then slides moved to PBS (RT), and permeabilized (0.5% Triton X-100 V/V, 100mM glycine, in TBS) for 10 min. An optional EdU Click-it reaction was performed at this step according to the manufacturer protocol, then tissues washed (TBS), and blocked (1h, RT, 5% Goat serum V/V, 2% BSA w/V in TBST with 1:40 Mouse-on-mouse Ig blocking reagent). Samples were incubated with

primary antibody (4°C, overnight), washed (TBS), and secondary antibody dilute in TBST was added (1h, RT). DAPI counterstaining followed (0.2 mg/mL in TBS), and mounted with fluorescent mounting media. Where applicable, the TdTomato fluorescence signal was preserved through PFA perfusion (described above) and did not require any signal rescue. Immunofluorescence images were captured using a Zeiss Z1 inverted epifluorescent microscope.

Immunofluorescent staining of cell cultures. Cell cultures (primary myoblasts, C2C12) were fixed in PFA (4% w/V, 10 min, RT), washed (PBS), then permeabilized (5% Triton X-100 vol/vol, 100 mM glycine, 20 min, RT). If cells were pre-incubated with EdU, the EdU Click-It reaction was performed according to the manufacturer's protocol; otherwise, this step was omitted. Cells were blocked with blocking buffer (5% goat serum V/V, 2% BSA w/V, in TBST) for 1h, then incubated with primary antibody diluted in blocking buffer (4°C, overnight) according to the dilution in Table 5. Cells were washed (TBS), incubated with secondary antibody dilute in TBS (1h, RT), counterstained with DAPI, and resuspended in TBS. Cells maintained in culture dish during staining were covered with PBS and immediately imaged. Immunofluorescence images were captured using a Zeiss Z1 inverted epifluorescent microscope.

Real-time quantitative PCR. A subset population of FACS isolated MuSCs derived from the donor mice for engraftment experiments was set aside, and RNA isolated using a NucleoSpin RNA Plus XS micro kit for RNA purification kit (Macherey-Nagel) according to the manufacturer protocol. Reverse transcription was

performed to generate a cDNA library using random primers. Quantitative PCR was performed using Taqman gene expression assays according to the manufacturer protocol.

2.4. Sample preparation for deep-sequencing analysis

Single-cell RNA sequencing. Sample preparation for single-cell RNA sequencing were modified from protocols described in (151). Regenerating TdT^+ cells were isolated from mice at 72 hpi and purified by FACS as described above. TdT^+ cells were concentrated to approximately 600 cells / µL, and their concentrations verified by quantification on a hemocytometer. Cell viability was monitored to assure viability remained above 85%, then 2,000 cells were prepared for each sample according to the 10X platform manufacturing guidelines. Once complete, samples were sequenced on an Illumina NextSeq 500 Platform with a read depth of 50,000 reads per cell.

RNA-sequencing. TdT+ myogenic cells for *in vivo* RNA-seq regeneration studies were isolated and purified from mice at either 48 hpi or 120 hpi as described above. RNA was collected using a PureLink RNA mini kit according to the manufacturer's protocol. Total RNA (340 ng) underwent rRNA depletion, and cDNA library prepared using a KAPA stranded mRNA sequencing kit according to the manufacturer protocol. Sequencing was performed on an Illumina HiSeq 2500 platform.

Precision Run-On Sequencing. MuSCs were isolated from NELFb^{scKO} and WT mice as described above for primary myoblast culturing techniques. After 48h of colony expansion, myoblasts were exposed to 4-hydroxytamoxifen (5 µM in primary growth medium) for 72h, refreshing the primary growth medium and 4-OHT at 24h intervals. Primary myoblasts were maintained at low confluence to avoid cell-cell contacts. Cell permeabilization was performed as follows. Primary myoblasts were detached with trypsin, collected in chilled (4°C) PBS with 10% BGS, and immediately quantified. Using 10x10^6 cells per replicate, myoblasts were centrifuged (150 x g, 10 min, 4°C), resuspended in wash buffer (10 mM Tris-HCl pH 8, 10 mM KCl, 250 mM sucrose, 5 mM $MgCl_2$, 0.5 mM DTT, 10% glycerol), and passed through a 40 µm strainer. Samples were permeabilized with permeabilization buffer (wash buffer supplemented with 0.1% Igepal) for 90s on a nutator, then immediately centrifuged (100 x g, 5min, 4°C). Permeabilized myoblasts were resuspended in freezing buffer (50 mM Tris HCl pH 8.3, 40% glycerol, 5 mM $MgCl_2$, 0.5 mM DTT) to a final concentration of 10 x 10^6 cells / mL. Nuclear run-on was performed according to the run-on assay described in (152).

Genome-wide localization using CUT&Tag. Cleavage Under Target and Tagmentation (CUT & Tag) was performed as originally described in the protocols (153-155). Briefly, primary myoblasts were exposed to 4-hydroxytamoxifen (5 µM in primary growth medium) for 72h, refreshing the primary growth medium and 4-OHT at 24h intervals. Recovered myoblasts were then immobilized on Concanavalin A-coated paramagnetic beads and permeabilized with digitonin. Cells were incubated overnight with the corresponding antibodies: Nelf-E (Proteintech, Cat#10705-1-AP +

Nelf-E(F-9) Santacruz, Cat#SC – 377052, mixed 1:1 ratio); RNAPII S5P (D9N5I - Cell Signaling Cat #13523); and H3K4me3 (EMD Millipore, Cat# 07-473). Tethered cells were washed thoroughly to remove unbound antibody, and then with pA-Tn5 for 60 min. Tn5 transposase mediated tagmentation was then initiated by the addition of $MgCl_2$. Cellular DNA was extracted using Phenol/Chloroform/Isoamyl alcohol and then precipitated. Tagmented DNA libraries were generated as previously described (153, 154) and sequenced on an Illumina HiSeq 2500 platform.

2.5 Deep-sequencing analysis

No new code was generated for sequencing dataset analysis. All code used was obtained from previously published peer-reviewed journals indicated below.

Single-cell RNA sequencing. Single-cell RNA-sequencing data was analyzed on the 10X cellranger platform using v2.1.1 to generate a gene expression matrix. This was analyzed using Seurat V3.0 (156, 157) to remove non-myogenic populations and perform clustering occupancy analysis. Myogenic populations were identified and exported for further analysis using PAGA (partition-based graph abstraction) on Scanpy v1.4. Various trajectories were constructed using ForceAtlas2 embedding as previously described (158)

RNA-sequencing Analysis. RNA-seq reads were aligned using STAR v2.6.0a, counts summarized using FeatureCounts v1.6.1, and differential gene expression identified with DESeq2 v1.26.0. Significant genes were identified with a p-value cutoff

< 0.01. DotPlots were constructed using ggplot2, and Volcano Plots with EnhancedVolcano functions on R version 3.6.3. In all instances, gene ontology analysis was performed using DAVID 6.8 (159, 160), and values represented as DotPlots.

CUT&Tag Analysis. High-throughput sequencing of CUT&Tag samples were processed by first trimming adapters from raw reads with Cutadapt 2.6 (161). The trimmed reads were aligned to the mouse genome (mm10) with Bowtie2 (v2.3.4.1) using the following parameters "*—local --very-sensitive-local --no-unal --no-mixed --no-discordant --phred33 -I 10 -X 700*" (162). Samtools v1.10 was used for post-alignment processing i.e. duplicates were marked and removed; non-uniquely aligned reads were filtered and only reads mapped in proper pairs were retained for analysis.

Spike-in normalized genomic coverage was calculated using bamCoverage (deeptools v3.3.2) (163). For the normalization, trimmed reads were aligned to spike-in DNA with Bowtie2 (v2.3.4.1) and the resulting number of total mapped fragments was used to calculate the per-sample scaling factors. For each sample, this was done by dividing the min(total-mapped-fragments) by the total-mapped-fragments for that sample. Additionally, bamCoverage was used to generate bigWig tracks for visualization as well as normalized bedGraphs for downstream peak-calling.

SEACR was used to call "stringent" peaks for each spike-in normalized bedgraph target file (164). In the presence of an IgG control, the control data was used to calculate the empirical thresholds and conversely, in the absence of a control, top 5% of enriched regions were selected as peaks by AUC. ENCODE Blacklist

regions (165) were filtered from peaks using BEDTools v2.27.1 (166) and nearest-gene annotations were obtained with ChIPseeker v1.24.0 (167).

Signal intensity heatmaps for the Cut&Tag libraries were generated using deeptools v3.3.2 (163). Using both normalized bigwigs and the M25 mouse gene annotation file from Gencode, ComputeMatrix was used with the *scale-regions* mode (*--beforeRegionStartLength 1000 , --regionBodyLength 5000, --afterRegionStartLength 1000*). PlotHeatmap was used with the resulting matrix to plot the signal distribution.

PRO-Sequencing Analysis. FASTQ read pairs were trimmed to 41bp per mate, and read pairs with a minimum average base quality score of 20 were retained. Read pairs were then further trimmed using cutadapt 1.14 to remove adapter sequences and low-quality 3' bases (--match-read-wildcards -m 20 -q 10).

R1 reads were then aligned to the spike genome index (dm3) using Bowtie 1.2.2 (-v 2 -p 6 --best --un) (162), with those reads not mapping to the spike genome serving as input to the reference, i.e. primary, genome alignment step (again using the same Bowtie 1.2.2 options). Reads mapping to the mm10 reference genome were then sorted, via samtools 1.3.1 (-n), and subsequently converted to bedGraph format. Because PRO-seq reveals the position of the RNA 3' end, the "+" and "-" strands were swapped to generate bedGraphs representing 3' end positions. The bedGraphs were ultimately depth-normalized only, merged within conditions, and used to generate bigWig files binned at 10bp. TSS-centric read count matrices were calculated over a window of +/- 2kb with 25bp bins.

For direct comparison to PRO-Seq data, RNA-sequencing analysis was performed on proliferating primary myoblasts. FASTQ read pairs were aligned to a GRCm38 cDNA index and quantified using kallisto 0.45.1 (-b 30 --rf-stranded --genomebam --gtf --chromosomes -t 6). Replicate samples belonging to the same condition were merged and depth-normalized, and bigWigs were then generated with 10bp binning. Differentially expressed genes were determined via a combination of tximport v1.12.3 and DESeq2 v1.24.0, using a padj < 0.01 threshold.

To integrate the differentially expressed genes, determined via RNA-seq, with the PRO-seq analyses, all wild type R2 reads (i.e. 5' end) were aligned (in the same manner as 3' end R1 reads) to identify putative transcription start sites using TSScall (https://github.com/lavenderca/TSScall, --set_read_threshold 8 --annotation_join_distance 500 --annotation_search_window 200). A single, dominant TSS was then assigned to each gene based on having the highest number of reads within a +/-150 interval relative to each called TSS. Dominant TSS-centric 3' read count matrices were then intersected with lists of up- and down-regulated gene lists from the RNA-seq analyses to visualize TSS-proximal profiles. Gene body read counts (+250-2250 relative to dominant TSS's) were similarly intersected with the RNA-seq results and statistics were computed via Wilcoxon test.

2.6 Quantification and statistical analysis

Unless stated in the figure legends, all values are reported as the mean where error bars represent SEM. Statistical significance was identified among comparisons having a p-value below 0.01 in transcriptome data. For all other experiments *p<0.05,

**p<0.01, ***p<0.001, ****p<0.0001. Statistical quantification was performed on the statistical graphing software GraphPad Prism v7.0.

CHAPTER 3

The role of NELF in myogenic cell state transitions

3.1 – The NELF complex regulates C2C12 cell state transitions.

3.1.1 ***Creating and validating NELFb targeting shRNA knockdown.*** The reported expression of NELF in skeletal muscle (119) raises an interesting possibility that NELF may participate in myogenic cell state changes during myogenesis. As a starting point, we investigated the role of NELF in the C2C12 immortalized mouse myoblast cell line (168), as they recapitulate myogenic processes of proliferation, terminal differentiation and myocyte fusion. While immortalized C2C12 myoblasts typically remain engaged in the cell cycle to undergo continued proliferation, a switch to low-serum culturing medium can be used to forcibly commit these myoblasts towards terminal differentiation, where they fuse with one another and form multinucleated and functional myotubes evidenced through their spontaneous contractions. Because C2C12 myoblasts efficiently display processes of myogenic proliferation and differentiation, they have helped identify master transcription factors of myogenesis, epigenetic modifications which govern myogenic cell state changes, and signaling pathways (169-171).

To investigate implications of NELF in C2C12 myoblasts first requires an ability to render the NELF complex non-functional. To do so, we opted to use lentiviral-mediated transduction of C2C12 myoblasts with short-hairpin RNA (shRNA) which

targets NELFb mRNA for degradation. To do so, shRNA constructs expressed in a pLKO.1 plasmid were obtained. This included five shRNA constructs which targeted either the coding sequence or the 5'UTR of NELFb mRNA, and one additional shRNA which targets luciferase mRNA (not expressed in C2C12 myoblasts). In conjunction with HEK 293 cells, we used these pLKO.1-shRNA constructs to prepare lentivirus (172), transduce C2C12 cells, and used puromycin to positively select for transduced C2C12 myoblasts (Figure S3.1). Initial western blot analysis shows transduction of C2C12 with NELFbshRNA3 (C2C12-sh3) and NELFbshRNA5 (C2C12-sh5) nearly depletes NELFb compared to the transduction control (shLuc) (Figure 3.1A). In addition, immunofluorescence of the transduced cells supports an efficient puromycin selection strategy, evidenced by a low abundance of NELFb^{+} C2C12 cells (Figure 3.1B). This supports a reliable model system capable to generate a NELFb knockdown (NELFb-KD) in the immortalized C2C12 myogenic cells.

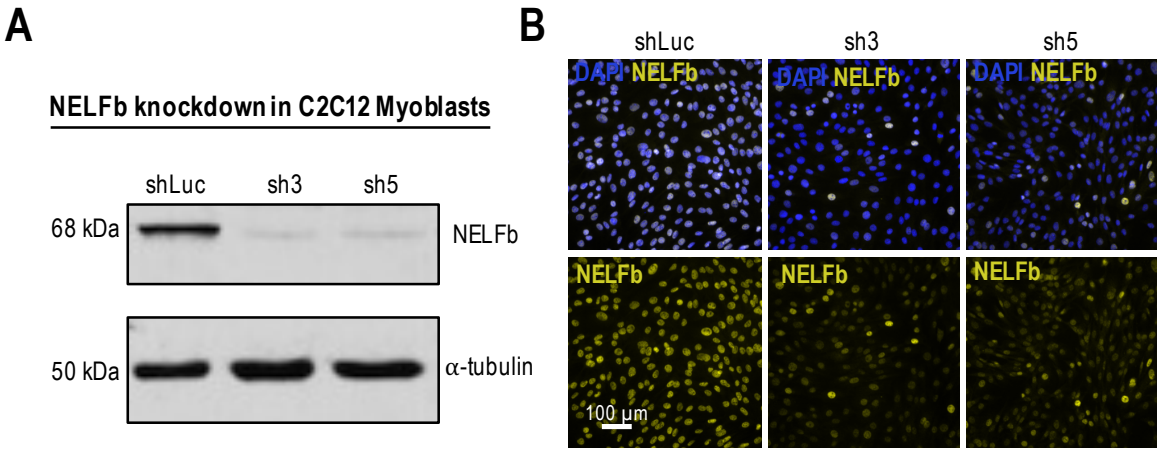

Figure 3.1 – NELFb knockdown efficacy in C2C12 myoblasts. ***(A)*** Whole cell extract western blots performed on the transduced C2C12 myoblasts show an >95% knockdown of NELFb protein in both NELFb-KD populations (sh3, sh5) when compared to control C2C12 populations transduced with luciferase targeting shRNA (shLuc). ***(B)*** Immunofluorescence for NELFb on C2C12 myoblasts fixed in culture plates shows an efficiency within puromycin selection, and reduced expression of NELFb upon transduction with NELFb targeting constructs.

3.1.2 ***C2C12 exhibit reduced proliferation upon a NELFb-KD.*** In response to a NELFb-KD, both C2C12-sh3 and C2C12-sh5 appeared to undergo a reduced expansion in their populations than the wildtype transduction control. To investigate, we performed an EdU incorporation assay to monitor for C2C12 proliferation. This revealed a twofold reduction in the abundance of EdU^+ cells in both NELFb-KD lines, namely C2C12-sh3 and C2C12-sh5, when compared to the transduction control (Figure 3.2A). In a parallel experiment, we monitored the abundance of C2C12 myoblasts over 72h to generate a growth curve. This shows a vastly reduced population expansion in both NELFb-KD lines when compared to transduction controls (Figure 3.2B). Taken together, these experiments suggest that a non-functional NELF complex produces dysfunctional C2C12 proliferation.

3.1.3 ***Myotube formation is not affected in NELFb-KD myoblasts.*** While a NELFb-KD causes an apparent defect in proliferation, we next desired to identify whether this would impair their ability to undergo terminal differentiation, fusion, and form multinucleated myotubes. To investigate, populations of C2C12 with either a NELFb-KD or control transduction were plated at high confluence and induced towards terminal differentiation with low-serum medium. Following a 72h incubation, both C2C12 NELFb-KD lines produced truncated multinucleated myotubes with an abnormal physiology when compared to the transduction controls (Figure 3.2C). While this suggests a defect inherent to terminal differentiation, both NELFb-KD lines displayed a high abundance of what appeared to be detached and contracted myotubes floating in the culture medium (not shown). This lead us to suppose that the NELFb-KD lines were capable of undergoing terminal differentiation and form

multinucleated myotubes, but could not remain adhered to the culturing plate. Thus, we pursued a similar differentiation experiment where differentiation was induced on Matrigel coated plates. Here, Matrigel provided an ECM mimick to support myotube adhesion to the plates and prevent detachment. Indeed, doing so produced multinucleated myotubes of similar morphology in the NELFb-KD and transduction control C2C12 lines (Figure 3.2D). Taken together, this shows the cellular processes

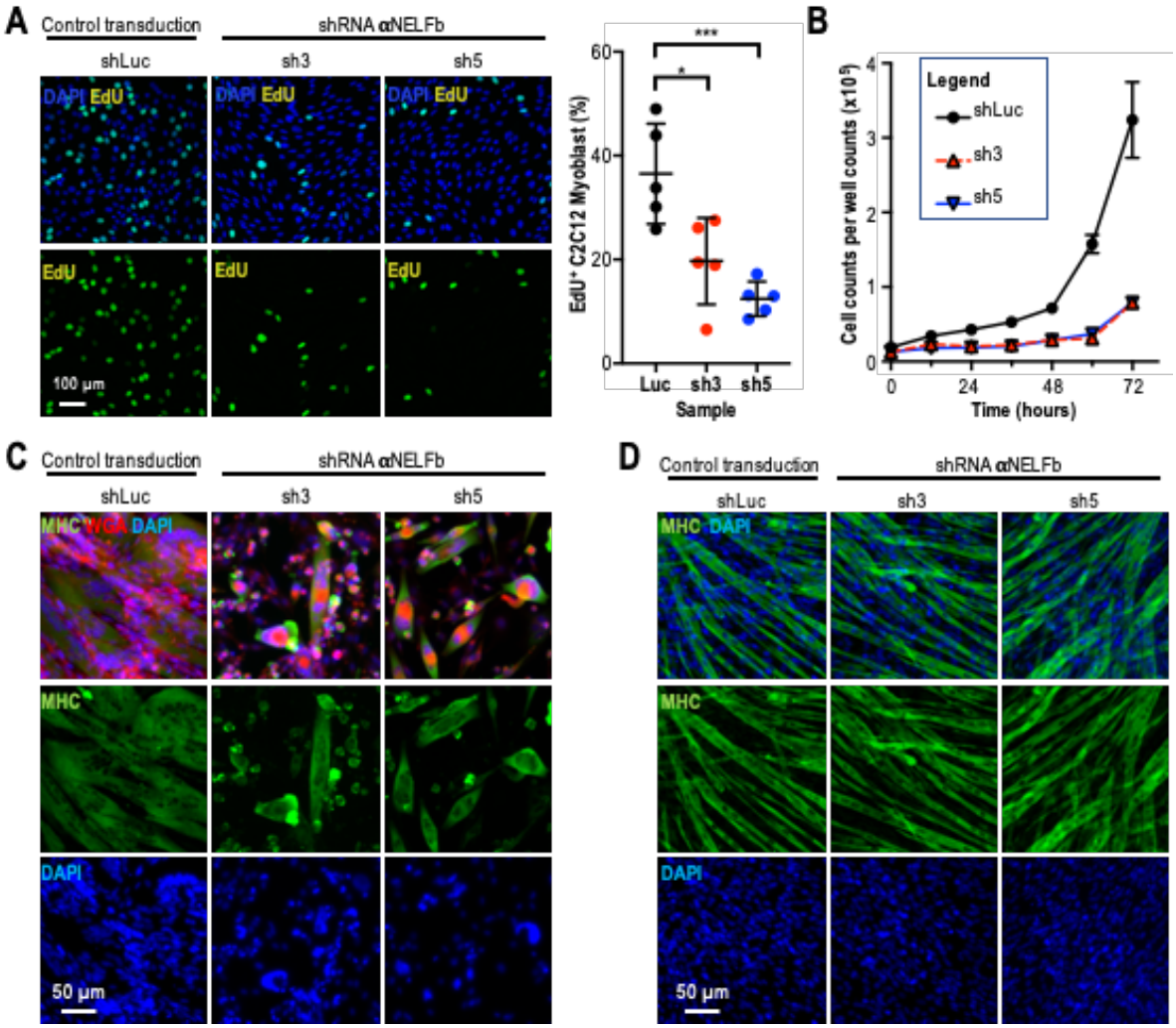

Figure 3.2 – Proliferation and differentiation assays upon a NELFb-KD. ***(A)*** Following a 4h EdU pulse, there is a significantly reduced abundance of EdU^+ populations in the NELFb-KD populations of C2C12-sh3 [19.7% ± 3.722, n=5] and C2C12-sh5 [12.43% ± 1.478, n=5] compared to the transduction control [36.52% ± 4.316, n=5]. ***(B)*** Growth curve analysis captured at 12h intervals over 72h shows a reduced expansion of NELFb-KD populations (sh3 and sh5) compared to the transduction controls. ***(C)*** Immunofluorescence staining following a 72h differentiation on uncoated culture plates for MHC (green), WGA (red), and DAPI (blue) shows truncated myotube morphology in NELFb-KD populations compared to transduction controls and ***(D)*** Immunofluorescence staining of myotubes after a 72h differentiation on Matrigel-coated culture plates for MHC (green) and DAPI (blue) shows no difference in myotube morphology in NELFb-KD populations compared to transduction controls.

which permit terminal differentiation and fusion of C2C12 myoblasts is not directly reliant on a functional NELF complex. Interestingly, the inability of the NELFb-KD myotubes to remain adhered to the culture plate suggests the NELF complex may be implicated in processes which relate to myotube adhesion. Because this defect can be rescued with a Matrigel coating means the NELF complex may regulate the production of factors which are secreted to the extracellular environment to support myotube adhesion.

3.2 – The role of NELF on primary myogenic cell state transitions in skeletal muscle regeneration

3.2.1 ***Production and validation of a NELFb^{scKO} mouse model.*** The function of NELF to control proliferation of C2C12 myoblasts suggests it may exhibit functional control on myogenic cell states during skeletal muscle regeneration. While C2C12 are a great myogenic model, they do not recapitulate the early events of myogenesis, such as MuSC quiescence and activation. In addition, the near-tetraploid karyotype of C2C12 (173) brings the possibility that NELF may have different effects on gene regulation and cellular activity than in diploid primary myogenic cells. To investigate whether NELF exerts regulatory effects on myogenic cell state changes, we generated an inducible MuSC specific NELFb knockout (NELFb^{sckO}) mouse model. Here, a mouse strain harbouring floxed NELFb alleles (124) crossed with those expressing CreERT2 under the Pax7 locus (32), produced a tamoxifen inducible NELFb knockout specific to MuSCs and their derived myogenic progenitors. Because the loss of NELFb will prevent functional assembly of the NELF complex, means this

model can be used to study functional implications of the NELF complex in adult MuSCs and their derived progenitors during skeletal muscle regeneration (Figure S3.2). In addition, a TdTomato (TdT) reporter which is activated in response to deletion of a floxed stop site by active CreERT2 (141) would permit to monitor CreERT2 activation and lineage tracking of downstream MuSC progenitors (Figure 3.3A, S3.2).

Initial characterization of the mouse models revealed a significantly reduced abundance of NELFb protein levels in quiescent MuSCs populations upon Cre recombinase induction with either tamoxifen administered *in vivo* (Figure 3.3B, top 2 panels**)**, or with 4-hydroxytamoxifen (4-OHT) supplemented in the growth medium of cultured primary myoblasts (Figure 3.3B, lower 2 panels). Together, this supports an

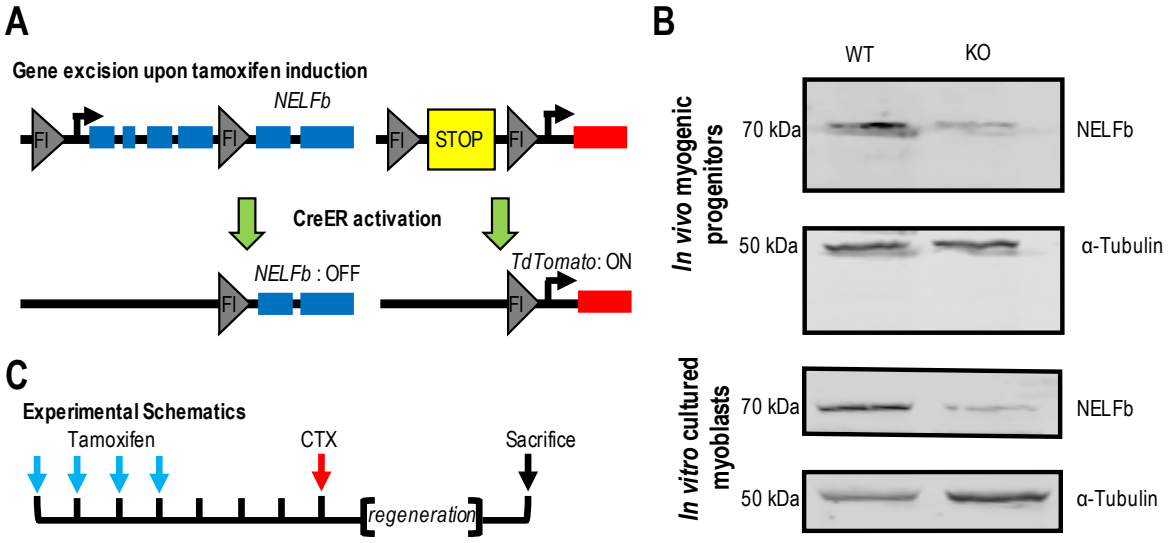

Figure 3.3. Graphical model and validation of the NELFb^{scKO} mouse model. ***(A)*** Schematic representation of recombination strategy. Tamoxifen administered *in vivo* activates CreERT2 to excise DNA segments flanked by loxP sites (Fl). This is followed with intramuscular injection(s) of cardiotoxin (CTX) to induce skeletal muscle damage. Floxed genomic regions include (left) exons 1 – 4 of NELFb, which generates a non-functional allele upon excision, and (right) a 'STOP' cassette at the 5' end of the TdTomato gene within the ROSA26 locus, which is removed and allows constitutive TdT expression upon CreERT2 activation. ***(B)*** Western blot of MuSCs whole cell extract isolated from NELFb^{scKO} and WT mice shows a 90% deletion efficiency of NELFb (68 kDa) when compared to the α-tubulin (50 kDa) loading control. ***(C)*** General experimental schematics for *in vivo* experiments includes tamoxifen induction with 4 consecutive intraperitoneal injections of tamoxifen at 24h intervals, followed by a 72h rest period, then intramuscular damage with CTX and an experiment-defined regeneration period.

efficient model system capable to generate a non-functional NELF complex both *in vivo* and *in vitro*.

3.2.2 ***Characterizing a functional role for NELF during skeletal muscle regeneration.*** As a first experiment, we desired to probe whether the NELF complex has any functional implications in myogenic cells during skeletal muscle regeneration. To do so, tamoxifen-induced NELFb^{scKO} and wildtype control mice were subject to intramuscular damage to the tibialis anterior (TA) muscle with cardiotoxin, and provided variable regeneration periods (Figure 3.3C). To assess the regenerative capacity of injured skeletal muscle, we first normalized the relative mass of the regenerated TA to the undamaged contralateral TA of a same mouse. At 7 days post-injury (7 dpi), this normalized weight was significantly lower in NELFb^{scKO} mice than in the wildtype controls (Figure S3.3A). Further, histological analysis performed on 10 µm cross-sections of the regenerated TA shows a significantly reduced minimal Feret diameter of the regenerated NELFb^{scKO} myofibers compared to the wildtype controls (Figure S3.3B). When provided a 28-day regeneration period, both the normalized weight and the myofiber diameter of the regenerated TA of NELFb^{scKO} mice remained inferior to that of wildtype controls (Figure 3.4A, B), which suggests myogenesis is impaired in response to a non-functional NELF complex. Despite this regeneration defect, the presence of mature myofibers without any necrotic or fibrotic tissue suggests NELFb^{scKO} myogenic cells were disrupted but not prevented from participating in skeletal muscle regeneration. In addition, the number of *de novo* myofibers in the regenerated TA compared to the undamaged contralateral TA was not changed upon a NELFb^{scKO} (Figure 3.4C). While this is expected as myofiber

formation is reliant on the extracellular matrix architecture (174) which is established during early development (175), it does indicate a critical contribution of NELFb^{scKO} MuSCs towards healthy skeletal muscle regeneration.

3.2.3 *The NELF complex does not affect myonuclei localization.*

Closer inspection of regenerated cross sections at 28 dpi revealed nearly half of *de novo* myofibers from NELFb^{scKO} muscle did not contain centrally-located myonuclei (Figure 3.4B, quantified in Figure 3.4D). Subsequent analysis of regenerated single myofibers

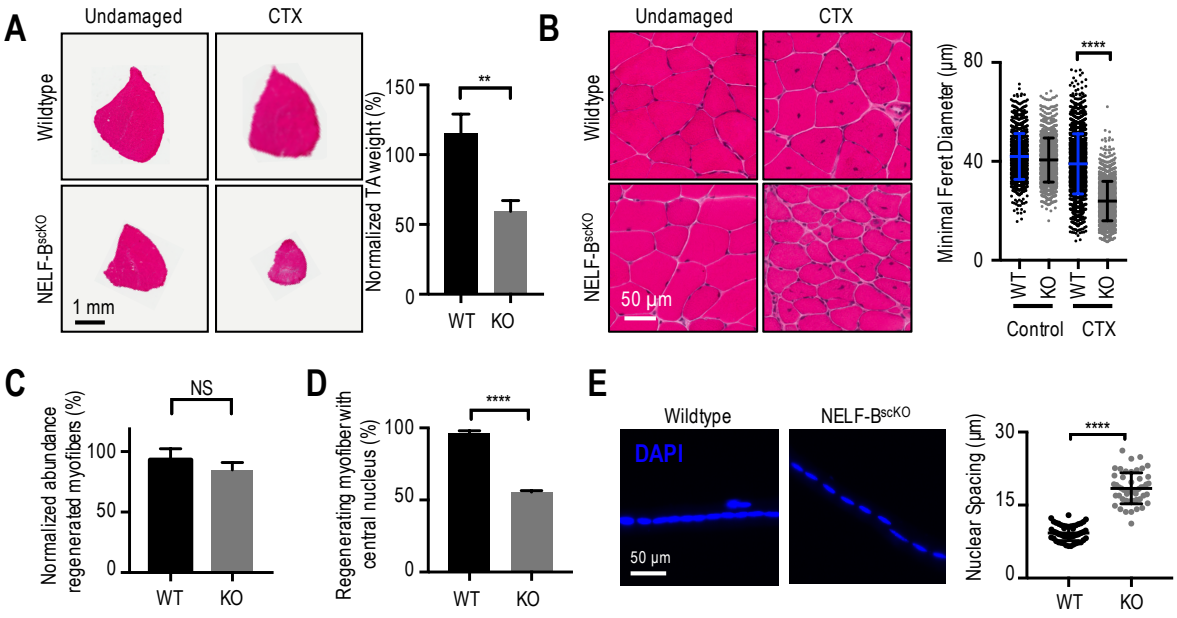

Figure 3.4. Skeletal muscle regeneration is impaired upon a NELFb^{scKO}. (*A*) Hematoxylin & Eosin staining of TA muscle cross-sections at 28 dpi with undamaged contralateral muscles as controls. The weight of the regenerated TA is presented relative to that of the undamaged contralateral leg shows a reduced size in NELFb^{scKO} mice [59.23% ± 4.53, n = 3] when compared to WT controls [115.30% ± 6.87, n = 3]. ***(B)*** Magnified view of the regenerated and undamaged TA cross-sections shown in **(*A*)** demonstrate a reduced minimal Feret's myofiber diameter in regenerated NELFb^{scKO} myofibers [23.94 μm ± 0.20, n=3] compared to WT controls [39.01 μm ± 0.29, n=3]. ***(C)*** Normalized amounts of newly regenerated myofibers to the undamaged contralateral leg at 28-days post injury reveal no difference in regenerated myofiber abundance in the NELFb^{scKO} population [84.89%± 3.55, n=3] compared to WT controls [93.17%± 5.29, n=3]. **(*D*)** The relative abundance of newly regenerated myofibers in which the central-located nucleus is captured in 10 μm cross-section is diminished in the NELFb^{scKO} population [55.56% ± 0.54 %, n = 3] compared to WT controls [96.24% ± 1.09, n=3]. **(*E*)** Single myofibers isolated from regenerated EDL at 21 dpi shows increased internuclear spacing in regenerated myofibers derived from NELFb^{scKO} [18.46 μm ± 0.45, n=50 myofibers from 3 biological replicates] compared to WT controls [9.27 μm ± 0.21, n=57 myofibers from 3 biological replicates]. Internuclear spacing is measured as the distance between the center of adjacent nuclei in a regenerated myofiber.

derived from the EDL at 21 dpi further shows the *de novo* myofibers in NELFb^{scKO} exhibit a nearly two-fold increase in spacing between adjacent centrally-located myonuclei when compared to wildtype controls (Figure 3.4E). This suggests the reduced abundance of central myonuclei in *de novo* myofibers of NELFb^{scKO} TA cross-sections is a defect stemming from increased myonuclear separation.

While these initial experiments demonstrate a clear defect in skeletal muscle regeneration upon a NELFb^{scKO}, they do not attribute the specific contributions of the NELF complex to the different myogenic cell states during regeneration. To further probe the functional requirements of NELF during skeletal muscle we examined how a loss of NELFb affected MuSC quiescence prior to injury, MuSC activation during injury, myogenic progenitor proliferation, commitment to terminal differentiation, and myocyte fusion. These various experiments are described in the following sections.

3.3 NELF retains myogenic progenitors in a proliferative expansive state

3.3.1 *Maintenance of quiescent MuSC pool in uninjured conditions.*

During skeletal muscle homeostasis, quiescent MuSCs undergo regular activation to fuse with muscle fibers and repair micro-tears sustained from regular use (5). Considering the abundance of poised Pol II in skeletal muscle (87) and G_0 induced C2C12 myoblasts (176), and the rapid changes in gene expression which accompany MuSC activation (74, 177) suggests a potential role for NELF to stabilize promoter proximal paused Pol II in quiescent MuSCs to permit rapid gene expression in response to damage. To investigate functional implications of NELF during MuSC quiescence, we provided initial tamoxifen induction to NELFb^{scKO} and wildtype

controls, and provided an extended hold over 8 weeks in the absence of skeletal muscle injury. Initial histological analysis on 10 µm cross-sections of the undamaged TA revealed there are no changes in the overall TA size, nor in minimal Feret myofiber diameter of the constituent myofibers in either NELFb^{scKO} or wildtype controls (Figure 3.5A**)**. Additional immunofluorescence analysis further reveals there are no significant differences in the abundance of Pax7^{+} MuSCs in the TA of NELFb^{scKO} compared to wildtype control populations (Figure 3.5B). Together, this suggests NELF may not be directly implicated in regulating cellular activity of quiescent MuSCs during skeletal muscle homeostasis.

3.3.2 ***MuSC activation upon injury*****.** Upon injury, both truly quiescent MuSCs and satellite progenitors may participate towards skeletal muscle regeneration. Here, truly quiescent MuSCs (Pax7^{+} Myf5^{-}) undergo either a symmetric or asymmetric division to produce two activated progenitors, while the satellite

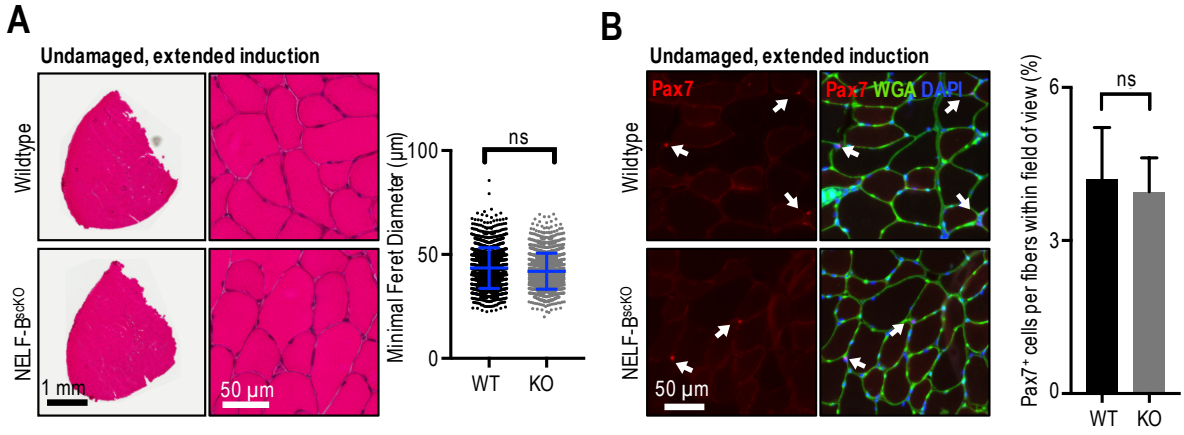

Figure 3.5 – NELF does not participate in skeletal muscle homeostasis. ***(A)*** Hematoxylin & Eosin staining on undamaged TA cross-sections following long-term tamoxifen induction (8 weeks) shows no change in TA morphology or myofiber minimal Feret diameter in the NELFb^{scKO} [43.48 µm ± 0.27, n=3] compared to WT controls [41.92 µm ± 0.24, n=3].***(B)*** Immunofluorescent characterization of the undamaged TA muscle cross-sections from ***(A)*** shows no significant difference in the abundance of Pax7^{+} MuSCs normalized to the amount of fibers within a field of view in NELFb^{scKO} populations [3.96% ± 0.38, n=3] compared to WT controls [4.20% ± 0.59, n=3].

progenitors (Pax7^{+} Myf5^{+}) are confined to symmetric divisions to produce two activated progenitors (reviewed in section 1.2). In either case, the vastly different transcriptome of activated MuSC from their originating MuSCs occurs in a small timeframe (74, 75, 177). This rapid change in transcriptome may emerge from promoter proximal paused Pol II in MuSCs (176). This presents a possible implication of NELF to stabilize and control poised Pol II to facilitate rapid changes in the transcriptome as quiescent MuSCs become activated.

To investigate functional implications of NELF in MuSC activation, the global rate of MuSC activation was probed using an EdU incorporation assay (178). Here, we reasoned that exposing MuSCs to an abundance of EdU during *in vivo* activation would cause EdU to stably incorporate into the DNA of activated MuSCs as they emerge from quiescent MuSCs and undergo their first division. Because MuSCs enter the cell cycle between 28 hpi to 40 hpi (179, 180), we focused on this time point to examine activation. Following CTX injury and intraperitoneal (IP) delivery of EdU at 28 hpi, mice were allowed to recover up to 40 hpi. Using FACS analysis to quantify the percentage MuSCs (TdT^{+} AI7^{+}) that had incorporated EdU (EdU^{+}) into their DNA, we observed no significant difference in overall MuSC activation of NELFb^{scKO} when compared to wildtype controls (Figure 3.6A, S3.4A). This suggests the NELF complex does not influence the ability of quiescent MuSCs to become activated in response to skeletal muscle injury.

3.3.3 ***Myogenic progenitor proliferation.*** In an analogous experiment, EdU administered at 60 hpi and provided a 12-hour *in vivo* incubation was sought to label proliferating myogenic progenitors with EdU as they pass through

the S-phase of the cell cycle. This timepoint was chosen as it represents a time typically marked by a high abundance of actively proliferating myogenic progenitors. Subsequent to FACS analysis, the abundance of myogenic progenitors (TdT^+ $AI7^+$) identified as proliferating (EdU^+) was significantly reduced in $NELFb^{scKO}$ populations when compared to wildtype controls (Figure 3.6B). Similarly, EdU pulse experiments performed in cultured myoblasts to favor myoblast proliferation again showed a significantly reduced number of EdU^+ myoblasts in the $NELFb^{scKO}$ samples compared to wildtype controls (Figure 3.6C). In addition, the growth curve of cultured primary myoblasts over a 72h period shows population expansion of $NELFb^{scKO}$ myoblasts is reduced when compared to wildtype controls (Figure 3.6D). Collectively, these experiments show that myogenic progenitors with a non-functional NELF complex cannot expand their populations as do the wildtype controls, which may contribute to the skeletal muscle regeneration defect reported (section 3.2.2).

3.3.4 ***Assessing apoptosis for reduced cell numbers*.** One potential reason $NELFb^{scKO}$ myogenic progenitors undergo reduced proliferation may arise from a general dysregulation in gene expression which prompts apoptosis. To explore this avenue, cultured primary myoblasts were assayed for expression of general apoptosis caspases 3 and 7 (181, 182). While neither caspase 3 or 7 were detected in $NELFb^{scKO}$ or wildtype controls, positive controls induced towards apoptosis with staurosporine did test positive for caspase 3/7, which supports a functional assay was used (Figure 3.6E). In addition, Sytox exclusion assays as a marker of cell viability were performed on primary myogenic cells isolated from freshly isolated MuSCs through to myogenic progenitors isolated at 5 dpi. In all instances, there was no

significant difference in the abundance of viable myogenic cells from NELFb^{scKO} to those from wildtype controls (Figure S3.4B). Taken together, both experiments support that a non-functional NELF complex does not affect cellular viability, which means the reduced proliferation of NELFb^{scKO} myogenic cells may produce a defect which deters cell cycle progression.

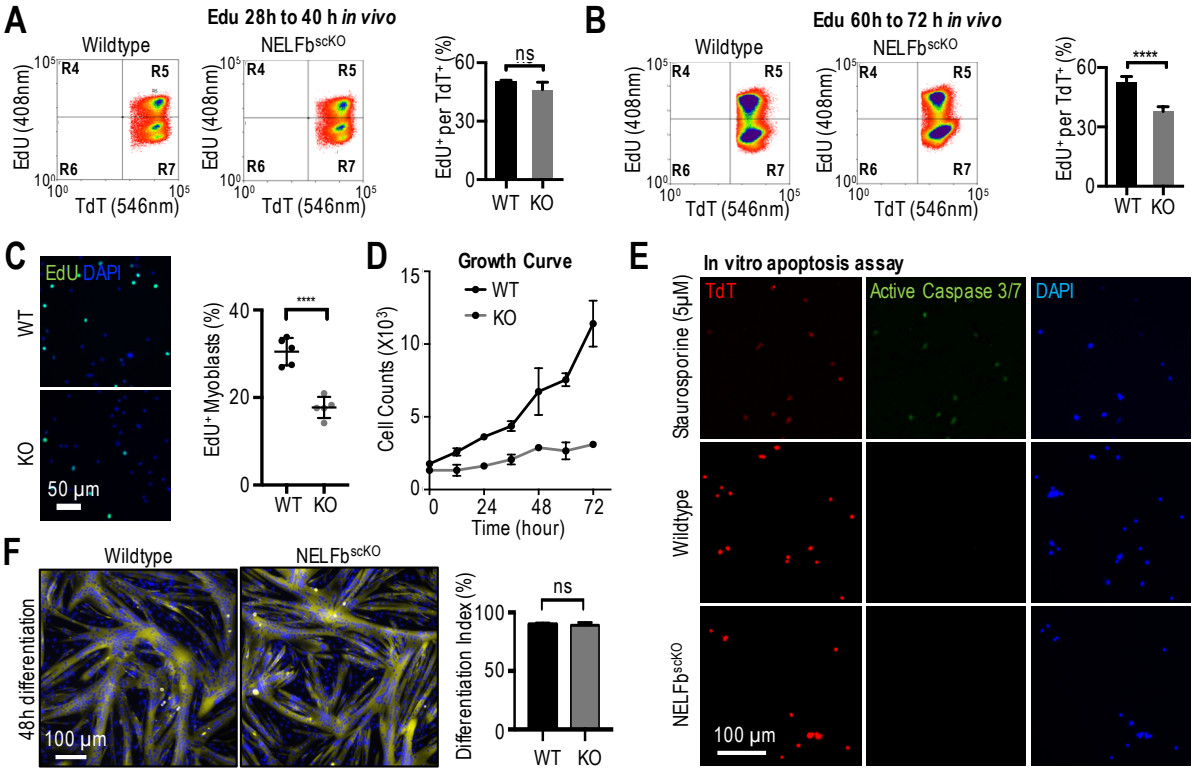

Figure 3.6 – The NELF complex impairs proliferation but no other myogenic cell states. ***(A)*** FACS-acquired quantification of EdU^{+} MuSCs (TdT^{+}/AI7^{+} populations) derived from skeletal muscle 40h post-injury to monitor MuSC activation reveals no significant difference in NELFb^{scKO} populations [46.24% ± 1.70, n = 4] compared to WT controls [(50.28% ± 0.58, n = 4]. ***(B)*** FACS-acquired quantification of EdU^{+} MuSCs (identified as TdT^{+}, AI7^{+} population) derived from skeletal muscle 72 hpi to monitor *in vivo* myoblast proliferation reveals a significant reduction of EdU^{+} NELFb^{scKO} populations [35.19% ± 2.04, n=5] compared to WT controls [50.65 ± 1.04, n=8]. ***(C)*** Analysis of cell cycle progression in *ex vivo* induced myoblasts shows reduced abundance of EdU^{+} myoblasts in NELFb^{scKO} myoblasts [17.72% ± 1.08, n=5] compared to WT controls [30.50% ± 1.40, n=5]. ***(D)*** Myoblasts from NELFb^{scKO} and WT mice were induced with 4-OHT, then population expansion monitored at 12h intervals for 72h to monitor growth curve. ***(E)*** Live caspase screening apoptosis assay was performed on NELFb^{scKO} and WT myoblasts to test whether a NELFb^{scKO} affects myoblast viability. No caspase^{+} cells were identified in either NELFb^{scKO} or WT conditions. Positive control created by treating WT myoblasts with staurosporine (5 µM, 4 hours), shows functionality of the apoptosis screening kit. ***(F)*** Primary myoblasts isolated from NELFb^{scKO} and WT controls were plated at high-density in low serum conditions to induce terminal differentiation. The ability to undergo terminal differentiation was quantified by the differentiation index (percentage of nuclei present in multinucleated myotubes). No significant difference was identified in the differentiation index for NELFb^{scKO} myoblasts [89.17% ± 1.36, n=3] and WT controls [89.77% ± 0.67, n=3].

3.3.5 ***Commitment to terminal differentiation and myocyte fusion*****.** Despite the ability of NELFb^{scKO} myocytes to participate in *de novo* myofiber formation (Figure 3.4A, 3.4E, S3.3), these results do not eliminate the possibility of a defect inherent to myocyte fusion. To investigate this possibility, primary myoblasts derived from NELFb^{scKO} and wildtype mice were induced with 4-OHT, replated at high cell densities, and induced towards terminal differentiation using low serum medium for 48h. Regardless of genotype, myoblasts underwent terminal differentiation, formed multinucleated myotubes which could spontaneously twitch, and exhibited no significant difference between their differentiation indices (Figure 3.6F). Thus, the NELF complex does not play a functional role relating to myoblast terminal differentiation and myocyte fusion. The observed spontaneous contractions in myotubes in both NELFb^{scKO} and wildtype populations further supports multinucleated myotube maturation is not affected by a non-functional NELF complex.

3.4 – Validating the functional role of NELF during multiple myogenic cell state changes.

Our *in vitro* and *in vivo* experiments suggest that the functional implications of the NELF complex is restricted to control the extent of myogenic progenitor proliferation. In the absence of NELF binding, this evokes premature differentiation of myogenic progenitors, fewer myocytes available for *de novo* myofiber formation, and a resulting reduced minimal Feret myofiber diameter observed. To validate this possibility, two critical experiments were performed for their ability to efficiently monitor myogenic cell stage transitions.

3.4.1 *Myogenic progenitor fate on ex vivo cultured myofibers.*

Single myofiber *ex vivo* culture is a powerful technique which can be used to monitor MuSC populations on their resident myofiber during activation, proliferation, and commitment to terminal differentiation in real time (146). The ability to do so relies on enzymatic digestion of structural collagen which forms the ECM, which releases single myofibers from their resident skeletal muscle. Doing so perturbs the MuSC niche environment and activates MuSCs towards the myogenic program, while remaining adhered to single myofibers.

Upon immediate release of myofibers from the extensor digitorum longus (EDL) muscle of induced NELFb^{scKO} and wildtype controls, there is no significant difference in the baseline amount of quiescent MuSCs (TdT^{+}) in NELFb^{scKO} and wildtype controls (Figure 3.7, panel I). Subsequent to a 72h *ex vivo* culture, the populations of TdT^{+} myogenic progenitors per myofiber in NELFb^{scKO} populations are significantly reduced compared to those in the wildtype controls (Figure 3.7, panel II), which agrees with the previously reported reduced population expansion of NELFb^{scKO} myogenic progenitors. In addition, an EdU pulse assay (Figure 3.7, panel III) performed from 66h to 72h in culture shows a reduced abundance of EdU^{+} myogenic progenitors (TdT^{+}) in the NELFb^{scKO} populations compared to wildtype controls, which further supports reduced proliferation of myogenic progenitors upon a NELFb^{scKO}. Prominently, the significant increase in Myog^{+} myogenic cells (TdT^{+}) in NELFb^{scKO} populations compared to the wildtype counterparts (Figure 3.7, panel IV)

suggests the reduced proliferation in NELFb^{scKO} populations arises from their precocious withdrawal from the cell cycle and commitment towards terminal differentiation.

3.4.2 ***Lineage tracking during in vivo regeneration.*** While *ex vivo* myofiber culture reveals myogenic cell behavior during their transition across many cell state transitions, it does so in the absence of the extracellular matrix which is known to affect myogenic cell behavior (reviewed in section 1.2). Thus, to investigate whether proliferating myogenic progenitors undergo precocious differentiation in response to a non-functional NELF complex, we performed an *in vivo* EdU pulse assay modelled on previous experiments (178, 183). To do so, mice were pulsed with

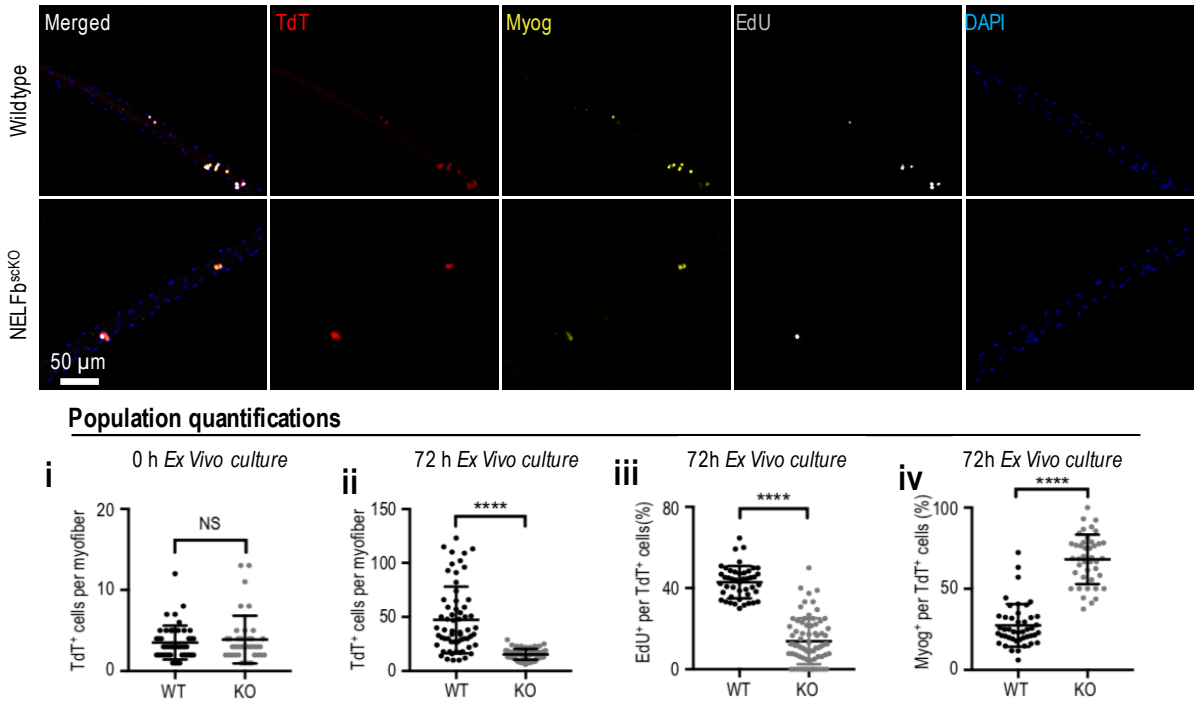

Figure 3.7 – NELFb^{scKO} myogenic progenitors undergo precocious differentiation during *ex vivo* myofiber culture. ***(i)*** Single myofibers isolated from the EDL muscle shows no significant difference in abundance of TdT$^+$ cells per myofiber in NELFb^{scKO} [4.21 ± 0.43, n=47 from 3 biological replicates] and WT controls [3.52 ± 0.31, n=46 from 3 biological replicates] at the time of isolation (0h). ***(ii)*** Following a 72h *ex vivo* culture, NELFb^{scKO} myofibers have reduced total population of TdT$^+$ cells per myofiber [15.42% ± 0.58, n=74 from 4 biological replicates] compared to WT controls [47.28% ± 3.94, n=61 from 4 biological replicates], ***(iii)*** reduced percentage of TdT$^+$ cells that incorporate EdU [13.85% ± 1.32, n=74 from 4 biological replicates] compared to WT controls [42.92% ±1.19, n=45 from 4 biological replicates], and ***(iv)*** increased percentage of TdT$^+$ cells that express Myog [68.20% ± 2.35, n=42 from 4 biological replicates] compared to WT controls [27.47% ±1.99, n=45 from 4 biological replicates].

EdU *in vivo* at either 48 hpi or 72 hpi, and provided a 7-day recovery period from the time of injury to monitor for cell populations which contained EdU in their DNA. The rapid bioavailability and short half-life of EdU (184) means that a single EdU pulse can efficiently label actively dividing cells at the time of exposure to track their location in regenerated skeletal muscle. Because most proliferating myogenic progenitors proceed to terminal differentiation for myofiber repair, we can expect that actively proliferating myogenic progenitors pulsed with EdU will produce an EdU^+ signal which will remain once they proceed to occupy a centrally-located myonuclear position in the regenerated *de novo* myofiber. When pulsed with EdU at 48 hpi, there was no significant difference in the abundance of *de novo* myofibers (TdT^+) with an EdU^+ centrally located nuclei (Figure 3.8) in $NELFb^{scKO}$ and wildtype populations. This indicates there is no difference within the transition of myogenic cells from late stages of activation towards early proliferation despite a non-functional NELF complex, in agreement with prior activation experiments performed (section 3.3.2). When EdU is pulsed at 72 hpi, the abundance of EdU^+ centrally located nuclei in *de novo* myofibers for $NELFb^{scKO}$ populations are significantly reduced to those in the wildtype controls (Figure 3.8). This suggests that most $NELFb^{scKO}$ myogenic progenitors had already undergone cell cycle withdrawal and commitment towards terminal differentiation by 72 hpi, while wildtype myogenic progenitors continued to proliferate. In agreement with single myofiber culture experiments, this supports that $NELFb^{scKO}$ myogenic progenitors undergo precocious terminal differentiation.

3.5 – The $NELFb^{scKO}$ reduces quiescent MuSC populations in regenerated skeletal muscle

3.5.1 *Reduced endogenous NELFb^{scKO} MuSC populations upon regeneration.*

Recent analyses focused on cellular kinetics during regeneration suggest MuSC self-renewal by quiescent MuSC populations begins around 3 dpi, peaks between 5 – 7 dpi, and continues with a lower occurrence up to 14 dpi (24). While the NELF complex had no apparent regulatory function in either MuSC homeostasis or activation, this does not preclude an implication of the NELF complex in MuSC self-renewal in the regenerated skeletal muscle milieu.

To investigate functional implications of the NELF complex in MuSC self-renewal, cross-sections from 7dpi and 28 dpi regeneration experiments were subject

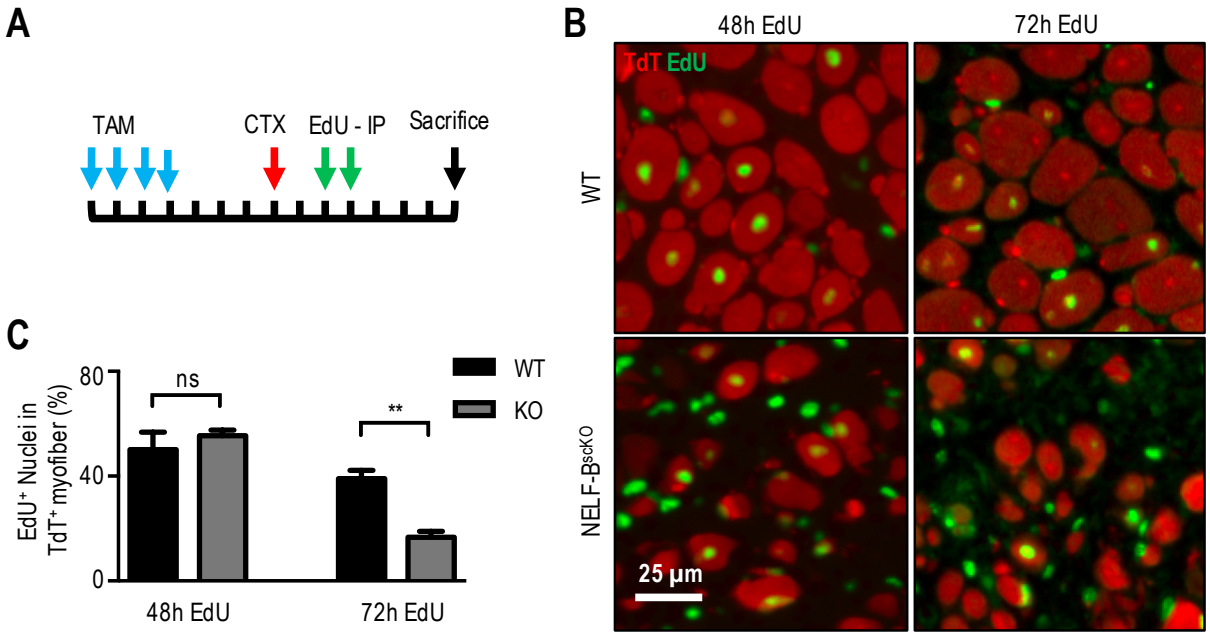

Figure 3.8 – *In vivo* EdU pulse-chase experiments suggest precocious differentiation of NELFb^{scKO} myogenic progenitors during regeneration. ***(A)*** Experimental schematics for the *in vivo* EdU pulse-chase experiment which is administered to mice through intraperitoneal injection at 48 hpi or 72 hpi, followed with a 7-day regeneration period from time of injury. ***(B)*** Immunofluorescence characterization performed on cross-sections (10 μm) of the regenerated skeletal muscle shows *de novo* myofibers (TdT$^+$) and identifies the actively dividing nuclei (EdU$^+$) at the time of the specific EdU pulse-chase experiment***. (C)*** No significant difference is observed in the abundance of EdU$^+$ centrally-located nuclei when EdU is administered at 48 hpi. When EdU is administered at 72 hpi ,a significantly reduced amount of EdU$^+$ centrally located nuclei are apparent in *de novo* myofibers of the NELFb^{scKO} populations [16.65% ± 2.33, n=4] compared to WT controls [39.01% ± 3.16, n=3].

to immunofluorescent characterization. Here, Pax7^{+} cells that reside within a peripheral location to *de novo* myofibers were categorized as MuSCs and quantified. Because the NELFb^{scKO} produces smaller *de novo* myofibers than their wildtype counterparts (Figure 3.4A, S3.3) we normalized the abundance of MuSCs to the amount of myofibers within a field of view to eliminate potential bias. Here, the normalized abundance of MuSCs in the regenerated TA of NELFb^{scKO} mice was significantly reduced at both 7 dpi and 28 dpi when compared to those of the wildtype controls (Figure 3.9, S3.5). This suggests a defect within MuSC self-renewal arises in response to a non-functional NELF complex.

3.5.2 *Skeletal muscle succumbs to serial injury upon a NELFb^{scKO}.* The reduced myofiber size and MuSC populations observed in regenerated skeletal muscle of NELFb^{scKO} populations presents a phenotype reminiscent to that in

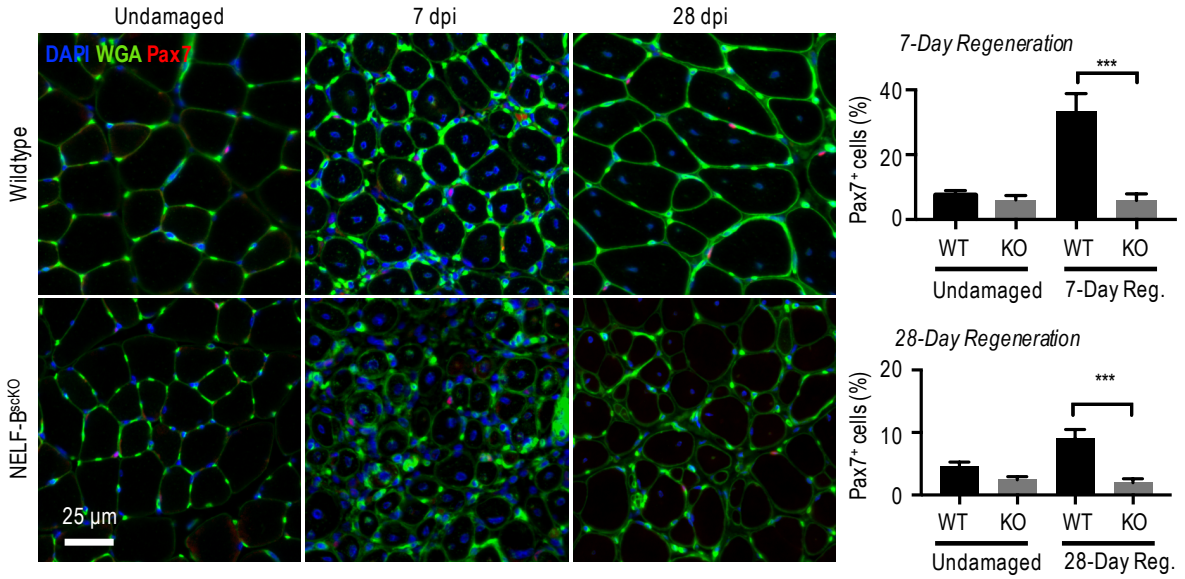

Figure 3.9 – *A non-functional NELF produces a severely reduced MuSC pool in regenerated skeletal muscle.* Immunofluorescence characterization of regenerated TA muscle shows a reduced population of Pax7^{+} cells normalized to the amount of fibers within a field of view for NELFb^{scKO} populations [5.89% ± 1.02, n=4] compared to WT controls [33.34% ± 3.20, n=3] at 7 dpi. The reduced normalized abundance of Pax7^{+} cells is sustained at 28-days post injury in the NELFb^{scKO} [1.96% ± 0.38, n = 3] compared to WT controls [9.07% ± 0.71, n=4].

sarcopenia (185). During sarcopenia, several defects in MuSC behavior precludes their regenerative capacity which leads to a progressive worsening in skeletal muscle function. To investigate whether the reduced MuSC populations in regenerated NELFb^{scKO} skeletal muscle would further worsen skeletal muscle, a repeat-injury experiment was performed. To do so, mice were subjected sequential intramuscular CTX injections in the TA muscle at 28-day intervals (Figure 3.10A), and regeneration assessed at 56 dpi from the first injury. At a first glance, the regenerated TA of NELFb^{scKO} mice exhibited a severely reduced size and overall mass (Figure 3.10B). Closer inspection of the cross-sections revealed a limited presence of *de novo* myofibers in the NELFb^{scKO} TA, and those present display a massively reduced myofiber diameter compared to wildtype controls (Figure 3.10C). In addition, an abundance of interstitial cells and general fibrosis in the NELFb^{scKO} cross-sections suggests an exhausted myogenic response from the NELFb^{scKO} MuSCs which are incapable to regenerate skeletal muscle.

3.6 – Discussion

3.6.1 ***Summary of results presented in the chapter*.** In this chapter, an inducible MuSC specific NELFb knockout mouse model (NELFb^{scKO}) was generated, validated, and used to study the functional role of NELF in skeletal muscle regeneration. Characterizing functional implications of NELF in general skeletal muscle regeneration and individual myogenic cell states clearly identified a role for the NELF complex to retain myogenic progenitors engaged in the cell cycle, which produces the pool of myogenic progenitors necessary to repair damaged myofibers.

In the absence of a functional NELF complex, myogenic progenitors undergo premature commitment to terminal differentiation, which prevents proper skeletal muscle regeneration. In addition, the insufficient repopulation of MuSCs in the regenerated muscle of NELFb^{scKO} populations severely impairs skeletal muscle from responding to future injury.

3.6.2 *Role of NELF in regulating proliferation expansion*.

Results presented within this chapter supports a functional role for NELF uniquely to the proliferating population of myogenic progenitor populations. While the presence of promoter proximal paused Pol II has been identified in other myogenic cell states (87), including quiescent MuSCs (176), our experiments reveal there is no functional implication for NELF in regulating myogenic cell state transitions at those instances.

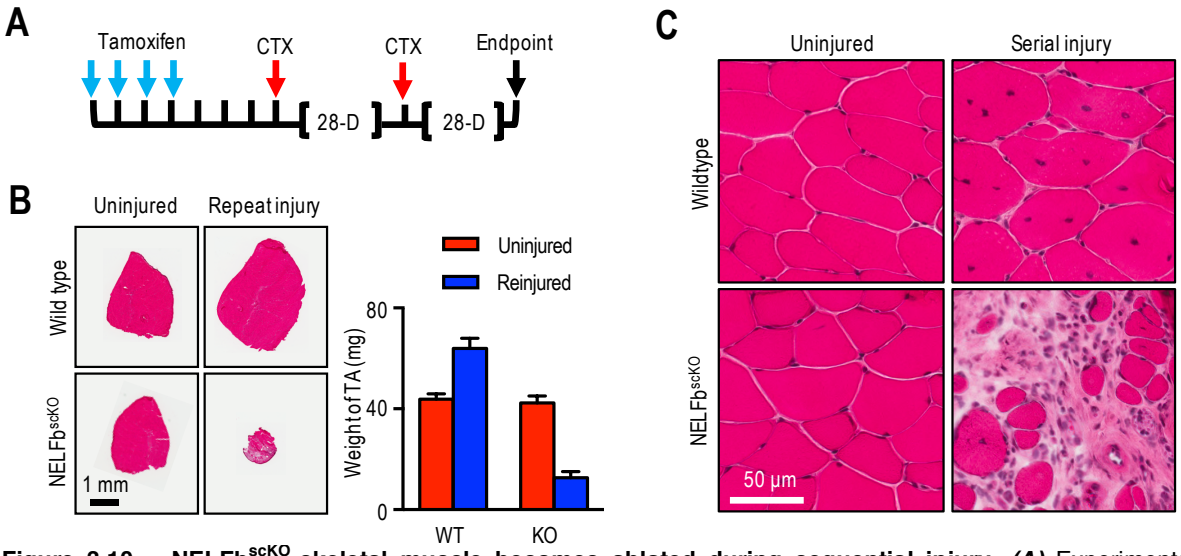

Figure 3.10 – NELFb^{scKO} skeletal muscle becomes ablated during sequential injury. ***(A)*** Experimental schematic showing the sequential injury approach, where mice that had undergone tamoxifen-induced recombination were subjected to two rounds of CTX treatment at 28-day intervals. ***(B)*** Haematoxylin & Eosin staining shows a reduced size and weight of the regenerated TA muscle of NELFb^{scKO} mice [12.69mg ± 1.39, n=3] when compared to the regenerated TA of the WT control [63.96mg ± 2.31, n = 3], while similar weights in the uninjured contralateral leg for the NELFb^{scKO} [42.34mg ±1.58, n=3] and WT [43.86mg ± 1.18, n = 3] are apparent. ***(C)*** Close-up of the repeat-injured TA from (***B***) shows small myofibers and a high abundance of interstitial cells in the NELF-B^{scKO} regenerated muscle, whereas the WT control exhibits muscle hypertrophy and no fibrosis.

Because Pol II promoter proximal pausing is a rate-limiting step in gene expression, this raises the intriguing possibility that additional mechanisms may regulate promoter proximal Pol II pausing in different situations to permit cell state changes.

In agreement with this model, several other factors have been implicated in regulating promoter proximal Pol II pausing (186). This includes the GAGA Factor (GAF) in *Drosophila* (187) and potential GAF homologs in eukaryotes (188). While overexpression of GAF factors tends to increase promoter proximal paused Pol II (189), its specific molecular functions and regulations are still under investigation. In addition, some studies indicate GAF may work in conjunction with NELF (190), although whether the function of GAF to control Pol II pausing is differentially influenced by the presence of NELF remains unanswered. Additional factors which have been implicated in the regulation promoter proximal Pol II pausing includes the histone chaperone FACT (191), the pre-exon junction complex (192), and the +1 nucleosome which acts as a secondary Pol II regulatory step further downstream from that typical for NELF (125). Additionally, several investigations have demonstrated the PAF complex associates with DSIF to control Pol II promoter proximal pausing (193-195). What remains interesting is PAF1c binds the same region of Pol II as does NELF (97, 196), which presents the possibility for mutually exclusive functions of NELF and PAF1c to control Pol II pausing at different gene networks, or function in different cell states. Indeed, a role for PAF1C to regulate Pol II elongation in C2C12 myoblasts (197) supports that multiple regulators of promoter proximal Pol II pausing may regulate gene expression. This raises the possibility that Pol II promoter proximal pausing of different gene regulatory networks and in different cell states are controlled through different mechanisms. Thus, considering promoter proximal Pol II pausing in

myogenesis, we have shown that NELF specifically regulates the transition from proliferation towards terminal differentiation but has no functional effects on other myogenic cell states, despite the reported presence of promoter proximal Pol II pausing within those other myogenic cell states (176). It remains interesting to determine whether different Pol II promoter proximal pausing regulators may inflict control on specific gene networks susceptible to rapid changes in expression, to elicit different responses. This could explain why a loss of function in NELF does not affect many myogenic cell state changes which are prone to Pol II promoter proximal pausing, such as those reported during MuSC activation (74, 75, 177).

3.6.3 ***Function of NELF on MuSC divisions*****.** The functional implication of NELF on MuSC activity was probed with two separate experiments. Here, populations of MuSCs during homeostasis were not afflicted by a NELFb^{scKO}, which suggests the NELF complex may not influence the asymmetric divisions of quiescent MuSCs during skeletal muscle homeostasis (5) (section 3.3.1). In addition, the ability of MuSCs to undergo symmetric divisions to produce two activated MuSCs in response to acute injury (23, 56) was not disrupted by a NELFb^{scKO} (section 3.3.2). This remains interesting, as the prevalence of promoter proximal paused Pol II found in skeletal muscle (87) and G_0 induced C2C12 myoblasts alike (176) suggests Pol II may be poised for rapid gene expression to permit MuSC activation (74, 75, 177). Thus, this process remaining unaffected despite a non-functional NELF complex suggests the poised Pol II in quiescent MuSCs may be stabilized by alternative factors, as discussed (section 3.6.2).

In either case, cellular functions of MuSCs during either asymmetric or symmetric divisions were not impaired by a NELFb^{scKO}, which suggests these processes may occur independent of the NELF complex. Despite the NELF complex showing no functional implications in MuSC asymmetric or symmetric divisions, there is a definite reduction in MuSC populations in the regenerated NELFb^{scKO} skeletal muscle, which stipulates a defect in MuSC self-renewal between 3 to 14 days after injury (24). To identify whether this defect in MuSC self-renewal is directly regulated by NELF, or an indirect effect which stems from defects in skeletal muscle regeneration will be addressed in the next chapter.

CHAPTER 4

Molecular functions of NELF in myogenic progenitor proliferation and MuSC self-renewal.

4.1 – MuSC allograft transplant of wildtype and NELFb^{scKO} donors into NSG recipient mice

4.1.1 ***Allograft transplant experiments*.** The reduced MuSC populations observed in the regenerated skeletal muscle of NELFb^{scKO} mice (section 3.5.1) poses an interesting observation which prompted further investigation. Considering the abundance of MuSC self-renewal typically occurs between 3 – 14 days post injury (198) presents a few possibilities for the reduced MuSC repopulation observed. First, the NELF complex may directly control MuSC divisions to permit self-renewal, so that this ability is compromised in response to a non-functional NELF complex. Alternatively, because MuSC self-renewal occurs predominantly within the milieu of regenerated skeletal muscle means that the reduced proliferation of NELFb^{scKO} myogenic progenitors may have produced a deficient extracellular environment unable to promote downstream MuSC self-renewal.

To investigate these possibilities, we proceeded with a series of allograft transplantation experiments to introduce donor MuSCs populations into a host recipient skeletal muscle (Figure 4.1). In all instances, NSG mice were used as host mice as their compromised immune system (142) would preclude immunorejection of

donor MuSC populations. Coupled with irradiation of the host hindlimb prior to transplantation would also incapacitate the endogenous host MuSC populations, so that observations are restricted to contributions by the donor MuSC populations (199, 200). In addition, performing allograft transplants of the NELFb^{scKO} and wildtype MuSC donors in the contralateral TA of a same host would expose the donor MuSC populations to nearly identical niche environments. This allows to normalize for molecular and accessory cell type interactions in the host niche environment on affecting MuSC self-renewal (see section 1.2.2) so that differences within donor

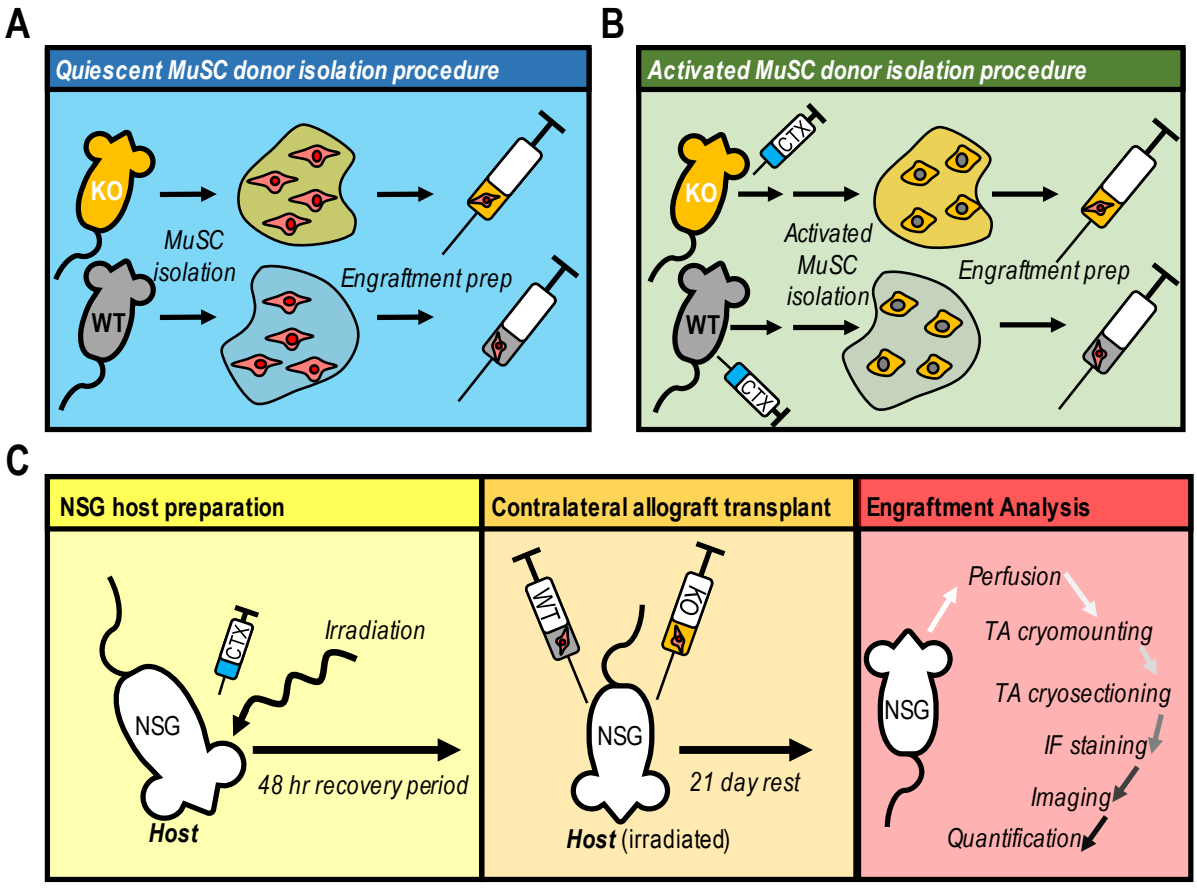

Figure 4.1 – Graphical representation of the different conditions of allograft transplant experiments. ***(A)*** Quiescent MuSC donours derived from tamoxifen-induced NELFb^{scKO} and WT donor mice are purified by fluorescence-based cell sorting (TdT^{+} AI7^{+}), and concentrated (200 cells/μL) for immediate allograft transplant experiments. ***(B)*** Activated MuScs are derived from skeletal muscle of donor mice harvested at 40 hpi, and prepared for engraftment as described in ***(A)***. ***(C)*** Host NSG recipient mice are prepared for allograft transplant through irradiation of the hindlimbs and cardiotoxin injury of both TA (if experimentally-specified) 48h prior to receipt of NELFb^{scKO} and WT donors in the contralateral TA. After a 21-day period to establish homeostasis, the host mice are sacrificed, and the TA muscle prepared for immunofluorescent characterization.

MuSCs behavior arises solely by the functional presence of NELF. Lastly, the TdT lineage tracer of donor populations provides easy tracking of the transplanted MuSCs, their progenitors, and of the host myofibers with which donor-derived myocytes have fused. This means that TdT^{+} host myofibers can be used to delimit the zone of homeostasis established by donor MuSCs as they engraft and proliferate upon their transplant in the undamaged host tissue (199), as represented in Figure 4.2. Thus, these experiments will clarify whether the reduced abundance of MuSC in the regenerated TA of $NELFb^{scKO}$ mice (section 3.5.1) arises from direct dysregulated expression of NELF target genes, or as an indirect effect where the reduced proliferation of $NELFb^{scKO}$ myogenic progenitors does not sufficiently rejuvenate the extracellular environment and cannot promote downstream MuSC self-renewal.

4.1.2 *Engraftment of quiescent donor MuSCs into undamaged recipient muscle.*

As a first trial, 12,000 freshly isolated quiescent MuSCs (TdT^{+} $AI7^{+}$) from undamaged $NELFb^{scKO}$ or wildtype skeletal muscle were engrafted into each of

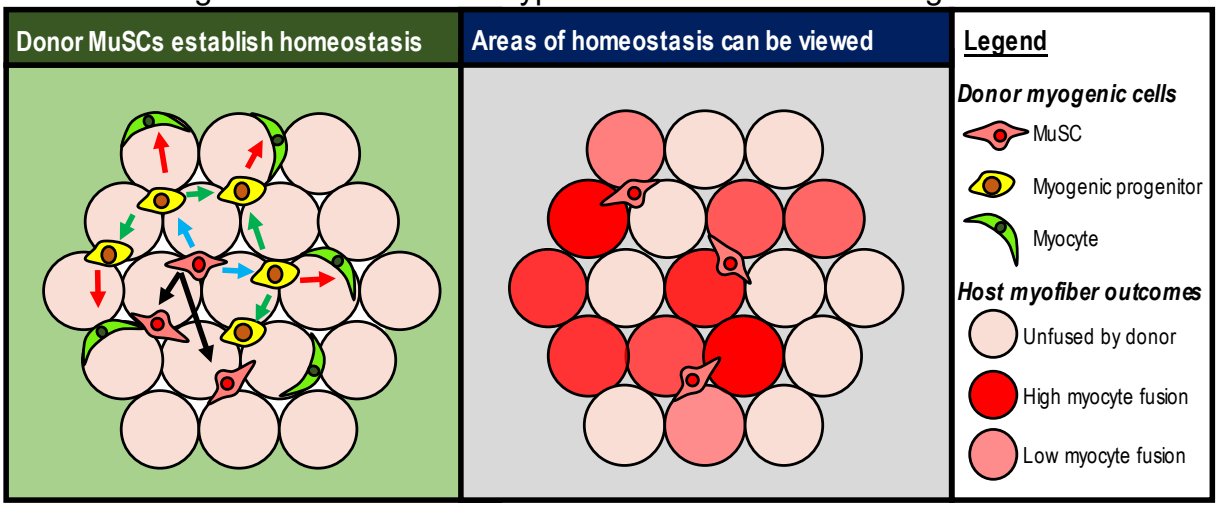

Figure 4.2 – Donor MuSCs establish homeostasis upon allograft transplant. Upon entry in recipient muscle, donor MuSC populations (TdT^{+}) engraft, proliferate, and self-renew to establish a zone of homeostasis within the host muscle. The donor proliferating myogenic progenitors differentiate and fuse with host myofibers, which are evidenced by expression of the donor TdT lineage tracker. The abundance of TdT^{+} host myofibers can be used to demark the established zone of homeostasis, and donor MuSCs identified by expression of TdT.

the undamaged contralateral TA of an irradiated host NSG mouse, and provided a 21-day engraftment period to permit donors to establish homeostasis. Initial immunofluorescent analysis of the host TA reveals the presence of donor-derived MuSCs ($Pax7^+$, TdT^+) regardless of the donor genotype (Figure 4.3A, S4.1A). In addition, unanimous expression of the calcitonin receptor (CalcR) as a mark of MuSC quiescence (201), and the complete absence of Ki67 as a marker of cells engaged in the cell cycle (202, 203) supports that all engrafted MuSCs derived from $NELFb^{scKO}$ and wildtype donors (TdT^+) are in a quiescent state (TdT^+, $CalcR^+$, $Ki67^-$) in the host TA (Figure 4.3B, S4.1C). In addition, presence of TdT^+ host myofibers in all recipient TA (Figure 4.3A, S4.1C) indicates that $NELFb^{scKO}$ and wildtype MuSC donors alike can engraft, produce proliferating myogenic progenitors to establish homeostasis, and undergo self-renewal upon allograft transplantation.

When quantified, there is a significantly reduced abundance of donor derived MuSCs ($Pax7^+$ TdT^+) and of host myofibers which have been fused by a donor-derived myocyte (TdT^+) for the host TA engrafted with $NELFb^{scKO}$ MuSC donors than in the contralateral control TA engrafted with wildtype MuSC donors (Figure S4.1). While the reduced abundance of TdT^+ host myofibers immediately suggests a reduced ability of engrafted $NELFb^{scKO}$ MuSC donors to establish homeostasis, this may stem from the intrinsic precocious differentiation of $NELFb^{scKO}$ myogenic progenitors (see section 3.3.3), which prevents their ability to proliferate and propagate and establish homeostasis. Thus, we reasoned that the reduced zone of homeostasis may in turn affect donor MuSC self-renewal. To account for this bias, we defined the normalized replenishment capacity as the abundance of donor MuSCs normalized to their zone of homeostasis demarked by TdT^+ host myofibers. Doing so shows there is no

significant difference in the normalized abundance of donor MuSCs upon allograft transplant of either NELFb^{sckO} or wildtype MuSC donors (Figure 4.3A). This suggests MuSC self-renewal is not intrinsically regulated by the NELF complex, but is highly susceptible to immediate interactions in the extracellular environment produced by proliferating myogenic progenitors.

4.1.3 ***Activated donor MuSCs into undamaged recipient muscle.*** During skeletal muscle regeneration, a subset of activated MuSCs may return to a dormant state to become satellite progenitors available to respond to future bouts of injury (23, 43). Because a NELFb^{scKO} evokes precocious differentiation, this may pull activated MuSCs towards the cell cycle and prevent their ability to become satellite progenitors, which could reduce the pool of dormant MuSCs in regenerated skeletal muscle. To investigate this possibility, we performed another allograft transplant using activated MuSCs donor populations. To do so, cardiotoxin-mediated injury performed to donor skeletal muscle 40h prior to their isolation assured that most isolated donor MuSCs would assume an activated state (Figure 4.1B, 4.1C). Upon isolation, these activated MuSCs were immediately used for allograft transplant into the undamaged TA of irradiated host NSG mice, and provided a 21-day recovery period to assure homeostasis of the donors was achieved.

Initial immunofluorescent characterization revealed all donor-derived MuSCs (Pax7^{+}, TdT^{+}) were present in a dormant state (Pax7^{+}, TdT^{+}, Ki67^{-}) in the host muscle regardless of the donor genotype (Figure 4.3C, S4.1D). In addition, there was no significant difference in the normalized replenishment capacity of NELFb^{scKO} and

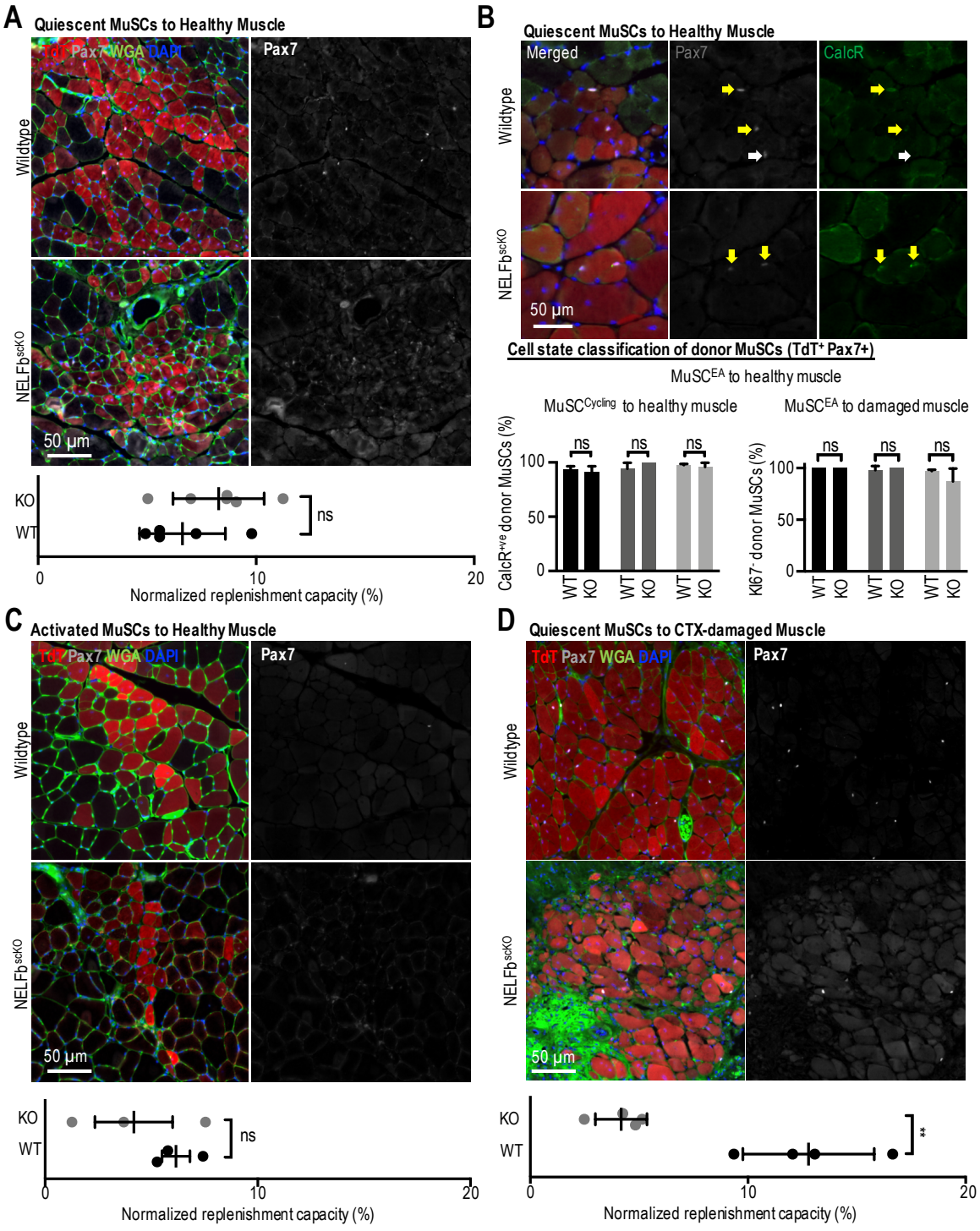

Figure 4.3 NELF is not required for muscle progenitors to return to quiescence and repopulated the MuSC niche. Allograft transplant experiments were performed as shown in Figure 4.1. Subsequent to a 21-day period to establish homeostasis, the host TA was characterized through immunofluorescence, and the abundance of donor-derived MuSCs (TdT^+ $Pax7^+$) was normalized to the region of homeostasis (TdT^+ myofibers) and termed the normalized replenishment capacity. Two-tailed paired t-tests were used to assess whether there was a significant difference within the normalized replenishment capacity of donor populations across biological replicates. ***(A)*** Quiescent donors transplanted into an undamaged host TA shows no significant difference in the

normalized replenishment capacity of NELFb^{scKO} and WT donors (*P*-value = 0.1025). ***(B)*** Immunofluorescence staining for CalcR as a marker of MuSC quiescence shows all Pax7^{+} cells are CalcR^{+} quiescent populations. ***(C)*** Activated MuSCs from NELFb^{scKO} and WT donors transplanted into an undamaged host TA have no significant difference in their normalized replenishment capacity (*P*-value = 0.2798). ***(D)*** When donors are transplanted to a regenerating host environment (48 hpi), the normalized replenishment capacity of the quiescent NELFb^{scKO} donors is significantly reduced than that of WT donors (*P*-value = 0.0034).

wildtype donors (Figure 4.3C, S4.1B, S4.1D), which suggests that the NELF complex does not influence the ability of activated MuSCs to return to a dormant state.

4.1.4 *Engraftment of quiescent donor MuSCs into regenerating recipient muscle.*

We next desired to assess whether the NELF complex controls the expression of genes which remodel the extracellular niche environment through a final allograft transplant experiment of quiescent MuSC donors into a damaged host skeletal muscle environment. To do so, the hindlimbs of host NSG mice were irradiated *and* damaged with CTX 48h prior to receiving 12,000 freshly isolated quiescent MuSCs donors derived from NELFb^{scKO} or wildtype mice (Figure 4.1A, 4.1C). As previously described, a 21-day regeneration period was provided to assure that donor populations had completed their myogenic programs to regenerate the damaged host skeletal muscle, and established homeostasis.

Upon immunofluorescence analysis, it is apparent that the NELFb^{scKO} donors are unable to regenerate the damaged host muscle, evidenced through collapsed ECM which is generally devoid of myofibers (Figure S4.1E), and very few donor-derived quiescent MuSCs (TdT^{+} Pax7^{+}) (Figure 4.3D, S4.1E). In stark contrast, wildtype donors could strongly contribute to the damaged host muscle, evidenced by a high abundance of donor-derived *de novo* myofibers (TdT^{+} with a centrally-located nuclei) and quiescent MuSCs populations (Pax7^{+} TdT^{+}) (Figure 4.3D, S4.1). What remains important is the normalized replenishment capacity of the NELFb^{scKO} donors

is significantly reduced to that of the wildtype donor controls (Figure 4.3D). This suggests an inability of the NELFb^{scKO} donors to undergo self-renewal, which extends beyond the reduced zone of homeostasis caused by precocious differentiation of NELFb^{scKO} myogenic progenitors. Because the previous allograft experiments show the NELF complex does not directly affect MuSC self-renewal, this raises the possibility that NELFb^{scKO} donors are unable to contribute to the extracellular environment during regeneration, which produces a deficient niche environment that remains incapable to promote donor MuSC maintenance and / or self-renewal. Thus, this implicates a potential role of NELF to regulate the expression of genes which remodel the niche environment during regeneration.

Taken together, these allograft transplant experiments suggest the NELF complex indirectly supports MuSC populations during skeletal muscle regeneration by (I) promoting extended myogenic progenitor proliferation, and (II) regulating the expression of genes which rejuvenate the MuSC niche environment. Together, this provides a downstream niche environment which supports MuSC self-renewal and maintenance. When the NELF complex is no longer functional, this produces a devoid extracellular environment which is no longer conducive towards MuSCs maintenance and / or self-renewal, which reduces the abundance of MuSCs.

4.2 Single-cell transcriptome analysis of myogenic progenitors

4.2.1 ***scRNA-seq model to understand effect of NELF in myogenesis.*** Both the phenotypic characterizations performed in chapter 3 and the allograft transplants described above support a role for NELF to sustain myogenic progenitor proliferation

during skeletal muscle regeneration. This sustained proliferation may assure sufficient expansion of myogenic progenitors available for myofiber repair, and supports replenishment of the extracellular environment to promote downstream MuSC self-renewal. While compelling, the mechanisms through which NELF may regulate gene expression for these functions remains unknown.

One suitable technique to investigate the molecular function of NELF in myogenic cell state changes is single-cell RNA-sequencing (scRNA-seq) owing to its ability to provide transcript information of individual cells across an entire sample population. While sequencing depth is limited, its use to identify new tissue-resident cell subtypes (204, 205), define tissue cellular composition (151), and provide directional pseudotime trajectories of cell state changes (206) supports its versatility to study cellular behavior. To study the effects of a non-functional NELF complex on myogenic cells in regeneration, isolated myogenic progenitors (TdT^{+}, $AI7^{+}$) collected from regenerating skeletal muscle at 72 hpi were subject to single-cell RNA sequencing using the $10X^{TM}$ platform. This specific time was chosen as our prior results shows divergence of $NELFb^{scKO}$ myogenic cell states occurs between 48hpi to 72 hpi (sections 3.3.2, 3.3.3, and 3.4.2).

4.2.2 ***Initial clustering using SEURAT algorithm.*** Initial analysis of the cell expression matrices with Seurat (157, 207) showed similar cluster topology for $NELFb^{scKO}$ and wildtype samples across biological and technical replicates ($NELFb^{scKO}$: KO-B, KO-C; Wildtype: WT-A, WT-B, WT-C) (Figure S4.2A, B). Because $NELFb^{sckO}$ and wildtype populations occupied a similar clustering topology, we treated all samples as a single population. While the topographical UMAP plots identify three

distinct islands (Figure S4.2C), transcriptional profiling suggests Islands I and III are contaminating populations composed of fibroblasts and immune cells respectively (Figure S4.2D, S4.2E). In addition, the expression of myogenic specific transcription factors *Pax7, Myf5, MyoD,* and *Myog* is restricted to cells clustered in island II (Figure S4.2F) which supports that only this island constitutes myogenic cells. Although fluorescence cell sorting was used to isolate for single-cell myogenic populations (TdT^{+} $AI7^{+}$), we attribute the presence of non-myogenic cells to limits of the sorting technology, which incorporated false-positives in the purified populations prior to sequencing. Because topological clustering is influenced by all cell populations provided for analysis, we reasoned that the contaminating populations could mask subtle differences between $NELFb^{scKO}$ and wildtype myogenic populations. Therefore, non-myogenic cells were excluded, so focus specifically on the effects of a non-functional NELF complex on myogenic populations. Looking at population distributions, an apparent difference in the relative abundance of $NELFb^{scKO}$ and wildtype populations distributed across the myogenic clusters suggests a $NELFb^{scKO}$ affects myogenic cell state transitions, as established in our previous results.

4.2.3 *PAGA clustering and trajectory analysis*. To inspect how myogenic cell state progression is affected by a $NELFb^{scKO}$, we processed the cell expression matrices of the myogenic populations with the PAGA algorithm (208) to construct pseudotime trajectories. Initial Louvain clustering of the combined wildtype and $NELFb^{scKO}$ populations revealed 16 interconnected myogenic clusters based on the transcriptome profiles of the myogenic cells (Figure 4.4A). To proceed to pseudotime trajectory reconstruction, PAGA first requires an anchor-point which denotes the

trajectory start. While high expression of *Pax7* is a logical starting point to denote myogenic cells closer to a quiescent state, its overall low expression across the 16 clusters (Figure 4.4C, red rectangle) means it could not confidently identify a start point. As an alternate, high expression of *Myog* specific to clusters 15, 12, and 6 (Figure 4.4C, blue rectangle), proved to be a suitable terminal anchor point for pseudotime trajectory reconstruction. Indeed, doing so produced a single proposed pseudotime trajectory (Figure 4.4B), which agreed with the differential expression patterns of myogenic regulatory factors *Pax7, Myod1,* and *Myog*, (Figure 4.4D) the cell cycle regulator *Cdkn3* involved in proliferation (209, 210), and *Cdkn1a* which denotes cell cycle withdrawal (Figure 4.4E) (211, 212). The coherence between the proposed pseudotime trajectory with established gene expression programs that accompany myogenic cell state transitions suggests accuracy within the proposed trajectory. Next, we assigned each of the 16 Louvain clusters to different myogenic cell states based on the differential gene expression signatures of each cluster (Figure 4.4C). This allowed to bin the clusters to denote MuSC quiescence (cluster 13), proliferation (clusters 2, 3, 4, 5, 7, 9, 11), early differentiation (clusters 0 and 8), and committed to terminal differentiation (clusters 1, 6, 12, 15).

Density plots which represent the relative population distributions of NELFb^{scKO} and wildtype populations within the pseudotime trajectory shows different populations occupancy along the trajectory as a result of a NELFb^{scKO} (Figure 4.5A). Indeed, the relative abundance of NELFb^{scKO} and wildtype cells in each of the myogenic cell states shows a different distribution along myogenic cell states: wildtype cells show a superior occupancy in proliferating clusters (60%) than NELFb^{scKO} populations (50%), while fewer wildtype cells occupied early or late differentiation clusters (39%)

compared to the NELFb^{scKO} populations (47%) (Figure 4.5B). Granted this is a static representation of myogenic progenitors captured at 72 hpi which excludes cells that had already fused into myofibers, the reduced amount of proliferating NELFb^{scKO} progenitors supports decreased proliferation and early commitment to terminal differentiation as described above. This reduced time in proliferation causes fewer progenitors to partake in population expansion, and therefore fewer myocytes

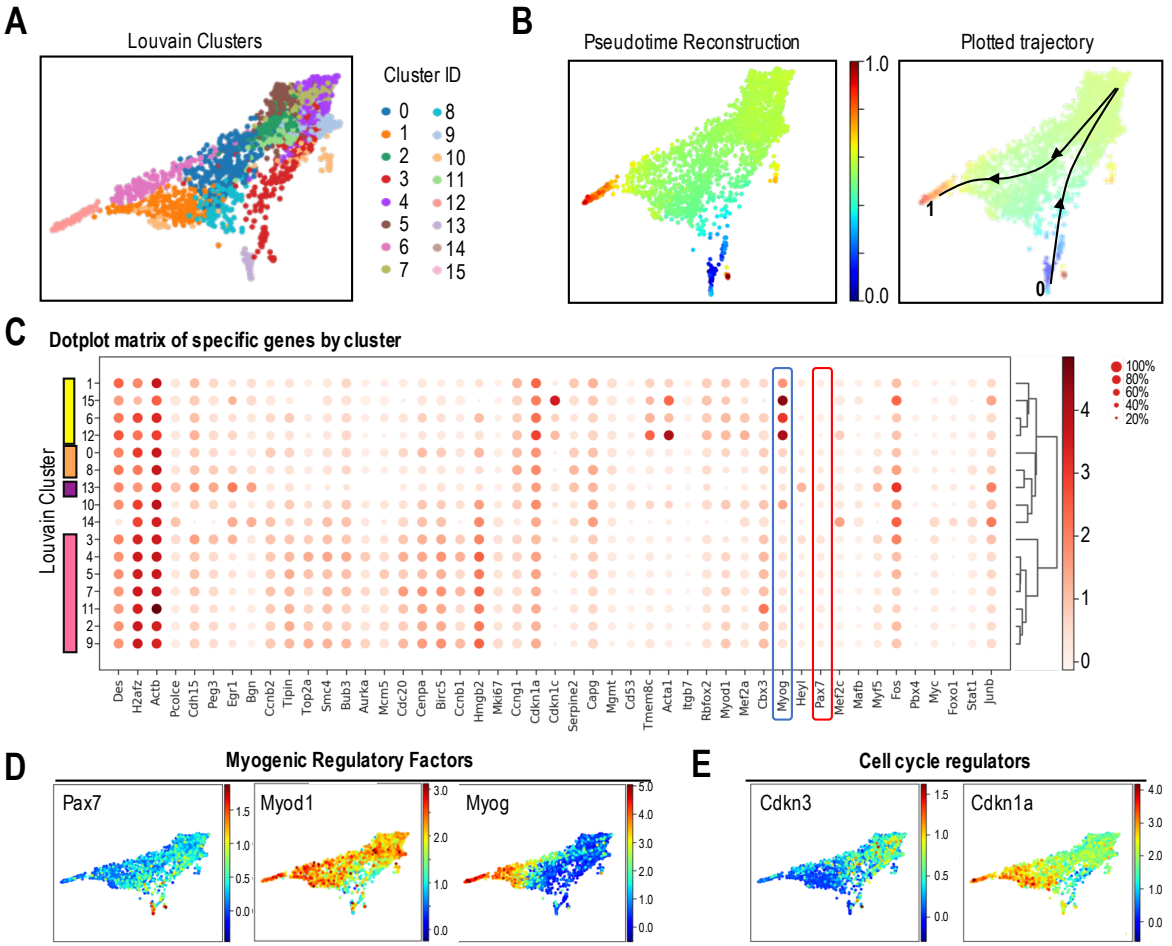

Figure 4.4 – Single cell transcriptome analysis of myogenic progenitors in regeneration. Myogenic progenitor cells (TdT^{+} AI7^{+}) were isolated from CTX injured hind-limb muscles at 72 hpi, sorted based on fluorescence, and subjected to scRNA-Seq using the 10x genomic platform. Subsequent to initial characterization with Seurat, the expression matrices of myogenic specific populations were re-processed on PAGA. ***(A)*** Myogenic cells clustered with the PAGA algorithm produces 16 different Louvain clusters on combined cell analysis for NELFb^{scKO} and WT samples. ***(B)*** Pseudotime trajectory re-construction using the PAGA algorithm shows the cell trajectory across 16 clusters from the Pax7^{+} MuSCs (blue), through to the Myog^{+} myocytes (red).***(C)*** Dotplot analysis of the 16 clusters on selected genes shows differences in Louvain cluster gene signatures. Expression mapping of ***(D)*** myogenic regulatory factors *Pax7, Myod1,* and *Myog* and ***(E)*** cell cycle regulators *Cdkn3* and *Cdkn1a* confirms the directional flow of the proposed pseudotime trajectory.

available to participate in *de novo* myofiber formation.

We next desired to look at molecular mechanisms which may lead to early terminal differentiation upon a non-functional NELF complex. To do so, we compared the relative population occupancy across the 16 Louvain clusters to identify those with a high discrepancy in the relative presence of NELFb^{scKO} and wildtype populations. This identified five key clusters enriched for either wildtype (clusters 2, 7, 9) or NELFb^{scKO} (clusters 0, 8) populations. Subsequent gene ontology analysis on the upregulated and downregulated genes which constitute these clusters was performed to identify pathways which may contribute towards early differentiation of NELFb^{scKO} populations. Clusters enriched with wildtype populations (2, 7, 9) displayed upregulation of terms which relate to the cell cycle and general proliferation (Figure 4.5C), and downregulation of genes relating to terminal differentiation. Clusters

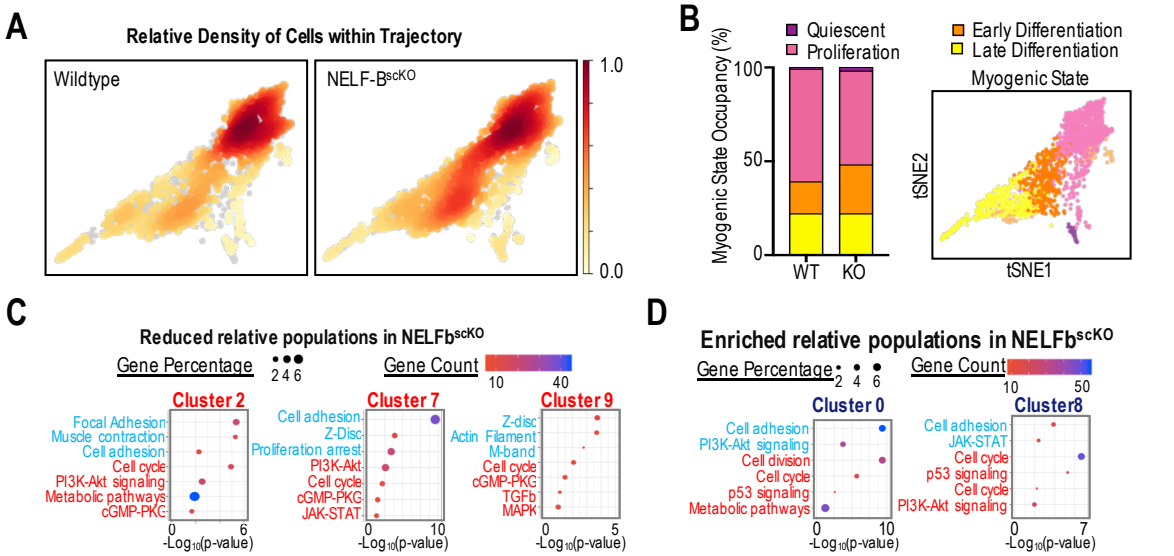

Figure 4.5 – scRNA-seq trajectory mapping indicates precocious differentiation amongst NELFb^{scKO} myogenic progenitor populations. *(A)*Density mapping of NELFb^{scKO} and WT myoblasts on the PAGA trajectory reveals differential population occupancy in clusters 0 and 8 (up in NELFb^{scKO}) as well as clusters 2, 7, and 9 (down in NELFb^{scKO}). ***(B)*** Cells were classified into different myogenic cell states based on global gene signatures representing quiescence (cluster 13), proliferation (cluster2,3,4,5,7,9,11), early differentiation (cluster 0,8), and late differentiation (cluster 1,6,12,15). (**C and D**) Gene Ontology analysis was performed on differentially expressed genes identified in the 5 clusters that were either underrepresented (**C**) or overrepresented (**D**) in NELFb^{scKO} mice. Representative upregulated (blue) and downregulated (red) GO terms are shown as a function of Log10(p-value).

enriched for NELFb^{scKO} populations (clusters 0 and 8) demonstrated an upregulation of terms which pertain to myogenic terminal differentiation, such as cell adhesion (213-218), JAK-STAT pathway (219-221) , and the PI3k-AKT pathway (222-225), while GO terms of the downregulated genes relate to the cell cycle, and cellular division (Figure 4.5D). In agreement with global population distributions (Figure 4.5A, B), this suggests NELFb^{scKO} populations are moving towards terminal differentiation while wildtype populations remain in a state of proliferation.

Collectively, the single-cell RNA-sequencing results support a mechanistic role for NELF to control the transitions from proliferation towards cell cycle withdrawal required for terminal differentiation. Because single-cell RNA sequencing offers limited sequencing resolution, higher resolution sequencing is required to understand the molecular mechanism through which NELF may controls the transition of myogenic progenitors from proliferation towards terminal differentiation.

4.3 Establishing specific molecular functions regulated by the NELF complex

4.3.1 *RNA-sequencing on myogenic progenitors captured at 48h post-injury.*

To identify early changes in gene expression from a non-functional NELF complex, RNA-seq analysis was performed on fluorescence-sorted myogenic progenitors (TdT^{+} AI7^{+}) gathered at 48 hpi. This earlier timepoint was chosen to study changes in the transcriptome upon a NELFb^{scKO} prior to these producing an observable phenotype as reported in sections 3.3.2 and 3.3.3. Initial differential gene expression analysis shows 305 upregulated and 343 downregulated genes in the NELFb^{scKO} samples when compared to wildtype controls (Figure 4.6A). Gene ontology

analysis performed on these upregulated genes returned terms which relate to skeletal muscle differentiation, extracellular matrix remodelling, and signaling pathways which typically function in terminal differentiation such as MAPK (226, 227) (Figure 4.6B, left panel). Contrarily, GO analysis of the downregulated genes suggests suppression of pathways which relate to the cell cycle, extracellular remodelling, and p53 signaling (Figure 4.6B, right panel). Together, this RNA-seq and GO analysis suggests that at 48 hpi, NELFb^{scKO} myogenic progenitors already have an aptitude towards terminal differentiation while wildtype populations gravitate towards maintenance withinin the cell cycle.

Amongst the GO terms produced, there were some contradictory results. Specifically, increased expression of genes which relate to the TGF-β pathway in NELFb^{scKO} progenitors (Figure 4.6B) seems counterintuitive as this pathway typically supports progenitor proliferation and prevents terminal differentiation (228). To investigate, we considered the specific dysregulated genes relating to the given GO terms, to identify whether they were positive or negative regulators of the pathways. Indeed, NELFb^{scKO} progenitors were marked with a general increased expression of myogenic genes typically observed during terminal differentiation such as *Myog, Mef2c, Des,* and *Mylpf* (Figure 4.6C). In addition, NELFb^{scKO} populations exhibit reduced expression of genes which sustain cellular proliferation (*Cdk6*, *Pcna*, and *CdC20*) (229-234) and upregulated expression of *Ccnd3* which supports cell cycle withdrawal prior to terminal differentiation (235-237). In addition, dysregulation of genes that function in extracellular matrix remodelling in NELFb^{scKO} progenitors included defects in expression of structural collagens *Col13a1* and *Col5a3* (238), matrix remodeling enzymes such as *Adamts1*, and genes such as *SerpinF1* which

produce the secreted protein Pigment Epithelium-Derived Factor (PEDF) (239) (Figure 4.6C). Collectively, these results demonstrate precocious differentiation upon a non-functional NELF complex occurs through early cell cycle arrest which prompts terminal differentiation. In addition, dysregulated expression of extracellular environment remodeling genes supports our prior implications of the NELF complex in remodeling the extracellular environment (section 4.1.4) to support downstream MuSC populations.

4.3.2 *Cut N Tag to identify direct NELF targets.* We next desired to identify whether the reported changes in gene expression arise from a direct loss of NELF binding, or as an indirect secondary effect produced by a loss of NELF function.

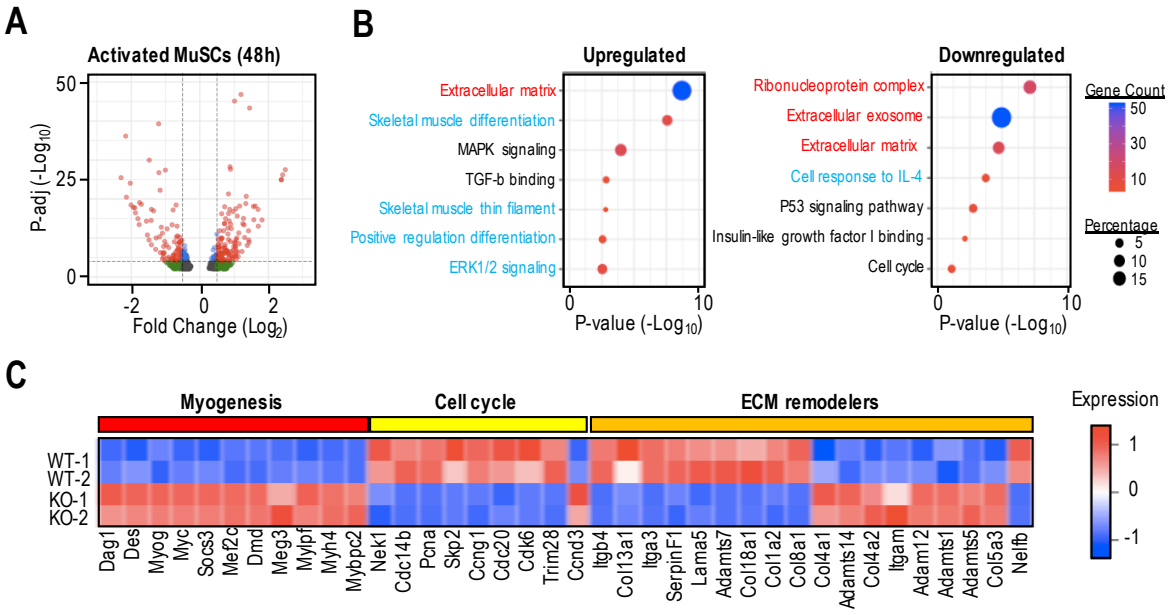

Figure 4.6 –*Transcriptome profiling of myogenic progenitors during early regeneration.* RNA-seq analysis performed on fluorescence-sorted NELFb^{scKO} and WT myogenic progenitors (TdT^{+} AI7^{+}) isolated from skeletal muscle at 48 hpi using an adjusted p-value < 0.01 as a cutoff. ***(A)*** Data represented as a Volcano plot shows 305 upregulated and 343 downregulated genes. ***(B)*** Representative GO terms of upregulated and downregulated genes upon a NELFb^{scKO} are represented as biological processes (blue), cell component (red), or Kegg pathway (black). ***(C)*** Heatmap plot for select genes are grouped on their contributions towards myogenesis, cell cycle regulation, and ECM remodeling.

To do so, we identified the direct NELF target genes by Cut & Tag using a dual-antibody approach to target the NELFe subunit (240) on cultured wildtype myoblasts (Figure 4.7A). Because the NELF complex may help pause Pol II at DNA double-stranded break repair in the gene body (241, 242), analysis of the sequencing results was confined to the promoter-proximal region. Subsequent overlap analysis between genes with promoter-proximal bound NELF to the differentially expressed genes in response to a NELFb^{scKO} identified direct NELF target genes which may evoke precocious differentiation. To investigate potential pathways, we performed GO analysis on these NELF target genes which are either upregulated or downregulated in response to a NELFb^{scKO} (section 4.3.1). The GO terms of the upregulated genes strongly related to terminal differentiation (Figure 4.7B) and encompass genes such as *Des, Myog,* and *Mylpf,* in addition to the cell cycle withdrawal gene *Ccnd3* (Figure 4.7C). Similarly, GO analysis of the downregulated NELF target genes produced terms relating to proliferation and mitosis (Figure 4.7B), owing to reduced expression of genes which promote cell cycle maintenance such as *Pcna, Cdc20,* and *Cdk6* (Figure 4.7C). In addition, direct NELF target genes which relate to extracellular remodelling were both upregulated (*Adamts1, Col5a3*) and downregulated (*SerpinF1, Col13a1*) (Figure 4.7C). Collectively, this data supports a direct role of NELF to regulate the expression of genes which favour maintenance within the cell cycle, and in extracellular remodelling.

4.3.3 *PRO-seq supports a role for NELF to stabilize rather than pause Pol II.*

To interrogate how a non-functional NELF complex affects Pol II activity and the resulting changes in gene expression, we proceeded to precisely map global Pol II positioning on cultured myoblasts derived from NELFb^{scKO} and wildtype populations using Precision Run-On sequencing (PRO-seq). This modified nuclear run-on assay uses biotin-labelled RNA precursors pulsed in permeabilized nuclei so that capture and sequencing of the biotin-labelled RNA transcripts can be used to map global Pol

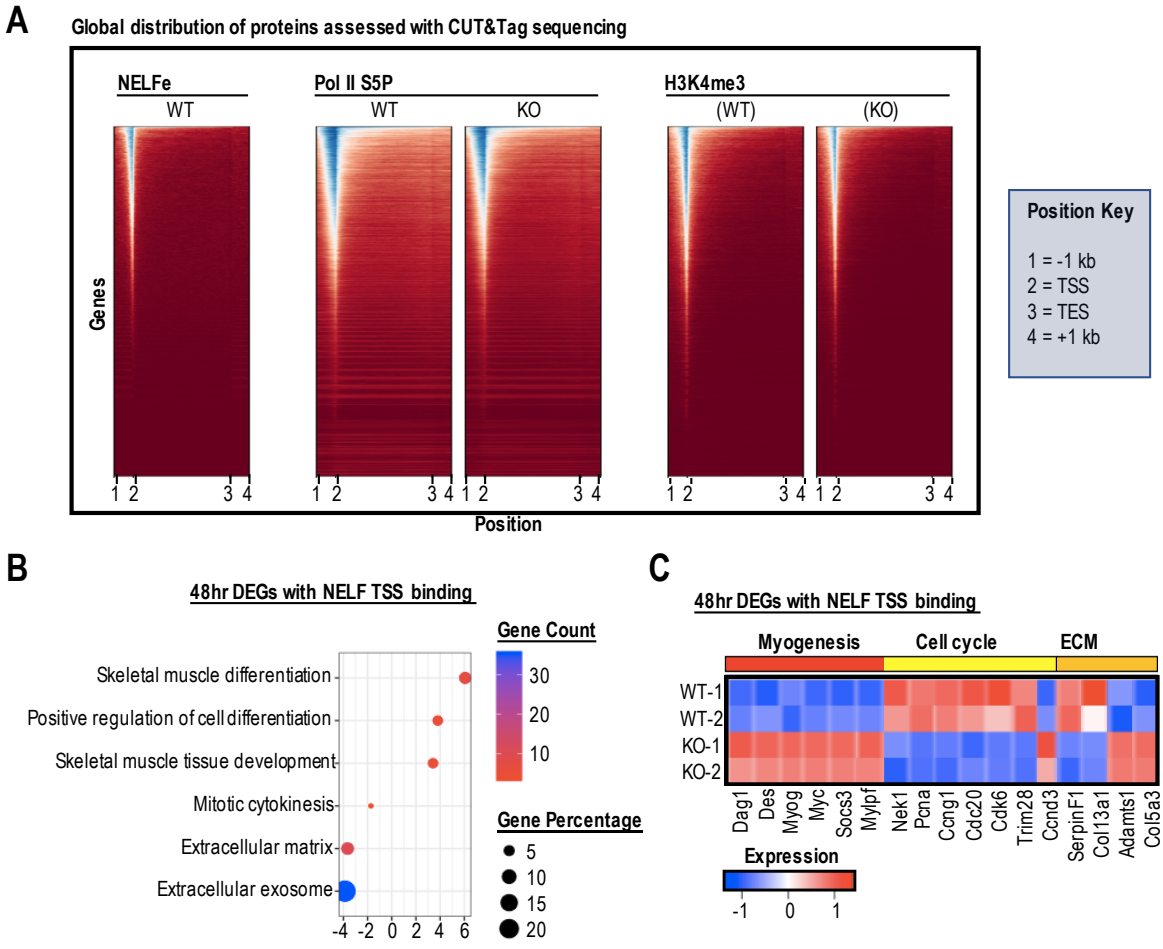

Figure 4.7 – Mapping NELF binding sites and inferring genes directly regulated by NELF. ***(A)*** CUT&Tag coupled with deep-sequencing was used to map global positioning of NELFe, Pol II S5P, and H3K4me3 marks. Data represented as global distribution plots between -1kb to +1kb relative to the TSS according to the position key (right). ***(B)*** Representative GO terms of genes with NELF bound in the promoter proximal region which are dysregulated in response to a NELFb^{scKO}. ***(C)*** Heatmap of select dysregulated NELF target genes grouped on their effect on myogenesis, cell cycle, and ECM remodelling.

II occupancy with single nucleotide resolution. Further, the transcript abundance is directly representative of Pol II abundance and activity, where elevated transcript content signals high Pol II density, and low transcript abundance denotes low Pol II density within the genomic region (88, 152, 243). In addition, comparative analysis between PRO-seq and RNA-seq datasets obtained in parallel conditions means the activity of Pol II within the promoter proximal region can be overlapped with RNA-sequencing. Thus, this can identify how a NELFb^{scKO} affects Pol II activity, and whether NELF stabilizes transcripts to promote their expression, or acts to block their active elongation (reviewed in section 1.3).

First, we focused on the effects of a NELFb^{scKO} on Pol II activity in genes which are specifically downregulated in response to a NELFb^{scKO}. Doing so reveals a reduced abundance of nascent transcript at both the TSS (Figure 4.8A), and within the gene body (Figure 4.8C). This suggests that in response to a non-functional NELF complex, the promoter proximal paused Pol II within these genes becomes destabilized and prone to abortive transcription, as explained in section 1.3.2. In addition, the reduced PRO-seq signal within these genes correlates with a reduced presence of both serine-5 phosphorylated RNA Pol II, and the histone mark H3K4me3 (Figure 4.7A), which are marks which denote paused promoter proximal Pol II and transcriptionally active genes, respectively. Thus, this signifies that genes which are downregulated in response to a non-functional NELF complex arises from destabilized Pol II in the promoter-proximal region which becomes susceptible to abortive transcription. In turn, this may promote gene silencing through reduced recruitment of general transcription factors and nucleosome encroachment, which leads to general downregulation and suppression, as introduced in section 1.3.4.

Next, we considered the PRO-seq signal at genes which are upregulated in response to a NELFb^{scKO}. This shows no significant difference within the abundance of Pol II accumulated at the TSS (Figure 4.8B), nor within the gene body (Figure 4.8C) when compared to the wildtype control PRO-seq signal. In addition, presence of H3K4me3 suggests these genes are transcriptionally active in response to a non-functional NELF complex. Taken together, this data supports that the upregulated expression of these genes in response to a NELFb^{scKO} occurs from a quicker release of paused Pol II from the promoter proximal region, without increasing the abundance of Pol II recruited within these regions. Thus, this supports an inhibitory role of NELF which binds promoter proximal paused Pol II to prevent the expression of these genes, so that a non-functional NELF complex allows release of promoter-proximal paused Pol II towards active elongation.

4.3.4 ***RNA-sequencing of cultured myogenic progenitors.*** During the PRO-seq experiments, RNA-seq analysis was performed on an adjacent population of NELFb^{scKO} and wildtype cultured myoblasts. Differential gene expression analysis

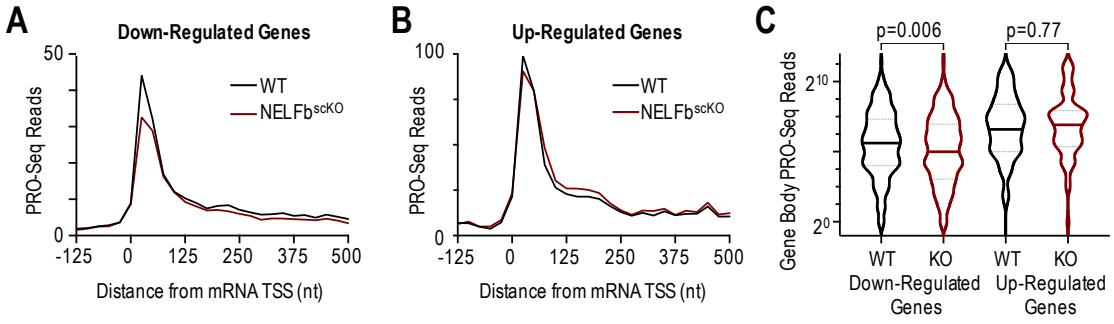

Figure 4.8 – Precision Run-On sequencing maps changes in global Pol II activity in response to a NELFb^{scKO}. Precision Run-On sequencing mapped onto RNA-sequencing results obtained from NELFb^{scKO} and WT cultured myoblasts show that ***(A)*** downregulated genes in the NELFb^{scKO} myoblasts have decreased nascent transcript levels at the promoter-proximal region as well as ***(C)*** the gene body (p-value = 0.006). ***(B)*** Genes which are upregulated in response to a NELFb^{scKO} show no significant change in nascent transcript levels compared with WT controls (p-value = 0.77), ***(C)*** nor in gene body occupancy.

identified 102 upregulated and 441 downregulated genes in NELFb^{scKO} populations when compared to the wildtype controls (Figure 4.9A). Gene ontology analysis of upregulated genes produced terms consistent with those obtained from myogenic progenitors collected at 48 hpi, including MAPK signaling, negative regulation of TGFβ, and skeletal muscle differentiation (Figure 4.9B, left panel). Similarly, GO analysis on the downregulated genes upon a NELFb^{scKO} produced terms relating to extracellular remodelling and cellular proliferation (Figure 4.9B, right panel). This data supports the previous conclusions (section 4.3.1), where dysregulated gene expression upon a NELFb^{scKO} causes cell cycle withdrawal and commitment to terminal differentiation, while dysregulation of genes pertaining to extracellular environment remodelling may prevent MuSC self-renewal. Thus, the early changes in gene expression which arise from a NELFb^{scKO} as early as 48 hpi may compound in later stages of proliferation to elicit precocious differentiation and defects in extracellular environment remodelling.

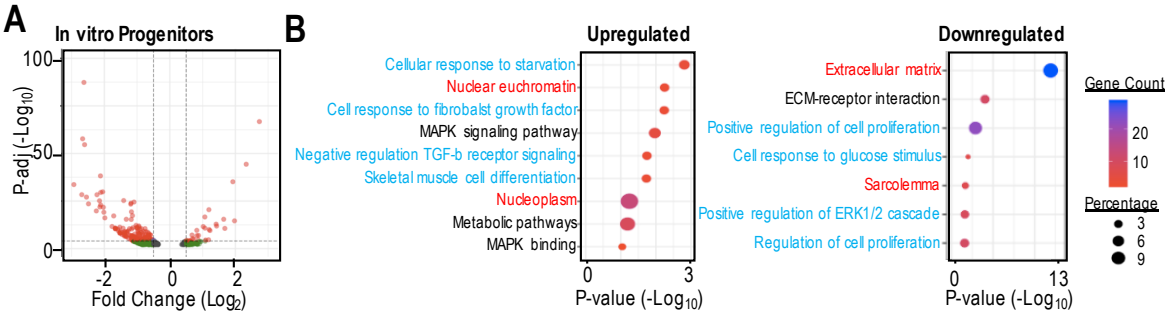

Figure 4.9 – Transcriptome profiling of cultured primary myogenic progenitors. RNA-seq analysis performed on cultured primary myoblasts derived from NELFb^{scKO} and WT mice, using an adjusted p-value < 0.01 as a cutoff shows 441 downregulated and 102 upregulated genes ***(A)*** Data represented as a Volcano plot; ***(B)*** Representative GO terms from upregulated and downregulated genes upon a NELFb^{scKO} show processes of biological processes (blue), cell component (red), or Kegg pathway (black).

4.4 Role of NELF in pathway regulation during skeletal muscle regeneration.

Collectively, the characterized phenotype and molecular analysis suggests NELF influences gene expression in two distinct pathways to support skeletal muscle regeneration. First, NELF regulates the expression of genes which favors myogenic cells to remain engaged in the cell cycle. This produces a massive expansion in myogenic progenitor populations to (I) adequately repair damaged myofibers, and (II) permit proliferating myogenic progenitors to rejuvenate the extracellular environment to support downstream MuSC self-renewal. Secondly, NELF directly regulates the expression of genes which rejuvenate the extracellular environment, which further supports downstream MuSC self-renewal in the regenerated environment. When NELF is rendered non-functional, dysregulated expression of genes relating to both these pathways culminates in fewer myogenic cells available to repair damaged myofibers, and a niche environment which cannot support MuSC self-renewal. To validate the proposed role of NELF in these pathways, we performed independent rescue experiments targeted towards each of the pathways.

4.4.1 ***NELF controls expression of cell cycle regulators to effect cell cycle withdrawal.*** Direct NELF target genes which are dysregulated in NELFb^{scKO} myogenic cells can be grouped as those which are either upregulated or downregulated in response to a non-functional NELF complex. Doing so reveals that genes which favours maintenance within the cell cycle such as *Ccng1, Pcna,* and *Cdc20*, are downregulated, while those which promote cell cycle withdrawal (*Cdkn1a, Ccnd3*) and terminal differentiation (*Myog*) are upregulated (Section 4.3.1). Thus, considering the temporal order of gene expression which accompanies myogenic cell

state changes suggests the reduced expression of cell cycle promoting genes may therefore initiate precocious differentiation, which is closely followed by upregulated expression of the cell cycle withdrawal and terminal differentiation genes.

Focusing on the downregulated NELF target genes reveals a reduced expression of *Ccng1*, which is a regulator of the p53 pathway which is well-known to elicit terminal differentiation during myogenesis (244-246). Here, Cyclin G1 dephosphorylates to activate the ubiquitin ligase MDM2, which ubiquitinates p53 so that p53 levels remain low (Figure S4.3A). In the absence of Cyclin G1, MDM2 remains in an inactive phosphorylated state, so it can no longer ubiquitinate p53, and this causes p53 protein levels to elevate (Figure S4.3B). In turn, p53 activates its target genes which includes *Cdkn1a,* and this produces the p21 protein to induce cell-cycle arrest. Thus, the reduced expression of *Ccng1* in NELFb^{scKO} populations could therefore cascade towards an increase in p53 to prompt cell cycle withdrawal and precocious differentiation. Indeed, deep-sequencing results supports *Ccng1* is a direct NELF target, where a NELFb^{scKO} reduces promoter-proximal paused Pol II (PolII-S5P), and decreases expression of *Ccng1* (Figure S4.4). This culminates in increased expression of p53, which drives production of p21 (Figure S4.5) to initiate precocious differentiation.

To investigate whether precocious differentiation of NELFb^{scKO} myogenic progenitors can be rescued through the p53 pathway, we cultured primary myoblasts in the presence of the p53 molecular inhibitor pifithrin-α, and measured proliferation through an EdU incorporation assay. A similar abundance of EdU^{+} myoblasts in NELFb^{scKO} and wildtype populations treated with pifithrin-α (Figure 4.10) suggests that a block in the activity of p53 rescues the precocious differentiation typically observed

in NELFb^{scKO} myoblasts. In addition, pifithrin-α treatment had no significant effect on the proliferation of wildtype myoblasts when compared to vehicle-treated controls, while the proliferation of untreated NELFb^{scKO} myoblasts remained significantly inferior to that of the untreated wildtype controls (Figure 4.10). This suggests that early expression of p53 may be responsible for the precocious differentiation of NELFb^{scKO} myogenic progenitors.

Next, pifithrin-α treatment was assessed *in vivo* to determine if blocking p53 could rescue the skeletal muscle regeneration defect previously described for NELFb^{scKO} mice. To do so, NELFb^{scKO} and wildtype mice were either provided pifithrin-α or a vehicle control at 40 hpi, 64 hpi, and 88 hpi, then assessed for total regeneration at a time of 7 dpi. Characterization of the regenerated TA through minimal Feret diameter measurements reveals a partial but significant rescue in the myofiber diameter of treated NELFb^{sckO} compared to the untreated population (Figure 4.11A).

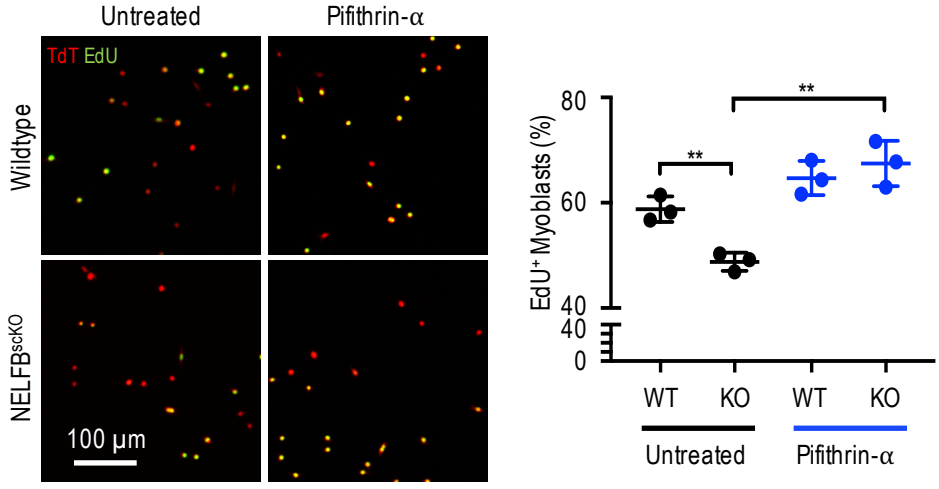

Figure 4.10 – Culturing primary myoblasts with pifithrin-α rescues proliferation of NELFb^{scKO} populations. Cultured primary myoblasts from NELFb^{scKO} and wildtype mice were induced with 4-OHT (72h), then treated with either pifithrin-α (27 μM) or a DMSO vehicle control (48h). Proliferation assessed through an EdU incorporation assay shows proliferation of vehicle-treated NELFb^{scKO} populations [48.79 ± 0.9975, n=3] are significantly reduced to that of vehicle-treated wildtype controls [58.79 ± 1.396, n=3]. Treatment with pifithrin-α significantly increases the proliferation of NELFb^{scKO} populations [58.92 ± 1.681, n=3], while having no significant effect on the proliferation of wildtype populations [62.56 ± 2.703, n=3].

This suggests the NELFb^{scKO} myogenic progenitors underwent extended proliferation *in vivo*, which allowed a higher abundance of myocytes to participate in myofiber repair. In addition, treatment with pifithrin- α had no effect on myofiber diameter of wildtype populations when compared to untreated wildtype controls. Because proliferating myogenic progenitors may rejuvenate the niche environment in support of MuSC self-renewal (section 4.1), we further quantified the abundance of Pax7^{+} MuSCs normalized to the amount of myofibers within a field of view. Indeed, a partial but significant increase in the abundance of Pax7^{+} MuSCs is apparent in the regenerated skeletal muscle of pifithrin-α treated NELFb^{scKO} mice when compared to untreated NELFb^{scKO} controls, whereas pifithrin-α had no effect on the MuSC populations of the wildtype groups (Figure 4.11B, S4.6). This suggests that pifithrin-α does not directly impact MuSC populations, rather the partial rescue in proliferation

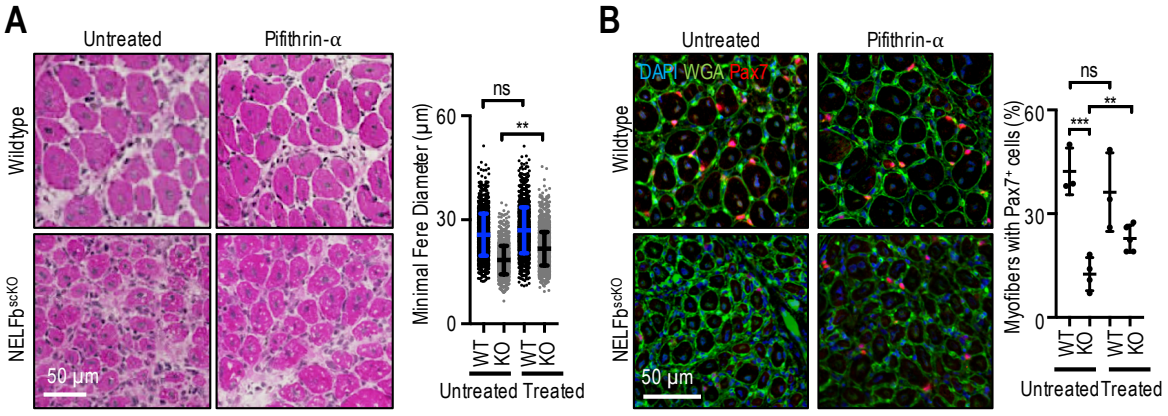

Figure 4.11 – Pfithrin-α administered during skeletal muscle regeneration yields a partial rescue in myofiber diameter and Pax7^{+} populations in NELFb^{scKO} populations. Tamoxifen-induced NELFb^{scKO} and wildtype mice received treatment with a vehicle control or pifithrin-α during skeletal muscle regeneration, and the regenerated TA isolated at 7 dpi for characterization. ***(A)*** Hematoxylin & Eosin staining of cross-sections obtained from the regenerating TA. Minimal Feret diameter measurements shows a significant increase in the myofiber diameter of the regenerated TA of NELFb^{scKO} populations treated with pifithrin-α [22.81 ± 1.747, n=5] compared to the NELFb^{scKO} populations which received an vehicle control [12.53 ± 2.386, n=4]. Treatment with pifithrin-α did not produce a significant difference in the myofiber diameter of wildtype populations [26.99 ± 0.4838, n=3] when compared to vehicle-treated controls [25.69 ± 1.602, n=3]. ***(B)*** Immunofluorescent staining identified the abundance of Pax7^{+} cells normalized to the abundance of myofibers within a field of view. Treatment of NELFb^{scKO} populations with pifithrin-α significantly increases the normalized abundance of Pax7^{+} populations [22.81 ± 1.747, n=5] compared to vehicle-treated NELFb^{scKO} populations [12.53 ± 2.386, n=4], while pifithrin-α treatment of wildtype populations causes no significant difference of normalized Pax7^{+} populations [36.24 ± 6.564, n=3] compared to vehicle-treated controls [42.23 ± 3.889, n=3]. Individual immunofluorescence fields are shown in Figure S4.6.

permits increased time for niche environment rejuvenation by myogenic progenitors, which permits downstream MuSC self-renewal. These rescue experiments support precocious differentiation of NELFb^{scKO} myogenic progenitors occurs in response to dysregulated expression of *Ccng1*, which prompts cell cycle withdrawal through a p53-dependent pathway.

4.4.2 *NELF directly controls the expression of niche rejuvenation factors for MuSC self-renewal.* During analysis of allograft transplant experiments (section 4.1) we noted a remarkable positive correlation which suggested proliferating myogenic progenitors actively reformulate the extracellular niche environment to support downstream MuSC self-renewal (section 4.1.2, 4.1.3). Further, deep-sequencing analysis showed NELF directly controls the expression on some of these environment remodelling factors. This included *SerpinF1* which produces the PEDF protein which is known to affect cellular behavior through anti-angiogenic , (247, 248), anti-tumorigenic (249, 250), neurotrophic (251) (252), and myogenic effects (239, 253). Thus, we reasoned that the reduced expression of *SerpinF1* in NELFb^{scKO} myogenic progenitors could also contribute to a diminished niche environment which is incapable to support downstream MuSC self-renewal during regeneration.

To investigate, we provided intramuscular PEDF to the regenerating TA of NELFb^{scKO} and wildtype mice at 3dpi and 5dpi, then characterized the regenerated skeletal muscle at 7dpi. Because PEDF had no significant effects on myofiber diameter in NELFb^{scKO} and wildtype populations (Figure 4.12A) suggests this factor does not affect the myogenic progenitor proliferation, and therefore does not influence *de novo* myofiber diameter. However, immunofluorescence analysis does reveal a

significant increase in the normalized abundance of Pax7^{+} MuSC populations in the regenerated TA of NELFb^{scKO} mice compared to vehicle treated NELFb^{scKO} controls. In addition, PEDF has no effect on Pax7^{+} MuSC populations in the regenerated TA of wildtype mice when compared to those of vehicle-treated wildtype controls (Figure 4.12B, S4.7). This implies a direct role for PEDF to promote MuSC self-renewal, which is directly regulated by NELF. Thus, this supports a role for NELF in myogenic progenitors to regulate the expression of genes which remodel the niche environment to promote downstream MuSC self-renewal, which occurs as an independent process from myogenic progenitor proliferation.

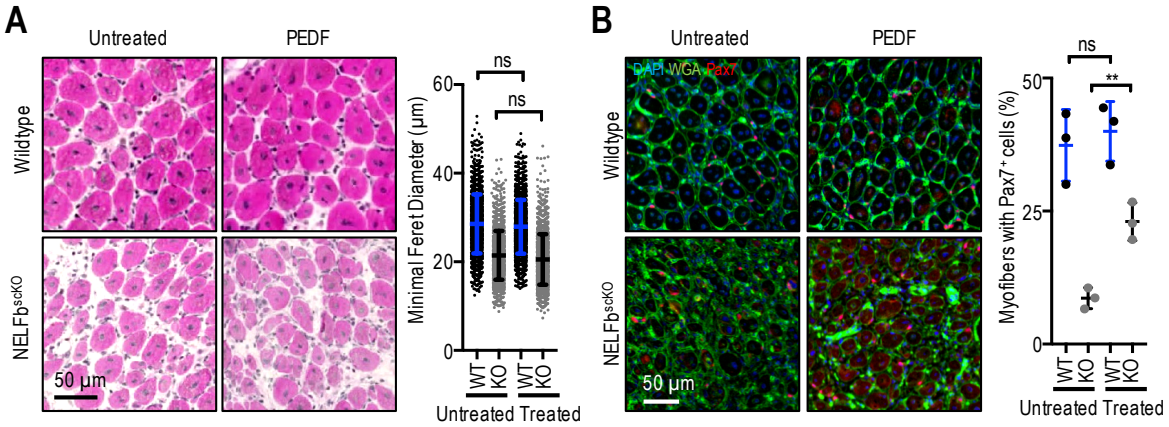

Figure 4.12 – PEDF supplemented to the regenerating skeletal muscle environment increases regeneration. Subsequent to tamoxifen-induced Cre-recombination, the TA of NELFb^{scKO} and WT mice was injured with intramuscular injury, and supplemented with intramuscular PEDF (50µM) in 2% alginate solution, or a vehicle control at 24 hpi and 48 hpi. Regenerated TA isolated at 7 dpi are characterized. ***(A)*** Hematoxylin & Eosin stain of the cross-sections shows there is no significant difference in the minimal Feret myofiber diameter of NELFb^{scKO} populations whether treated with PEDF [20.59 ± 1.368, n=3] or a vehicle control [21.51 ± 0.857, n=3]. Similarly, there is no significant difference in myofiber diameter of wildtype populations treated with PEDF [27.94 ± 0.9834, n=3] compared to vehicle controls [28.56 ± 0.6189, n=3]. ***(B)*** Immunofluorescence of the cross-sections was used to quantify the abundance of Pax7^{+} cells normalized to the abundance of myofibers within a field of view. Upon PEDF treatment, NELFb^{scKO} populations shows a significant increase in the normalized abundance of Pax7^{+} cells [23.03% ± 2.046, n=3] compared to vehicle-treated controls [10.54% ± 2.069, n=3], while PEDF had no significant effect on the abundance of Pax7^{+} populations [39.99% ± 3.239, n=3] compared to vehicle-treated controls [37.36 % ± 3.896, n=3]. Individual immunofluorescence fields are shown in Figure S4.7.

4.5 – Discussion

4.5.1 *The NELF complex does not influence cell state transitions of quiescent and activated MuSCs.*

The reduced abundance of MuSC populations in regenerated skeletal muscle of NELFb^{scKO} (section 3.5.1) prompted us to further investigate *how* a NELFb^{scKO} may affect MuSC self-renewal using a series of allograft transplant experiments. Considering the behavior of donor MuSCs during allograft transplantations, they are known to engraft and proliferate to establish a zone of homeostasis within their transplanted region (199). Understanding that the extracellular environment strongly influences MuSC activity (section 1.1.3), this means that differences in progenitor proliferation while establishing homeostasis could influence downstream MuSCs self-renewal. Thus, to account for the inherent reduced proliferation caused by a NELFb^{scKO} (section 3.3.3) and its potential impact to affect donor MuSC self-renewal, we decided to normalize the abundance of donor-derived MuSCs to the established zone of homeostasis, denoted by TdT^{+} host myofibers, and termed this parameter the normalized replenishment capacity.

Upon transplantation of quiescent MuSCs in the undamaged host TA, there was no significant difference in the normalized replenishment capacity of NELFb^{scKO} and wildtype donors. This suggests that NELFb^{scKO} MuSCs have an equal ability to engraft and undergo self-renewal than their wildtype counterparts. In addition, there were no significant differences within the normalized replenishment capacity when activated MuSC donors were transplanted into a healthy host muscle. This equally suggests that the NELF complex does not influence the ability of activated MuSCs to return to a dormant state. Thus, this data suggests the NELF complex poses no

influence on the cellular activity of MuSCs regarding their activity prior to entering the cell cycle, and therefore has no influence on cellular activity of MuSCs in quiescence and activated states, nor in MuSC self-renewal.

4.5.2 *NELF controls the expression of extracellular remodelling genes.*

When quiescent MuSCs were transplanted into a regenerating host milieu, we observed a significantly reduced normalized replenishment capacity of NELFb^{scKO} donors compared to wildtype donors. This suggests that MuSC self-renewal is impaired even when accounting for the reduced proliferation of myogenic progenitors in response to a non-functional NELF complex. Because NELF does not inherently affect MuSC self-renewal, this suggests a defect in the extracellular environment is affecting the ability of donor MuSCs to undergo self-renewal. In addition, we may exclude the effects of pre-existing niche factors and accessory cell types to influence MuSC self-renewal, as the NELFb^{scKO} and wildtype donors were transplanted into the contralateral TA of a same host NSG mouse, meaning they are exposed to near-identical extracellular conditions upon transplant. Thus, the only variable in the transplant experiments remains with the donor populations, and these only differed in the function of the NELF complex. This presents the possibility that the NELFb^{scKO} MuSC donors have an impaired ability to reformulate their extracellular environment during acute injury, beyond that arising from their reduced proliferation. This supposes that gene dysregulation from a NELFb^{scKO} causes aberrant expression of genes which reformulate the extracellular environment, and this produced the reduced normalized replenishment capacity of the NELFb^{scKO} donors when transplanted into a regenerating host milieu.

Indeed, subsequent deep-sequencing experiments do show NELF directly regulates the expression of several genes which reformulate the extracellular environment. Amongst these genes was downregulation of *SerpinF1,* which produces the PEDF protein that is a known influencer of cellular activity (239, 247-253). When PEDF is supplemented to the regenerating skeletal muscle environment, it produced a partial rescue in the abundance of endogenous MuSC populations in NELFb^{scKO} muscle, with no effect on wildtype controls. This supports a role for NELF to directly control the expression of genes which remodel the extracellular environment, and this permits downstream MuSC self-renewal. While the dysregulation of these genes did not appear to affect self-renewal of NELFb^{scKO} donors transplanted to an undamaged host environment, this is likely because host factors present within the undamaged niche environment were able to compensate and promote MuSC self-renewal.

While we can exclude the function of NELF in affecting MuSC self-renewal, it remains unclear whether the differences in MuSC population arose from an inability of MuSC to undergo self-renewal, or from a hostile niche environment which could not retain MuSCs in a quiescent state. To investigate, an extended EdU exposure should be provided to host mice between 5 days – 10 days following allograft transplant, reminiscent to an experiment previously described (24). Doing so would incorporate EdU into the nucleus of MuSCs as they divide during self-renewal, so that quiescent MuSC populations can be differentiated as those that arose from donor self-renewal (Pax7^{+}, TdT^{+}, EdU^{+}) versus those which engrafted and did not divide (Pax7^{+}, TdT^{+}, EdU^{-}). Comparative analysis of the abundance of self-renewing MuSCs versus those which engraft with no proliferation to the normalized engraftment capacity would

identify whether the depleted niche environment upon a NELFb^{scKO} impairs MuSC self-renewal or maintenance within a quiescent state in the host environment.

4.5.3 NELF supports promoter proximal Pol II pausing during chromatin rearrangements. The role of NELF to stabilize promoter proximal paused Pol II (80) may permit a period for regulatory signals to integrate (99), and control the ability of Pol II to express a specific gene. When NELF is associated with Pol II, it largely prevents Pol II from escaping into the gene body, which may be a regulatory step to permit chromatin rearrangement and render the downstream genes more permissive. Upon recruitment of pTEFb, NELF is disengaged and Pol II proceeds into the gene body. By remaining associated with Pol II and stabilizing it towards elongation through Ser2 phosphorylation of the Pol II CTD, this confers stability to permit Pol II elongation and subsequent gene expression.

The role of NELF has been proposed to both (I) stabilize Pol II against abortive transcription by the integrator complex in support of gene expression, and (II) to prevent Pol II release into the gene body, as a transcriptional inhibitor (section 1.3). Thus, when NELF is depleted, the fate of the promoter proximal paused Pol II may either proceed towards active gene expression or towards promoter-proximal termination (80). Here, the fate of Pol II may largely depend on the epigenetic signature of the gene (254). Permissive genes with low thermodynamic barriers would remain susceptible to active elongation, so that an increased expression occurs upon a non-functional NELF complex. Genes with thermodynamic barriers such as tightly bound nucleosomes, repressive histone marks, and other inhibitory factors may present a high thermodynamic barrier to Pol II upon its release into the gene body.

Here, Pol II may not be able to overcome these steric and thermodynamic barriers which entice Pol II termination (51, 80), potentially mediated through endonuclease cleavage by the integrator complex, as described in section 1.3. In addition, Pol II escape in response to a non-functional NELF complex may not be bound by pTEFb so that the CTD Ser2 remains un-phosphorylated. This further destabilizes Pol II, which may be more susceptible to transcription termination when faced with destabilizing factors on the gene body.

In the case of a non-functional NELF complex generated by a NELFb^{scKO}, our sequencing data shows Pol II undergoes both active elongation and promoter-proximal termination at NELF target genes, with a bias of the gene class. Specifically, Pol II termination was predominant at genes which promote maintenance within the cell cycle, while active elongation was observed at genes which promote cell cycle arrest and terminal differentiation. This may arise from early rearrangements in the chromatin landscape as activated MuSCs become engaged in the cell cycle (51, 255). As an example, cell cycle maintenance genes are typically marked with activating H3K4me3 marks on their nucleosomes during the early stages of myogenic progenitor proliferation (256), to assure their expression and maintenance within the cell cycle (255). Therefore, a loss of functional NELF at these genes would permit Pol II escape prior to chromatin rearrangements. However, as Pol II encounters thermodynamic barriers it could prompt abortive transcription which would prevent gene expression.

The ability of escaped Pol II to undergo active elongation amongst genes which participate towards terminal differentiation may additionally arise from early changes to the chromatin networks. Indeed, a recent study suggests Pax7 directs changes in chromatin looping networks to prime genes required for terminal differentiation (66).

Thus, this open chromatin state could be conducive towards active Pol II elongation early in proliferation, so that ablated NELF permits Pol II escape into permissive chromatin which supports active elongation. Additionally, this early expression of genes implicated in terminal differentiation such as *Myog* would further contribute to cell cycle withdrawal. Specifically, Myog induction of p21 would coax cell cycle and terminal differentiation, whilst diminishing the expression of cell cycle promoting genes.

While the above scenarios remain speculative, the correlation between gene class and the fate of escaped Pol II in response to non-functional NELF remains an interesting observation. Future comparative investigations to consider NELF binding sites, chromatin accessibility with ATAC-seq, and the fate of the escaped Pol II in response to a non-functional NELF complex may clarify whether NELF exerts Pol II pausing to regulate between chromatin rearrangements and transcription regulation. Additional bioinformatics comparisons to accessible databases such as ENCODE (257, 258) will provide additional insight into spatio-temporal interactions between chromatin rearrangements and transcriptional control evoked by NELF. Lastly, bioinformatics modelling to consider the spatio-temporal activity of chromatin modifiers along myogenic cell state changes in conjunction with changes in chromatin and Pol II processivity will help shape the regulatory network which ties chromatin accessibility and the resulting activity of Pol II.

4.5.4 NELF acts as a point of convergence between multiple signaling pathways to initiate terminal differentiation and acts in a feed-forward loop.

The ability of NELF to control the onset of terminal differentiation was proposed

to proceed through direct regulation of *Ccng1* expression, which is an upstream regulator of p53. Indeed, a block in p53 activity did extend myoblast proliferation, which supports a mechanism of action where NELF can initiate terminal differentiation by regulating the abundance of p53 regulators. This remains interesting, given several signaling pathways in myogenesis are known to relay extracellular signals to induce terminal differentiation by modulating the activity of p53, such as PI3K/Akt, MAPK, and JAK/STAT signaling pathways (259-261). This presents an interesting possibility when considering the general function of NELF to control rapid changes in gene expression in response to extracellular stimulus, and the proposed ability of NELF to induce terminal differentiation through p53 signaling. Here, extracellular signals may activate diverse signaling pathways, which culminate in dissociation of NELF and subsequent gene dysregulation which favours accumulation of p53 to evoke cell cycle withdrawal and commitment to terminal differentiation.

Gene ontology analysis of dysregulated genes in NELFb^{scKO} samples revealed prevalent upregulation of signaling pathway components known to entice myogenic progenitors towards terminal differentiation. This included genes relating to the JAK-STAT (219-221) , PI3k-AKT (222-225), and MAPK (226, 227) pathways. This presents an interesting implication of NELF to support the onset of terminal differentiation. As a release of NELF starts priming cells towards cell cycle withdrawal, this also causes increased expression of functional components of signaling pathways which prompt terminal differentiation. In turn, this may potentiate the cellular response towards extracellular signaling, in a type of feed-forward loop which assures commitment to terminal differentiation. This remains an interesting possibility owing to previous

studies that have demonstrated the importance of NELF to mitigate gene expression in response to extracellular signals (section 1.3).

Lastly, while a block in p53 activity did provide a partial rescue in myogenic progenitor proliferation, it did not rescue myofiber size to that of wildtype controls. This could arise from an unoptimized protocol, or because NELF may additionally induce terminal differentiation through a p53-independent pathway. Therefore, while the activity of p53 is blocked, these dysregulated p53-independent pathways could still entice cell cycle withdrawal and precocious terminal differentiation. To investigate, shRNA silencing could be used to eliminate p53 and abolish p53-mediated cell cycle withdrawal. From here, the ability of NELFb^{scKO} and wildtype populations could be assessed for their ability to undergo terminal differentiation. If the NELFb^{scKO} populations still undergo precocious differentiation compared to the controls, this would support the ability of NELF to initiate cell cycle withdrawal and terminal differentiation through a p53-independent pathway.

4.5.5 *General conclusions*

Results presented within this chapter describe an important role of NELF to retain myogenic progenitors in an expansive state. Doing so accomplishes two critical components to effectuate skeletal muscle regeneration. As a direct effect, population expansion assures sufficient myocytes are present for *de novo* myofiber fusion. As an indirect effect, the sustained proliferation allows myogenic progenitors to reformulate the niche environment in support of MuSC self-renewal during regeneration. In addition, NELF regulates the expression of genes to assure rejuvenation of the extracellular environment to promote MuSC self-renewal (Figure 4.13). At the

molecular level, NELF appears to stabilize promoter proximal Pol II of many genes to retain myogenic progenitors in a proliferating state. Upon terminal differentiation, various signaling pathways may converge to induce a release of NELF from promoter proximal paused Pol II, and initiate the expression of gene programs required for terminal differentiation.

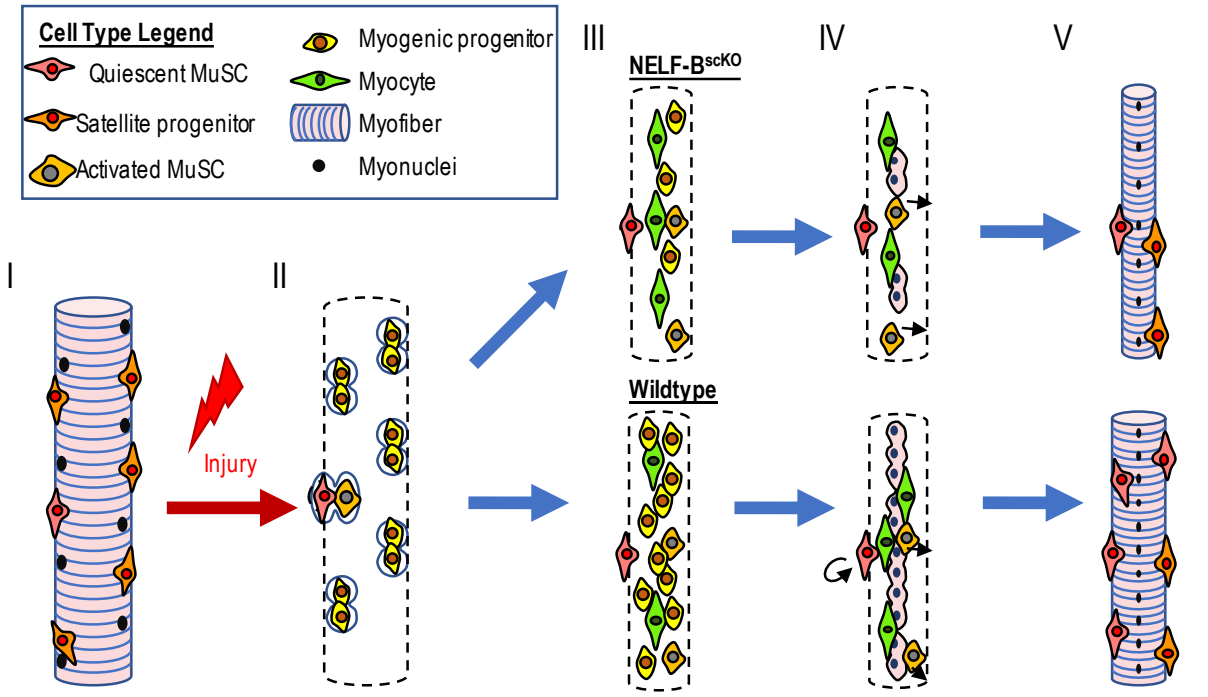

Figure 4.13 – Proposed mechanism for the implication of NELF in skeletal muscle regeneration. Healthy skeletal muscle (I) remains adaptive to injury. In response to injury, (II) MuSCs are activated and begin dividing to permit population expansion. (III) In response to a NELFb^{scKO}, myogenic progenitors exhibit reduced proliferation than in WT conditions, and begin undergoing precocious differentiation. This reduces the amount of progenitors available for regeneration, and does not rejuvenate the extracellular niche environment. (IV) As regeneration progresses myotubes begin forming. In addition, some activated MuSCs may become a dormant satellite progenitor, while quiescent MuSCs undergo self-renewal. The reduced replenishment of the niche environment in NELFb^{scKO} populations impairs MuSC self-renewal. (V) The mature myofiber is characterized by a contractile myofiber and repopulated MuSC populations, both of which are reduced in NELFb^{scKO} populations.

CHAPTER 5

Regulating myogenic cell proliferation through the NELF-pTEFb axis

5.1 – Modelling prolonged myoblast proliferation through molecular inhibition

5.1.1 ***Effects of Flavopiridol on primary myoblast proliferation*.** The ability of NELF to regulate myogenic progenitor proliferation poses interesting therapeutic perspectives. Specifically, sustaining NELF binding at its target genes is a strategy which could retain myogenic progenitors engaged in proliferation, and increase the abundance of myogenic progenitors available to contribute towards degenerated skeletal muscle. Because NELF remains engaged until its release is induced by phosphorylation of DSIF by pTEFb, this leads to the possibility that disabling the function of pTEFb could be used to retain NELF bound to its target genes, and support gene expression patterns which favour proliferation.

Considering molecular inhibitors of cyclin dependent kinases, one promising candidate is Flavopiridol as it can specifically inhibit the catalytic activity of the pTEFb constituent Cdk9 (262). In C2C12 myoblasts, a non-functional pTEFb complex generated through either exogenous overexpression of a catalytically dead Cdk9 (Cdk9dn) or with low concentrations of Flavopiridol prevents the expression of genes expressed in terminal differentiation such as *Myog, Mck, and MHC* (263) and general myotube formation (264). Thus, this supports a role for pTEFb to initiate terminal differentiation in C2C12 myoblasts. Considering the similar functional roles of NELF

in C2C12 myoblasts and primary myoblasts (chapter 3) leads to suppose that a block in pTEFb causes NELF to remain associated with its target genes and prevents their terminal differentiation.

Despite the ability of Flavopiridol to block terminal differentiation of C2C12 myoblasts, its effects on primary myogenic cells has yet to be characterized. In addition, because concentrations of Flavopiridol impacts cyclin dependent kinases differently, this has the potential to elicit a range of effects ranging from increased proliferation to induced apoptosis. Therefore, we desired to investigate the effects of low concentrations of Flavopiridol on primary myogenic progenitors, and assess its impact on myogenic behavior. To do so, primary myoblasts with a TdT^+ lineage reporter were separated into two groups and received either Flavopiridol treatment (25 nM) or a vehicle control as a 48h pre-treatment (Figure 5.1). Under continued treatment, we assessed proliferation with an EdU incorporation assay, which shows there is no significant difference in EdU incorporation between treated and control

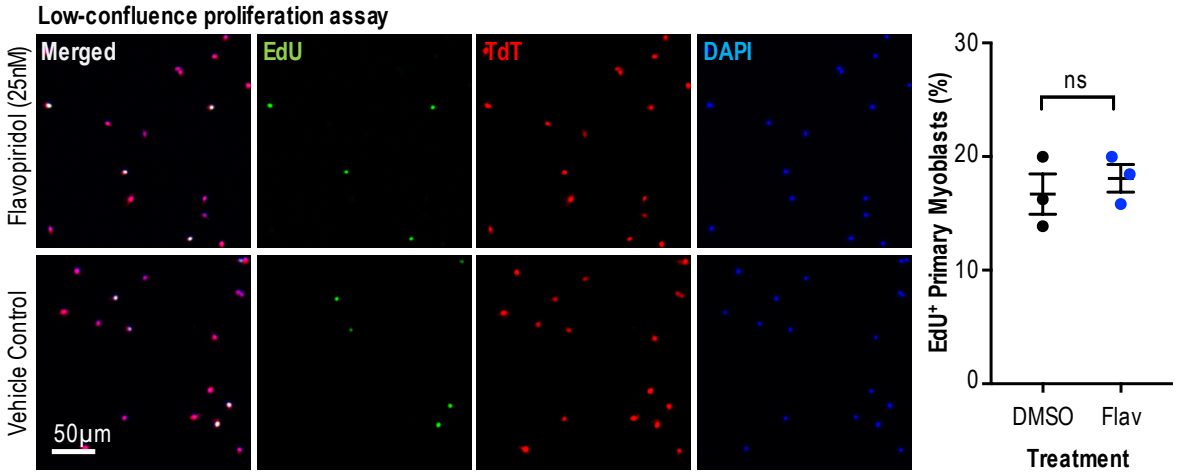

Figure 5.1 – Proliferation of primary cultured myoblasts during Flavopiridol treatment. Primary myoblasts isolated from TdT^+ mice and subcultured in Flavopiridol (25 nM in DMSO) or vehicle control (DMSO) for 48h prior to a 4h EdU incorporation assay. There is no significant difference in the abundance of EdU^+ myoblasts in Flavopiridol treated populations [18.09 ± 1.211, n=3] and vehicle controls [16.69 ± 1.781, n=3].

populations. Thus, this low concentration of Flavopiridol does not appear to influence general proliferation of primary myoblasts.

5.1.2 ***Differentiation upon Flavopiridol withdrawal*****.** Although Flavopiridol can inhibit terminal differentiation of C2C12 myoblasts, whether differentiation remains impaired upon treatment withdrawal remains elusive. To investigate, primary myoblasts were subdivided into two groups and treated with either Flavopiridol or a vehicle control for 3 days. After treatment, both groups were further cultured at low-confluence in treatment-devoid primary growth medium for an additional two days, to permit complete treatment withdrawal from these myoblasts. Finally, we assessed the ability of these populations to undergo terminal differentiation when plated at high-confluence and exposed to low-serum treatment-devoid differentiation medium (Figure 5.2A). The presence of multinucleated myotubes with similar morphology in both populations (Figure 5.2B) supports that the inhibitory effect of Flavopiridol on pTEFb is transitory, so that withdrawal of Flavopiridol restores activity to pTEFb and allows terminal differentiation to proceed as normal.

5.1.3 ***Flavopiridol inhibits terminal differentiation*****.** The ability of Flavopiridol to inhibit terminal differentiation in C2C12 myoblasts has yet to be validated in primary myoblasts. To investigate this possibility, a population of cultured primary myoblasts was sub-divided into two groups and treated with varying concentrations of Flavopiridol or a vehicle control for 48h, then coaxed towards terminal differentiation with low-serum medium over 72h. The ability to undergo terminal differentiation and form multinucleated myotubes appeared to be inversely

correlated to the concentration of Flavopiridol (Figure S5.1A). Of interest, populations treated with the highest concentration of Flavopiridol formed very thin myotubes and displayed large aggregates of myogenic cells which remained largely unfused (Figure S5.1B). While this suggests terminal differentiation may be partially impaired by Flavopiridol, it does not show a complete block in terminal differentiation. Because the

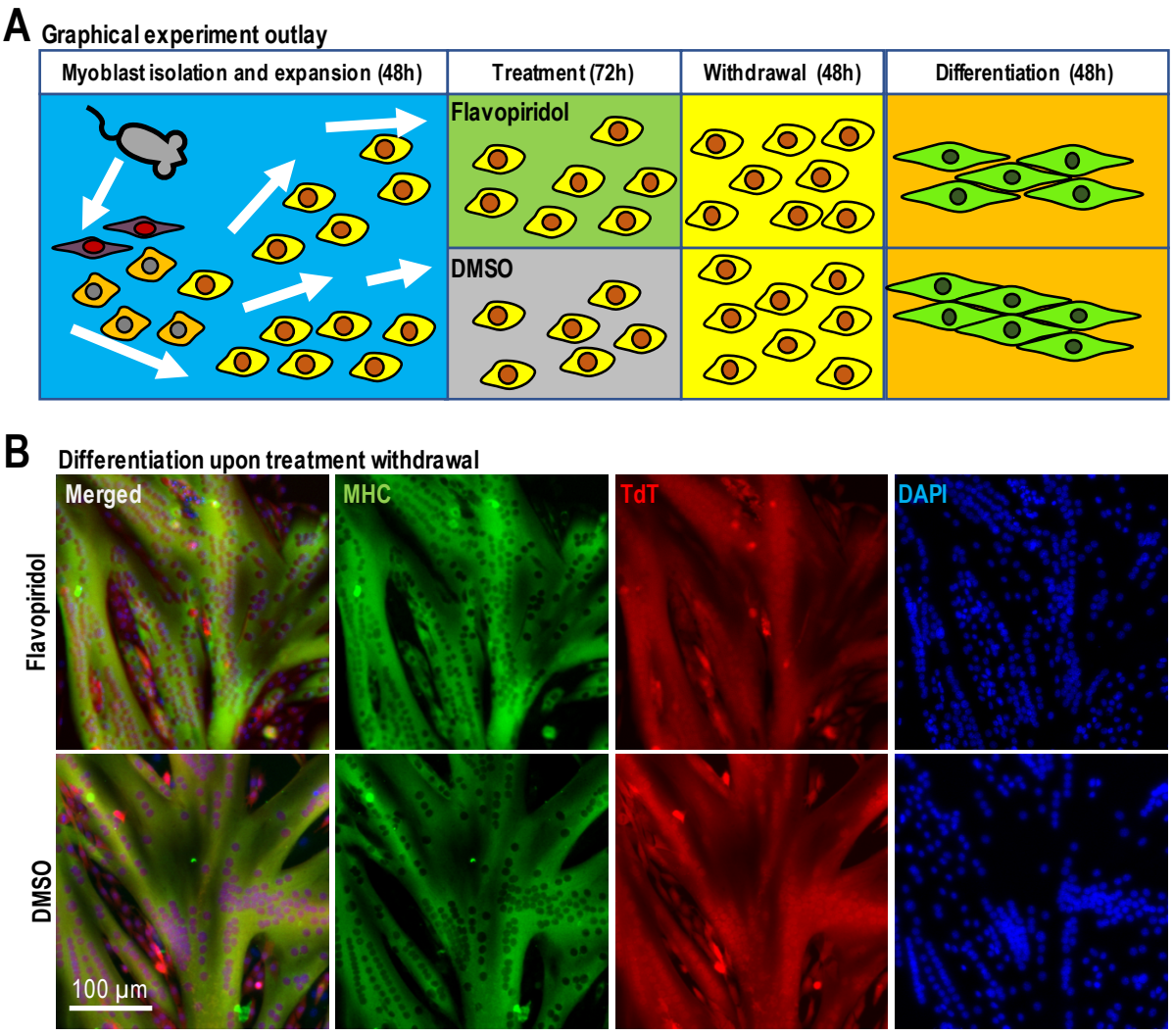

Figure 5.2 –Myoblasts retain their ability to differentiate upon withdrawal from Flavopiridol treatment. ***(A)*** Graphical outlay of the experiment performed: Primary myoblasts derived from TdT^{+} mice are subcultured for 48h in 4-OHT, then divided in two populations for either Flavopiridol (25 nM in DMSO) or vehicle control (DMSO) treatment for 72h. These populations are further subcultured in treatment-devoid primary growth medium (48h), then plated at high density in low serum medium to induce terminal differentiation. ***(B)*** Immunofluorescence for MHC, endogenous TdT, and DAPI shows the preceeding populations retain similar ability to robustly undergo terminal differentiation and form large multinucleated myotubes.

myogenic cells used in the prior experiment were subcultured over a few days prior to Flavopiridol treatment, we reasoned that some populations may have already been primed to undergo cell cycle withdrawal towards terminal differentiation. To verify, we isolated fresh primary myoblasts, and immediately subdivided them to receive either Flavopiridol or a vehicle control. Here, myoblasts were retained in treated growth medium, and allowed to expand to high-confluence. Upon doing so, the vehicle-treated populations underwent terminal differentiation to form multinucleated myotubes, whereas those under Flavopiridol treatment remained as single-cell aggregates which were mostly devoid of the myotube marker MHC (Figure 5.3). This supports the ability of Flavopiridol treatment to retain cultured primary myoblasts in a proliferative which would have normally undergone terminal differentiation and formation of multinucleated myotubes.

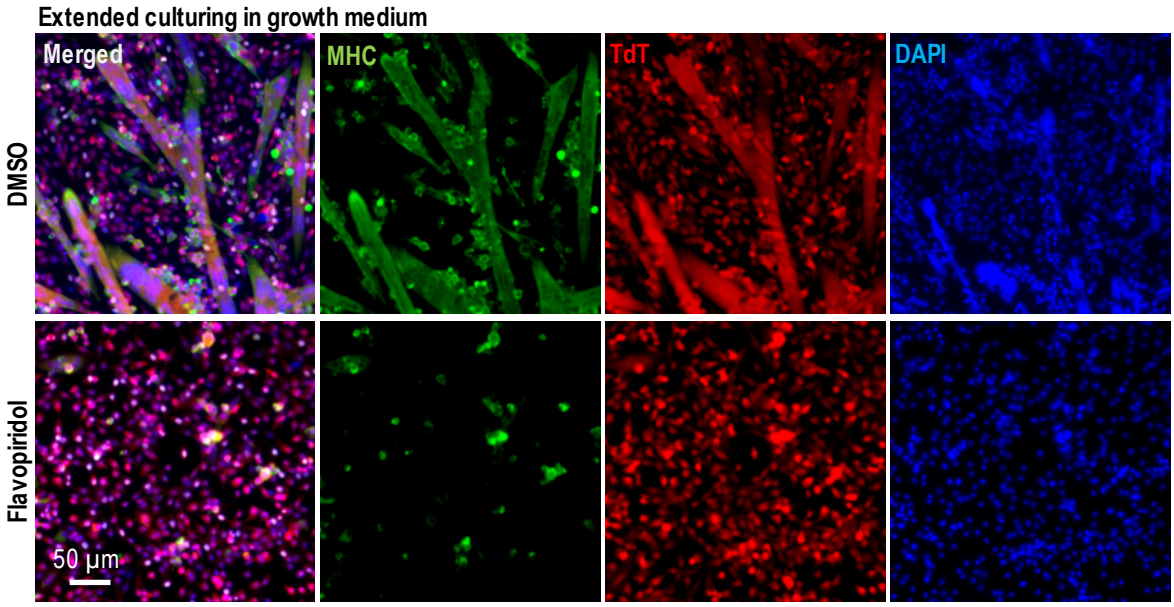

Figure 5.3 – Flavopiridol inhibits spontaneous differentiation. Primary myoblast populations induced with 4-OHT to permit TdT^+ expression are treated with either Flavopiridol (25 nM in DMSO) or a vehicle control. While primary growth medium spiked with the specified treatment is refreshed at 24h intervals, vehicle control populations undergo spontaneous differentiation and form multinucleated myotubes (MHC, green), while those treated with Flavopiridol undergo extended proliferation, produce high-density single-cell aggregates, and do not undergo terminal differentiation.

5.2 – Discussion to the chapter

5.2.1. ***Significance of results.*** The results presented in this chapter support an important function of the NELF-pTEFb axis which regulates gene expression to control maintenance and withdrawal from the cell cycle. Specifically, our results support the necessity of functional pTEFb to induce terminal differentiation in primary myogenic progenitors, as previously reported in C2C12 myoblasts (132, 137, 264). Considering the functional role of NELF which retains myogenic progenitors engaged in the cell cycle presented in chapters 3 and 4, this presents a potential mechanism critical to terminal differentiation in myogenic progenitors: while NELF regulates gene expression in favor of progenitor proliferation, dissociation of NELF induced by pTEFb provokes dysregulation in the expression of NELF-gated genes, which culminates in cell cycle withdrawal and terminal differentiation. In addition, while the NELF-pTEFb axis may act as a molecular switch to control the transition from proliferation towards cell cycle withdrawal, this axis appears to be highly susceptible to exogenous manipulation with small molecular inhibitors such as Flavopiridol. This raises the possibility that supplementing damaged skeletal muscle with Flavopiridol *in vivo,* could be used to increase the abundance of proliferating myogenic progenitors, produce more downstream myocytes available to fuse with myofibers, and lead to a general increase in myofiber size and contractile function, to restore strength in persons affected by muscle degenerative disease (Figure 5.4). In addition, extended myogenic progenitor proliferation may additionally rejuvenate the extracellular environment in support of MuSC self-renewal, as discussed in chapter 4. While

speculative, this poses an interesting direction for therapeutics towards skeletal muscle wasting disease.

5.2.2 *Flavopiridol has broad functions.* While our results support a role for Flavopiridol to extend the duration of myogenic progenitor proliferation, we must consider prior reports provide critical insight on the different effects Flavopiridol concentrations can entice. contradicts prior reports which boasts the anti-neoplastic effects of the compound. In fact, Flavopiridol which is also known as Alvocidib, has proceeded through phase 2 clinical trials to study its safety to delay progression of multiple lymphomas (265-267). Although results were promising, harmful secondary effects (265, 268-271) have prevented its progression towards phase 3 clinical trials.

The contradictory effects of Flavopiridol to sustain proliferation in myogenic progenitors, but demonstrating antitumour activity *(272)* by cell cycle arrest of carcinogenic cells (273, 274) presents an interesting dichotomy of its function. This arises from the molecular kinetics of Flavopiridol which regulates its ability to interact with the family of cyclin dependent kinases (275). At moderate concentrations (150nM – 300nM), Flavopiridol outcompetes ATP and binds the ATP-binding pocket of Cdks 1, 2, 4, 6, 7, and 9 (276-279). This restricts the energy currency which affords function to Cdks, and causes these Cdks to become non-functional and unable to participate in cell-cycle checkpoints. This produces cell cycle arrest and an inability to continue cellular division. Administered at even higher concentrations, Flavopiridol induces apoptosis in a p53-independent pathway (280, 281). Therefore, while moderate to high concentrations of Flavopiridol does strongly inhibit cell proliferation, it does so by

acting on many Cdks, and this occurs in a mechanism not related to the NELF-pTEFb axis of cell state regulation proposed.

At lower concentrations (5nM – 30nM) region, Flavopiridol solely inhibits Cdk9 through an unknown mechanism which occurs independently from binding to the ATP-binding pocket (282). Because the other Cdks retain functionality, the cell cycle and cellular divisions proceed as intended, but with a block in the functional activity of pTEFb. In the case of myogenesis, low concentrations of Flavopiridol means renders pTEFB non-functional, so it can no longer phosphorylate DSIF to release NELF at specific target genes. As a result, low expression of these genes retains myoblast proliferation and offsets cell cycle withdrawal and terminal differentiation. Upon withdrawal of Flavopiridol, pTEFb activity is restored so it may phosphorylate DSIF and Pol II, causes NELF to disengage, and allows expression of specific genes which

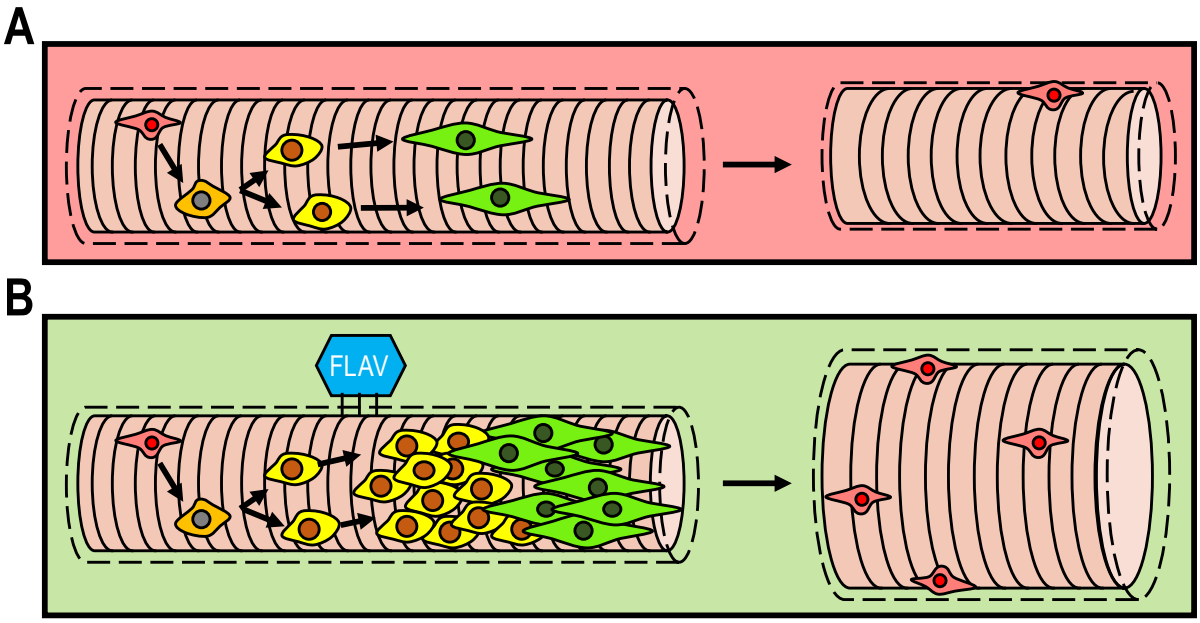

Figure 5.4 – Proposed therapeutic use of Flavopiridol towards skeletal muscle wasting disease. *(**A**)* Persons affected by muscle degenerative disease see a gradual decline in skeletal muscle mass, and reduced contributions of MuSC populations to maintain myofibers. ***(B)*** Targeted delivery of Flavopiridol could coax an extended proliferation of myogenic progenitor cells (yellow) during the contributions of MuSCs towards skeletal muscle in homeostasis. This could increase the abundance of myocytes (green) to produce larger myofibers, and rejuvenate the extracellular environment to support MuSC self-renewal (red). This could theoretically increase muscle mass, strength, and restore the ability of MuSCs to participate in skeletal muscle maintenance.

favours cell cycle exit and terminal differentiation (Figure 6.1A). Whether Flavopiridol may be used to coax extended proliferation of myogenic progenitors *in vivo* remains to be investigated, but will surely be an interesting area for future research.

CHAPTER 6

General discussion

6.1 – Summary of results.

Results presented within this thesis have rigorously characterized the functional role of the Negative Elongation Factor (NELF) complex in controlling cell state transitions of myogenic cells. As a general function, NELF stabilizes promoter proximal paused Pol II, where it acts as a signal integration hub to control the outcome of paused Pol II at specific genes. In myogenic cells, we show that NELF has a dual function to (I) stabilize promoter proximal paused Pol II in favour of gene expression, or (II) prevent promoter proximal Pol II from progressing towards processive elongation. While the role of NELF appears to be influenced by the specific gene class, its ability to retain myogenic cells engaged in the cell cycle is largely attributed to its ability to stabilize Pol II to promote expression of genes which favour maintenance within the cell cycle. Specifically, we propose that NELF stabilizes paused Pol II in the promoter proximal region of cell cycle regulatory genes such as *Ccng1,* which supports its stable expression to maintain low levels of p53 so that myogenic cells remain engaged in the cell cycle. In response to a non-functional NELF complex, destabilized Pol II in the *Ccng1* promoter region becomes susceptible to integrator-mediated abortive transcription. This lowers the levels of Cyclin G1, which cascades towards an increase in the abundance of p53, and prompts early withdrawal from the cell cycle towards terminal differentiation. This affects skeletal muscle regeneration as fewer available myocytes produces thinner *de novo*

myotubes, and the reduced proliferation of myogenic progenitors does not sufficiently rejuvenate the extracellular niche environment (Figure 4.13), which severely reduces downstream MuSC self-renewal. In addition, NELF regulates the expression of several genes which remodel the extracellular environment of regenerating skeletal muscle, such as *SerpinF1*, and this is critical for downstream MuSC self-renewal. In response to a NELFb^{scKO}, dysregulation of these extracellular remodelling genes prevents myogenic progenitors from remodelling the extracellular niche environment, which impairs downstream MuSC self-renewal.

6.2 – New insights on myogenesis

6.2.1 ***Myogenic progenitors rejuvenate the niche environment for MuSC self-renewal.*** The MuSC niche microenvironment is well known for its regulatory function towards MuSC maintenance and self-renewal, which arise from both biophysical interactions and embedded ligands within the niche environment (reviewed in section 1.1.3). To support the MuSC niche environment, many accessory cell types such as T cells, monocytes, macrophages, fibroblasts, fibro-adipogenic progenitors, and mesenchymal cells, influence the immediate niche environment of MuSCs (32, 35, 38, 283-288). Doing so regulates several signaling pathways modulated by Wnt7a and fibronectin (289, 290), Fibroblast growth factor receptor 1 (291), the JAK/STAT pathway (292, 293), and p38 MAPk, and this controls the ability of MuSC to remain quiescent, undergo self-renewal, and become activated. When these pathways are perturbed, this often restricts the ability of MuSCs to remain quiescent and/or undergo self-renewal (291, 292, 294, 295).

Despite the importance of cellular cross-talk in support of skeletal muscle regeneration, there is limited literature which alludes to an ability of proliferating myogenic progenitors to influence downstream MuSC self-renewal during skeletal muscle regeneration. Some prior reports have shown that MuSC self-renewal remains responsive to the extent of skeletal muscle injury (21, 56, 296), and the extent with which quiescent MuSCs undergo self-renewal has been shown to positively correlate to myogenic progenitor proliferation (23). In another instance, ablated fibroblasts were shown to elicit precocious differentiation of myogenic progenitors and reduced populations of quiescent MuSCs in the regenerated skeletal muscle (32).

Thus, during the allograft experiments, it remained interesting to find a strong positive correlation between the extent with which myogenic cells proliferate to establish homeostasis within their niche environment, and the resulting abundance of quiescent MuSCs. Because the NELF complex does not affect MuSC quiescence (section 3.3.1) or activation (section 3.3.2), does not restrict the ability of activated MuSCs to become dormant (section 4.1.3), nor in MuSC self-renewal (4.1.2, 4.1.3), suggests that the inherently reduced MuSC populations upon NELFb^{scKO} donors occured from extracellular effects which impaired MuSC self-renewal. In addition, because NELFb^{scKO} and wildtype donors were administered to the contralateral TA of a same host mouse, this allowed us to exclude potential effects of the host niche cytokines and accessory cell types to influence donor MuSC self-renewal. Thus, the only variable which impaired donor MuSC self-renewal in these experiments is the proliferation of donor-derived myogenic progenitors, where reduced myogenic progenitor proliferation impairs MuSC self-renewal.

Understanding a role for myogenic progenitors to rejuvenate the niche environment and support downstream MuSC self-renewal may partially be explained by cellular kinetics during myogenesis. Specifically, while myogenic progenitors typically proliferate between 3 – 5 dpi, predominant MuSC self-renewal tends to occur immediately afterwards, between 5 – 7 dpi (24). Considering the positive correlation between myogenic progenitor proliferation and the abundance of quiescent MuSCs in the allograft transplant experiments, this poses the possibility that while myogenic progenitors are engaged in proliferation, they actively contribute towards remodelling the extracellular environment to promote MuSC self-renewal. Whether myogenic progenitors do so through biophysical or biochemical contributions remains unknown. In addition, whether myogenic progenitors directly act on quiescent MuSCs to evoke self-renewal (Figure 6.1A), or do so by through an intermediary cell type (Figure 6.1B) remains to be established.

To investigate the specific mechanisms through which myogenic progenitors affect downstream MuSC activity could be supported with computational modelling. To do so, a connectome approach as described in (297, 298) may be particularly

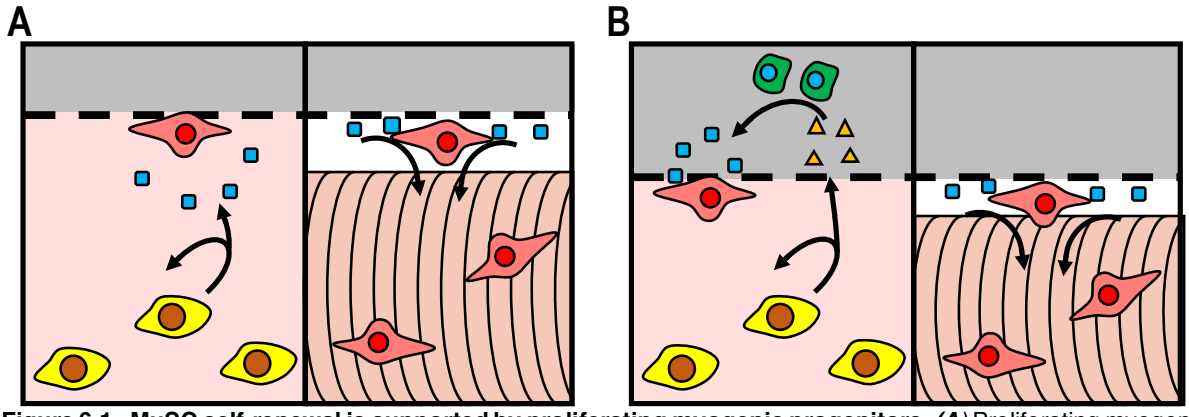

Figure 6.1 - MuSC self-renewal is supported by proliferating myogenic progenitors. ***(A)*** Proliferating myogenic progenitors (yellow) may either directly secrete factors in the extracellular environment (blue squares) to support downstream MuSC self-renewal (red), or ***(B)*** secrete recruiting factors (orange triangle) to localize accessory cell types (green) in support of downstream MuSC self-renewal.

useful. This would compare the MuSC receptome to the secretome of proliferating myogenic progenitors and other accessory cell types in skeletal muscle, to identify specific ligands which could be detected by and influence MuSC activity. Identifying specific cytokines, extracellular matrix proteins or other components which promote MuSC self-renewal would validate our reported role for proliferating myogenic progenitors in reformulating the MuSC niche microenvironment. In addition, it would be beneficial to extend the connectome analysis to consider how secreted factors by myogenic progenitors may interact with and recruit accessory cell types, and identify whether these accessory cell types may interact with MuSCs to influence their self-renewal. While computationally heavy, this would provide an unbiased approach to identify cellular cross-talk networks which influence MuSC activity during skeletal muscle regeneration. Once candidate pathways are identified, they will need to be validated *in vivo.* This could be achieved through gene silencing of candidate receptors in MuSCs and ligands secreted by myogenic progenitors and accessory cells to study how this may affect (I) general skeletal muscle regeneration, (II) MuSC populations, and (III) cellular localization between accessory cell types and myogenic cells. This may be facilitated using advanced multiplexed imaging systems (e.g. CODEX by Akoya Biosystems^{TM}) to study how candidate interactomes affect skeletal muscle regeneration from a systems biology perspective. Lastly, these interaction networks could be investigated in different muscle degenerative diseases to identify whether ligand exposure strategies could be used to manipulate MuSC activity and restore skeletal muscle strength and volume.

6.2.2. *Harnessing myogenic progenitor activity as a therapeutic approach.*

The influence of proliferating myogenic progenitors on MuSC self-renewal presents an intriguing therapeutic strategy towards muscle degenerative disease. Specifically, a forced increase in myogenic progenitor proliferation would (I) provide more downstream myocytes available to strengthen deteriorating myofibers, and (II) rejuvenate the niche microenvironment to promote MuSC self-renewal. Considering the role of Flavopiridol in extending myoblast proliferation (section 5.1) confers great therapeutic interest to Flavopirdiol, as described in section 5.3. As Flavopiridol may exert effects on non-myogenic cell populations which reside in skeletal muscle, means optimized drug-delivery strategies are required to assure targeted delivery of Flavopiridol remains specific towards myogenic progenitors. Additionally, this will require that Flavopiridol concentrations remain low enough to avoid secondary effects such as inhibiting other Cdks and initiating apoptosis (299, 300).

One feasible strategy includes MuSC transplant approaches, where the alginate gel used to encapsulate donors MuSC populations (301-303) could be treated with Flavopiridol. Doing so would promote an extended proliferation of the donor-derived proliferating myogenic progenitors while establishing homeostasis, and this could increase the zone of homeostasis, increase donor MuSC self-renewal, and provide a more efficient contribution towards the degenerating muscle. As an alternative, systemic delivery of Flavopiridol payloads could be targeted specifically to ailing skeletal muscle with muscle-homing peptides (304) or nanoparticle delivery systems (305, 306). Here, shuttled Flavopiridol would act directly on endogenous myogenic progenitor populations, and strengthen skeletal muscle through increased progenitor production, and increased MuSC self-renewal, as previously described.

This would increase skeletal muscle volume and strength, while a rejuvenated niche environment would support MuSC self-renewal to provide long-term support to the skeletal muscle.

While this seems promising, further investigations are required to assess the potential therapeutic benefit of Flavopiridol *in vivo*, and its ability to remediate degenerated skeletal muscle arising from different muscle wasting diseases. These studies should be focused to assess the effects of Flavopiridol in different mouse models of (I) injury-mediated regeneration, (II) long-term exposure in uninjured homeostatic muscle, (III) various myopathies, (IV) cachexia, and (V) sarcopenia. In all instances, myofiber diameter can be measured to loosely screen for increased proliferation of myogenic progenitors, and quiescent MuSC populations quantified to investigate increases in MuSC maintenance and self-renewal. In addition, a long-term *in vivo* EdU pulse could be used to differentiate the abundance of MuSC self-renewal (EdU^+) as performed in (24) and described in section 4.5. The possible effects of Flavopiridol to reverse sarcopenia will be particularly interesting, given recent studies which allude that biophysical and biochemical modifications within the extracellular environment may alter MuSC fates (294, 307), and reverse their reduced ability to undergo self-renewal which was previously thought to be permanent (291, 294, 295, 308, 309). Thus, this leads to speculate that extended proliferation of myogenic progenitors in aged skeletal muscle by Flavopiridol could sufficiently rejuvenate the niche environment and support MuSC self-renewal, to restore skeletal muscle strength, volume, and function.

6.3 – Significance of our results towards global functions of NELF

6.3.1 Different regulators of Pol II promoter proximal pausing may control different gene subsets.

The presence of promoter proximal paused Pol II across various cell types in higher eukaryotes infers important regulatory functions of this process. Indeed, the results presented within this thesis show an important ability of NELF to control Pol II activity at specific genes to effectuate cell cycle withdrawal. What remains unanswered is whether NELF is a global regulator of promoter proximal paused Pol II, or acts at a specific subset of genes. Indeed, other proteins known to regulate promoter proximal paused Pol II includes GAF, the +1 nucleosome, and Paf1C, but whether these do so exclusively of NELF remains under debate. In the context of myogenesis, the presence of promoter proximal Pol II peaks in quiescent MuSCs are rapidly reduced during MuSC activation (176). This suggests that promoter proximal paused Pol II is rapidly disengaged from the promoter proximal region and proceeds towards active elongation during activation. Despite this observation, results in this thesis show a loss in function of NELF does not affect cellular functions of MuSC during quiescence or activation. This poses the possibility that either regulatory complexes other than NELF may control Pol II pausing in quiescent MuSCs to effect cell state changes, or that rapid changes in gene expression which accompany MuSC activation relies on other mechanisms, such as rapid translation of the sequestered mRNA of Myf5 and MyoD discussed in section 1.2.2. To investigate, overlap analysis between promoter proximal paused Pol II, and different regulators of paused Pol II such as NELF, DSIF, GAF, Paf1C, and the +1 nucleosome will need to be performed in quiescent and activated MuSCs populations. Particularly, it will be important to identify (I) the classes of genes with diminished

promoter proximal Pol II pausing during MuSC activation, and (II) which regulators of Pol II pausing co-localize with these peaks. It will be interesting to identify whether different regulators of paused Pol II control the expression of different subsets of genes associated with different cellular processes and states.

6.3.2 – NELF is a master regulator which controls cellular proliferation.

Results presented in Chapters 3 – 5 demonstrate an important role for NELF to regulate the extent of myogenic progenitor proliferation by modulating their ability to undergo cell cycle arrest and terminal differentiation. Intriguingly, a role for the NELF complex to retain cells engaged in the cell cycle is apparent in other cell systems. As an example, NELFb is typically overexpressed in several carcinogenic cell populations such as hepatocellular carcinomas (310), upper gastrointestinal carcinomas (311), and prostate cancer (312). Similarly, NELFe is overexpressed in pancreatic (313) and gastric (314) cancerous tissues. Further, when NELF is inactivated through silencing of any one of its subunits, these carcinogenic cells tend to exhibit reduced proliferation and migration, while ectopic overexpression of NELF in non-carcinogenic cells tends to increase cellular viability, proliferation, and migration, a phenotype reminiscent to that of carcinogenic cells (312, 314). A role for NELF to retain cellular proliferation has also been reported in non-cancerous cell systems, where a NELFb knockdown in murine embryos induces spontaneous cell differentiation and prevents further embryonic development (116). In addition, NELF supports embryonic stem cell proliferation towards embryo patterning and development (117, 118), and does so in response to extracellular signaling (108). Thus, these studies and the work presented in this thesis suggests a global role for

NELF to retains cells engaged in the cell cycle, and acts as a master regulator of cellular proliferation responsive to extracellular stimulus.

Prior studies have demonstrated an importance of 'bookmarked' genes that permit rapid changes in gene expression upon mitotic exit. Here, genes are bookmarked through histone modifications, transcription factors, and promoter proximal paused Pol II which retains the ability to undergo rapid expression in support of mitotic exit (315, 316), and cellular identity (317-319). The observed 'leaky' expression of these genes further supports presence of promoter proximal paused Pol II (320). Although these studies have not specifically considered the role for NELF to control Pol II pausing at these genes, the oft reported implication of NELF to sustain cellular proliferation leads to speculate that NELF supports Pol II pausing at these bookmarked genes to retain cells engaged in the cell cycle. Thus, this offers a potential mechanistic role wherein NELF stabilizes paused promoter-proximal Pol II at cell cycle regulatory genes, which permits rapid changes in the expression of specific genes to induce cell cycle withdrawal in response to specific stimulus.

6.3.3 – Evolutionary conservation of NELF as a cellular proliferation regulator.

A broad-scale role for NELF to regulate cellular proliferation critical for development in humans, mouse, and drosophila (113, 114, 117) suggests NELF may have been evolutionary conserved. Indeed, prior reports have identified orthologs of NELF across insects and vertebrates (119), and the emergence of all four subunits of NELF are traced to the early metazoan (321). Considering other processes which evolved in early metazoa includes refined cell-adhesion interactions (322), tyrosine kinase signaling to relay extracellular signals and permit cell-cell communications

(323), and the emergence of multicellular organisms that undergo spatial rather than temporal differentiation (324). Thus, NELF may have emerged as a regulator of Pol II activity to permit responsive gene regulation towards extracellular stimulus, to evoke spatial rather than temporal cellular differentiation. From a speculative perspective, this would allow multicellular organisms to competitively respond to carbon sources. When faced with nutrient deprived environments, harsh external conditions would be transduced and elicit a release of NELF at specific genes to permit rapid withdrawal from the cell cycle, stop cellular divisions, and reduce the overall energy requirements of the organism. During an abundance of carbon sources, NELF would remain engaged at these genes, so that the sustained proliferation would provide a competitive advantage to a multicellular organism through increased size, and the ability to obtain additional nutrients. Thus, while NELF may have evolved to permit spatial differentiation, its inherent function may have been conserved in higher eukaryotes, where it acts as a spatial regulator to control proliferation and differentiation (Figure 6.2).

The evolutionary implication of NELF to mitigate environmental responses on the expression of cell cycle genes may have further diverged to control the expression of several rapid-response genes towards extracellular stimulus. This includes the role for NELF to permit rapid gene expression during the heat shock response in *Drosophila* (113, 114), and for rapid induction of immediate early genes in differentiated neurons in response to external stimulus (115). In addition, recent work has demonstrated a role for the NELFa and NELFe subunits to arrest elongating Pol II in response to double stranded DNA breaks (241, 242), although NELFb and

NELFcd do not co-localize at these sites. These roles may have emerged at a later evolutionary time owing to the refined ability of NELF to stabilize paused Pol II.

6.4 – Multiple signaling pathways may converge on NELF to elicit cell cycle withdrawal

6.4.1 Regulation of pTEFb functions is affected by various factors. Despite the role of pTEFb to disengage NELF, it interacts with additional protein partners to modulate housekeeping gene expression programs. This includes the role of pTEFb to phosphorylate Ser2 of the Pol II CTD to permit elongation (325, 326), and of histone H1.4 to render nucleosomes more permissive in the promoter region of active genes (263, 327). This remains enigmatic, as Flavopiridol treatment to inhibit Cdk9 and therefore pTEFb does not affect cellular viability, as demonstrated by both our results, and prior studies which show Pol II CTD hyperphosphorylation remains during

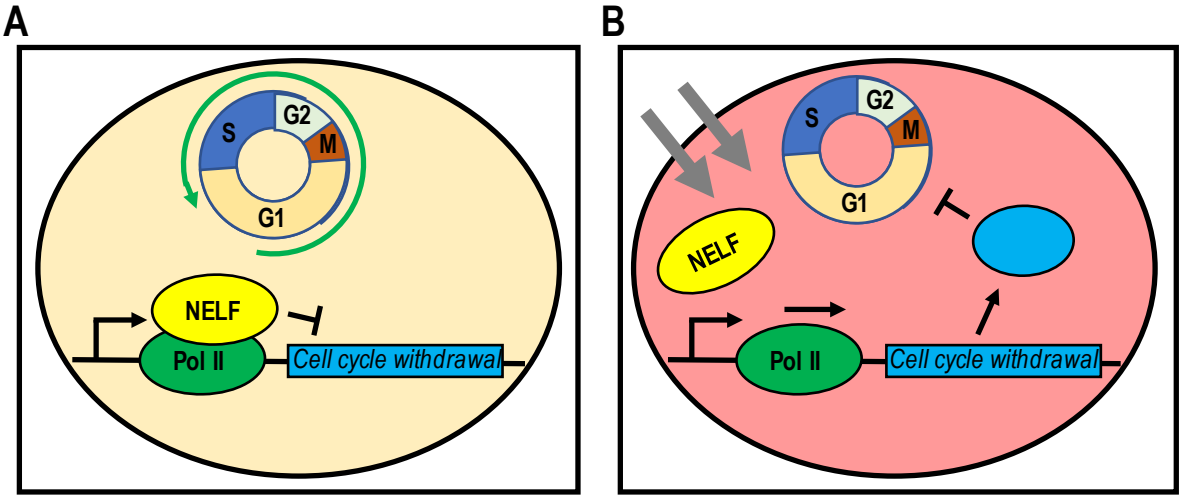

Figure 6.2 Early evolutionary role of NELF to control cellular proliferation responsive to external stimulus. (*A*) NELF associates with Pol II and prevents the expression of cell cycle withdrawal genes. This retains cells in a state of proliferation, leading to population expansion within a multicellular organism. ***(B)*** In response to extracellular stressors (grey arrows), NELF disengages Pol II, which allows expression of cell cycle withdrawal genes, whose effector proteins (blue) coax withdrawal from the cell cycle.

Flavopiridol treatment (328). While this may occur from compensatory mechanisms such as Cdk12/13 to undertake Ser2 CTD phosphorylation (329-331), the composition of pTEFb may additionally influence its susceptibility to inhibitors. Here, differences in the pTEFb constituent isoforms of Cdk9 may cause pTEFb to interact with different regulatory proteins, and elicit different functional roles in cells.

Cdk9 isoforms. The two isoforms of Cdk9, namely Cdk9-42 kDa (Cdk9-42) or Cdk9-55 kDa (Cdk9-55) (332, 333) exhibit different cellular functions. First, the promoter regions of the Cdk9 isoforms suggests their expression is independently regulated. The TATA-less promoter of Cdk9-42 implies its expression may be mediated alongside that of general housekeeping genes (332), while E-box (264) and TATA box (333) motifs in the Cdk9-55 isoform imply its expression may be dependent on stress-responsive factors (334, 335) and transcription factors. In addition, the dynamic abundance of Cdk9 isoforms is highly responsive to external stimulus (336-338), where the Cdk9-55 is dominant in G_0 cell states, but entry within the cell cycle causes a shift and prevalence of the Cdk9-42 isoform (264, 339, 340). This implies the Cdk9 isoforms which constitute pTEFb may well influence its downstream activity.

Cdk9 isoform localization. In addition to dynamic changes in their expression, Cdk9 isoforms localize to different regions in the nucleus, which further affects its functional role (341). Here, Cdk9-42 localized to the nucleoplasm supports a role for general transcription (342), whereas Cdk9-55 localized to the nucleolus may support cellular stress response pathways mediated by the nucleolus (343). Indeed, nucleoli

formation is cell-cycle dependent (344, 345), and perturbations to the nucleoli structure is known to trigger a cellular stress-response (346) which evokes cell cycle arrest through p53-dependent (347-349) and p53-independent pathways (350, 351). This leads to speculate that in response to cellular stress, the nucleolus induces cell cycle arrest with synergistic contributions by the p53 pathway and a rapid release of sequestered Cdk9-55. The increased abundance of active pTEFb becomes available to phosphorylate DSIF and release NELF, which produces changes in Pol II activity at these genes to evoke cell cycle withdrawal. Thus, while the Cdk9-42 isoform may participate in general housekeeping functions, it is the increased abundance of previously sequestered Cdk9-55 which targets NELF to permit cell cycle withdrawal. Indeed, this agrees with prior studies which suggest the availability of active and free pTEFb is a rate limiting step in regulating Pol II activity at NELF-bound genes (352) to evoke a change in gene expression. In addition, this presents the possibility that the housekeeping Cdk9-42 is sheltered by accessory proteins such as the super elongation complex, which hinders Flavopiridol interactions, whereas Cdk9-55 released by the nucleolus is free and susceptible to inhibition by Flavopiridol.

6.4.2 – Accessory proteins guide pTEFb to gene loci independent of the Cdk9 isoform. The increased availability of active pTEFb to facilitate large-scale release of NELF binding must also be able to interact with localizing proteins to direct it to stalled Pol II. Generally, much of the free pTEFb associates with the super elongation complex (134), while the remainder associates with transcription factors and other RNA-binding proteins (353-356) to localize it towards paused promoter-proximal Pol II. In the case of C2C12 myoblasts, prior studies have shown that MyoD

interacts with the N-terminal tail of Cdk9-42 and chromatin remodellers p300, PCAF, and Brg1 (137, 357). This allows MyoD to co-localize chromatin remodelers and pTEFb to elicit rapid gene expression at specific target sites. Thus, the role of MyoD towards gene activation during terminal differentiation may be further supported by localizing pTEFb to paused Pol II within these genes and allow their rapid expression.

Although western blots of the MyoD immunoprecipitations identified a Cdk9-42 protein band, the western blots did not include the 55 kDa region to identify whether MyoD interacts with the Cdk9-55 isoform (137). Thus, it remains unclear whether MyoD interacts in a selective manner with each of the Cdk9 isoforms, and whether the increased abundance of Cdk9-55 during myogenic terminal differentiation (264) permits association of this isoform with specific DNA binding proteins, or acts merely to elevate levels of free pTEFb. Some evidence may come from an earlier study, which showed that ectopic overexpression of a non-functional Cdk9-42 (Cdk9dn) prevents myoblast terminal differentiation (132, 264). This raises the possibility that the high levels of Cdk9dn can outcompete the endogenous Cdk9 isoforms to interact with pTEFb localizing proteins such as MyoD, so that the Cdk9dn becomes localized to NELF binding sites. In turn, the lost kinase function of the Cdk9dn would not be able to relieve NELF binding at target genes, so that myoblasts remain in a state of proliferation. Thus, this suggests a non-discriminatory role of the N-terminal tail of Cdk9 isoforms to interact with localizing proteins such as MyoD, and the interaction of pTEFb with MyoD may be reliant only on elevated availability of pTEFb regardless of its constituent Cdk9 isoform. Thus, while a shorter Cdk9-42 isoform may be incorporated into housekeeping complexes such as the super elongation complex (Figure 6.3A), the arginine-rich N-terminal tail of Cdk9-55 localizes the larger isoform

to the nucleolus as part of the cellular stress response pathway (358). This allows to sequester active Cdk9, which can be suddenly released in response to cellular stressors (Figure 6.3B). The sudden abundance of free pTEFb becomes available to interact with specific DNA-localizing proteins such as MyoD, which recruits pTEFb to promoter proximal paused Pol II to phosphorylate DSIF, disengage NELF, and permit rapid gene expression.

6.4.3 Multiple signaling pathways may elicit release of functional pTEFb. An increased abundance of free pTEFb is also achieved when pTEFb is released from a

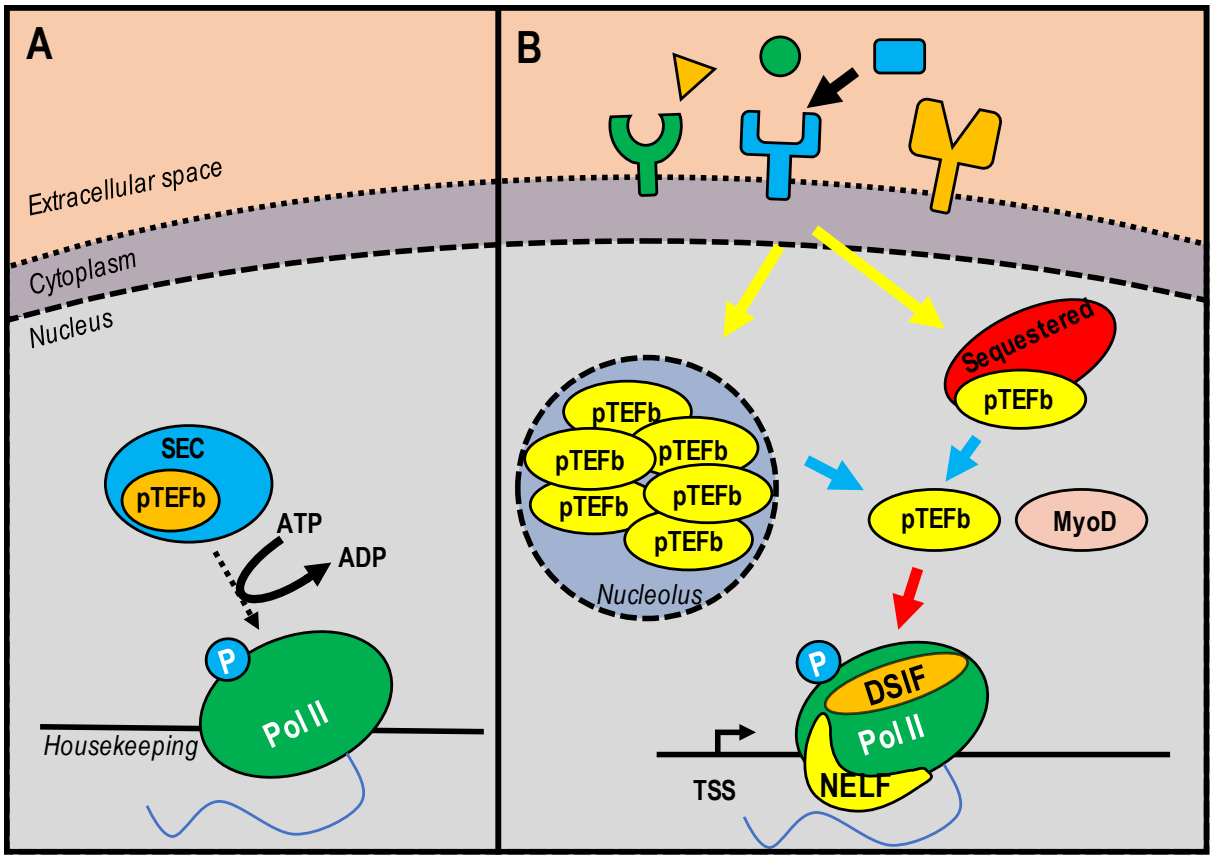

Figure 6.3 – Isoforms of Cdk9 assume different regulatory functions. Cdk9 isoforms localize to different cellular regions which influences its activity. ***(A)*** The smaller Cdk9-42 isoform may be captured by the super elongation complex to participate in housekeeping activities, such as Ser2-P of the Pol II CTD. ***(B)*** Cdk9-55 is sequestered to the nucleolus or to the HEXIM1/2 complex, which inactivates it. Upon extracellular signaling (black arrow), signaling cascades (yellow arrow) perturb either the nucleolus and / or the HEXIM1/2 sequestering complex, which releases free pTEFb composed with the Cdk9-55 isoform (blue arrow). This becomes available to interact with DNA-localizing proteins such as MyoD (pink), which shuttles it towards NELF-bound loci (red arrow), where pTEFb phosphorylates DSIF to evoke a release of NELF and permits active gene expression.

sequestering complex composed of 7SKsnRNA, MeCPE, LARP, and HEXIM1/2 (359). Previous reports indicate this occurs in response to a vast array of contributing factors. For instance, chromatin remodelers such as histone deacetylases and bromodomain and extra-terminal (BET) domains affect the stability of the sequestering complex to regulate the release of free pTEFb (360, 361). The histone modifier JMJD6 (362, 363) can also demethylate the 7SK snRNA (364) and cleave MeCPE (365) to dismantle the sequestering complex and release active pTEFb (364). In addition, signaling pathways such as PI3k/Akt (366) and ERK (367) have been shown to disrupt this sequestering complex, and thereby elevate levels of free pTEFb. In addition, the nucleolus remains responsive to several extracellular stress response pathways (343) to produce a rapid increase in free pTEFb. Therefore, several pathways may contribute to a sudden increase in abundance of free pTEFb to provoke a release of NELF, and permit expression of genes which cause cell cycle withdrawal.

This brings an interesting perspective on the previously discussed role of NELF to retain cellular proliferation and permit spatial differentiation. Here, vast cellular proliferation could proceed until extracellular conditions become unfavorable to do so. This extracellular stress is detected through diverse signaling pathways which disrupt the nucleolus or the pTEFb sequestering complex, and this causes a rapid elevation in nuclear levels of active pTEFb. The abundance of free pTEFb is now available to relieve NELF binding and permit rapid changes in gene expression which culminate in cell cycle arrest and spatial differentiation to occur. In the case of myogenesis, cell-cell contacts (368), PI3K/AKT(222, 369), p38 MAPK (370), ERK/MAPK (371, 372), and JAK-STAT (373) pathways are all known for their ability to induce terminal differentiation. Therefore, while these pathways detect different extracellular stressors

to evoke terminal differentiation, they may contribute individually or collectively to elevate the abundance of free pTEFb, alleviate NELF binding, and induce cell cycle withdrawal for terminal differentiation to occur.

While this remains an interesting pathway, further investigations are required to validate it. To investigate, the ability of myoblasts to undergo terminal differentiation in response to a Cdk9-55 knockdown would reveal whether this isoform may influence terminal differentiation. If these knockdown myoblasts can no longer undergo terminal differentiation, a follow-up rescue experiment with exogenous expression of Cdk9-42 and Cdk9-55 could identify whether the Cdk9 isoforms occupy non-discriminate roles to induce terminal differentiation. In complimentary experiments, immunofluorescence imaging focused on Cdk9-55 localization relative to the nucleolus in proliferating and differentiating myoblasts could further identify whether a release of Cdk9-55 from the nucleolus occurs during terminal differentiation. If the antibodies provide sufficient resolution to show Cdk9-55 colocalization within the nucleolus, subsequent proliferating myoblast populations could be treated with ligands which activate these various pathways, and visualized with immunofluorescence to see whether they promote a release of Cdk9-55 from the nucleolus.

6.4.4 *The NELF-pTEFb axis exerts control on the cell cycle of myogenic cells.*

Previous studies have shown that a loss of functional NELF or DSIF allows transcription to proceed independent of pTEFb (104, 139, 140). Thus, while a difference in pTEFb isoforms is typically required to release NELF and permit expression of genes for terminal differentiation, a non-functional NELF complex

causes spontaneous expression of these genes to evoke terminal differentiation fully independent from pTEFb availability.

Considering the role of NELF to retain myogenic progenitor proliferation, and the translation of extracellular events which coax an increased abundance of pTEFb to alleviate NELF binding for cell cycle withdrawal allows to propose a model of the NELF-pTEFb axis in myogenesis. First, NELF stabilizes paused Pol II at upstream regulators of p53 such as *Ccng1*, which retains low levels of cellular p53, and permits myogenic progenitors to remain engaged in an expansive state. In response to exogenous stimulus through signaling pathways, sequestered pTEFb is rapidly released from the nucleolus and / or HEXIM1/2 sequestering complexes. The elevated abundance of active pTEFb interacts with DNA-localizing proteins such as MyoD, which shuttles pTEFb to NELF-bound genes. Here, pTEFb phosphorylates DSIF which prompts NELF to disengage, and leaves Pol II susceptible to different fates. In some instances, Pol II proceeds towards active elongation to elevate gene expression, while in others, the integrator complex may more freely bind with Pol II and initiate abortive transcription. This produces dysregulated expression of cell cycle regulating genes, which increases levels of p53 to promote production of the cell-cycle arrest protein p21 by *Cdkn1a* (374). Indeed, phenotype rescue experiments performed in chapter 4 supports that a block in p53 activity in NELFb^{scKO} populations does extended myogenic progenitor proliferation in cultured myoblasts and during *in vivo* skeletal muscle regeneration.

6.5 – Potential Mechanisms at play in the context of myogenesis

The results presented in this thesis presents a critical role for the NELF-pTEFb axis in mediating skeletal muscle regeneration. While the axis only exerts effects in proliferating myogenic progenitors, its direct and indirect impacts strongly influence the outcome of the regenerated skeletal muscle. A detailed mechanism is presented below, and summarized in Figure 6.4.

Muscle stem cells during regeneration: from quiescence to proliferation.

Prior to skeletal muscle damage, quiescent MuSCs associated with individual myofibers are maintained in quiescent state, which is supported by various niche microenvironment factors (309). In this quiescent state, many genes have paused Pol II in the promoter-proximal region which may prime them for rapid induction (176). While the factors which support this promoter proximal Pol II pausing are currently unknown, our results suggest the NELF complex may not directly influence the Pol II pausing to elicit changes in the MuSC cell state. Upon damage to skeletal muscle, MuSCs are activated, rapidly enters the cell cycle (23), and undergo a massive expansion in their populations. While doing so, NELF and DSIF associate with paused Pol II at various genes, which stabilize paused Pol II to regulate the expression of these genes. Doing so locks myogenic progenitors in the cell cycle where they undergo a massive population expansion between 2 – 5 dpi. While undergoing proliferation, the myogenic progenitor cells additionally secretes factors in the extracellular environment, such as PEDF. These factors help rejuvenate the niche environment, which will promote downstream quiescent MuSC self-renewal.

External stress signals cell cycle arrest and commitment to terminal differentiation.

Near the end of proliferation, a combination of signaling ligands and cell-cell contacts evoke an internal stress response in myogenic progenitor cells. These pathways cause an abrupt release of sequestered pTEFb from the nucleolus and the HEXIM1/2 sequestering complexes (341). The sudden increase of free pTEFb is available to alleviate NELF binding, and the paused Pol II becomes susceptible towards gene elongation, or abortive transcription. Together, this produces dysregulated expression of cell cycle regulatory genes, which culminates in increased levels of p53. In a NELF-independent pathway, the nucleolus also secretes proteins which support increased abundance of p53 (343). In turn, this prompts cell cycle arrest, withdrawal, and permits myogenic progenitors to become myocytes committed

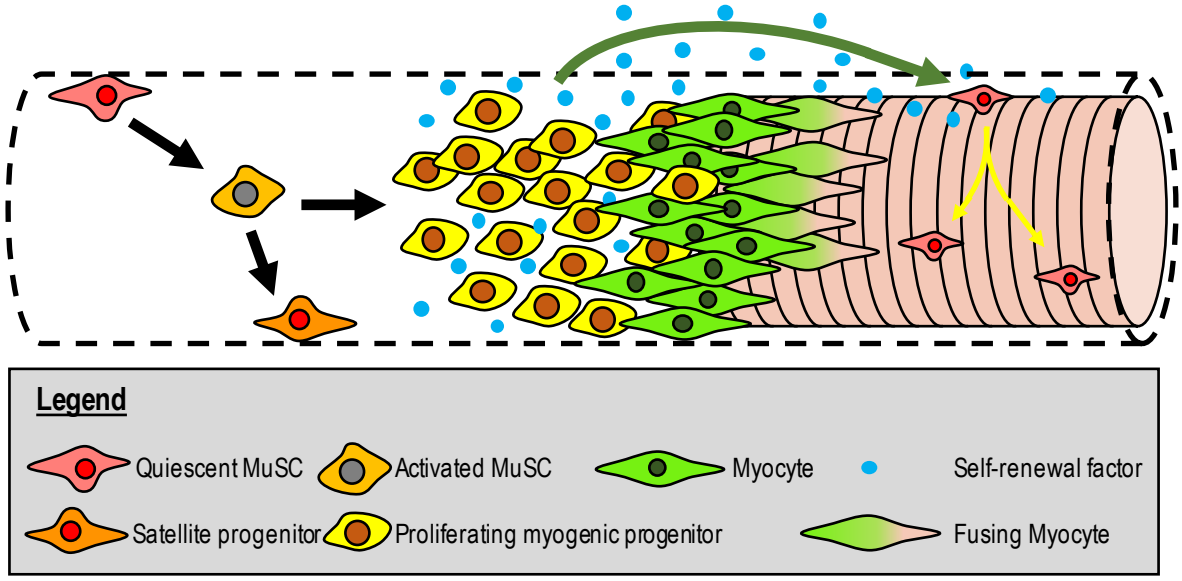

Figure 6.4 – Proposed model on the role of myogenic progenitor cells to promote MuSC self-renewal during skeletal muscle regeneration. In response to acute injury, quiescent MuSCs become activated. While the majority enter the cell cycle to undergo massive expansion, a small subset may return to a dormant state as a satellite progenitor available to participate in future regeneration. During proliferation, myogenic progenitor cells undergo a massive population expansion, and secrete renewing factors in the extracellular environment. In response to extracellular signaling cues, myogenic progenitors withdraw from the cell cycle, and become myocytes committed to terminal differentiation. Myocytes fuse with one another to produce *de novo* myofibers. While this occurs, the renewing factors secreted by myogenic progenitor cells effectuate self-renewal of the quiescent MuSCs which did not participate in regeneration.

to terminal differentiation. In turn, myocytes fuse with one another or with damaged myofibers to generate multinucleated myofibers.

MuSC self-renewal. At the end of myogenic progenitor proliferation, terminal differentiation allows myocytes to produce *de novo* myofibers. In addition, the rejuvenated niche microenvironment causes self-renewal of MuSCs which have remained quiescent, which typically occurs from 5 – 7 days post injury (24). The niche environment plays a critical role towards this self-renewal and subsequent maintenance of MuSC quiescence (309). At this point, the skeletal muscle is functional and ready to respond to future damage and general skeletal muscle homeostasis.

6.6 – Closing remarks

The results presented within this thesis have contributed to our understanding of cellular processes during skeletal muscle regeneration. In particular, we uncovered a previously unappreciated ability of proliferating myogenic progenitors to reformulate the extracellular environment in support of downstream MuSC self-renewal. This presents the potential that increasing the extent of myogenic progenitor proliferation *in vivo* could promote downstream MuSC self-renewal. One method to do so could be through targeted delivery of Flavopiridol to myogenic progenitors, owing to our preliminary *in vitro* results which shows the ability of Flavopiridol to sustain myogenic progenitors in a state of proliferation. Whether these results translate *in vivo* will remain an interesting area for further investigation.

Investigations into the functional implications of NELF on myogenic cell states has identified the NELF-pTEFb axis as a key modulator which controls maintenance

and exit from the cell cycle. This accompanies recent results which suggest NELF may be a master regulator of the cell cycle (108), which elicits withdrawal from the cell cycle in response to extracellular signaling. Indeed, we present a potential mechanism which explains that various extracellular signaling pathways may be able to induce a release of sequestered pTEFb to specifically alleviate NELF binding and permit withdrawal from the cell cycle. While further investigations will be required to validate this axis, it could pose novel approaches to regulate cellular activity towards therapeutic applications which range from tissue regeneration through to tumor suppressors.

Lastly, our results suggest that regulation of promoter proximal Pol II by NELF may be restricted to the population of proliferating myogenic progenitor populations. While the presence of promoter proximal Pol II is apparent in other myogenic cell states such as in quiescent MuSCs, a non-functional NELF complex does not impact the ability of those myogenic to participate in cell state changes. This raises the possibility that either (I) different regulatory proteins assist promoter proximal Pol II pausing to regulate gene expression during these myogenic cell state changes, or that (II) promoter proximal pausing of Pol II is not a rate-limiting step required for those cell state changes.

While intensive research efforts will be required to further explore these concepts, the results presented within this thesis in conjunction with research efforts led by many other groups provide a foundation to direct exciting future investigations.

References

1. Rando, T. A. 2006. Stem cells, ageing and the quest for immortality. *Nature* 441: 1080-1086.

2. Wagers, A. J., and I. L. Weissman. 2004. Plasticity of adult stem cells. *Cell* 116: 639-648.

3. Chatterjee, T., R. S. Sarkar, P. S. Dhot, S. Kumar, and V. K. Kumar. 2010. Adult Stem Cell Plasticity: Dream or Reality? *Med J Armed Forces India* 66: 56-60.

4. Fukada, S. I. 2018. The roles of muscle stem cells in muscle injury, atrophy and hypertrophy. *J Biochem* 163: 353-358.

5. Pawlikowski, B., C. Pulliam, N. D. Betta, G. Kardon, and B. B. Olwin. 2015. Pervasive satellite cell contribution to uninjured adult muscle fibers. *Skeletal muscle* 5: 42.

6. Mitchell, P. O., and G. K. Pavlath. 2004. Skeletal muscle atrophy leads to loss and dysfunction of muscle precursor cells. *American journal of physiology. Cell physiology* 287: C1753-1762.

7. Snijders, T., B. T. Wall, M. L. Dirks, J. M. Senden, F. Hartgens, J. Dolmans, M. Losen, L. B. Verdijk, and L. J. van Loon. 2014. Muscle disuse atrophy is not accompanied by changes in skeletal muscle satellite cell content. *Clinical science* 126: 557-566.

8. McCarthy, J. J., J. Mula, M. Miyazaki, R. Erfani, K. Garrison, A. B. Farooqui, R. Srikuea, B. A. Lawson, B. Grimes, C. Keller, G. Van Zant, K. S. Campbell, K. A. Esser, E. E. Dupont-Versteegden, and C. A. Peterson. 2011. Effective fiber hypertrophy in satellite cell-depleted skeletal muscle. *Development* 138: 3657-3666.

9. Egner, I. M., J. C. Bruusgaard, and K. Gundersen. 2016. Satellite cell depletion prevents fiber hypertrophy in skeletal muscle. *Development* 143: 2898-2906.

10. Goh, Q., and D. P. Millay. 2017. Requirement of myomaker-mediated stem cell fusion for skeletal muscle hypertrophy. *eLife* 6.

11. Latil, M., P. Rocheteau, L. Chatre, S. Sanulli, S. Memet, M. Ricchetti, S. Tajbakhsh, and F. Chretien. 2012. Skeletal muscle stem cells adopt a dormant cell state post mortem and retain regenerative capacity. *Nat Commun* 3: 903.

12. Frontera, W. R., and J. Ochala. 2015. Skeletal muscle: a brief review of structure and function. *Calcif Tissue Int* 96: 183-195.

13. Dasgupta, R., and D. A. Rodeberg. 2012. Update on rhabdomyosarcoma. *Semin Pediatr Surg* 21: 68-78.

14. Koscielniak, E., M. Morgan, and J. Treuner. 2002. Soft tissue sarcoma in children: prognosis and management. *Paediatr Drugs* 4: 21-28.

15. Egas-Bejar, D., and W. W. Huh. 2014. Rhabdomyosarcoma in adolescent and young adult patients: current perspectives. *Adolesc Health Med Ther* 5: 115-125.

16. Ferrari, A., P. Dileo, M. Casanova, R. Bertulli, C. Meazza, L. Gandola, P. Navarria, P. Collini, A. Gronchi, P. Olmi, F. Fossati-Bellani, and P. G. Casali. 2003. Rhabdomyosarcoma in adults. A retrospective analysis of 171 patients treated at a single institution. *Cancer* 98: 571-580.

17. Mauro, A. 1961. Satellite cell of skeletal muscle fibers. *J Biophys Biochem Cytol* 9: 493-495.

18. Charge, S. B., and M. A. Rudnicki. 2004. Cellular and molecular regulation of muscle regeneration. *Physiol Rev* 84: 209-238.

19. Fuchs, E., and H. M. Blau. 2020. Tissue Stem Cells: Architects of Their Niches. *Cell Stem Cell* 27: 532-556.

20. Bischoff, R. 1990. Interaction between satellite cells and skeletal muscle fibers. *Development* 109: 943-952.

21. Morrison, S. J., and J. Kimble. 2006. Asymmetric and symmetric stem-cell divisions in development and cancer. *Nature* 441: 1068-1074.

22. Holterman, C. E., and M. A. Rudnicki. 2005. Molecular regulation of satellite cell function. *Seminars in cell & developmental biology* 16: 575-584.

23. Yin, H., F. Price, and M. A. Rudnicki. 2013. Satellite cells and the muscle stem cell niche. *Physiol Rev* 93: 23-67.

24. Cutler, A. A., B. Pawlikowski, J. R. Wheeler, N. D. Betta, T. Elston, R. O'Rourke, K. Jones, and B. B. Olwin. 2021. The regenerating skeletal muscle niche guides muscle stem cell self-renewal
. *BioRXIV*.

25. Evano, B., S. Khalilian, G. Le Carrou, G. Almouzni, and S. Tajbakhsh. 2020. Dynamics of Asymmetric and Symmetric Divisions of Muscle Stem Cells In Vivo and on Artificial Niches. *Cell reports* 30: 3195-3206 e3197.

26. Yang, W., and P. Hu. 2018. Skeletal muscle regeneration is modulated by inflammation. *J Orthop Translat* 13: 25-32.

27. Arnold, L., A. Henry, F. Poron, Y. Baba-Amer, N. van Rooijen, A. Plonquet, R. K. Gherardi, and B. Chazaud. 2007. Inflammatory monocytes recruited after skeletal muscle injury switch into antiinflammatory macrophages to support myogenesis. *J Exp Med* 204: 1057-1069.

28. Mourkioti, F., and N. Rosenthal. 2005. IGF-1, inflammation and stem cells: interactions during muscle regeneration. *Trends Immunol* 26: 535-542.

29. Zhang, J., Z. Xiao, C. Qu, W. Cui, X. Wang, and J. Du. 2014. CD8 T cells are involved in skeletal muscle regeneration through facilitating MCP-1 secretion and Gr1(high) macrophage infiltration. *J Immunol* 193: 5149-5160.

30. Yennek, S., M. Burute, M. Thery, and S. Tajbakhsh. 2014. Cell adhesion geometry regulates non-random DNA segregation and asymmetric cell fates in mouse skeletal muscle stem cells. *Cell reports* 7: 961-970.

31. Chapman, M. A., R. Meza, and R. L. Lieber. 2016. Skeletal muscle fibroblasts in health and disease. *Differentiation* 92: 108-115.

32. Murphy, M. M., J. A. Lawson, S. J. Mathew, D. A. Hutcheson, and G. Kardon. 2011. Satellite cells, connective tissue fibroblasts and their interactions are crucial for muscle regeneration. *Development* 138: 3625-3637.

33. Mathew, S. J., J. M. Hansen, A. J. Merrell, M. M. Murphy, J. A. Lawson, D. A. Hutcheson, M. S. Hansen, M. Angus-Hill, and G. Kardon. 2011. Connective tissue fibroblasts and Tcf4 regulate myogenesis. *Development* 138: 371-384.

34. Uezumi, A., T. Ito, D. Morikawa, N. Shimizu, T. Yoneda, M. Segawa, M. Yamaguchi, R. Ogawa, M. M. Matev, Y. Miyagoe-Suzuki, S. Takeda, K. Tsujikawa, K. Tsuchida, H.

Yamamoto, and S. Fukada. 2011. Fibrosis and adipogenesis originate from a common mesenchymal progenitor in skeletal muscle. *J Cell Sci* 124: 3654-3664.

35. Joe, A. W., L. Yi, A. Natarajan, F. Le Grand, L. So, J. Wang, M. A. Rudnicki, and F. M. Rossi. 2010. Muscle injury activates resident fibro/adipogenic progenitors that facilitate myogenesis. *Nat Cell Biol* 12: 153-163.

36. Koirala, S., L. V. Reddy, and C. P. Ko. 2003. Roles of glial cells in the formation, function, and maintenance of the neuromuscular junction. *J Neurocytol* 32: 987-1002.

37. Latroche, C., C. Gitiaux, F. Chretien, I. Desguerre, R. Mounier, and B. Chazaud. 2015. Skeletal Muscle Microvasculature: A Highly Dynamic Lifeline. *Physiology (Bethesda)* 30: 417-427.

38. Verma, M., Y. Asakura, B. S. R. Murakonda, T. Pengo, C. Latroche, B. Chazaud, L. K. McLoon, and A. Asakura. 2018. Muscle Satellite Cell Cross-Talk with a Vascular Niche Maintains Quiescence via VEGF and Notch Signaling. *Cell Stem Cell* 23: 530-543 e539.

39. Lira, V. A., C. R. Benton, Z. Yan, and A. Bonen. 2010. PGC-1alpha regulation by exercise training and its influences on muscle function and insulin sensitivity. *Am J Physiol Endocrinol Metab* 299: E145-161.

40. Rowe, G. C., S. Raghuram, C. Jang, J. A. Nagy, I. S. Patten, A. Goyal, M. C. Chan, L. X. Liu, A. Jiang, K. C. Spokes, D. Beeler, H. Dvorak, W. C. Aird, and Z. Arany. 2014. PGC-1alpha induces SPP1 to activate macrophages and orchestrate functional angiogenesis in skeletal muscle. *Circ Res* 115: 504-517.

41. Bjornson, C. R., T. H. Cheung, L. Liu, P. V. Tripathi, K. M. Steeper, and T. A. Rando. 2012. Notch signaling is necessary to maintain quiescence in adult muscle stem cells. *Stem Cells* 30: 232-242.

42. Mourikis, P., R. Sambasivan, D. Castel, P. Rocheteau, V. Bizzarro, and S. Tajbakhsh. 2012. A critical requirement for notch signaling in maintenance of the quiescent skeletal muscle stem cell state. *Stem Cells* 30: 243-252.

43. Relaix, F., M. Bencze, M. J. Borok, A. Der Vartanian, F. Gattazzo, D. Mademtzoglou, S. Perez-Diaz, A. Prola, P. C. Reyes-Fernandez, A. Rotini, and t. Taglietti. 2021. Perspectives on skeletal muscle stem cells. *Nat Commun* 12: 692.

44. Biferali, B., D. Proietti, C. Mozzetta, and L. Madaro. 2019. Fibro-Adipogenic Progenitors Cross-Talk in Skeletal Muscle: The Social Network. *Front Physiol* 10: 1074.

45. Lukjanenko, L., S. Karaz, P. Stuelsatz, U. Gurriaran-Rodriguez, J. Michaud, G. Dammone, F. Sizzano, O. Mashinchian, S. Ancel, E. Migliavacca, S. Liot, G. Jacot, S. Metairon, F. Raymond, P. Descombes, A. Palini, B. Chazaud, M. A. Rudnicki, C. F. Bentzinger, and J. N. Feige. 2019. Aging Disrupts Muscle Stem Cell Function by Impairing Matricellular WISP1 Secretion from Fibro-Adipogenic Progenitors. *Cell Stem Cell* 24: 433-446 e437.

46. Mozzetta, C., S. Consalvi, V. Saccone, M. Tierney, A. Diamantini, K. J. Mitchell, G. Marazzi, G. Borsellino, L. Battistini, D. Sassoon, A. Sacco, and P. L. Puri. 2013. Fibroadipogenic progenitors mediate the ability of HDAC inhibitors to promote regeneration in dystrophic muscles of young, but not old Mdx mice. *EMBO molecular medicine* 5: 626-639.

47. Burzyn, D., W. Kuswanto, D. Kolodin, J. L. Shadrach, M. Cerletti, Y. Jang, E. Sefik, T. G. Tan, A. J. Wagers, C. Benoist, and D. Mathis. 2013. A special population of regulatory T cells potentiates muscle repair. *Cell* 155: 1282-1295.

48. Fry, C. S., T. J. Kirby, K. Kosmac, J. J. McCarthy, and C. A. Peterson. 2017. Myogenic Progenitor Cells Control Extracellular Matrix Production by Fibroblasts during Skeletal Muscle Hypertrophy. *Cell Stem Cell* 20: 56-69.

49. De Micheli, A. J., E. J. Laurilliard, C. L. Heinke, H. Ravichandran, P. Fraczek, S. Soueid-Baumgarten, I. De Vlaminck, O. Elemento, and B. D. Cosgrove. 2020. Single-Cell Analysis of the Muscle Stem Cell Hierarchy Identifies Heterotypic Communication Signals Involved in Skeletal Muscle Regeneration. *Cell reports* 30: 3583-3595 e3585.

50. Riuzzi, F., G. Sorci, C. Arcuri, I. Giambanco, I. Bellezza, A. Minelli, and R. Donato. 2018. Cellular and molecular mechanisms of sarcopenia: the S100B perspective. *J Cachexia Sarcopenia Muscle* 9: 1255-1268.

51. Robinson, D. C. L., and F. J. Dilworth. 2018. Epigenetic Regulation of Adult Myogenesis. *Curr Top Dev Biol* 126: 235-284.

52. Liu, Y., A. Chu, I. Chakroun, U. Islam, and A. Blais. 2010. Cooperation between myogenic regulatory factors and SIX family transcription factors is important for myoblast differentiation. *Nucleic Acids Res* 38: 6857-6871.

53. Niro, C., J. Demignon, S. Vincent, Y. Liu, J. Giordani, N. Sgarioto, M. Favier, I. Guillet-Deniau, A. Blais, and P. Maire. 2010. Six1 and Six4 gene expression is necessary to activate the fast-type muscle gene program in the mouse primary myotome. *Dev Biol* 338: 168-182.

54. Black, B. L., and E. N. Olson. 1998. Transcriptional control of muscle development by myocyte enhancer factor-2 (MEF2) proteins. *Annu Rev Cell Dev Biol* 14: 167-196.

55. Moncaut, N., P. W. Rigby, and J. J. Carvajal. 2013. Dial M(RF) for myogenesis. *FEBS J* 280: 3980-3990.

56. Kuang, S., K. Kuroda, F. Le Grand, and M. A. Rudnicki. 2007. Asymmetric self-renewal and commitment of satellite stem cells in muscle. *Cell* 129: 999-1010.

57. Zammit, P. S., T. A. Partridge, and Z. Yablonka-Reuveni. 2006. The skeletal muscle satellite cell: the stem cell that came in from the cold. *J Histochem Cytochem* 54: 1177-1191.

58. Megeney, L. A., B. Kablar, K. Garrett, J. E. Anderson, and M. A. Rudnicki. 1996. MyoD is required for myogenic stem cell function in adult skeletal muscle. *Genes Dev* 10: 1173-1183.

59. Ustanina, S., J. Carvajal, P. Rigby, and T. Braun. 2007. The myogenic factor Myf5 supports efficient skeletal muscle regeneration by enabling transient myoblast amplification. *Stem Cells* 25: 2006-2016.

60. Tintignac, L. A., M. P. Leibovitch, M. Kitzmann, A. Fernandez, B. Ducommun, L. Meijer, and S. A. Leibovitch. 2000. Cyclin E-cdk2 phosphorylation promotes late G1-phase degradation of MyoD in muscle cells. *Exp Cell Res* 259: 300-307.

61. Batonnet-Pichon, S., L. J. Tintignac, A. Castro, V. Sirri, M. P. Leibovitch, T. Lorca, and S. A. Leibovitch. 2006. MyoD undergoes a distinct G2/M-specific regulation in muscle cells. *Exp Cell Res* 312: 3999-4010.

62. Singh, K., and F. J. Dilworth. 2013. Differential modulation of cell cycle progression distinguishes members of the myogenic regulatory factor family of transcription factors. *FEBS J*.

63. Zammit, P. S., J. P. Golding, Y. Nagata, V. Hudon, T. A. Partridge, and J. R. Beauchamp. 2004. Muscle satellite cells adopt divergent fates: a mechanism for self-renewal? *J Cell Biol* 166: 347-357.

64. Olguin, H. C., and B. B. Olwin. 2004. Pax-7 up-regulation inhibits myogenesis and cell cycle progression in satellite cells: a potential mechanism for self-renewal. *Dev Biol* 275: 375-388.

65. Olguin, H. C., Z. Yang, S. J. Tapscott, and B. B. Olwin. 2007. Reciprocal inhibition between Pax7 and muscle regulatory factors modulates myogenic cell fate determination. *J Cell Biol* 177: 769-779.

66. Zhang, N., J. Mendieta-Esteban, A. Magli, K. C. Lilja, R. C. R. Perlingeiro, M. A. Marti-Renom, A. Tsirigos, and B. D. Dynlacht. 2020. Muscle progenitor specification and myogenic differentiation are associated with changes in chromatin topology. *Nat Commun* 11: 6222.

67. Deato, M. D., M. T. Marr, T. Sottero, C. Inouye, P. Hu, and R. Tjian. 2008. MyoD targets TAF3/TRF3 to activate myogenin transcription. *Mol Cell* 32: 96-105.

68. Liu, Q. C., X. H. Zha, H. Faralli, H. Yin, C. Louis-Jeune, E. Perdiguero, E. Pranckeviciene, P. Munoz-Canoves, M. A. Rudnicki, M. Brand, C. Perez-Iratxeta, and F. J. Dilworth. 2012. Comparative expression profiling identifies differential roles for Myogenin and p38alpha MAPK signaling in myogenesis. *Journal of molecular cell biology* 4: 386-397.

69. Zhang, P., C. Wong, D. Liu, M. Finegold, J. W. Harper, and S. J. Elledge. 1999. p21(CIP1) and p57(KIP2) control muscle differentiation at the myogenin step. *Genes Dev* 13: 213-224.

70. Hinterberger, T. J., D. A. Sassoon, S. J. Rhodes, and S. F. Konieczny. 1991. Expression of the muscle regulatory factor MRF4 during somite and skeletal myofiber development. *Dev Biol* 147: 144-156.

71. Cornelison, D. D., B. B. Olwin, M. A. Rudnicki, and B. J. Wold. 2000. MyoD(-/-) satellite cells in single-fiber culture are differentiation defective and MRF4 deficient. *Dev Biol* 224: 122-137.

72. Miska, E. A., C. Karlsson, E. Langley, S. J. Nielsen, J. Pines, and T. Kouzarides. 1999. HDAC4 deacetylase associates with and represses the MEF2 transcription factor. *EMBO J* 18: 5099-5107.

73. Moretti, I., S. Ciciliot, K. A. Dyar, R. Abraham, M. Murgia, L. Agatea, T. Akimoto, S. Bicciato, M. Forcato, P. Pierre, N. H. Uhlenhaut, P. W. Rigby, J. J. Carvajal, B. Blaauw, E. Calabria, and S. Schiaffino. 2016. MRF4 negatively regulates adult skeletal muscle growth by repressing MEF2 activity. *Nat Commun* 7: 12397.

74. Machado, L., J. Esteves de Lima, O. Fabre, C. Proux, R. Legendre, A. Szegedi, H. Varet, L. R. Ingerslev, R. Barres, F. Relaix, and P. Mourikis. 2017. In Situ Fixation Redefines Quiescence and Early Activation of Skeletal Muscle Stem Cells. *Cell reports* 21: 1982-1993.

75. van Velthoven, C. T. J., A. de Morree, I. M. Egner, J. O. Brett, and T. A. Rando. 2017. Transcriptional Profiling of Quiescent Muscle Stem Cells In Vivo. *Cell reports* 21: 1994-2004.

76. Crist, C. G., D. Montarras, and M. Buckingham. 2012. Muscle satellite cells are primed for myogenesis but maintain quiescence with sequestration of Myf5 mRNA targeted by microRNA-31 in mRNP granules. *Cell Stem Cell* 11: 118-126.

77. Hausburg, M. A., J. D. Doles, S. L. Clement, A. B. Cadwallader, M. N. Hall, P. J. Blackshear, J. Lykke-Andersen, and B. B. Olwin. 2015. Post-transcriptional regulation of satellite cell quiescence by TTP-mediated mRNA decay. *eLife* 4: e03390.

78. Nikolov, D. B., and S. K. Burley. 1997. RNA polymerase II transcription initiation: a structural view. *Proc Natl Acad Sci U S A* 94: 15-22.

79. Phatnani, H. P., and A. L. Greenleaf. 2006. Phosphorylation and functions of the RNA polymerase II CTD. *Genes Dev* 20: 2922-2936.

80. Core, L., and K. Adelman. 2019. Promoter-proximal pausing of RNA polymerase II: a nexus of gene regulation. *Genes Dev* 33: 960-982.

81. Komarnitsky, P., E. J. Cho, and S. Buratowski. 2000. Different phosphorylated forms of RNA polymerase II and associated mRNA processing factors during transcription. *Genes Dev* 14: 2452-2460.

82. Asfour, H. A., M. Z. Allouh, and R. S. Said. 2018. Myogenic regulatory factors: The orchestrators of myogenesis after 30 years of discovery. *Exp Biol Med (Maywood)* 243: 118-128.

83. Massenet, J., E. Gardner, B. Chazaud, and F. J. Dilworth. 2021. Epigenetic regulation of satellite cell fate during skeletal muscle regeneration. *Skeletal muscle* 11: 4.

84. Kim, T. H., L. O. Barrera, M. Zheng, C. Qu, M. A. Singer, T. A. Richmond, Y. Wu, R. D. Green, and B. Ren. 2005. A high-resolution map of active promoters in the human genome. *Nature* 436: 876-880.

85. Guenther, M. G., S. S. Levine, L. A. Boyer, R. Jaenisch, and R. A. Young. 2007. A chromatin landmark and transcription initiation at most promoters in human cells. *Cell* 130: 77-88.

86. Muse, G. W., D. A. Gilchrist, S. Nechaev, R. Shah, J. S. Parker, S. F. Grissom, J. Zeitlinger, and K. Adelman. 2007. RNA polymerase is poised for activation across the genome. *Nat Genet* 39: 1507-1511.

87. Zeitlinger, J., A. Stark, M. Kellis, J. W. Hong, S. Nechaev, K. Adelman, M. Levine, and R. A. Young. 2007. RNA polymerase stalling at developmental control genes in the Drosophila melanogaster embryo. *Nat Genet* 39: 1512-1516.

88. Core, L. J., J. J. Waterfall, and J. T. Lis. 2008. Nascent RNA sequencing reveals widespread pausing and divergent initiation at human promoters. *Science* 322: 1845-1848.

89. Core, L. J., J. J. Waterfall, D. A. Gilchrist, D. C. Fargo, H. Kwak, K. Adelman, and J. T. Lis. 2012. Defining the status of RNA polymerase at promoters. *Cell reports* 2: 1025-1035.

90. Gilmour, D. S., and J. T. Lis. 1986. RNA polymerase II interacts with the promoter region of the noninduced hsp70 gene in Drosophila melanogaster cells. *Mol Cell Biol* 6: 3984-3989.

91. Fant, C. B., C. B. Levandowski, K. Gupta, Z. L. Maas, J. Moir, J. D. Rubin, A. Sawyer, M. N. Esbin, J. K. Rimel, O. Luyties, M. T. Marr, I. Berger, R. D. Dowell, and D. J. Taatjes. 2020. TFIID Enables RNA Polymerase II Promoter-Proximal Pausing. *Mol Cell* 78: 785-793 e788.

92. Aida, M., Y. Chen, K. Nakajima, Y. Yamaguchi, T. Wada, and H. Handa. 2006. Transcriptional pausing caused by NELF plays a dual role in regulating immediate-early expression of the junB gene. *Mol Cell Biol* 26: 6094-6104.

93. Vos, S. M., L. Farnung, H. Urlaub, and P. Cramer. 2018. Structure of paused transcription complex Pol II-DSIF-NELF. *Nature* 560: 601-606.

94. Sheridan, R. M., N. Fong, A. D'Alessandro, and D. L. Bentley. 2019. Widespread Backtracking by RNA Pol II Is a Major Effector of Gene Activation, 5' Pause Release, Termination, and Transcription Elongation Rate. *Mol Cell* 73: 107-118 e104.

95. Adelman, K., M. T. Marr, J. Werner, A. Saunders, Z. Ni, E. D. Andrulis, and J. T. Lis. 2005. Efficient release from promoter-proximal stall sites requires transcript cleavage factor TFIIS. *Mol Cell* 17: 103-112.

96. Adelman, K., and T. Henriques. 2018. Transcriptional speed bumps revealed in high resolution. *Nature* 560: 560-561.

97. Vos, S. M., L. Farnung, M. Boehning, C. Wigge, A. Linden, H. Urlaub, and P. Cramer. 2018. Structure of activated transcription complex Pol II-DSIF-PAF-SPT6. *Nature* 560: 607-612.

98. Titov, D. V., B. Gilman, Q. L. He, S. Bhat, W. K. Low, Y. Dang, M. Smeaton, A. L. Demain, P. S. Miller, J. F. Kugel, J. A. Goodrich, and J. O. Liu. 2011. XPB, a subunit of TFIIH, is a target of the natural product triptolide. *Nat Chem Biol* 7: 182-188.

99. Henriques, T., D. A. Gilchrist, S. Nechaev, M. Bern, G. W. Muse, A. Burkholder, D. C. Fargo, and K. Adelman. 2013. Stable pausing by RNA polymerase II provides an opportunity to target and integrate regulatory signals. *Mol Cell* 52: 517-528.

100. Buckley, M. S., H. Kwak, W. R. Zipfel, and J. T. Lis. 2014. Kinetics of promoter Pol II on Hsp70 reveal stable pausing and key insights into its regulation. *Genes Dev* 28: 14-19.

101. Erickson, B., R. M. Sheridan, M. Cortazar, and D. L. Bentley. 2018. Dynamic turnover of paused Pol II complexes at human promoters. *Genes Dev* 32: 1215-1225.

102. Chen, F., X. Gao, and A. Shilatifard. 2015. Stably paused genes revealed through inhibition of transcription initiation by the TFIIH inhibitor triptolide. *Genes Dev* 29: 39-47.

103. Gilchrist, D. A., G. Dos Santos, D. C. Fargo, B. Xie, Y. Gao, L. Li, and K. Adelman. 2010. Pausing of RNA polymerase II disrupts DNA-specified nucleosome organization to enable precise gene regulation. *Cell* 143: 540-551.

104. Cheng, B., and D. H. Price. 2007. Properties of RNA polymerase II elongation complexes before and after the P-TEFb-mediated transition into productive elongation. *J Biol Chem* 282: 21901-21912.

105. Missra, A., and D. S. Gilmour. 2010. Interactions between DSIF (DRB sensitivity inducing factor), NELF (negative elongation factor), and the Drosophila RNA polymerase II transcription elongation complex. *Proc Natl Acad Sci U S A* 107: 11301-11306.

106. Shao, W., and J. Zeitlinger. 2017. Paused RNA polymerase II inhibits new transcriptional initiation. *Nat Genet* 49: 1045-1051.

107. Gilchrist, D. A., S. Nechaev, C. Lee, S. K. Ghosh, J. B. Collins, L. Li, D. S. Gilmour, and K. Adelman. 2008. NELF-mediated stalling of Pol II can enhance gene expression by blocking promoter-proximal nucleosome assembly. *Genes Dev* 22: 1921-1933.

108. Williams, L. H., G. Fromm, N. G. Gokey, T. Henriques, G. W. Muse, A. Burkholder, D. C. Fargo, G. Hu, and K. Adelman. 2015. Pausing of RNA polymerase II regulates mammalian developmental potential through control of signaling networks. *Mol Cell* 58: 311-322.

109. Elrod, N. D., T. Henriques, K. L. Huang, D. C. Tatomer, J. E. Wilusz, E. J. Wagner, and K. Adelman. 2019. The Integrator Complex Attenuates Promoter-Proximal Transcription at Protein-Coding Genes. *Mol Cell* 76: 738-752 e737.

110. Tatomer, D. C., N. D. Elrod, D. Liang, M. S. Xiao, J. Z. Jiang, M. Jonathan, K. L. Huang, E. J. Wagner, S. Cherry, and J. E. Wilusz. 2019. The Integrator complex cleaves nascent mRNAs to attenuate transcription. *Genes Dev* 33: 1525-1538.

111. Aiyar, S. E., J. L. Sun, A. L. Blair, C. A. Moskaluk, Y. Z. Lu, Q. N. Ye, Y. Yamaguchi, A. Mukherjee, D. M. Ren, H. Handa, and R. Li. 2004. Attenuation of estrogen receptor alpha-mediated transcription through estrogen-stimulated recruitment of a negative elongation factor. *Genes Dev* 18: 2134-2146.

112. Adelman, K., M. A. Kennedy, S. Nechaev, D. A. Gilchrist, G. W. Muse, Y. Chinenov, and I. Rogatsky. 2009. Immediate mediators of the inflammatory response are poised for gene activation through RNA polymerase II stalling. *Proc Natl Acad Sci U S A* 106: 18207-18212.

113. Wu, C. H., Y. Yamaguchi, L. R. Benjamin, M. Horvat-Gordon, J. Washinsky, E. Enerly, J. Larsson, A. Lambertsson, H. Handa, and D. Gilmour. 2003. NELF and DSIF cause promoter proximal pausing on the hsp70 promoter in Drosophila. *Genes Dev* 17: 1402-1414.

114. Ghosh, S. K., A. Missra, and D. S. Gilmour. 2011. Negative elongation factor accelerates the rate at which heat shock genes are shut off by facilitating dissociation of heat shock factor. *Mol Cell Biol* 31: 4232-4243.

115. Schaukowitch, K., J. Y. Joo, X. Liu, J. K. Watts, C. Martinez, and T. K. Kim. 2014. Enhancer RNA facilitates NELF release from immediate early genes. *Mol Cell* 56: 29-42.

116. Amleh, A., S. J. Nair, J. Sun, A. Sutherland, P. Hasty, and R. Li. 2009. Mouse cofactor of BRCA1 (Cobra1) is required for early embryogenesis. *PLoS One* 4: e5034.

117. Wang, X., S. Hang, L. Prazak, and J. P. Gergen. 2010. NELF potentiates gene transcription in the Drosophila embryo. *PLoS One* 5: e11498.

118. Mazina, M. Y., E. V. Kovalenko, and N. E. Vorobyeva. 2021. The negative elongation factor NELF promotes induced transcriptional response of Drosophila ecdysone-dependent genes. *Scientific reports* 11: 172.

119. Narita, T., Y. Yamaguchi, K. Yano, S. Sugimoto, S. Chanarat, T. Wada, D. K. Kim, J. Hasegawa, M. Omori, N. Inukai, M. Endoh, T. Yamada, and H. Handa. 2003. Human transcription elongation factor NELF: identification of novel subunits and reconstitution of the functionally active complex. *Mol Cell Biol* 23: 1863-1873.

120. Bernecky, C., J. M. Plitzko, and P. Cramer. 2017. Structure of a transcribing RNA polymerase II-DSIF complex reveals a multidentate DNA-RNA clamp. *Nat Struct Mol Biol* 24: 809-815.

121. Hein, P. P., K. E. Kolb, T. Windgassen, M. J. Bellecourt, S. A. Darst, R. A. Mooney, and R. Landick. 2014. RNA polymerase pausing and nascent-RNA structure formation are linked through clamp-domain movement. *Nat Struct Mol Biol* 21: 794-802.

122. Szlachta, K., R. G. Thys, N. D. Atkin, L. C. T. Pierce, S. Bekiranov, and Y. H. Wang. 2018. Alternative DNA secondary structure formation affects RNA polymerase II promoter-proximal pausing in human. *Genome Biol* 19: 89.

123. Nechaev, S., D. C. Fargo, G. dos Santos, L. Liu, Y. Gao, and K. Adelman. 2010. Global analysis of short RNAs reveals widespread promoter-proximal stalling and arrest of Pol II in Drosophila. *Science* 327: 335-338.

124. Gupte, R., G. W. Muse, Y. Chinenov, K. Adelman, and I. Rogatsky. 2013. Glucocorticoid receptor represses proinflammatory genes at distinct steps of the transcription cycle. *Proc Natl Acad Sci U S A* 110: 14616-14621.

125. Aoi, Y., E. R. Smith, A. P. Shah, E. J. Rendleman, S. A. Marshall, A. R. Woodfin, F. X. Chen, R. Shiekhattar, and A. Shilatifard. 2020. NELF Regulates a Promoter-Proximal Step Distinct from RNA Pol II Pause-Release. *Mol Cell* 78: 261-274 e265.

126. Gilchrist, D. A., G. Fromm, G. dos Santos, L. N. Pham, I. E. McDaniel, A. Burkholder, D. C. Fargo, and K. Adelman. 2012. Regulating the regulators: the pervasive effects of Pol II pausing on stimulus-responsive gene networks. *Genes Dev* 26: 933-944.

127. Lagha, M., J. P. Bothma, E. Esposito, S. Ng, L. Stefanik, C. Tsui, J. Johnston, K. Chen, D. S. Gilmour, J. Zeitlinger, and M. S. Levine. 2013. Paused Pol II coordinates tissue morphogenesis in the Drosophila embryo. *Cell* 153: 976-987.

128. Boettiger, A. N., and M. Levine. 2009. Synchronous and stochastic patterns of gene activation in the Drosophila embryo. *Science* 325: 471-473.

129. Yamada, T., Y. Yamaguchi, N. Inukai, S. Okamoto, T. Mura, and H. Handa. 2006. P-TEFb-mediated phosphorylation of hSpt5 C-terminal repeats is critical for processive transcription elongation. *Mol Cell* 21: 227-237.

130. Li, Q., J. P. Price, S. A. Byers, D. Cheng, J. Peng, and D. H. Price. 2005. Analysis of the large inactive P-TEFb complex indicates that it contains one 7SK molecule, a dimer of HEXIM1 or HEXIM2, and two P-TEFb molecules containing Cdk9 phosphorylated at threonine 186. *J Biol Chem* 280: 28819-28826.

131. Sonawane, Y. A., M. A. Taylor, J. V. Napoleon, S. Rana, J. I. Contreras, and A. Natarajan. 2016. Cyclin Dependent Kinase 9 Inhibitors for Cancer Therapy. *J Med Chem* 59: 8667-8684.

132. Simone, C., P. Stiegler, L. Bagella, B. Pucci, C. Bellan, G. De Falco, A. De Luca, G. Guanti, P. L. Puri, and A. Giordano. 2002. Activation of MyoD-dependent transcription by cdk9/cyclin T2. *Oncogene* 21: 4137-4148.

133. Fujinaga, K. 2020. P-TEFb as A Promising Therapeutic Target. *Molecules* 25.

134. Luo, Z., C. Lin, E. Guest, A. S. Garrett, N. Mohaghegh, S. Swanson, S. Marshall, L. Florens, M. P. Washburn, and A. Shilatifard. 2012. The super elongation complex family of RNA polymerase II elongation factors: gene target specificity and transcriptional output. *Mol Cell Biol* 32: 2608-2617.

135. De Luca, A., V. Esposito, A. Baldi, P. P. Claudio, Y. Fu, M. Caputi, M. M. Pisano, F. Baldi, and A. Giordano. 1997. CDC2-related kinase PITALRE phosphorylates pRb exclusively on serine and is widely expressed in human tissues. *J Cell Physiol* 172: 265-273.

136. de Falco, G., and A. Giordano. 1998. CDK9 (PITALRE): a multifunctional cdc2-related kinase. *J Cell Physiol* 177: 501-506.

137. Giacinti, C., L. Bagella, P. L. Puri, A. Giordano, and C. Simone. 2006. MyoD recruits the cdk9/cyclin T2 complex on myogenic-genes regulatory regions. *J Cell Physiol* 206: 807-813.

138. Sanso, M., R. S. Levin, J. J. Lipp, V. Y. Wang, A. K. Greifenberg, E. M. Quezada, A. Ali, A. Ghosh, S. Larochelle, T. M. Rana, M. Geyer, L. Tong, K. M. Shokat, and R. P. Fisher. 2016. P-TEFb regulation of transcription termination factor Xrn2 revealed by a chemical genetic screen for Cdk9 substrates. *Genes Dev* 30: 117-131.

139. Wada, T., T. Takagi, Y. Yamaguchi, A. Ferdous, T. Imai, S. Hirose, S. Sugimoto, K. Yano, G. A. Hartzog, F. Winston, S. Buratowski, and H. Handa. 1998. DSIF, a novel transcription elongation factor that regulates RNA polymerase II processivity, is composed of human Spt4 and Spt5 homologs. *Genes Dev* 12: 343-356.

140. Yamaguchi, Y., T. Takagi, T. Wada, K. Yano, A. Furuya, S. Sugimoto, J. Hasegawa, and H. Handa. 1999. NELF, a multisubunit complex containing RD, cooperates with DSIF to repress RNA polymerase II elongation. *Cell* 97: 41-51.

141. Madisen, L., T. A. Zwingman, S. M. Sunkin, S. W. Oh, H. A. Zariwala, H. Gu, L. L. Ng, R. D. Palmiter, M. J. Hawrylycz, A. R. Jones, E. S. Lein, and H. Zeng. 2010. A robust and high-throughput Cre reporting and characterization system for the whole mouse brain. *Nature neuroscience* 13: 133-140.

142. Shultz, L. D., B. L. Lyons, L. M. Burzenski, B. Gott, X. Chen, S. Chaleff, M. Kotb, S. D. Gillies, M. King, J. Mangada, D. L. Greiner, and R. Handgretinger. 2005. Human lymphoid and myeloid cell development in NOD/LtSz-scid IL2R gamma null mice engrafted with mobilized human hemopoietic stem cells. *J Immunol* 174: 6477-6489.

143. Sancak, Y., T. R. Peterson, Y. D. Shaul, R. A. Lindquist, C. C. Thoreen, L. Bar-Peled, and D. M. Sabatini. 2008. The Rag GTPases bind raptor and mediate amino acid signaling to mTORC1. *Science* 320: 1496-1501.

144. Shea, K. L., W. Xiang, V. S. LaPorta, J. D. Licht, C. Keller, M. A. Basson, and A. S. Brack. 2010. Sprouty1 regulates reversible quiescence of a self-renewing adult muscle stem cell pool during regeneration. *Cell Stem Cell* 6: 117-129.

145. Le Moal, E., G. Juban, A. S. Bernard, T. Varga, C. Policar, B. Chazaud, and R. Mounier. 2018. Macrophage-derived superoxide production and antioxidant response following skeletal muscle injury. *Free radical biology & medicine* 120: 33-40.

146. Brun, C. E., Y. X. Wang, and M. A. Rudnicki. 2018. Single EDL Myofiber Isolation for Analyses of Quiescent and Activated Muscle Stem Cells. *Methods Mol Biol* 1686: 149-159.

147. Hindi, L., J. D. McMillan, D. Afroze, S. M. Hindi, and A. Kumar. 2017. Isolation, Culturing, and Differentiation of Primary Myoblasts from Skeletal Muscle of Adult Mice. *Bio Protoc* 7.

148. Guttridge, D. C., M. W. Mayo, L. V. Madrid, C. Y. Wang, and A. S. Baldwin, Jr. 2000. NF-kappaB-induced loss of MyoD messenger RNA: possible role in muscle decay and cachexia. *Science* 289: 2363-2366.

149. Thompson, W. R., B. Nadal-Ginard, and V. Mahdavi. 1991. A MyoD1-independent muscle-specific enhancer controls the expression of the beta-myosin heavy chain gene in skeletal and cardiac muscle cells. *J Biol Chem* 266: 22678-22688.

150. Feige, P., and M. A. Rudnicki. 2020. Isolation of satellite cells and transplantation into mice for lineage tracing in muscle. *Nat Protoc* 15: 1082-1097.

151. Giordani, L., G. J. He, E. Negroni, H. Sakai, J. Y. C. Law, M. M. Siu, R. Wan, A. Corneau, S. Tajbakhsh, T. H. Cheung, and F. Le Grand. 2019. High-Dimensional Single-Cell Cartography Reveals Novel Skeletal Muscle-Resident Cell Populations. *Mol Cell* 74: 609-621 e606.

152. Mahat, D. B., H. Kwak, G. T. Booth, I. H. Jonkers, C. G. Danko, R. K. Patel, C. T. Waters, K. Munson, L. J. Core, and J. T. Lis. 2016. Base-pair-resolution genome-wide mapping of active RNA polymerases using precision nuclear run-on (PRO-seq). *Nat Protoc* 11: 1455-1476.

153. Kaya-Okur, H. S., D. H. Janssens, J. G. Henikoff, K. Ahmad, and S. Henikoff. 2020. Efficient low-cost chromatin profiling with CUT&Tag. *Nat Protoc* 15: 3264-3283.

154. Kaya-Okur, H. S., S. J. Wu, C. A. Codomo, E. S. Pledger, T. D. Bryson, J. G. Henikoff, K. Ahmad, and S. Henikoff. 2019. CUT&Tag for efficient epigenomic profiling of small samples and single cells. *Nat Commun* 10: 1930.

155. Li, Y., K. Nakka, T. Olender, P. Gingras-Gelinas, M. M. Wong, D. C. L. Robinson, H. Bandukwala, C. G. Palii, O. Neyret, M. Brand, A. Blais, and F. J. Dilworth. 2021. Chromatin and transcription factor profiling in rare stem cell populations using CUT&Tag. *STAR Protoc* 2: 100751.

156. Butler, A., P. Hoffman, P. Smibert, E. Papalexi, and R. Satija. 2018. Integrating single-cell transcriptomic data across different conditions, technologies, and species. *Nat Biotechnol* 36: 411-420.

157. Stuart, T., A. Butler, P. Hoffman, C. Hafemeister, E. Papalexi, W. M. Mauck, 3rd, Y. Hao, M. Stoeckius, P. Smibert, and R. Satija. 2019. Comprehensive Integration of Single-Cell Data. *Cell* 177: 1888-1902 e1821.

158. Jacomy, M., T. Venturini, S. Heymann, and M. Bastian. 2014. ForceAtlas2, a continuous graph layout algorithm for handy network visualization designed for the Gephi software. *PLoS One* 9: e98679.

159. Huang da, W., B. T. Sherman, and R. A. Lempicki. 2009. Bioinformatics enrichment tools: paths toward the comprehensive functional analysis of large gene lists. *Nucleic Acids Res* 37: 1-13.

160. Huang da, W., B. T. Sherman, and R. A. Lempicki. 2009. Systematic and integrative analysis of large gene lists using DAVID bioinformatics resources. *Nat Protoc* 4: 44-57.

161. Martin, M. 2011. Cutadapt removes adapter sequences from high-throughput sequencing reads. *EMBnet.journal* 17: 10 - 12.

162. Langmead, B., and S. L. Salzberg. 2012. Fast gapped-read alignment with Bowtie 2. *Nat Methods* 9: 357-359.

163. Ramirez, F., D. P. Ryan, B. Gruning, V. Bhardwaj, F. Kilpert, A. S. Richter, S. Heyne, F. Dundar, and T. Manke. 2016. deepTools2: a next generation web server for deep-sequencing data analysis. *Nucleic Acids Res* 44: W160-165.

164. Meers, M. P., D. Tenenbaum, and S. Henikoff. 2019. Peak calling by Sparse Enrichment Analysis for CUT&RUN chromatin profiling. *Epigenetics Chromatin* 12: 42.

165. Amemiya, H. M., A. Kundaje, and A. P. Boyle. 2019. The ENCODE Blacklist: Identification of Problematic Regions of the Genome. *Scientific reports* 9: 9354.

166. Quinlan, A. R., and I. M. Hall. 2010. BEDTools: a flexible suite of utilities for comparing genomic features. *Bioinformatics* 26: 841-842.

167. Yu, G., L. G. Wang, and Q. Y. He. 2015. ChIPseeker: an R/Bioconductor package for ChIP peak annotation, comparison and visualization. *Bioinformatics* 31: 2382-2383.

168. Yaffe, D., and O. Saxel. 1977. Serial passaging and differentiation of myogenic cells isolated from dystrophic mouse muscle. *Nature* 270: 725-727.

169. Pieper, F. R., R. L. Slobbe, F. C. Ramaekers, H. T. Cuypers, and H. Bloemendal. 1987. Upstream regions of the hamster desmin and vimentin genes regulate expression during in vitro myogenesis. *EMBO J* 6: 3611-3618.

170. Lassar, A. B., B. M. Paterson, and H. Weintraub. 1986. Transfection of a DNA locus that mediates the conversion of 10T1/2 fibroblasts to myoblasts. *Cell* 47: 649-656.

171. Segales, J., A. B. Islam, R. Kumar, Q. C. Liu, P. Sousa-Victor, F. J. Dilworth, E. Ballestar, E. Perdiguero, and P. Munoz-Canoves. 2016. Chromatin-wide and transcriptome profiling integration uncovers p38alpha MAPK as a global regulator of skeletal muscle differentiation. *Skeletal muscle* 6: 9.

172. Song, H., and P. C. Yang. 2010. Construction of shRNA lentiviral vector. *N Am J Med Sci* 2: 598-601.

173. Zacharaki, P., G. Stephanou, and N. A. Demopoulos. 2013. Comparison of the aneugenic properties of nocodazole, paclitaxel and griseofulvin in vitro. Centrosome defects and alterations in protein expression profiles. *J Appl Toxicol* 33: 869-879.

174. Webster, M. T., U. Manor, J. Lippincott-Schwartz, and C. M. Fan. 2016. Intravital Imaging Reveals Ghost Fibers as Architectural Units Guiding Myogenic Progenitors during Regeneration. *Cell Stem Cell* 18: 243-252.

175. Li, M., X. Zhou, Y. Chen, Y. Nie, H. Huang, H. Chen, and D. Mo. 2015. Not all the number of skeletal muscle fibers is determined prenatally. *BMC Dev Biol* 15: 42.

176. Gala, H. P., D. Saha, N. Venugopal, A. Aloysius, and J. Dhawan. 2018. RNA polymerase II pausing regulates a quiescence-dependent transcriptional program, priming cells for cell cycle reentry. *BioRXIV*.

177. van den Brink, S. C., F. Sage, A. Vertesy, B. Spanjaard, J. Peterson-Maduro, C. S. Baron, C. Robin, and A. van Oudenaarden. 2017. Single-cell sequencing reveals dissociation-induced gene expression in tissue subpopulations. *Nat Methods* 14: 935-936.

178. Salic, A., and T. J. Mitchison. 2008. A chemical method for fast and sensitive detection of DNA synthesis in vivo. *Proc Natl Acad Sci U S A* 105: 2415-2420.

179. Rodgers, J. T., K. Y. King, J. O. Brett, M. J. Cromie, G. W. Charville, K. K. Maguire, C. Brunson, N. Mastey, L. Liu, C. R. Tsai, M. A. Goodell, and T. A. Rando. 2014. mTORC1 controls the adaptive transition of quiescent stem cells from G0 to G(Alert). *Nature* 510: 393-396.

180. Siegel, A. L., P. K. Kuhlmann, and D. D. Cornelison. 2011. Muscle satellite cell proliferation and association: new insights from myofiber time-lapse imaging. *Skelet Muscle* 1: 7.

181. Luthi, A. U., and S. J. Martin. 2007. The CASBAH: a searchable database of caspase substrates. *Cell Death Differ* 14: 641-650.

182. Timmer, J. C., and G. S. Salvesen. 2007. Caspase substrates. *Cell Death Differ* 14: 66-72.

183. Zeng, C., F. Pan, L. A. Jones, M. M. Lim, E. A. Griffin, Y. I. Sheline, M. A. Mintun, D. M. Holtzman, and R. H. Mach. 2010. Evaluation of 5-ethynyl-2'-deoxyuridine staining as a sensitive and reliable method for studying cell proliferation in the adult nervous system. *Brain Res* 1319: 21-32.

184. Maltsev, D. I., K. A. Mellanson, V. V. Belousov, G. N. Enikolopov, and O. V. Podgorny. 2021. The bioavailability time of commonly used thymidine analogues after intraperitoneal delivery in mice: labeling kinetics in vivo and clearance from blood serum. *Histochem Cell Biol*.

185. Walston, J. D. 2012. Sarcopenia in older adults. *Curr Opin Rheumatol* 24: 623-627.

186. Dollinger, R., and D. S. Gilmour. 2021. Regulation of Promoter Proximal Pausing of RNA Polymerase II in Metazoans. *J Mol Biol* 433: 166897.

187. Wang, Y. V., H. Tang, and D. S. Gilmour. 2005. Identification in vivo of different rate-limiting steps associated with transcriptional activators in the presence and absence of a GAGA element. *Mol Cell Biol* 25: 3543-3552.

188. Matharu, N. K., T. Hussain, R. Sankaranarayanan, and R. K. Mishra. 2010. Vertebrate homologue of Drosophila GAGA factor. *J Mol Biol* 400: 434-447.

189. Tsai, S. Y., Y. L. Chang, K. B. Swamy, R. L. Chiang, and D. H. Huang. 2016. GAGA factor, a positive regulator of global gene expression, modulates transcriptional pausing and organization of upstream nucleosomes. *Epigenetics Chromatin* 9: 32.

190. Li, J., Y. Liu, H. S. Rhee, S. K. Ghosh, L. Bai, B. F. Pugh, and D. S. Gilmour. 2013. Kinetic competition between elongation rate and binding of NELF controls promoter-proximal pausing. *Mol Cell* 50: 711-722.

191. Tettey, T. T., X. Gao, W. Shao, H. Li, B. A. Story, A. D. Chitsazan, R. L. Glaser, Z. H. Goode, C. W. Seidel, R. C. Conaway, J. Zeitlinger, M. Blanchette, and J. W. Conaway. 2019. A Role for FACT in RNA Polymerase II Promoter-Proximal Pausing. *Cell reports* 27: 3770-3779 e3777.

192. Akhtar, J., N. Kreim, F. Marini, G. Mohana, D. Brune, H. Binder, and J. Y. Roignant. 2019. Promoter-proximal pausing mediated by the exon junction complex regulates splicing. *Nat Commun* 10: 521.

193. Chen, F. X., A. R. Woodfin, A. Gardini, R. A. Rickels, S. A. Marshall, E. R. Smith, R. Shiekhattar, and A. Shilatifard. 2015. PAF1, a Molecular Regulator of Promoter-Proximal Pausing by RNA Polymerase II. *Cell* 162: 1003-1015.

194. Lu, X., X. Zhu, Y. Li, M. Liu, B. Yu, Y. Wang, M. Rao, H. Yang, K. Zhou, Y. Wang, Y. Chen, M. Chen, S. Zhuang, L. F. Chen, R. Liu, and R. Chen. 2016. Multiple P-TEFbs cooperatively regulate the release of promoter-proximally paused RNA polymerase II. *Nucleic Acids Res* 44: 6853-6867.

195. Yu, M., W. Yang, T. Ni, Z. Tang, T. Nakadai, J. Zhu, and R. G. Roeder. 2015. RNA polymerase II-associated factor 1 regulates the release and phosphorylation of paused RNA polymerase II. *Science* 350: 1383-1386.

196. Vos, S. M., L. Farnung, A. Linden, H. Urlaub, and P. Cramer. 2020. Structure of complete Pol II-DSIF-PAF-SPT6 transcription complex reveals RTF1 allosteric activation. *Nat Struct Mol Biol* 27: 668-677.

197. Hou, L., Y. Wang, Y. Liu, N. Zhang, I. Shamovsky, E. Nudler, B. Tian, and B. D. Dynlacht. 2019. Paf1C regulates RNA polymerase II progression by modulating elongation rate. *Proc Natl Acad Sci U S A* 116: 14583-14592.

198. Cutler, A. A., B. Pawlikowski, J. R. Wheeler, N. D. Betta, T. Elston, R. O'Rourke, K. Jones, and B. B. Olwin. 2021. The regenerating skeletal muscle niche guides muscle stem cell self-renewal. *BioRXIV*.

199. Sacco, A., R. Doyonnas, P. Kraft, S. Vitorovic, and H. M. Blau. 2008. Self-renewal and expansion of single transplanted muscle stem cells. *Nature* 456: 502-506.

200. Boldrin, L., A. Neal, P. S. Zammit, F. Muntoni, and J. E. Morgan. 2012. Donor satellite cell engraftment is significantly augmented when the host niche is preserved and endogenous satellite cells are incapacitated. *Stem Cells* 30: 1971-1984.

201. Baghdadi, M. B., D. Castel, L. Machado, S. I. Fukada, D. E. Birk, F. Relaix, S. Tajbakhsh, and P. Mourikis. 2018. Reciprocal signalling by Notch-Collagen V-CALCR retains muscle stem cells in their niche. *Nature* 557: 714-718.

202. Gerdes, J., U. Schwab, H. Lemke, and H. Stein. 1983. Production of a mouse monoclonal antibody reactive with a human nuclear antigen associated with cell proliferation. *Int J Cancer* 31: 13-20.

203. Gerdes, J., H. Lemke, H. Baisch, H. H. Wacker, U. Schwab, and H. Stein. 1984. Cell cycle analysis of a cell proliferation-associated human nuclear antigen defined by the monoclonal antibody Ki-67. *J Immunol* 133: 1710-1715.

204. Villani, A. C., R. Satija, G. Reynolds, S. Sarkizova, K. Shekhar, J. Fletcher, M. Griesbeck, A. Butler, S. Zheng, S. Lazo, L. Jardine, D. Dixon, E. Stephenson, E. Nilsson, I. Grundberg, D. McDonald, A. Filby, W. Li, P. L. De Jager, O. Rozenblatt-Rosen, A. A. Lane, M. Haniffa, A. Regev, and N. Hacohen. 2017. Single-cell RNA-seq reveals new types of human blood dendritic cells, monocytes, and progenitors. *Science* 356.

205. Gury-BenAri, M., C. A. Thaiss, N. Serafini, D. R. Winter, A. Giladi, D. Lara-Astiaso, M. Levy, T. M. Salame, A. Weiner, E. David, H. Shapiro, M. Dori-Bachash, M. Pevsner-Fischer, E. Lorenzo-Vivas, H. Keren-Shaul, F. Paul, A. Harmelin, G. Eberl, S. Itzkovitz, A. Tanay, J. P. Di Santo, E. Elinav, and I. Amit. 2016. The Spectrum and Regulatory Landscape of Intestinal Innate Lymphoid Cells Are Shaped by the Microbiome. *Cell* 166: 1231-1246 e1213.

206. La Manno, G., R. Soldatov, A. Zeisel, E. Braun, H. Hochgerner, V. Petukhov, K. Lidschreiber, M. E. Kastriti, P. Lonnerberg, A. Furlan, J. Fan, L. E. Borm, Z. Liu, D. van Bruggen, J. Guo, X. He, R. Barker, E. Sundstrom, G. Castelo-Branco, P. Cramer, I. Adameyko, S. Linnarsson, and P. V. Kharchenko. 2018. RNA velocity of single cells. *Nature* 560: 494-498.

207. Satija, R., J. A. Farrell, D. Gennert, A. F. Schier, and A. Regev. 2015. Spatial reconstruction of single-cell gene expression data. *Nat Biotechnol* 33: 495-502.

208. Wolf, F. A., F. K. Hamey, M. Plass, J. Solana, J. S. Dahlin, B. Gottgens, N. Rajewsky, L. Simon, and F. J. Theis. 2019. PAGA: graph abstraction reconciles clustering with trajectory inference through a topology preserving map of single cells. *Genome Biol* 20: 59.

209. Hannon, G. J., D. Casso, and D. Beach. 1994. KAP: a dual specificity phosphatase that interacts with cyclin-dependent kinases. *Proc Natl Acad Sci U S A* 91: 1731-1735.

210. Moran, J. L., Y. Li, A. A. Hill, W. M. Mounts, and C. P. Miller. 2002. Gene expression changes during mouse skeletal myoblast differentiation revealed by transcriptional profiling. *Physiol Genomics* 10: 103-111.

211. Hawke, T. J., A. P. Meeson, N. Jiang, S. Graham, K. Hutcheson, J. M. DiMaio, and D. J. Garry. 2003. p21 is essential for normal myogenic progenitor cell function in regenerating skeletal muscle. *American journal of physiology. Cell physiology* 285: C1019-1027.

212. Halevy, O., B. G. Novitch, D. B. Spicer, S. X. Skapek, J. Rhee, G. J. Hannon, D. Beach, and A. B. Lassar. 1995. Correlation of terminal cell cycle arrest of skeletal muscle with induction of p21 by MyoD. *Science* 267: 1018-1021.

213. Quach, N. L., S. Biressi, L. F. Reichardt, C. Keller, and T. A. Rando. 2009. Focal adhesion kinase signaling regulates the expression of caveolin 3 and beta1 integrin, genes essential for normal myoblast fusion. *Mol Biol Cell* 20: 3422-3435.

214. Schwander, M., M. Leu, M. Stumm, O. M. Dorchies, U. T. Ruegg, J. Schittny, and U. Muller. 2003. Beta1 integrins regulate myoblast fusion and sarcomere assembly. *Developmental cell* 4: 673-685.

215. McDonald, K. A., M. Lakonishok, and A. F. Horwitz. 1995. Alpha v and alpha 3 integrin subunits are associated with myofibrils during myofibrillogenesis. *J Cell Sci* 108 (Pt 7): 2573-2581.

216. Tachibana, I., and M. E. Hemler. 1999. Role of transmembrane 4 superfamily (TM4SF) proteins CD9 and CD81 in muscle cell fusion and myotube maintenance. *J Cell Biol* 146: 893-904.

217. Kurisaki, T., A. Masuda, K. Sudo, J. Sakagami, S. Higashiyama, Y. Matsuda, A. Nagabukuro, A. Tsuji, Y. Nabeshima, M. Asano, Y. Iwakura, and A. Sehara-Fujisawa. 2003. Phenotypic analysis of Meltrin alpha (ADAM12)-deficient mice: involvement of Meltrin alpha in adipogenesis and myogenesis. *Mol Cell Biol* 23: 55-61.

218. Yagami-Hiromasa, T., T. Sato, T. Kurisaki, K. Kamijo, Y. Nabeshima, and A. Fujisawa-Sehara. 1995. A metalloprotease-disintegrin participating in myoblast fusion. *Nature* 377: 652-656.

219. Tamir, Y., and E. Bengal. 2000. Phosphoinositide 3-kinase induces the transcriptional activity of MEF2 proteins during muscle differentiation. *J Biol Chem* 275: 34424-34432.

220. Guillet-Deniau, I., A. F. Burnol, and J. Girard. 1997. Identification and localization of a skeletal muscle secrotonin 5-HT2A receptor coupled to the Jak/STAT pathway. *J Biol Chem* 272: 14825-14829.

221. Mancinelli, R., T. Pietrangelo, G. Burnstock, G. Fano, and S. Fulle. 2012. Transcriptional profile of GTP-mediated differentiation of C2C12 skeletal muscle cells. *Purinergic signalling* 8: 207-221.

222. Briata, P., W. J. Lin, M. Giovarelli, M. Pasero, C. F. Chou, M. Trabucchi, M. G. Rosenfeld, C. Y. Chen, and R. Gherzi. 2012. PI3K/AKT signaling determines a dynamic switch between distinct KSRP functions favoring skeletal myogenesis. *Cell Death Differ* 19: 478-487.

223. Li, Y., B. Jiang, W. Y. Ensign, P. K. Vogt, and J. Han. 2000. Myogenic differentiation requires signalling through both phosphatidylinositol 3-kinase and p38 MAP kinase. *Cellular signalling* 12: 751-757.

224. Coolican, S. A., D. S. Samuel, D. Z. Ewton, F. J. McWade, and J. R. Florini. 1997. The mitogenic and myogenic actions of insulin-like growth factors utilize distinct signaling pathways. *J Biol Chem* 272: 6653-6662.

225. Tureckova, J., E. M. Wilson, J. L. Cappalonga, and P. Rotwein. 2001. Insulin-like growth factor-mediated muscle differentiation: collaboration between phosphatidylinositol 3-kinase-Akt-signaling pathways and myogenin. *J Biol Chem* 276: 39264-39270.

226. Zetser, A., E. Gredinger, and E. Bengal. 1999. p38 mitogen-activated protein kinase pathway promotes skeletal muscle differentiation. Participation of the Mef2c transcription factor. *J Biol Chem* 274: 5193-5200.

227. Lluis, F., E. Ballestar, M. Suelves, M. Esteller, and P. Munoz-Canoves. 2005. E47 phosphorylation by p38 MAPK promotes MyoD/E47 association and muscle-specific gene transcription. *Embo J* 24: 974-984.

228. Delaney, K., P. Kasprzycka, M. A. Ciemerych, and M. Zimowska. 2017. The role of TGF-beta1 during skeletal muscle regeneration. *Cell Biol Int* 41: 706-715.

229. Matushansky, I., F. Radparvar, and A. I. Skoultchi. 2003. CDK6 blocks differentiation: coupling cell proliferation to the block to differentiation in leukemic cells. *Oncogene* 22: 4143-4149.

230. Strzalka, W., and A. Ziemienowicz. 2011. Proliferating cell nuclear antigen (PCNA): a key factor in DNA replication and cell cycle regulation. *Annals of botany* 107: 1127-1140.

231. Yablonka-Reuveni, Z., and A. J. Rivera. 1994. Temporal expression of regulatory and structural muscle proteins during myogenesis of satellite cells on isolated adult rat fibers. *Dev Biol* 164: 588-603.

232. Gurden, M. D., A. J. Holland, W. van Zon, A. Tighe, M. A. Vergnolle, D. A. Andres, H. P. Spielmann, M. Malumbres, R. M. Wolthuis, D. W. Cleveland, and S. S. Taylor. 2010. Cdc20 is required for the post-anaphase, KEN-dependent degradation of centromere protein F. *J Cell Sci* 123: 321-330.

233. Badodi, S., F. Baruffaldi, M. Ganassi, R. Battini, and S. Molinari. 2015. Phosphorylation-dependent degradation of MEF2C contributes to regulate G2/M transition. *Cell Cycle* 14: 1517-1528.

234. Qiao, R., F. Weissmann, M. Yamaguchi, N. G. Brown, R. VanderLinden, R. Imre, M. A. Jarvis, M. R. Brunner, I. F. Davidson, G. Litos, D. Haselbach, K. Mechtler, H. Stark, B. A. Schulman, and J. M. Peters. 2016. Mechanism of APC/CCDC20 activation by mitotic phosphorylation. *Proc Natl Acad Sci U S A* 113: E2570-2578.

235. Cenciarelli, C., F. De Santa, P. L. Puri, E. Mattei, L. Ricci, F. Bucci, A. Felsani, and M. Caruso. 1999. Critical role played by cyclin D3 in the MyoD-mediated arrest of cell cycle during myoblast differentiation. *Mol Cell Biol* 19: 5203-5217.

236. Kiess, M., R. M. Gill, and P. A. Hamel. 1995. Expression of the positive regulator of cell cycle progression, cyclin D3, is induced during differentiation of myoblasts into quiescent myotubes. *Oncogene* 10: 159-166.

237. Gurung, R., and V. K. Parnaik. 2012. Cyclin D3 promotes myogenic differentiation and Pax7 transcription. *J Cell Biochem* 113: 209-219.

238. Haronen, H., Z. Zainul, N. Naumenko, R. Sormunen, I. Miinalainen, A. Shakirzyanova, S. Santoleri, A. V. Kemppainen, R. Giniatullin, T. Pihlajaniemi, and A. Heikkinen. 2019. Correct expression and localization of collagen XIII are crucial for the normal formation and function of the neuromuscular system. *Eur J Neurosci* 49: 1491-1511.

239. Ho, T. C., Y. P. Chiang, C. K. Chuang, S. L. Chen, J. W. Hsieh, Y. W. Lan, and Y. P. Tsao. 2015. PEDF-derived peptide promotes skeletal muscle regeneration through its mitogenic effect on muscle progenitor cells. *American journal of physiology. Cell physiology* 309: C159-168.

240. Yu, L., B. Zhang, D. Deochand, M. A. Sacta, M. Coppo, Y. Shang, Z. Guo, X. Zeng, D. A. Rollins, B. Tharmalingam, R. Li, Y. Chinenov, I. Rogatsky, and X. Hu. 2020. Negative elongation factor complex enables macrophage inflammatory responses by controlling anti-inflammatory gene expression. *Nat Commun* 11: 2286.

241. Awwad, S. W., E. R. Abu-Zhayia, N. Guttmann-Raviv, and N. Ayoub. 2017. NELF-E is recruited to DNA double-strand break sites to promote transcriptional repression and repair. *EMBO Rep* 18: 745-764.

242. Bishara, L. A., F. E. Machour, S. W. Awwad, and N. Ayoub. 2021. NELF complex fosters BRCA1 and RAD51 recruitment to DNA damage sites and modulates sensitivity to PARP inhibition. *DNA Repair (Amst)* 97: 103025.

243. Kwak, H., N. J. Fuda, L. J. Core, and J. T. Lis. 2013. Precise maps of RNA polymerase reveal how promoters direct initiation and pausing. *Science* 339: 950-953.

244. Porrello, A., M. A. Cerone, S. Coen, A. Gurtner, G. Fontemaggi, L. Cimino, G. Piaggio, A. Sacchi, and S. Soddu. 2000. p53 regulates myogenesis by triggering the differentiation activity of pRb. *J Cell Biol* 151: 1295-1304.

245. Cerone, M. A., A. Marchetti, G. Bossi, G. Blandino, A. Sacchi, and S. Soddu. 2000. p53 is involved in the differentiation but not in the differentiation-associated apoptosis of myoblasts. *Cell Death Differ* 7: 506-508.

246. Soddu, S., G. Blandino, R. Scardigli, S. Coen, A. Marchetti, M. G. Rizzo, G. Bossi, L. Cimino, M. Crescenzi, and A. Sacchi. 1996. Interference with p53 protein inhibits hematopoietic and muscle differentiation. *J Cell Biol* 134: 193-204.

247. Dawson, D. W., O. V. Volpert, P. Gillis, S. E. Crawford, H. Xu, W. Benedict, and N. P. Bouck. 1999. Pigment epithelium-derived factor: a potent inhibitor of angiogenesis. *Science* 285: 245-248.

248. Bouck, N. 2002. PEDF: anti-angiogenic guardian of ocular function. *Trends Mol Med* 8: 330-334.

249. Phillips, N. J., M. R. Ziegler, D. M. Radford, K. L. Fair, T. Steinbrueck, F. P. Xynos, and H. Donis-Keller. 1996. Allelic deletion on chromosome 17p13.3 in early ovarian cancer. *Cancer Res* 56: 606-611.

250. Slavc, I., I. R. Rodriguez, K. Mazuruk, G. J. Chader, and J. A. Biegel. 1997. Mutation analysis and loss of heterozygosity of PEDF in central nervous system primitive neuroectodermal tumors. *Int J Cancer* 72: 277-282.

251. Houenou, L. J., A. P. D'Costa, L. Li, V. L. Turgeon, C. Enyadike, E. Alberdi, and S. P. Becerra. 1999. Pigment epithelium-derived factor promotes the survival and differentiation of developing spinal motor neurons. *J Comp Neurol* 412: 506-514.

252. Filleur, S., T. Nelius, W. de Riese, and R. C. Kennedy. 2009. Characterization of PEDF: a multi-functional serpin family protein. *J Cell Biochem* 106: 769-775.

253. Ho, T. C., S. H. Tsai, S. I. Yeh, S. L. Chen, K. Y. Tung, H. Y. Chien, Y. C. Lu, C. H. Huang, and Y. P. Tsao. 2019. PEDF-derived peptide promotes tendon regeneration through its mitogenic effect on tendon stem/progenitor cells. *Stem Cell Res Ther* 10: 2.

254. Chiu, A. C., H. I. Suzuki, X. Wu, D. B. Mahat, A. J. Kriz, and P. A. Sharp. 2018. Transcriptional Pause Sites Delineate Stable Nucleosome-Associated Premature Polyadenylation Suppressed by U1 snRNP. *Mol Cell* 69: 648-663 e647.

255. Dilworth, F. J., and A. Blais. 2011. Epigenetic regulation of satellite cell activation during muscle regeneration. *Stem Cell Res Ther* 2: 18.

256. Sebastian, S., P. Sreenivas, R. Sambasivan, S. Cheedipudi, P. Kandalla, G. K. Pavlath, and J. Dhawan. 2009. MLL5, a trithorax homolog, indirectly regulates H3K4 methylation, represses cyclin A2 expression, and promotes myogenic differentiation. *Proc Natl Acad Sci U S A* 106: 4719-4724.

257. Dunham, I., A. Kundaje, S. F. Aldred, P. J. Collins, C. A. Davis, F. Doyle, C. B. Epstein, S. Frietze, J. Harrow, R. Kaul, J. Khatun, B. R. Lajoie, S. G. Landt, B. K. Lee, F. Pauli, K. R. Rosenbloom, P. Sabo, A. Safi, A. Sanyal, N. Shoresh, J. M. Simon, L. Song, N. D. Trinklein, R. C. Altshuler, E. Birney, J. B. Brown, C. Cheng, S. Djebali, X. Dong, I. Dunham, J. Ernst, T. S. Furey, M. Gerstein, B. Giardine, M. Greven, R. C. Hardison, R. S. Harris, J. Herrero, M. M. Hoffman, S. Iyer, M. Kelllis, J. Khatun, P. Kheradpour, A. Kundaje, T. Lassman, Q. Li, X. Lin, G. K. Marinov, A. Merkel, A. Mortazavi, S. C. Parker, T. E. Reddy, J. Rozowsky, F. Schlesinger, R. E. Thurman, J. Wang, L. D. Ward, T. W. Whitfield, S. P. Wilder, W. Wu, H. S. Xi, K. Y. Yip, J. Zhuang, B. E. Bernstein, E. Birney, I. Dunham, E. D. Green, C. Gunter, M. Snyder, M. J. Pazin, R. F. Lowdon, L. A. Dillon, L. B. Adams, C. J. Kelly, J. Zhang, J. R. Wexler, E. D. Green, P. J. Good, E. A. Feingold, B. E. Bernstein, E. Birney, G. E. Crawford, J. Dekker, L. Elinitski, P. J. Farnham, M. Gerstein, M. C. Giddings, T. R. Gingeras, E. D. Green, R. Guigo, R. C. Hardison, T. J. Hubbard, M. Kellis, W. J. Kent, J. D. Lieb, E. H. Margulies, R. M. Myers, M. Snyder, J. A. Starnatoyannopoulos, S. A. Tennebaum, Z. Weng, K. P. White, B. Wold, J. Khatun, Y. Yu, J. Wrobel, B. A. Risk, H. P. Gunawardena, H. C. Kuiper, C. W. Maier, L. Xie, X. Chen, M. C. Giddings, B. E. Bernstein, C. B. Epstein, N. Shoresh, J. Ernst, P. Kheradpour, T. S. Mikkelsen, S. Gillespie, A. Goren, O. Ram, X. Zhang, L. Wang, R. Issner, M. J. Coyne, T. Durham, M. Ku, T. Truong, L. D. Ward, R. C. Altshuler, M. L. Eaton, M. Kellis, S. Djebali, C. A. Davis, A. Merkel, A. Dobin, T.

Lassmann, A. Mortazavi, A. Tanzer, J. Lagarde, W. Lin, F. Schlesinger, C. Xue, G. K. Marinov, J. Khatun, B. A. Williams, C. Zaleski, J. Rozowsky, M. Roder, F. Kokocinski, R. F. Abdelhamid, T. Alioto, I. Antoshechkin, M. T. Baer, P. Batut, I. Bell, K. Bell, S. Chakrabortty, X. Chen, J. Chrast, J. Curado, T. Derrien, J. Drenkow, E. Dumais, J. Dumais, R. Duttagupta, M. Fastuca, K. Fejes-Toth, P. Ferreira, S. Foissac, M. J. Fullwood, H. Gao, D. Gonzalez, A. Gordon, H. P. Gunawardena, C. Howald, S. Jha, R. Johnson, P. Kapranov, B. King, C. Kingswood, G. Li, O. J. Luo, E. Park, J. B. Preall, K. Presaud, P. Ribeca, B. A. Risk, D. Robyr, X. Ruan, M. Sammeth, K. S. Sandu, L. Schaeffer, L. H. See, A. Shahab, J. Skancke, A. M. Suzuki, H. Takahashi, H. Tilgner, D. Trout, N. Walters, H. Wang, J. Wrobel, Y. Yu, Y. Hayashizaki, J. Harrow, M. Gerstein, T. J. Hubbard, A. Reymond, S. E. Antonarakis, G. J. Hannon, M. C. Giddings, Y. Ruan, B. Wold, P. Carninci, R. Guigo, T. R. Gingeras, K. R. Rosenbloom, C. A. Sloan, K. Learned, V. S. Malladi, M. C. Wong, G. P. Barber, M. S. Cline, T. R. Dreszer, S. G. Heitner, D. Karolchik, W. J. Kent, V. M. Kirkup, L. R. Meyer, J. C. Long, M. Maddren, B. J. Raney, T. S. Furey, L. Song, L. L. Grasfeder, P. G. Giresi, B. K. Lee, A. Battenhouse, N. C. Sheffield, J. M. Simon, K. A. Showers, A. Safi, D. London, A. A. Bhinge, C. Shestak, M. R. Schaner, S. K. Kim, Z. Z. Zhang, P. A. Mieczkowski, J. O. Mieczkowska, Z. Liu, R. M. McDaniell, Y. Ni, N. U. Rashid, M. J. Kim, S. Adar, Z. Zhang, T. Wang, D. Winter, D. Keefe, E. Birney, V. R. Iyer, J. D. Lieb, G. E. Crawford, G. Li, K. S. Sandhu, M. Zheng, P. Wang, O. J. Luo, A. Shahab, M. J. Fullwood, X. Ruan, Y. Ruan, R. M. Myers, F. Pauli, B. A. Williams, J. Gertz, G. K. Marinov, T. E. Reddy, J. Vielmetter, E. C. Partridge, D. Trout, K. E. Varley, C. Gasper, A. Bansal, S. Pepke, P. Jain, H. Amrhein, K. M. Bowling, M. Anaya, M. K. Cross, B. King, M. A. Muratet, I. Antoshechkin, K. M. Newberry, K. McCue, A. S. Nesmith, K. I. Fisher-Aylor, B. Pusey, G. DeSalvo, S. L. Parker, S. Balasubramanian, N. S. Davis, S. K. Meadows, T. Eggleston, C. Gunter, J. S. Newberry, S. E. Levy, D. M. Absher, A. Mortazavi, W. H. Wong, B. Wold, M. J. Blow, A. Visel, L. A. Pennachio, L. Elnitski, E. H. Margulies, S. C. Parker, H. M. Petrykowska, A. Abyzov, B. Aken, D. Barrell, G. Barson, A. Berry, A. Bignell, V. Boychenko, G. Bussotti, J. Chrast, C. Davidson, T. Derrien, G. Despacio-Reyes, M. Diekhans, I. Ezkurdia, A. Frankish, J. Gilbert, J. M. Gonzalez, E. Griffiths, R. Harte, D. A. Hendrix, C. Howald, T. Hunt, I. Jungreis, M. Kay, E. Khurana, F. Kokocinski, J. Leng, M. F. Lin, J. Loveland, Z. Lu, D. Manthravadi, M. Mariotti, J. Mudge, G. Mukherjee, C. Notredame, B. Pei, J. M. Rodriguez, G. Saunders, A. Sboner, S. Searle, C. Sisu, C. Snow, C. Steward, A. Tanzer, E. Tapanan, M. L. Tress, M. J. van Baren, N. Walters, S. Washieti, L. Wilming, A. Zadissa, Z. Zhengdong, M. Brent, D. Haussler, M. Kellis, A. Valencia, M. Gerstein, A. Raymond, R. Guigo, J. Harrow, T. J. Hubbard, S. G. Landt, S. Frietze, A. Abyzov, N. Addleman, R. P. Alexander, R. K. Auerbach, S. Balasubramanian, K. Bettinger, N. Bhardwaj, A. P. Boyle, A. R. Cao, P. Cayting, A. Charos, Y. Cheng, C. Cheng, C. Eastman, G. Euskirchen, J. D. Fleming, F. Grubert, L. Habegger, M. Hariharan, A. Harmanci, S. Iyenger, V. X. Jin, K. J. Karczewski, M. Kasowski, P. Lacroute, H. Lam, N. Larnarre-Vincent, J. Leng, J. Lian, M. Lindahl-Allen, R. Min, B. Miotto, H. Monahan, Z. Moqtaderi, X. J. Mu, H. O'Geen, Z. Ouyang, D. Patacsil, B. Pei, D. Raha, L. Ramirez, B. Reed, J. Rozowsky, A. Sboner, M. Shi, C. Sisu, T. Slifer, H. Witt, L. Wu, X. Xu, K. K. Yan, X. Yang, K. Y. Yip, Z. Zhang, K.

Struhl, S. M. Weissman, M. Gerstein, P. J. Farnham, M. Snyder, S. A. Tenebaum, L. O. Penalva, F. Doyle, S. Karmakar, S. G. Landt, R. R. Bhanvadia, A. Choudhury, M. Domanus, L. Ma, J. Moran, D. Patacsil, T. Slifer, A. Victorsen, X. Yang, M. Snyder, K. P. White, T. Auer, L. Centarin, M. Eichenlaub, F. Gruhl, S. Heerman, B. Hoeckendorf, D. Inoue, T. Kellner, S. Kirchmaier, C. Mueller, R. Reinhardt, L. Schertel, S. Schneider, R. Sinn, B. Wittbrodt, J. Wittbrodt, Z. Weng, T. W. Whitfield, J. Wang, P. J. Collins, S. F. Aldred, N. D. Trinklein, E. C. Partridge, R. M. Myers, J. Dekker, G. Jain, B. R. Lajoie, A. Sanyal, G. Balasundaram, D. L. Bates, R. Byron, T. K. Canfield, M. J. Diegel, D. Dunn, A. K. Ebersol, A. K. Ebersol, T. Frum, K. Garg, E. Gist, R. S. Hansen, L. Boatman, E. Haugen, R. Humbert, G. Jain, A. K. Johnson, E. M. Johnson, T. M. Kutyavin, B. R. Lajoie, K. Lee, D. Lotakis, M. T. Maurano, S. J. Neph, F. V. Neri, E. D. Nguyen, H. Qu, A. P. Reynolds, V. Roach, E. Rynes, P. Sabo, M. E. Sanchez, R. S. Sandstrom, A. Sanyal, A. O. Shafer, A. B. Stergachis, S. Thomas, R. E. Thurman, B. Vernot, J. Vierstra, S. Vong, H. Wang, M. A. Weaver, Y. Yan, M. Zhang, J. A. Akey, M. Bender, M. O. Dorschner, M. Groudine, M. J. MacCoss, P. Navas, G. Stamatoyannopoulos, R. Kaul, J. Dekker, J. A. Stamatoyannopoulos, I. Dunham, K. Beal, A. Brazma, P. Flicek, J. Herrero, N. Johnson, D. Keefe, M. Lukk, N. M. Luscombe, D. Sobral, J. M. Vaquerizas, S. P. Wilder, S. Batzoglou, A. Sidow, N. Hussami, S. Kyriazopoulou-Panagiotopoulou, M. W. Libbrecht, M. A. Schaub, A. Kundaje, R. C. Hardison, W. Miller, B. Giardine, R. S. Harris, W. Wu, P. J. Bickel, B. Banfai, N. P. Boley, J. B. Brown, H. Huang, Q. Li, J. J. Li, W. S. Noble, J. A. Bilmes, O. J. Buske, M. M. Hoffman, A. O. Sahu, P. V. Kharchenko, P. J. Park, D. Baker, J. Taylor, Z. Weng, S. Iyer, X. Dong, M. Greven, X. Lin, J. Wang, H. S. Xi, J. Zhuang, M. Gerstein, R. P. Alexander, S. Balasubramanian, C. Cheng, A. Harmanci, L. Lochovsky, R. Min, X. J. Mu, J. Rozowsky, K. K. Yan, K. Y. Yip, and E. Birney. 2012. An integrated encyclopedia of DNA elements in the human genome. *Nature* 489: 57-74.

258. Consortium, E. P. 2012. An integrated encyclopedia of DNA elements in the human genome. *Nature* 489: 57-74.

259. Abraham, A. G., and E. O'Neill. 2014. PI3K/Akt-mediated regulation of p53 in cancer. *Biochem Soc Trans* 42: 798-803.

260. Wu, G. S. 2004. The functional interactions between the p53 and MAPK signaling pathways. *Cancer Biol Ther* 3: 156-161.

261. Goyal, H., I. Chachoua, C. Pecquet, W. Vainchenker, and S. N. Constantinescu. 2020. A p53-JAK-STAT connection involved in myeloproliferative neoplasm pathogenesis and progression to secondary acute myeloid leukemia. *Blood Rev* 42: 100712.

262. de Azevedo, W. F., Jr., F. Canduri, and N. J. da Silveira. 2002. Structural basis for inhibition of cyclin-dependent kinase 9 by flavopiridol. *Biochem Biophys Res Commun* 293: 566-571.

263. O'Brien, S. K., K. L. Knight, and T. M. Rana. 2012. Phosphorylation of histone H1 by P-TEFb is a necessary step in skeletal muscle differentiation. *J Cell Physiol* 227: 383-389.

264. Giacinti, C., A. Musaro, G. De Falco, I. Jourdan, M. Molinaro, L. Bagella, C. Simone, and A. Giordano. 2008. Cdk9-55: a new player in muscle regeneration. *J Cell Physiol* 216: 576-582.

265. Kouroukis, C. T., A. Belch, M. Crump, E. Eisenhauer, R. D. Gascoyne, R. Meyer, R. Lohmann, P. Lopez, J. Powers, R. Turner, J. M. Connors, and G. National Cancer Institute of Canada Clinical Trials. 2003. Flavopiridol in untreated or relapsed mantle-cell lymphoma: results of a phase II study of the National Cancer Institute of Canada Clinical Trials Group. *J Clin Oncol* 21: 1740-1745.

266. Wang, H. K. 2001. Flavopiridol. National Cancer Institute. *Curr Opin Investig Drugs* 2: 1149-1155.

267. Lanasa, M. C., L. Andritsos, J. R. Brown, J. Gabrilove, F. Caligaris-Cappio, P. Ghia, R. A. Larson, T. J. Kipps, V. Leblond, D. W. Milligan, A. Janssens, A. J. Johnson, N. A. Heerema, A. Buhler, S. Stilgenbauer, J. Devin, M. Hallek, J. C. Byrd, and M. R. Grever. 2015. Final results of EFC6663: a multicenter, international, phase 2 study of alvocidib for patients with fludarabine-refractory chronic lymphocytic leukemia. *Leuk Res* 39: 495-500.

268. Jessen, B. A., L. Lee, T. Koudriakova, M. Haines, K. Lundgren, S. Price, J. Nonomiya, C. Lewis, and G. J. Stevens. 2007. Peripheral white blood cell toxicity induced by broad spectrum cyclin-dependent kinase inhibitors. *J Appl Toxicol* 27: 133-142.

269. Konecny, G. E. 2016. Cyclin-dependent kinase pathways as targets for women's cancer treatment. *Curr Opin Obstet Gynecol* 28: 42-48.

270. Shapiro, G. I. 2006. Cyclin-dependent kinase pathways as targets for cancer treatment. *J Clin Oncol* 24: 1770-1783.

271. Hu, Y., J. Gao, M. Wang, and M. Li. 2021. Potential Prospect of CDK4/6 Inhibitors in Triple-Negative Breast Cancer. *Cancer Manag Res* 13: 5223-5237.

272. Drees, M., W. A. Dengler, T. Roth, H. Labonte, J. Mayo, L. Malspeis, M. Grever, E. A. Sausville, and H. H. Fiebig. 1997. Flavopiridol (L86-8275): selective antitumor activity in vitro and activity in vivo for prostate carcinoma cells. *Clin Cancer Res* 3: 273-279.

273. Senderowicz, A. M. 1999. Flavopiridol: the first cyclin-dependent kinase inhibitor in human clinical trials. *Invest New Drugs* 17: 313-320.

274. Hanahan, D., and R. A. Weinberg. 2011. Hallmarks of cancer: the next generation. *Cell* 144: 646-674.

275. Ding, L., J. Cao, W. Lin, H. Chen, X. Xiong, H. Ao, M. Yu, J. Lin, and Q. Cui. 2020. The Roles of Cyclin-Dependent Kinases in Cell-Cycle Progression and Therapeutic Strategies in Human Breast Cancer. *Int J Mol Sci* 21.

276. Senderowicz, A. M., and E. A. Sausville. 2000. Preclinical and clinical development of cyclin-dependent kinase modulators. *J Natl Cancer Inst* 92: 376-387.

277. Losiewicz, M. D., B. A. Carlson, G. Kaur, E. A. Sausville, and P. J. Worland. 1994. Potent inhibition of CDC2 kinase activity by the flavonoid L86-8275. *Biochem Biophys Res Commun* 201: 589-595.

278. Carlson, B. A., M. M. Dubay, E. A. Sausville, L. Brizuela, and P. J. Worland. 1996. Flavopiridol induces G1 arrest with inhibition of cyclin-dependent kinase (CDK) 2 and CDK4 in human breast carcinoma cells. *Cancer Res* 56: 2973-2978.

279. Sedlacek, H. H. 2001. Mechanisms of action of flavopiridol. *Crit Rev Oncol Hematol* 38: 139-170.

280. Bible, K. C., and S. H. Kaufmann. 1996. Flavopiridol: a cytotoxic flavone that induces cell death in noncycling A549 human lung carcinoma cells. *Cancer Res* 56: 4856-4861.

281. Shapiro, G. I., D. A. Koestner, C. B. Matranga, and B. J. Rollins. 1999. Flavopiridol induces cell cycle arrest and p53-independent apoptosis in non-small cell lung cancer cell lines. *Clin Cancer Res* 5: 2925-2938.

282. Chao, S. H., K. Fujinaga, J. E. Marion, R. Taube, E. A. Sausville, A. M. Senderowicz, B. M. Peterlin, and D. H. Price. 2000. Flavopiridol inhibits P-TEFb and blocks HIV-1 replication. *J Biol Chem* 275: 28345-28348.

283. Castiglioni, A., G. Corna, E. Rigamonti, V. Basso, M. Vezzoli, A. Monno, A. E. Almada, A. Mondino, A. J. Wagers, A. A. Manfredi, and P. Rovere-Querini. 2015. FOXP3+ T Cells Recruited to Sites of Sterile Skeletal Muscle Injury Regulate the Fate of Satellite Cells and Guide Effective Tissue Regeneration. *PLoS One* 10: e0128094.

284. Saclier, M., S. Cuvellier, M. Magnan, R. Mounier, and B. Chazaud. 2013. Monocyte/macrophage interactions with myogenic precursor cells during skeletal muscle regeneration. *FEBS J* 280: 4118-4130.

285. Saclier, M., H. Yacoub-Youssef, A. L. Mackey, L. Arnold, H. Ardjoune, M. Magnan, F. Sailhan, J. Chelly, G. K. Pavlath, R. Mounier, M. Kjaer, and B. Chazaud. 2013. Differentially activated macrophages orchestrate myogenic precursor cell fate during human skeletal muscle regeneration. *Stem Cells* 31: 384-396.

286. Tidball, J. G. 2017. Regulation of muscle growth and regeneration by the immune system. *Nat Rev Immunol* 17: 165-178.

287. Uezumi, A., S. Fukada, N. Yamamoto, S. Takeda, and K. Tsuchida. 2010. Mesenchymal progenitors distinct from satellite cells contribute to ectopic fat cell formation in skeletal muscle. *Nat Cell Biol* 12: 143-152.

288. Heredia, J. E., L. Mukundan, F. M. Chen, A. A. Mueller, R. C. Deo, R. M. Locksley, T. A. Rando, and A. Chawla. 2013. Type 2 innate signals stimulate fibro/adipogenic progenitors to facilitate muscle regeneration. *Cell* 153: 376-388.

289. Le Grand, F., A. E. Jones, V. Seale, A. Scime, and M. A. Rudnicki. 2009. Wnt7a activates the planar cell polarity pathway to drive the symmetric expansion of satellite stem cells. *Cell Stem Cell* 4: 535-547.

290. Bentzinger, C. F., Y. X. Wang, J. von Maltzahn, V. D. Soleimani, H. Yin, and M. A. Rudnicki. 2013. Fibronectin regulates Wnt7a signaling and satellite cell expansion. *Cell Stem Cell* 12: 75-87.

291. Bernet, J. D., J. D. Doles, J. K. Hall, K. Kelly Tanaka, T. A. Carter, and B. B. Olwin. 2014. p38 MAPK signaling underlies a cell-autonomous loss of stem cell self-renewal in skeletal muscle of aged mice. *Nat Med* 20: 265-271.

292. Tierney, M. T., T. Aydogdu, D. Sala, B. Malecova, S. Gatto, P. L. Puri, L. Latella, and A. Sacco. 2014. STAT3 signaling controls satellite cell expansion and skeletal muscle repair. *Nat Med* 20: 1182-1186.

293. Zhu, H., F. Xiao, G. Wang, X. Wei, L. Jiang, Y. Chen, L. Zhu, H. Wang, Y. Diao, H. Wang, N. Y. Ip, T. H. Cheung, and Z. Wu. 2016. STAT3 Regulates Self-Renewal of Adult Muscle Satellite Cells during Injury-Induced Muscle Regeneration. *Cell reports* 16: 2102-2115.

294. Cosgrove, B. D., P. M. Gilbert, E. Porpiglia, F. Mourkioti, S. P. Lee, S. Y. Corbel, M. E. Llewellyn, S. L. Delp, and H. M. Blau. 2014. Rejuvenation of the muscle stem cell population restores strength to injured aged muscles. *Nat Med* 20: 255-264.

295. Price, F. D., J. von Maltzahn, C. F. Bentzinger, N. A. Dumont, H. Yin, N. C. Chang, D. H. Wilson, J. Frenette, and M. A. Rudnicki. 2014. Inhibition of JAK-STAT signaling stimulates adult satellite cell function. *Nat Med* 20: 1174-1181.

296. Kuang, S., M. A. Gillespie, and M. A. Rudnicki. 2008. Niche regulation of muscle satellite cell self-renewal and differentiation. *Cell Stem Cell* 2: 22-31.

297. Zhou, J. X., R. Taramelli, E. Pedrini, T. Knijnenburg, and S. Huang. 2017. Extracting Intercellular Signaling Network of Cancer Tissues using Ligand-Receptor Expression Patterns from Whole-tumor and Single-cell Transcriptomes. *Scientific reports* 7: 8815.

298. Zepp, J. A., W. J. Zacharias, D. B. Frank, C. A. Cavanaugh, S. Zhou, M. P. Morley, and E. E. Morrisey. 2017. Distinct Mesenchymal Lineages and Niches Promote Epithelial Self-Renewal and Myofibrogenesis in the Lung. *Cell* 170: 1134-1148 e1110.

299. Ebner, D. C., P. Bialek, A. F. El-Kattan, C. M. Ambler, and M. Tu. 2015. Strategies for skeletal muscle targeting in drug discovery. *Current pharmaceutical design* 21: 1327-1336.

300. Li, Y., M. Chen, Y. Zhao, M. Li, Y. Qin, S. Cheng, Y. Yang, P. Yin, L. Zhang, and P. Tang. 2020. Advance in Drug Delivery for Ageing Skeletal Muscle. *Front Pharmacol* 11: 1016.

301. Ashimova, A., S. Yegorov, B. Negmetzhanov, and G. Hortelano. 2019. Cell Encapsulation Within Alginate Microcapsules: Immunological Challenges and Outlook. *Front Bioeng Biotechnol* 7: 380.

302. Sleep, E., B. D. Cosgrove, M. T. McClendon, A. T. Preslar, C. H. Chen, M. H. Sangji, C. M. R. Perez, R. D. Haynes, T. J. Meade, H. M. Blau, and S. I. Stupp. 2017. Injectable biomimetic liquid crystalline scaffolds enhance muscle stem cell transplantation. *Proc Natl Acad Sci U S A* 114: E7919-E7928.

303. Judson, R. N., and F. M. V. Rossi. 2020. Towards stem cell therapies for skeletal muscle repair. *NPJ Regen Med* 5: 10.

304. Gao, X., J. Zhao, G. Han, Y. Zhang, X. Dong, L. Cao, Q. Wang, H. M. Moulton, and H. Yin. 2020. Effective Dystrophin Restoration by a Novel Muscle-Homing Peptide-Morpholino Conjugate in Dystrophin-Deficient mdx Mice. *Mol Ther* 28: 2299-2301.

305. Poussard, S., M. Decossas, O. Le Bihan, S. Mornet, G. Naudin, and O. Lambert. 2015. Internalization and fate of silica nanoparticles in C2C12 skeletal muscle cells: evidence of a beneficial effect on myoblast fusion. *Int J Nanomedicine* 10: 1479-1492.

306. Nance, M. E., C. H. Hakim, N. N. Yang, and D. Duan. 2018. Nanotherapy for Duchenne muscular dystrophy. *Wiley Interdiscip Rev Nanomed Nanobiotechnol* 10.

307. Madl, C. M., I. A. Flaig, C. A. Holbrook, Y. X. Wang, and H. M. Blau. 2021. Biophysical matrix cues from the regenerating niche direct muscle stem cell fate in engineered microenvironments. *Biomaterials* 275: 120973.

308. Sousa-Victor, P., S. Gutarra, L. Garcia-Prat, J. Rodriguez-Ubreva, L. Ortet, V. Ruiz-Bonilla, M. Jardi, E. Ballestar, S. Gonzalez, A. L. Serrano, E. Perdiguero, and P. Munoz-Canoves. 2014. Geriatric muscle stem cells switch reversible quiescence into senescence. *Nature* 506: 316-321.

309. Blau, H. M., B. D. Cosgrove, and A. T. Ho. 2015. The central role of muscle stem cells in regenerative failure with aging. *Nat Med* 21: 854-862.

310. El Zeneini, E., S. Kamel, M. El-Meteini, and A. Amleh. 2017. Knockdown of COBRA1 decreases the proliferation and migration of hepatocellular carcinoma cells. *Oncol Rep* 37: 1896-1906.

311. McChesney, P. A., S. E. Aiyar, O. J. Lee, A. Zaika, C. Moskaluk, R. Li, and W. El-Rifai. 2006. Cofactor of BRCA1: a novel transcription factor regulator in upper gastrointestinal adenocarcinomas. *Cancer Res* 66: 1346-1353.

312. Yun, H., R. Bedolla, A. Horning, R. Li, H. C. Chiang, T. H. Huang, R. Reddick, A. F. Olumi, R. Ghosh, and A. P. Kumar. 2018. BRCA1 Interacting Protein COBRA1 Facilitates Adaptation to Castrate-Resistant Growth Conditions. *Int J Mol Sci* 19.

313. Han, L., Y. Zan, C. Huang, and S. Zhang. 2019. NELFE promoted pancreatic cancer metastasis and the epithelialtomesenchymal transition by decreasing the stabilization of NDRG2 mRNA. *Int J Oncol* 55: 1313-1323.

314. Yu, S., L. Li, H. Cai, B. He, Y. Gao, and Y. Li. 2021. Overexpression of NELFE contributes to gastric cancer progression via Wnt/beta-catenin signaling-mediated activation of CSNK2B expression. *J Exp Clin Cancer Res* 40: 54.

315. Michelotti, E. F., S. Sanford, and D. Levens. 1997. Marking of active genes on mitotic chromosomes. *Nature* 388: 895-899.

316. Kadauke, S., and G. A. Blobel. 2013. Mitotic bookmarking by transcription factors. *Epigenetics Chromatin* 6: 6.

317. Kadauke, S., M. I. Udugama, J. M. Pawlicki, J. C. Achtman, D. P. Jain, Y. Cheng, R. C. Hardison, and G. A. Blobel. 2012. Tissue-specific mitotic bookmarking by hematopoietic transcription factor GATA1. *Cell* 150: 725-737.

318. Teves, S. S., L. An, A. S. Hansen, L. Xie, X. Darzacq, and R. Tjian. 2016. A dynamic mode of mitotic bookmarking by transcription factors. *eLife* 5.

319. Liu, Y., B. Pelham-Webb, D. C. Di Giammartino, J. Li, D. Kim, K. Kita, N. Saiz, V. Garg, A. Doane, P. Giannakakou, A. K. Hadjantonakis, O. Elemento, and E. Apostolou. 2017. Widespread Mitotic Bookmarking by Histone Marks and Transcription Factors in Pluripotent Stem Cells. *Cell reports* 19: 1283-1293.

320. Palozola, K. C., G. Donahue, H. Liu, G. R. Grant, J. S. Becker, A. Cote, H. Yu, A. Raj, and K. S. Zaret. 2017. Mitotic transcription and waves of gene reactivation during mitotic exit. *Science* 358: 119-122.

321. Reddy, P. C., S. J. Pradhan, K. Karmodiya, and S. Galande. 2020. Origin of RNA Polymerase II pause in eumetazoans: Insights from Hydra. *J Biosci* 45.

322. King, N., M. J. Westbrook, S. L. Young, A. Kuo, M. Abedin, J. Chapman, S. Fairclough, U. Hellsten, Y. Isogai, I. Letunic, M. Marr, D. Pincus, N. Putnam, A. Rokas, K. J. Wright, R. Zuzow, W. Dirks, M. Good, D. Goodstein, D. Lemons, W. Li, J. B. Lyons, A. Morris, S. Nichols, D. J. Richter, A. Salamov, J. G. Sequencing, P. Bork, W. A. Lim, G. Manning, W. T. Miller, W. McGinnis, H. Shapiro, R. Tjian, I. V. Grigoriev, and D. Rokhsar. 2008. The genome of the choanoflagellate Monosiga brevicollis and the origin of metazoans. *Nature* 451: 783-788.

323. Segawa, Y., H. Suga, N. Iwabe, C. Oneyama, T. Akagi, T. Miyata, and M. Okada. 2006. Functional development of Src tyrosine kinases during evolution from a unicellular ancestor to multicellular animals. *Proc Natl Acad Sci U S A* 103: 12021-12026.

324. Mikhailov, K. V., A. V. Konstantinova, M. A. Nikitin, P. V. Troshin, L. Y. Rusin, V. A. Lyubetsky, Y. V. Panchin, A. P. Mylnikov, L. L. Moroz, S. Kumar, and V. V. Aleoshin. 2009. The origin of Metazoa: a transition from temporal to spatial cell differentiation. *Bioessays* 31: 758-768.

325. Price, D. H. 2000. P-TEFb, a cyclin-dependent kinase controlling elongation by RNA polymerase II. *Mol Cell Biol* 20: 2629-2634.

326. Chao, S. H., and D. H. Price. 2001. Flavopiridol inactivates P-TEFb and blocks most RNA polymerase II transcription in vivo. *J Biol Chem* 276: 31793-31799.

327. Saha, A., C. H. Seward, L. Stubbs, and C. A. Mizzen. 2020. Site-Specific Phosphorylation of Histone H1.4 Is Associated with Transcription Activation. *Int J Mol Sci* 21.

328. Sordet, O., S. Larochelle, E. Nicolas, E. V. Stevens, C. Zhang, K. M. Shokat, R. P. Fisher, and Y. Pommier. 2008. Hyperphosphorylation of RNA polymerase II in response to topoisomerase I cleavage complexes and its association with transcription- and BRCA1-dependent degradation of topoisomerase I. *J Mol Biol* 381: 540-549.

329. Liang, K., X. Gao, J. M. Gilmore, L. Florens, M. P. Washburn, E. Smith, and A. Shilatifard. 2015. Characterization of human cyclin-dependent kinase 12 (CDK12) and CDK13 complexes in C-terminal domain phosphorylation, gene transcription, and RNA processing. *Mol Cell Biol* 35: 928-938.

330. Bartkowiak, B., P. Liu, H. P. Phatnani, N. J. Fuda, J. J. Cooper, D. H. Price, K. Adelman, J. T. Lis, and A. L. Greenleaf. 2010. CDK12 is a transcription elongation-associated CTD kinase, the metazoan ortholog of yeast Ctk1. *Genes Dev* 24: 2303-2316.

331. Blazek, D., J. Kohoutek, K. Bartholomeeusen, E. Johansen, P. Hulinkova, Z. Luo, P. Cimermancic, J. Ule, and B. M. Peterlin. 2011. The Cyclin K/Cdk12 complex maintains genomic stability via regulation of expression of DNA damage response genes. *Genes Dev* 25: 2158-2172.

332. Liu, H., and A. P. Rice. 2000. Genomic organization and characterization of promoter function of the human CDK9 gene. *Gene* 252: 51-59.

333. Shore, S. M., S. A. Byers, W. Maury, and D. H. Price. 2003. Identification of a novel isoform of Cdk9. *Gene* 307: 175-182.

334. Tirosh, I., A. Weinberger, M. Carmi, and N. Barkai. 2006. A genetic signature of interspecies variations in gene expression. *Nat Genet* 38: 830-834.

335. Yang, L., J. Wang, Y. Lv, D. Hao, Y. Zuo, X. Li, and W. Jiang. 2014. Characterization of TATA-containing genes and TATA-less genes in S. cerevisiae by network topologies and biological properties. *Genomics* 104: 562-571.

336. Peng, J., Y. Zhu, J. T. Milton, and D. H. Price. 1998. Identification of multiple cyclin subunits of human P-TEFb. *Genes Dev* 12: 755-762.

337. Garriga, J., J. Peng, M. Parreno, D. H. Price, E. E. Henderson, and X. Grana. 1998. Upregulation of cyclin T1/CDK9 complexes during T cell activation. *Oncogene* 17: 3093-3102.

338. Herrmann, C. H., R. G. Carroll, P. Wei, K. A. Jones, and A. P. Rice. 1998. Tat-associated kinase, TAK, activity is regulated by distinct mechanisms in peripheral blood lymphocytes and promonocytic cell lines. *J Virol* 72: 9881-9888.

339. Shore, S. M., S. A. Byers, P. Dent, and D. H. Price. 2005. Characterization of Cdk9(55) and differential regulation of two Cdk9 isoforms. *Gene* 350: 51-58.

340. MacLachlan, T. K., N. Sang, A. De Luca, P. L. Puri, M. Levrero, and A. Giordano. 1998. Binding of CDK9 to TRAF2. *J Cell Biochem* 71: 467-478.

341. Liu, H., and C. H. Herrmann. 2005. Differential localization and expression of the Cdk9 42k and 55k isoforms. *J Cell Physiol* 203: 251-260.

342. Szentirmay, M. N., and M. Sawadogo. 2000. Spatial organization of RNA polymerase II transcription in the nucleus. *Nucleic Acids Res* 28: 2019-2025.

343. Pfister, A. S. 2019. Emerging Role of the Nucleolar Stress Response in Autophagy. *Front Cell Neurosci* 13: 156.

344. Potmesil, M., and A. Goldfeder. 1977. Identification and kinetics of G1 phase-confined cells in experimental mammary carcinomas. *Cancer Res* 37: 857-864.

345. Mangan, H., M. O. Gailin, and B. McStay. 2017. Integrating the genomic architecture of human nucleolar organizer regions with the biophysical properties of nucleoli. *FEBS J* 284: 3977-3985.

346. Boulon, S., B. J. Westman, S. Hutten, F. M. Boisvert, and A. I. Lamond. 2010. The nucleolus under stress. *Mol Cell* 40: 216-227.

347. Dai, M. S., S. X. Zeng, Y. Jin, X. X. Sun, L. David, and H. Lu. 2004. Ribosomal protein L23 activates p53 by inhibiting MDM2 function in response to ribosomal perturbation but not to translation inhibition. *Mol Cell Biol* 24: 7654-7668.

348. Rubbi, C. P., and J. Milner. 2003. Disruption of the nucleolus mediates stabilization of p53 in response to DNA damage and other stresses. *EMBO J* 22: 6068-6077.

349. Lindstrom, M. S., D. Jurada, S. Bursac, I. Orsolic, J. Bartek, and S. Volarevic. 2018. Nucleolus as an emerging hub in maintenance of genome stability and cancer pathogenesis. *Oncogene* 37: 2351-2366.

350. James, A., Y. Wang, H. Raje, R. Rosby, and P. DiMario. 2014. Nucleolar stress with and without p53. *Nucleus* 5: 402-426.

351. Holmberg Olausson, K., M. Nister, and M. S. Lindstrom. 2012. p53 -Dependent and -Independent Nucleolar Stress Responses. *Cells* 1: 774-798.

352. Lis, J. T., P. Mason, J. Peng, D. H. Price, and J. Werner. 2000. P-TEFb kinase recruitment and function at heat shock loci. *Genes Dev* 14: 792-803.

353. Barrandon, C., F. Bonnet, V. T. Nguyen, V. Labas, and O. Bensaude. 2007. The transcription-dependent dissociation of P-TEFb-HEXIM1-7SK RNA relies upon formation of hnRNP-7SK RNA complexes. *Mol Cell Biol* 27: 6996-7006.

354. Ji, X., Y. Zhou, S. Pandit, J. Huang, H. Li, C. Y. Lin, R. Xiao, C. B. Burge, and X. D. Fu. 2013. SR proteins collaborate with 7SK and promoter-associated nascent RNA to release paused polymerase. *Cell* 153: 855-868.

355. Van Herreweghe, E., S. Egloff, I. Goiffon, B. E. Jady, C. Froment, B. Monsarrat, and T. Kiss. 2007. Dynamic remodelling of human 7SK snRNP controls the nuclear level of active P-TEFb. *EMBO J* 26: 3570-3580.

356. Calo, E., R. A. Flynn, L. Martin, R. C. Spitale, H. Y. Chang, and J. Wysocka. 2015. RNA helicase DDX21 coordinates transcription and ribosomal RNA processing. *Nature* 518: 249-253.

357. Albini, S., and P. L. Puri. 2010. SWI/SNF complexes, chromatin remodeling and skeletal myogenesis: it's time to exchange! *Exp Cell Res* 316: 3073-3080.

358. Martin, R. M., G. Ter-Avetisyan, H. D. Herce, A. K. Ludwig, G. Lattig-Tunnemann, and M. C. Cardoso. 2015. Principles of protein targeting to the nucleolus. *Nucleus* 6: 314-325.

359. Zhou, Q., T. Li, and D. H. Price. 2012. RNA polymerase II elongation control. *Annu Rev Biochem* 81: 119-143.

360. Bartholomeeusen, K., K. Fujinaga, Y. Xiang, and B. M. Peterlin. 2013. Histone deacetylase inhibitors (HDACis) that release the positive transcription elongation factor b (P-TEFb) from its inhibitory complex also activate HIV transcription. *J Biol Chem* 288: 14400-14407.

361. Bartholomeeusen, K., Y. Xiang, K. Fujinaga, and B. M. Peterlin. 2012. Bromodomain and extra-terminal (BET) bromodomain inhibition activate transcription via transient release of positive transcription elongation factor b (P-TEFb) from 7SK small nuclear ribonucleoprotein. *J Biol Chem* 287: 36609-36616.

362. Han, G., J. Li, Y. Wang, X. Li, H. Mao, Y. Liu, and C. D. Chen. 2012. The hydroxylation activity of Jmjd6 is required for its homo-oligomerization. *J Cell Biochem* 113: 1663-1670.

363. Chang, B., Y. Chen, Y. Zhao, and R. K. Bruick. 2007. JMJD6 is a histone arginine demethylase. *Science* 318: 444-447.

364. Liu, W., Q. Ma, K. Wong, W. Li, K. Ohgi, J. Zhang, A. K. Aggarwal, and M. G. Rosenfeld. 2013. Brd4 and JMJD6-Associated Anti-Pause Enhancers in Regulation of Transcriptional Pause Release. *Cell* 155: 1581-1595.

365. Lee, S., H. Liu, R. Hill, C. Chen, X. Hong, F. Crawford, M. Kingsley, Q. Zhang, X. Liu, Z. Chen, A. Lengeling, K. M. Bernt, P. Marrack, J. Kappler, Q. Zhou, C. Y. Li, Y. Xue, K. Hansen, and G. Zhang. 2020. JMJD6 cleaves MePCE to release positive transcription elongation factor b (P-TEFb) in higher eukaryotes. *eLife* 9.

366. Contreras, X., M. Barboric, T. Lenasi, and B. M. Peterlin. 2007. HMBA releases P-TEFb from HEXIM1 and 7SK snRNA via PI3K/Akt and activates HIV transcription. *PLoS Pathog* 3: 1459-1469.

367. Kim, Y. K., U. Mbonye, J. Hokello, and J. Karn. 2011. T-cell receptor signaling enhances transcriptional elongation from latent HIV proviruses by activating P-TEFb through an ERK-dependent pathway. *J Mol Biol* 410: 896-916.

368. Krauss, R. S., F. Cole, U. Gaio, G. Takaesu, W. Zhang, and J. S. Kang. 2005. Close encounters: regulation of vertebrate skeletal myogenesis by cell-cell contact. *J Cell Sci* 118: 2355-2362.

369. Sumitani, S., K. Goya, J. R. Testa, H. Kouhara, and S. Kasayama. 2002. Akt1 and Akt2 differently regulate muscle creatine kinase and myogenin gene transcription in insulin-induced differentiation of C2C12 myoblasts. *Endocrinology* 143: 820-828.

370. Kook, S. H., K. C. Choi, Y. O. Son, K. Y. Lee, I. H. Hwang, H. J. Lee, W. T. Chung, C. B. Lee, J. S. Park, and J. C. Lee. 2008. Involvement of p38 MAPK-mediated signaling in the calpeptin-mediated suppression of myogenic differentiation and fusion in C2C12 cells. *Mol Cell Biochem* 310: 85-92.

371. Wu, Z., P. J. Woodring, K. S. Bhakta, K. Tamura, F. Wen, J. R. Feramisco, M. Karin, J. Y. Wang, and P. L. Puri. 2000. p38 and extracellular signal-regulated kinases regulate the myogenic program at multiple steps. *Mol Cell Biol* 20: 3951-3964.

372. Li, J., and S. E. Johnson. 2006. ERK2 is required for efficient terminal differentiation of skeletal myoblasts. *Biochem Biophys Res Commun* 345: 1425-1433.

373. Jang, Y. N., and E. J. Baik. 2013. JAK-STAT pathway and myogenic differentiation. *JAKSTAT* 2: e23282.

374. el-Deiry, W. S., J. W. Harper, P. M. O'Connor, V. E. Velculescu, C. E. Canman, J. Jackman, J. A. Pietenpol, M. Burrell, D. E. Hill, Y. Wang, and et al. 1994. WAF1/CIP1 is induced in p53-mediated G1 arrest and apoptosis. *Cancer Res* 54: 1169-1174.

374. Robinson, D. C. L., M. Ritso, G. M. Nelson, Z. Mokhtari, K. Nakka, H. Bandukwala, S. R. Goldman, P. J. Park, R. Mounier, B. Chazaud, M. Brand, M. A. Rudnicki, K. Adelman, and F. J. Dilworth. 2021. Negative elongation factor regulates muscle progenitor expansion for efficient myofiber repair and stem cell pool repopulation. *Dev Cell* 56: 1014-1029 e1017.

Copyright Permissions

Some materials included in this thesis have been obtained from their original publication. As per Elsevier's publishing guidelines, primary authors retain the right to include published articles in a thesis, provided the thesis is not published commercially. Doing so does not require publisher permission, granted the original journal is cited. Work which was included in this thesis from the original publication (374) includes Chapter 2 (modified), and modifications to the following main figures present in the thesis: 1.2, 3.3, 3.4 – 3.10, 4.3 – 4.13, and the following supplementary figures located in the appendices : S3.2 – S3.5, S4.1, S4.3 – S4.7.

Collaborator Contributions

The work presented within this thesis was largely performed by myself. However, there were some experiments which received technical support by lab personnel and core facilities, in addition to collaborations with other labs. The nature of these contributions is indicated below.

Laboratory collaborations.

Adelman Lab (Harvard Medical School)

Precision Run-On sequencing described in section 4.3.3 was performed in collaboration with the Adelman lab (Harvard Medical School), and supported by Dr. Seth Goldman and Dr. Geoff Nelson under Dr. Adelman's supervision. For this collaboration, I prepared and permeabilized the myoblast samples (NELFb^{scKO} and WT), Dr. Goldman performed the run-on assay and sequencing, and Dr. Nelson

performed the sequencing analysis. Dr. Adelman assisted in interpretation of the results and provided useful insights.

Brand Lab (Ottawa Hospital Research Institute)

Single-cell RNA-seq analysis described in section 4.2.3 was in part supported by Dr. Zeinab Mokhtari, under the supervision of Dr. Brand. Here, I performed initial analysis of the single-cell RNA-seq gene expression matrices using Seurat, and identified the population of myogenic cells. These were provided to Dr. Mokhtari who performed analysis with PAGA focusing on specific parameters and outputs suggested by myself.

Rudnicki Lab (Ottawa Hospital Research Institute)

Allograft transplant experiments described in section 4.1 were in part supported by Dr. Morten Ritso, under the supervision of Dr. Michael Rudnicki. Dr. Ritso prepared the NSG mice for engraftment (irradiation and CTX injury if applicable), and performed engraftment of donor MuSC populations prepared by myself. Tissue processing and immunofluorescence characterization was performed by myself, and interpretation of results was assisted by Dr. Ritso and Dr. Rudnicki.

Personnel and Core Facility support.

Mr. Fernando Ortiz (StemCore, Ottawa Hospital Research Institute) performed all of the FACS experiments described in this thesis. Kathy Sheikheleslamy (StemCore, Ottawa Hospital Research Institute) prepared sorted myogenic progenitor cells for single-cell RNA-seq experiments on the 10X platform, and preparation of single cell

expression matrices was performed by Christopher Porter (StemCore, Ottawa Hospital Research Institute)

Sample preparation for CUT&Tag (section 4.3.2) was performed by Dr. Kiran Nakka (Dilworth Lab, Ottawa Hospital Research Institute), and sequencing analysis performed by Ms. Hina Bandukwala (Dilworth Lab). Animal husbandry was supported by Mr. Magid Fallahi (Dilworth Lab, Ottawa Hospital Research Institute) and Debbie King (Dilworth Lab, Ottawa Hospital Research Institute).

Appendix I – Supplementary Figures to Chapter 3

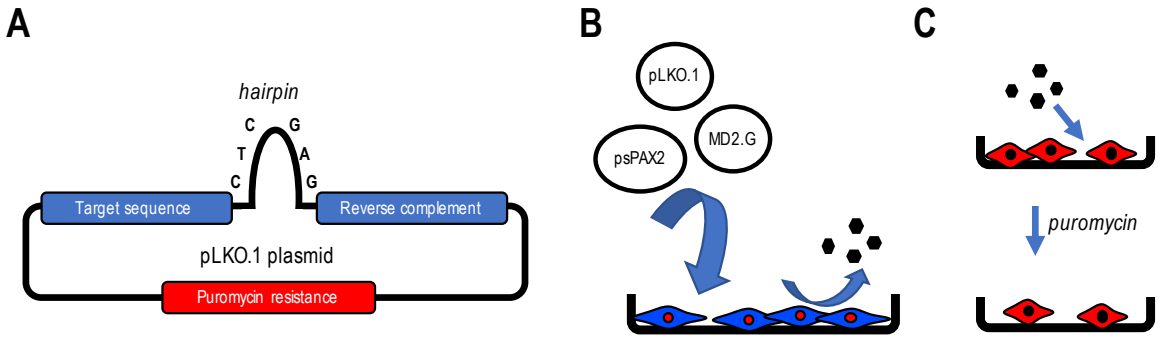

Figure S3.1 – Generating lentivirus to deliver shRNA to C2C12 cells. ***(A)*** shRNA target sequences are cloned into the pLKO.1 plasmid. ***(B)*** Calcium phosphate transfection using pLKO.1, pMD2.G, and psPAX2 plasmids are performed on HEK 293T cells. Assembly of functional virus is expelled in the culturing medium which is collected. ***(C)*** Harvested viral medium from ***(B)*** is used to transduce C2C12 cells. Puromycin selection is used to positively screen for transduced C2C12 cells, which are used in subsequent experiments.

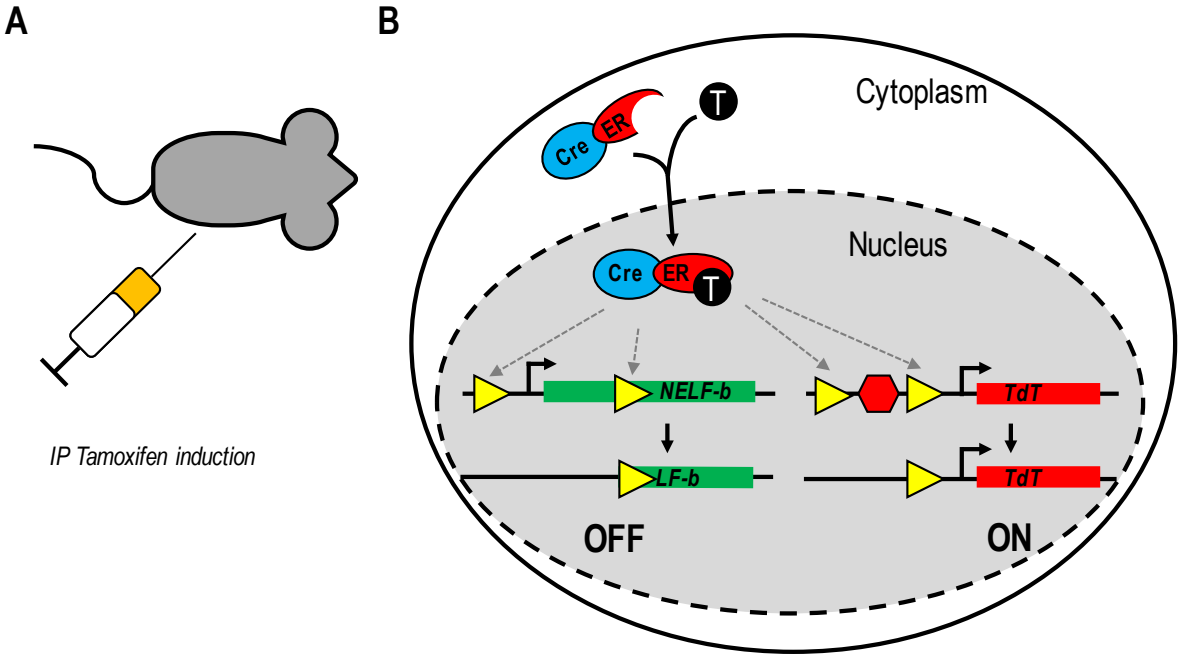

Figure S3.2 – Graphical representation of tamoxifen-induced CreERT2 recombination in mouse models. ***(A)*** Tamoxifen is delivered to mice through four consecutive intraperitoneal injections at 24h intervals. ***(B)*** Systemic tamoxifen is internalized by the constituent cells. In MuSCs, Pax7 drives the expression of CreERT2, which is inactivate and remains in the cytoplasm. In response to tamoxifen induction, the ER receptor binds tamoxifen, translocates to the nucleus, where the Cre recombinase performs homologous recombination of floxed sites to remove the DNA within those regions. This causes a deletion of *NELFb,* and activation of TdTomato.

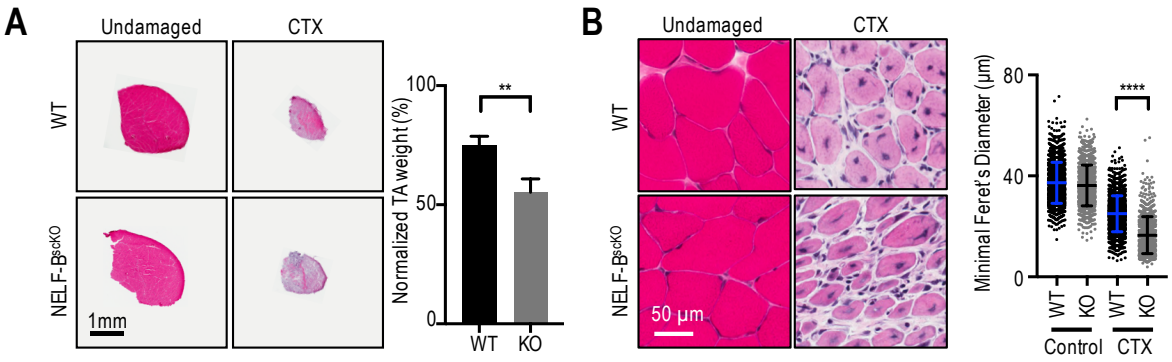

Figure S3.3 – **Regenerated TA cross-sections at 7dpi.** ***(A)*** Hematoxylin & Eosin staining of regenerated TA at 7 dpi shows a reduced size of the regenerating TA muscle from NELFb^{scKO} compared to WT controls. The normalized regenerated weight to the undamaged contralateral leg is significantly reduced in the NELFb^{scKO} [55.24% ± 2.79, n=4] compared to WT controls [74.75% ± 2.33, n=3]. ***(B)*** Magnified images from (***A***) show a reduced minimal Feret's myofiber diameter in the NELFb^{scKO} population [16.54 µm ± 0.24, n=3] compared to WT controls [25.01 µm ± 0.18, n=3].

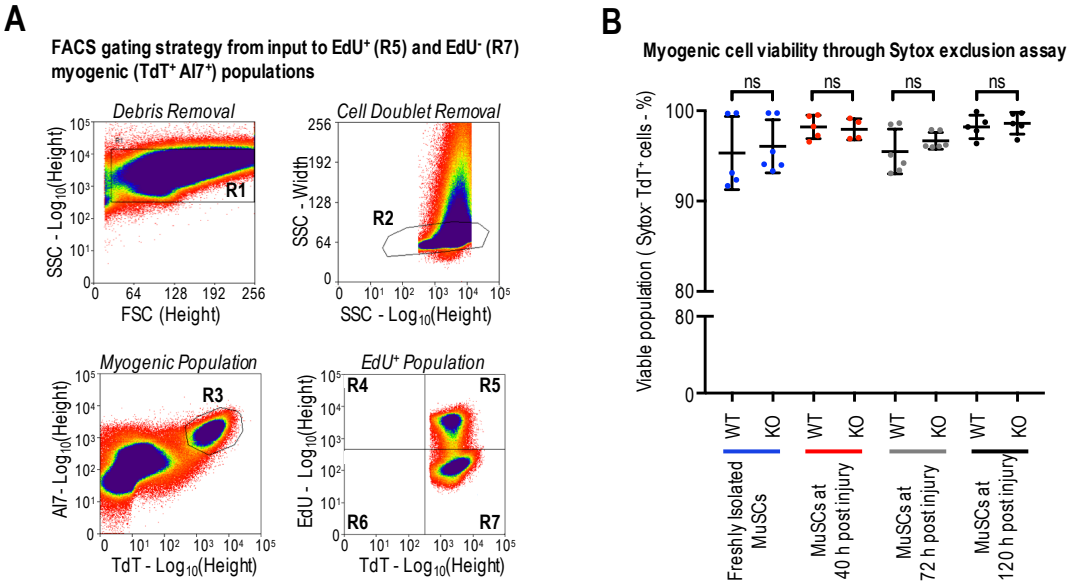

Figure S3.4 – **Fluorescence cell sorting used in different experiments** ***(A)*** FACS gating strategy applied to quantify abundance of EdU^{+} MuSCs (TdT^{+} AI7^{+}) shown in Figure 3.6A and 3.6B. First, cell debris are excluded and only cells are selected (R1); from the cell population, doublets are removed (R2) to yield only single-cell populations, which are then selected for the MuSC specific population (TdT^{+}, AI7^{+}, R3), and finally for EdU^{+} populations (R5) and EdU^{-} populations (R7). ***(B)*** Analysis of viable (Sytox^{-}) muscle progenitor cells (TdT^{+} AI7^{+}) from all experiments performed did not show significant differences in viable cell populations between NELFb^{scKO} and WT muscle progenitors. Samples included viability sorting for freshly isolated MuSCs [WT : 95.32% ± 1.81, n=5; NELFb^{scKO} : 96.06 ± 1.2, n=6], MuSCs from skeletal muscle at 40 hpi [WT : 98.21% ± 0.58, n=5; NELFb^{scKO} : 97.96% ± 0.58, n=4], MuSCs from skeletal muscle at 72 hpi [WT : 95.50% ± 1.02, n=6; NELFb^{scKO} : 96.68% ± 0.379, n=6], and myogenic progenitors from skeletal muscle at 120 hpi [WT : 98.21% ± 0.58, n=5; NELFb^{scKO} : 98.61 ± 0.538, n=5].

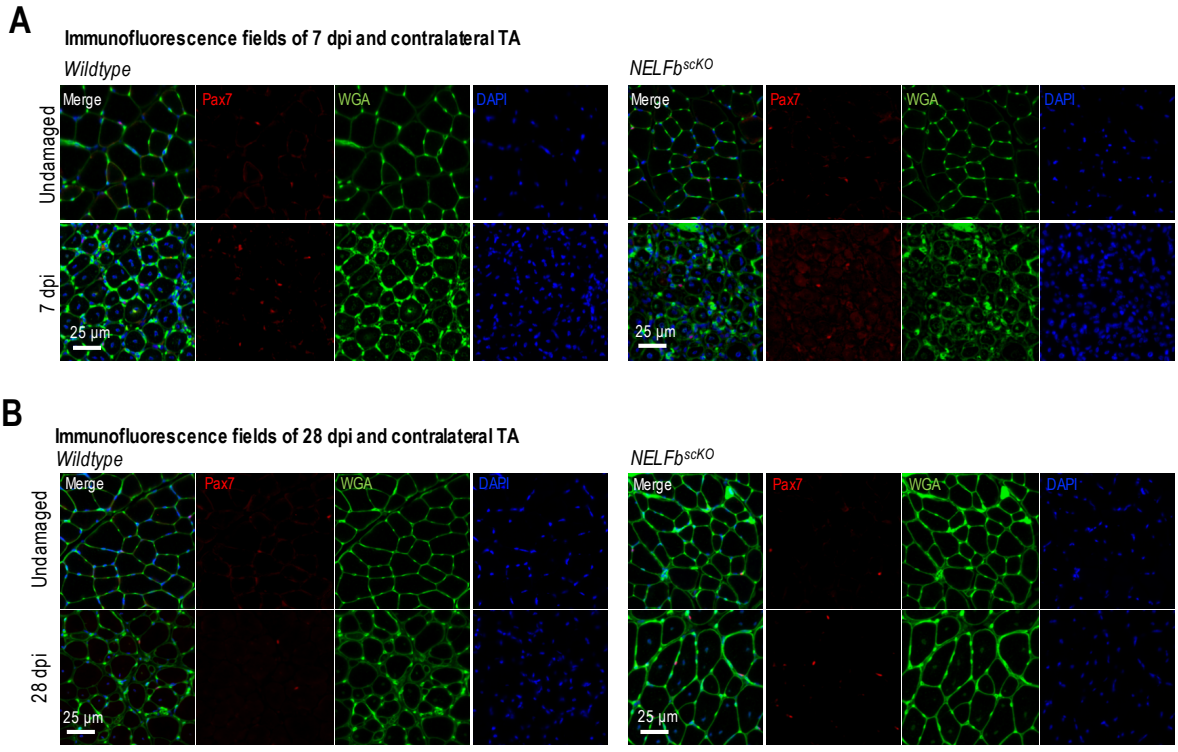

Figure S3.5 – **Individual immunofluorescence fields of skeletal muscle icharacterized at 7dpi and 28dpi.** Merged and individual fields showing MuSC (Pax7), myofibers (WGA), and all nuclei (DAPI) in cross-sections of the TA muscle which is either undamaged or regenerated obtained at 7 dpi ***(A)*** and 28 dpi ***(B)***.

Appendix II – Supplementary Figures to Chapter 4

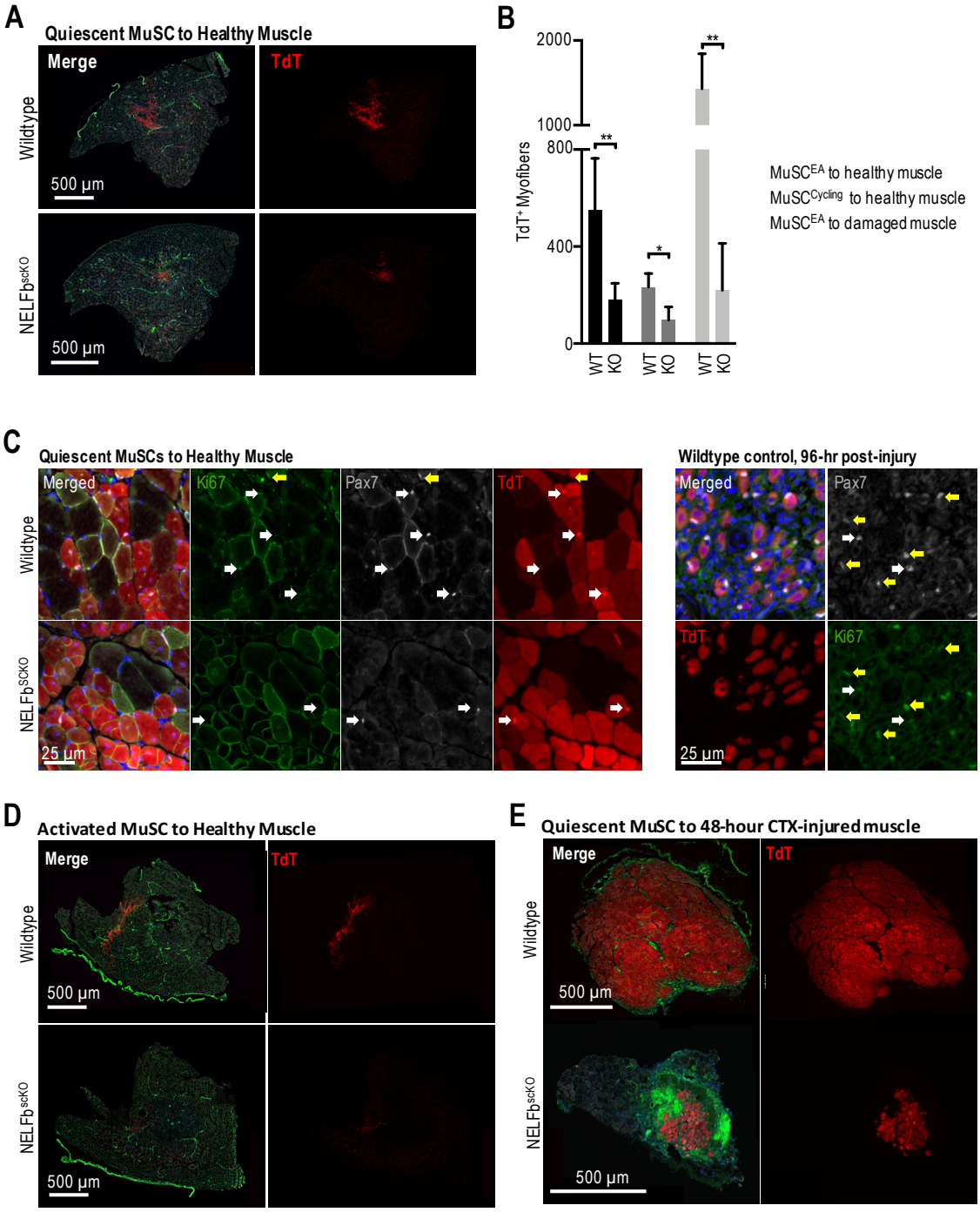

Figure S4.1 – (Related to Figure 4.3). Transplantation of MuSCs from NELFb^{scKO} mice show reduced incorporation into myofibers. Immunofluorescence characterization on 10 µm cross-sections from allograft recipient mice 21-days after transplantation. In all instances, 12,000 MuSCs from NELFb^{scKO} or WT were transplanted into irradiated NSG recipient mice. ***(A)*** Freshly isolated MuSCs from healthy muscle of WT and NELFb^{scKO} donors into uninjured irradiated recipient NSG

muscle. ***(B)*** Abundance of TdT^+ myofibers for : transplants of freshly isolated MuSCs into healthy uninjured irradiated recipient muscle shows reduced TdT^+ myofibers upon a transplant of $NELFb^{scKO}$ MuSCs [181.5 ± 27.6, n=5] compared to WT [548.2 ± 96.7, n=5]; reduced amount of TdT+ myofibers for transplant of activated MuSC from $NELFb^{scKO}$ [97.33 ± 31.39, n=3] compared to WT [233.2 ± 25.1, n=3], and reduced TdT^+ myofibers for transplants of freshly isolated MuSCs into regenerating skeletal muscle at 48 hpifor $NELFb^{scKO}$ [220.0 ± 96.7, n=4] compared to WT [1431 ± 207, n=4] counterparts. ***(C)*** Representative images for Ki67 and Pax7 co-stain of transplanted freshly isolated MuSCs from $NELFb^{scKO}$ and WT mice into healthy uninjured recipient NSG muscle, with positive control performed on WT muscle collected at 96-hours post-injury. ***(D)*** Transplant of 12,000 activated MuSCs isolated from regenerating muscle of WT and $NELFb^{scKO}$ donors (40h after CTX injection) into uninjured irradiated recipient NSG muscle; and ***(E)*** transplant of freshly isolated MuSCs from healthy muscle of WT and NELF-BscKO donors into irradiated recipient muscle at 48 hours after CTX damage.

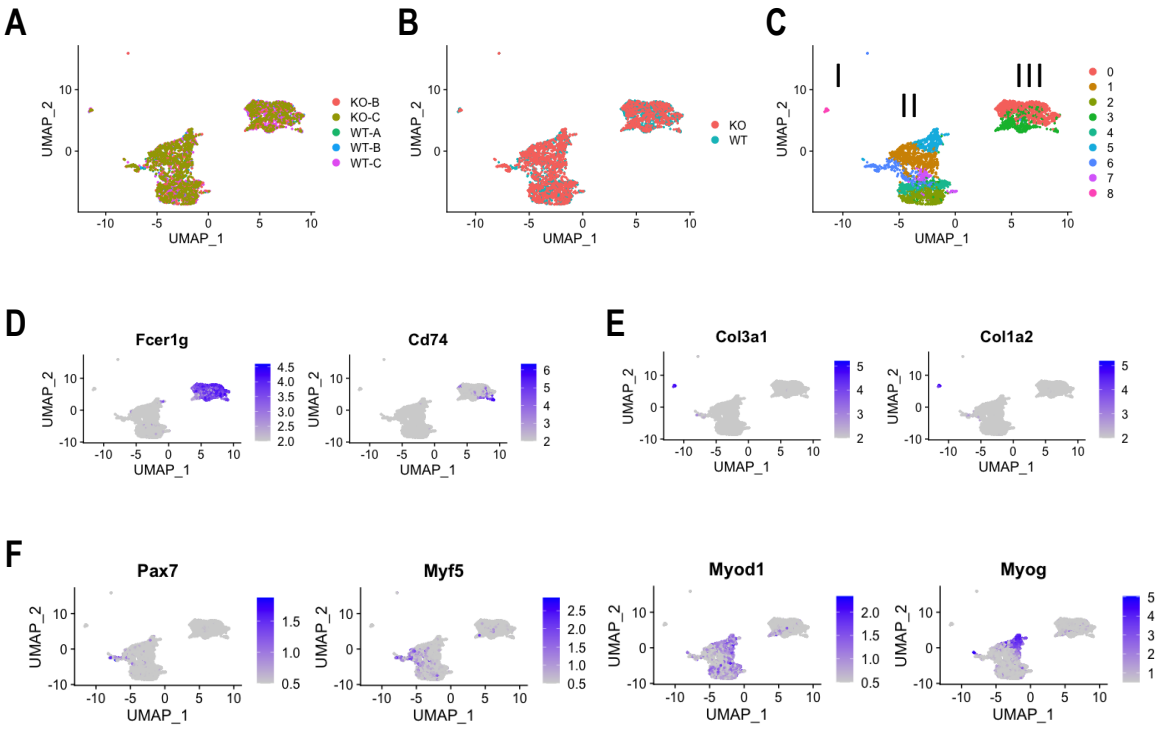

Figure S4.2 – Single cell transcriptome analysis with Seurat. Myogenic progenitors were isolated from skeletal muscle at 72 hpi, purified by FACS (TdT^+ $AI7^+$), and prepared for single-cell RNA-seq using the 10X platform. The resulting single cell expression matrices for $NELFb^{scKO}$ (KO-B, KO-C) and wildtype (WT-A, WT-B, WT-C) populations were analyzed with Seurat. All KO and WT populations distribute equally amongst the topographical map produced when considered by sample (***A***) or by population ***(B)***, and occupy 3 distinct islands ***(C).*** Gene expression analysis reveals cluster III is composed of immune cells owing to their expression of *Fcer1g* and *Cd74* ***(D)***, whereas island 1 constitutes fibroblasts based on their high expression of collagens such as *Col3a1* and *Col1a2* ***(E)***. Island 2 contains the myogenic progenitor cells, evidenced by their expression of the myogenic specific transcription factors *Pax7, Myf5, Myod1, and Myog* ***(F)***.

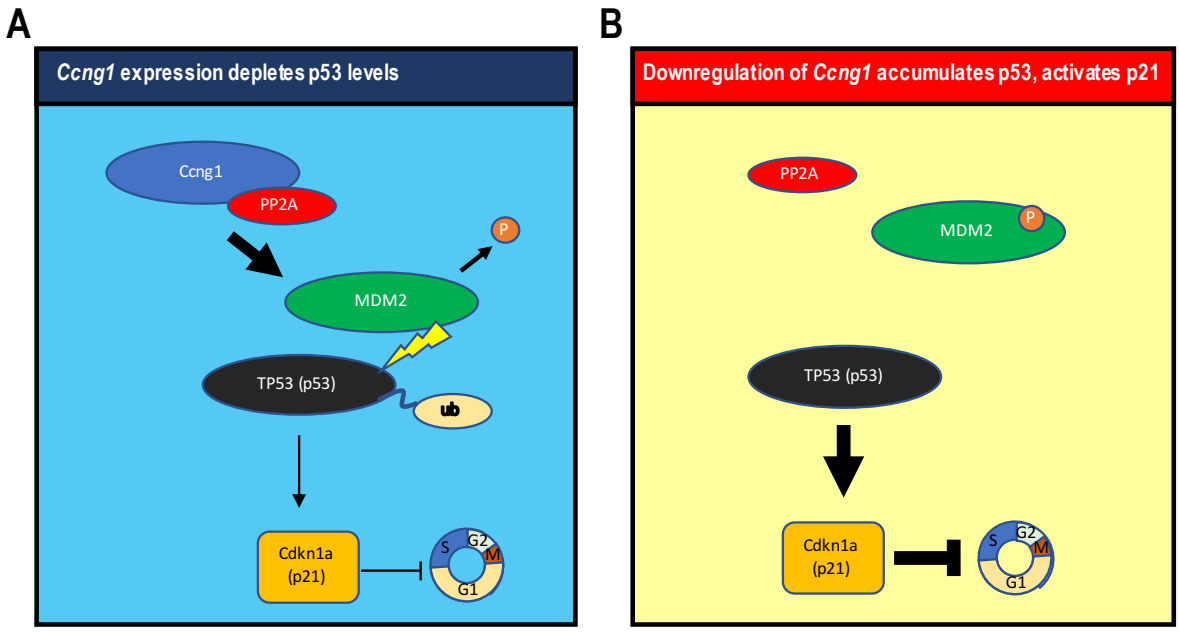

Figure S4.3 – The role of CycIn G1 in modulating p53 activity. ***(A)*** When expressed, Cyclin G1 and PP2A de-phosphorylate MDM2. This activates MDM2, which ubiquitinates p53, and targets it for degradation. ***(B)*** When *Ccng1* is downregulated, PP2A can no longer de-phosphorylate MDM2 so it remains inactive. This allows p53 to accumulate, induce the expression of *Cdkn1a,* whose protein product p21 induces cell cycle withdrawal.

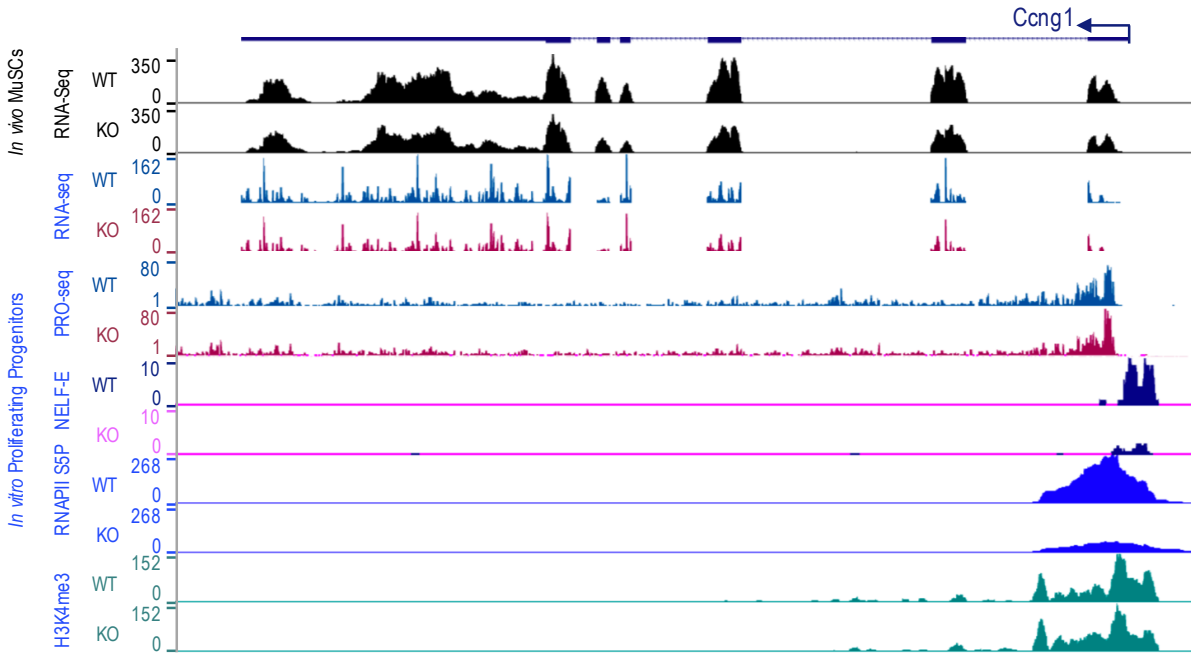

Figure S4.4 – Non-functional NELF causes a drop in promoter-proximal bound Pol II and reduced expression of *Ccng1.* Representative UCSC track for Ccng1 shows reduced Ccng1 expression for NELFb^{scKO} samples compared to WT counterparts for RNA derived from MuSCs at 48h postinjuryand from RNA-seq obtained from cultured myoblasts. PRO-seq analysis shows no effect on nascent transcript, while Cut & Tag experiments show reduced NELFe and Pol II (S5P) binding at the promoter region in NELFb^{scKO} samples compared to WT counterparts.

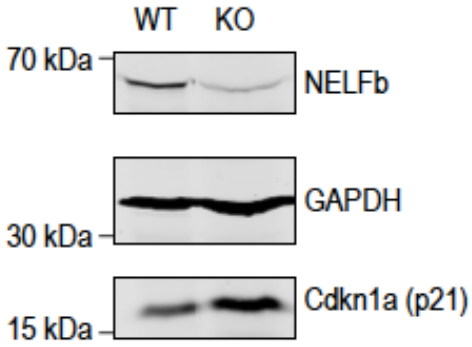

Figure S4.5 – Western blot of cultured primary myoblasts shows an elevated level of p21 among NELFb^{scKO} populations. Whole cell extracts of proliferating primary myoblasts derived from NELFb^{scKO} and WT mice reveals an upregulation of p21 in NELFb^{scKO} populations. This likely prompts precocious differentiation.

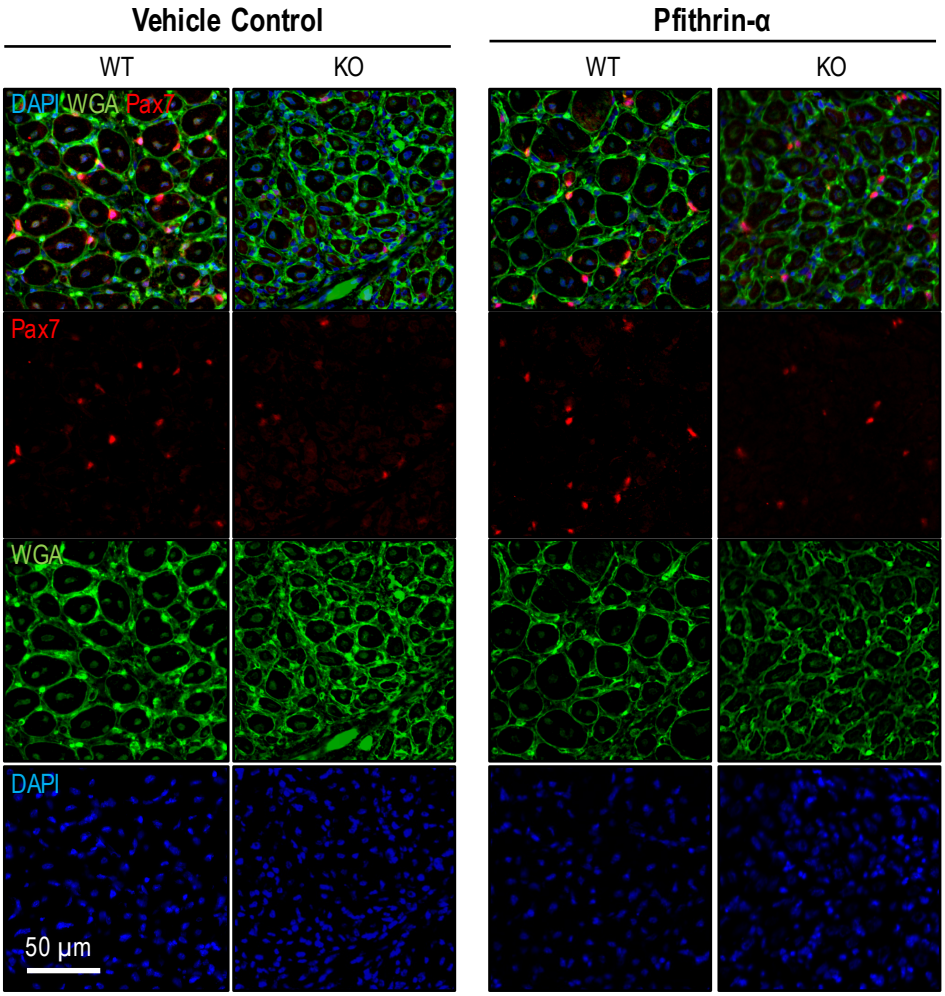

Figure S4.6 – (Related to Figure 4.11) Individual immunofluorescence fields of regenerating TA cross-sections during pifithirin-α treatment. Merged and individual immunofluorescence fields performed on regenerated skeletal muscle (7 dpi) of NELFb^{scKO} and WT mice when untreated or having received intraperitoneal pifithirin-α during regeneration.

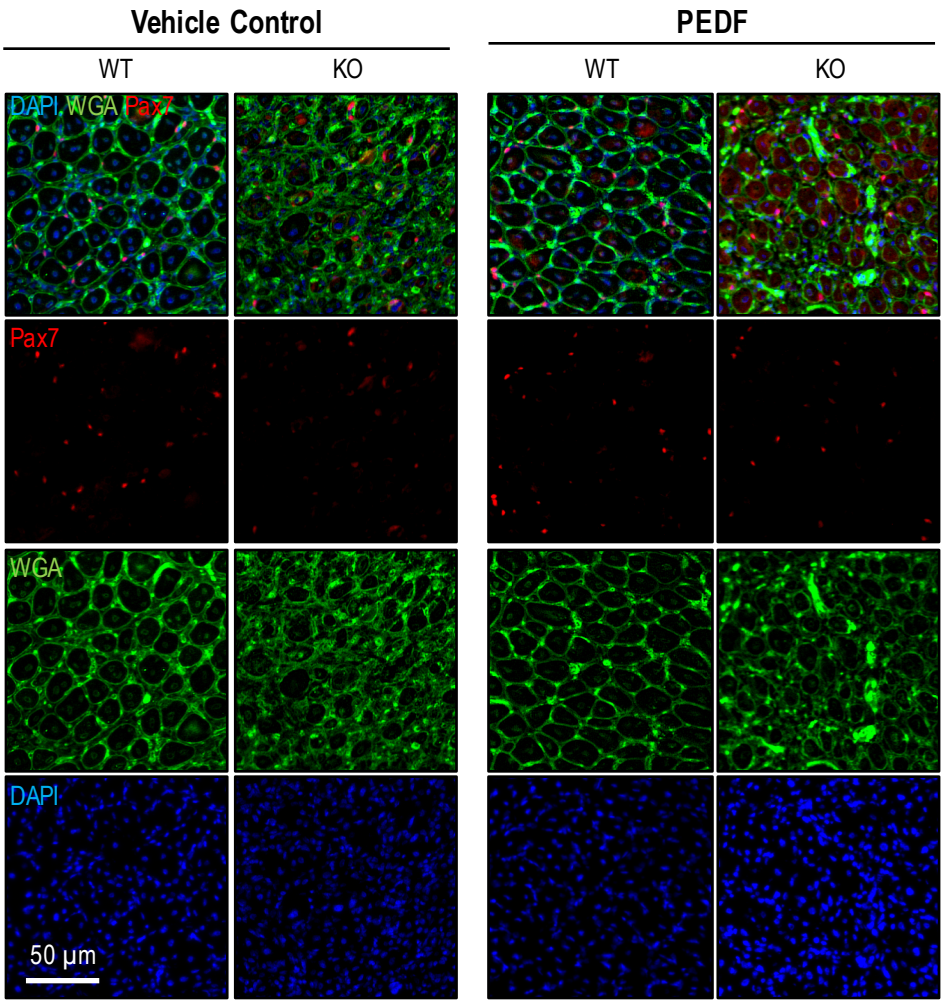

Figure S4.7 – (Related to Figure 4.12) Individual immunofluorescence fields of regenerating TA cross-sections during intramuscular PEDF supplementation experiments. Merged and individual immunofluorescence fields performed on regenerated skeletal muscle (7 dpi) of NELFb^{scKO} and WT mice when untreated or having received intramuscular PEDF during regeneration.

Appendix III – Supplementary Figures to Chapter 5

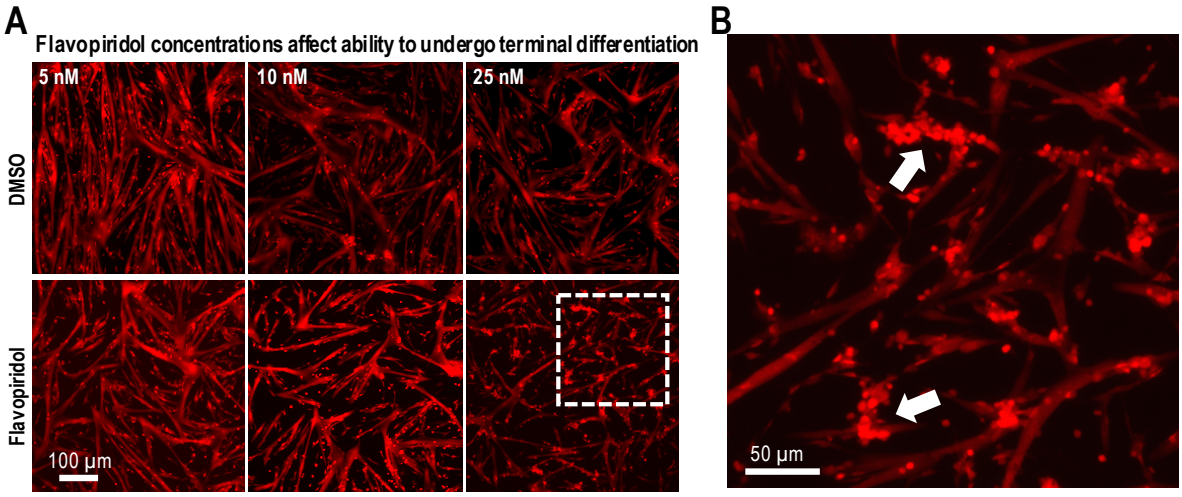

Figure S5.1 – Flavopiridol impairs primary myoblasts from undergoing terminal differentiation. Cultured primary myoblasts derived from WT mice (TdT^+) were subdivided into different groups and received varying doses of Flavopiridol or a vehicle control (DMSO). Myoblast populations were imaged live, monitoring for TdT^+. ***(A)*** The ability to form myotubes is affected by increased concentrations of Flavopiridol. ***(B)*** In response to high doses of Flavopiridol, myoblasts form large single-cell aggregates (white arrows), which appear to be myoblasts which are unable to commit to terminal differentiation.

DANIEL C.L. ROBINSON
Academic CV

EDUCATION

Doctor of Philosophy, Cell and Molecular Medicine, University of Ottawa (Ottawa Hospital Research Institute), 2015 – ongoing. Supervised by Dr. Jeffrey Dilworth. Anticipated defense date: December 2021.

Bachelor of Science (hons), Biochemistry (2015), University of Manitoba, graduated with First Class Honours

---

RESEARCH EXPERIENCE

Doctoral Thesis, (2015 – ongoing)
Research work for my doctoral thesis has identified a novel implication of the Negative Elongation Factor (NELF) complex on regulating gene expression during terminal differentiation of myogenic progenitors.

Research Assistant, University of Manitoba, 2014 – 2015
Research performed in Dr. Joe O'Neil's Proteomics lab (Department of Biochemistry) focused on studying protein dynamics of the glycerol facilitator and glycerol kinase proteins using Nuclear Magnetic Resonance (NMR).

Research Assistant, University of Manitoba, 2013
Work performed in Dr. Frank Schweizer's organic chemistry lab (Department of Chemistry) focused on constructing modified hydrophobic proline building blocks to synthesize novel antimicrobial peptides.

TEACHING EXPERIENCE

Teaching Assistant, University of Manitoba, 2013 – 2015
Courses taught: General Chemistry I & II, Introduction to Biochemistry I & II, Organic Chemistry I & II

ADDITIONAL TRAINING

Computational Genomics, Cold Spring Harbor Laboratory (December 2019). Introduction to performing independent computational genomic analysis on the Galaxy platform. Competitive course admission.

Michael Smith Foreign Study Supplement (May – July 2017).
Funding provided for training in the Chazaud lab (Lyon, France) towards histological and immunofluorescent preparation of skeletal muscle tissue.

PUBLICATIONS

Primary Research Articles

Robinson DCL, Ritso M, Nelson GM, Mokhtari, Z, Nakka, K, Bandukwala H, Goldman SR, Park PJ, Mounier R, Chazaud B, Brand M, Rudnicki MA, Adelman K, Dilworth FJ. (2021). Negative elongation factor regulates muscle progenitor expansion for efficient myofiber repair and stem cell pool repopulation. *Developmental cell*, *56*(7):1014–1029.

Sharma T, **Robinson DCL,** Witwicka H, Dilworth FJ, Imbalzano AN. The Bromodomains of the mammalian SWI/SNF (mSWI/SNF) ATPases Brahma (BRM) and Brahma Related Gene 1 (BRG1) promote chromatin interaction and are critical for skeletal muscle differentiation (2021). *Nucleic Acids Research, 49(14):8060-8077***.**

Li Y, Nakka K, Olender T, Gingras-Gelinas P, Wong MMK, **Robinson DCL**, Bandukwala H, Palii CG, Neyret O, Brand M, Blais A, Dilworth FJ. (2021). Chromatin and transcription factor profiling in rare stem cell populations using CUT&Tag. *STAR Protocols, 2(3):100751*.

Book Chapters

Robinson DCL, Dilworth FJ. *Epigenetic Regulation of Adult Myogenesis*. Curr Top Dev Biol, 2018. **126**: p. 235 – 284.

News Reports

Robinson DCL, *Persistent Organic Pollutants (POPs): a sneaky culprit of chronic disease*. Health Science Inquiry, 2018, 9 – 10.

Robinson DCL, *Developing CRISPR-Cas9 as a therapeutic tool to treat inherited genetic disorders*. Health Science Inquiry, 2017, 9 – 10.

FUNDING

Studentships

Ontario Graduate Scholarship (2020), University of Ottawa, (*$15,000* CAD).

Queen Elizabeth II Graduate Scholarship in Science and Technology (2019), University of Ottawa, (*$15,000* CAD).

Ontario Graduate Scholarship (2018), University of Ottawa, (*$15,000* CAD).

Queen Elizabeth II Graduate Scholarship in Science and Technology (2017), University of Ottawa, (*$15,000* CAD).

Canadian Graduate Scholarship – Masters (CIHR) (2016) University of Ottawa, (*$17,500* CAD).

Ontario Graduate Scholarship (2015) University of Ottawa, (*$15,000* CAD).

University of Manitoba Undergraduate Research Award (2014), University of Manitoba, (*$6,000* CAD).

Scholarships

University of Ottawa Excellence Scholarship (2015), University of Ottawa (tuition costs waived)

University of Ottawa Excellence Scholarship (2016), University of Ottawa (tuition costs waived)

University of Ottawa Excellence Scholarship (2017), University of Ottawa (tuition costs waived)

University of Ottawa Excellence Scholarship (2018), University of Ottawa (tuition costs waived)

University of Ottawa Excellence Scholarship (2019), University of Ottawa (tuition costs waived)

University of Ottawa Excellence Scholarship (2020), University of Ottawa (tuition costs waived)

University of Ottawa Tuition Fee Scholarship (2021), University of Ottawa (tuition costs waived)

Research Supplements and Travel Grants

Stem Cell Network International Travel Award (2019), Ottawa Hospital Research Institute (*$2,000* CAD). Funding provided to assist in tuition costs for the *Computational Genomics Course* (2019) taken at Cold Spring Harbor Laboratory, NY.

Canada Graduate Scholarship - Michael Smith Foreign Study Supplement, University of Ottawa, 2017 (*$6,000* CAD). Funding provided to assist in travel costs for research performed in the Chazaud lab (Lyon, France).

PRESENTATIONS

Conference Presentations

Robinson, Daniel C (2019). "Promoter-proximal stalling of RNA-Polymerase II is required for repopulation of the satellite cell niche after muscle injury". Talk presented at the Ottawa Hospital Research Institute Research Day, 8 November 2019.
**** Awarded 2nd place for oral presentation category***

Robinson, Daniel C (2019). "Promoter-proximal stalling of RNA-Polymerase II is required for repopulation of the satellite cell niche after muscle injury". Talk presented at the Ottawa Institute of Systems Biology Symposium, 7 May 2019.

Poster Presentations

3rd International Conference on Stem Cells (Aegean Conference) (03 – 08 October 2019)
Poster Title : *Expansion of the muscle stem cell population by modulation of RNA Pol II promoter-proximal stalling*
**** Awarded 2nd place for poster presentations***

5th Canadian Conference on Epigenetics *(30 September – 02 October 2018)*
Poster Title: *The Negative Elongation Factor (NELF) complex plays an apparent role in mediating myoblast differentiation during skeletal muscle regeneration*

OHRI Research Day *(9 November 2017)*
Poster Title: *Investigating the role of Negative Elongation Factor (NELF) in myogenesis*

4th Ottawa International Conference on Neuromuscular Disease and Biology – *(7 – 9 September 2017)*
Poster Title: *Investigating the role of Negative Elongation Factor (NELF) in myogenesis*

OHRI Research Day *(10 November 2016)*
Poster Title: *Investigating potential implications of the Negative Elongation Factor (NELF) in skeletal muscle regeneration*

3rd Canadian Conference on Epigenetics – *(18- 21 September 2016)*
Poster Title: *Investigating potential implications of the Negative Elongation Factor (NELF) in skeletal muscle regeneration*

University of Manitoba Undergraduate Research Day – *(30 October 2013)*
Poster Title: *Constructing modified proline building blocks to combat antibiotic resistance with antimicrobial peptides*
**** Awarded 2nd place category winner***

ADDITIONAL HONORS & AWARDS

3rd International Conference on Stem Cell (Aegean Conference) Travel Award (03 – 08 October 2019)

LEADERSHIP ROLES

Health Science Inquiry Senior Editor (2019 – 2020)

Health Science Inquiry News Manager (2018 – 2019)

University of Ottawa Graduate Student Association, student representative (2017 – 2019)

University of Manitoba Chemistry Undergraduate Society Treasurer (2013 – 2015)

2LT ROBINSON, Daniel C.L.
Military CV

TRAINING and COURSES

May – July 2021	Basic Military Officer Qualification – ARMY, Gagetown, NB
March 2018	Unit Environment Safety Officer course, London, ON
October 2017	Promotion to 2Lt (Second Lieutenant), Ottawa, ON
September 2017	Unit Recruiting Officer course, Valcartier, QC
May 2016	Basic Military Officer Qualification, Module 2, Ottawa, ON
June – July 2015	Basic Military Qualification, Nanaimo, BC
06 May 2015	Direct Entry Officer enrolment as Signals Officer (MOSID : 00341). Entry rank : Officer Cadet (OCdt)

HONOURS & AWARDS

May 2019	Junior Officer Leadership Recognition (Canadian Armed Forces, Primary Reserve) (May 2019)

LEADERSHIP ROLES

2018 – 2019	33 Signal Regiment, 703 squadron, C Troop commander
2017 – current	33 Signal Regiment, Unit Recruiting Officer
2016 – 2018	33 Signal Regiment, 763 squadron, A Troop commander